# MODERN PATHOLOGY

ABSTRACTS

GYNECOLOGIC AND OBSTETRIC PATHOLOGY

(1047-1234)

USCAP 109TH ANNUAL MEETING

2020

EYES ON YOU

FEBRUARY 29-MARCH 5, 2020

LOS ANGELES CONVENTION CENTER
LOS ANGELES, CALIFORNIA

EDUCATION COMMITTEE

ABSTRACT REVIEW BOARD

1047   P120 Catenin Staining Patterns Differentiate Mullerian Carcinosarcoma from its Mimics

Andres Acosta[1], Brooke Howitt[2], Kyle Strickland[3], Jelena Mirkovic[4], Carlos Parra-Herran[4], Michelle Hirsch[5], David Kolin[5], Marisa Nucci[1]

[1]Brigham and Women's Hospital, Harvard Medical School, Boston, MA, [2]Stanford University School of Medicine, Stanford, CA, [3]Duke University Medical Center, Durham, NC, [4]Sunnybrook Health Sciences Centre, University of Toronto, Toronto, ON, [5]Brigham and Women's Hospital, Boston, MA

Disclosures: Andres Acosta: None; Brooke Howitt: None; Kyle Strickland: None; Jelena Mirkovic: None; Carlos Parra-Herran: None; Michelle Hirsch: None; David Kolin: None; Marisa Nucci: None

Background: Loss and/or downregulation of E-Cadherin-mediated adhesion, which is a key event in epithelial-to-mesenchymal transition and the putative mechanism by which sarcomatous components of carcinosarcomas (CS) arise, results in cytoplasmic and/or nuclear translocation of P120, an integral component of the E-cadherin adhesion complex. Localization of P120 to the cytoplasm can induce a "mesenchymal" phenotype, and is thought to be one of the factors that underlie the sarcomatous transformation seen in some aggressive carcinomas. Therefore, we hypothesized that P120 staining patterns may help differentiate mullerian CS from some of its most common mimics, including corded and hyalinized endometrial carcinoma (CHEC), and dedifferentiated/undifferentiated endometrial carcinomas (D/UC).

Design: FFPE tissue sections of 29 CS, 24 D/UC and 14 CHEC were obtained from 4 institutions for P120 immunohistochemistry (IHC). Only the sarcomatous component of CS, the corded and hyalinized areas of CHEC and the undifferentiated component of D/UC were evaluated. IHC was performed using monoclonal anti-P120 primary antibodies (clone 98/pp120; BD Biosciences, San Jose, CA, USA) and the Leica Novolink (Leica Biosystems, Buffalo Grove, IL, USA) system.

Results: 24/25 (83%) CS, 14/15 (93%) CHEC and 20/24 (83%) D/UC were positive for P120. In CS, the predominant staining pattern was cytoplasmic (23/24; 96%), only 1 case was membranous (1/24; 4%). In contrast, most CHEC showed membranous staining (43%), followed by membranous and nuclear staining (21%). Similarly, the most common staining pattern in D/UC was membranous (50%), followed by cytoplasmic (25%). Staining for P120 was more often focal in D/UC (75%) and diffuse in both CS (83%) and CHEC (64%). Although sensitivity was suboptimal (60% for CHEC and 45.8% for D/UC), membranous P120 staining was 96.5% specific for the distinction of CHEC and D/UC from CS. Cytoplasmic P120 was 79% sensitive for CS, with a specificity of 80% and 75% for the distinction of CS from CHEC and D/UC, respectively.

		CS N (%)	CHEC N (%)	P [§]	D/UC N (%)	P [§]
N		29	15		24	
P120 IHC	Positive	24 (82.8)	14 (93.3)	0.647	20 (83.3)	1
	Negative	5 (17.2)	1 (6.7)		4 (16.7)	
COMPARTMENT	Membranous only	1 (4.2) *¥	6 (42.9) *¥	<0.001	10 (50) *¥	<0.001
	Cytoplasmic only	23 (95.8) *¥	2 (14.3) *¥		5 (25) *¥	
	Nucleus only	0 ¥	2 (14.3) *¥		3 (15) *¥	
	Membrane + nucleus °	0 ¥	3 (21.4) *¥		1 (5) *¥	
	Cytoplasm + nucleus °	0 ¥	1 (7.1) *¥		1 (5) *¥	
EXTENT	Focal ¶	4 (16.7) *¥	5 (35.7) *¥	0.245	15 (75) *¥	<0.001
	Non-focal ¤	20 (83.3) *¥	9 (64.3) *¥		5 (25) *¥	

*Percentages calculated based on the number of positive cases. ¥ The characteristics described in these sections correspond to the sarcomatous components of CS, the corded and hyalinized or spindle cell components of CHEC and the differentiated/undifferentiated components of D/UC. § P values reflect the significance of the difference between CHEC and CS and between D/UC and CS (Fisher's exact test, R version 3.6.1; R Foundation for Statistical Computing, Vienna, Austria). ¶ Positive staining in less than 10% of the cells of interest. ¤ Positive staining in 10% or more of the cells of interest. ° Staining patterns that are equally frequent but present in different cell populations. Abbreviations: CS = carcinosarcoma, CHEC = corded and hyalinized variant of endometrioid endometrial adencarcinoma, D/UC = Dedifferentiated/undifferentiated endometrial carcinoma.

Figure 1 - 1047
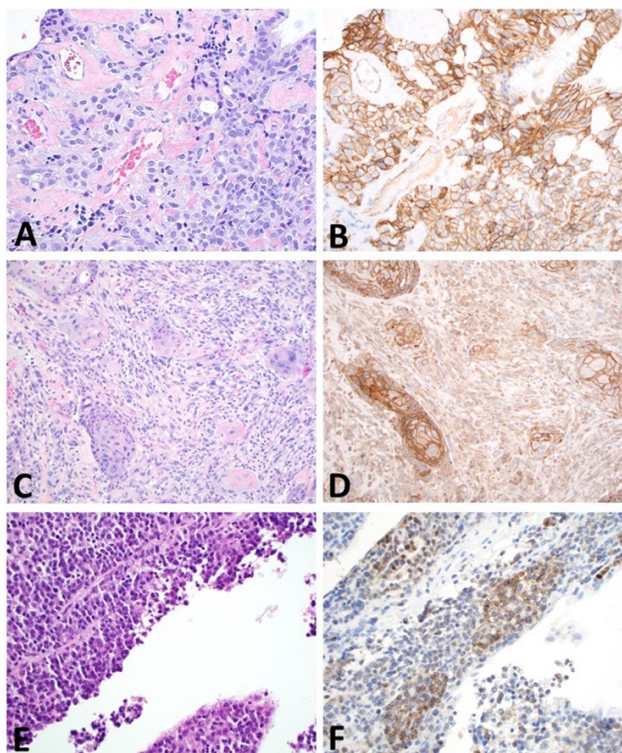
Corded and hyalinized endometrioid endometrial adenocarcinoma (A) with membranous expression of P120 (B). Carcinosarcoma (C) with cytoplasmic and membranous P120 in the sarcoma and carcinoma components, respectively (D). Undifferentiated endometrial carcinoma (E) with focally retained membranous P120 expression (F).

Conclusions: Membranous staining for P120 is highly supportive of malignant epithelial differentiation. Conversely, this staining pattern uncommonly occurs in the sarcomatous component of CS. Thus membranous staining helps differentiate CHEC and D/UC from the sarcomatous component of CS. Also, nuclear P120 argues against CS. Furthermore, diffuse cytoplasmic staining is significantly more common in sarcomatous elements of CS, albeit not specific.

1048 Tumors of the Female Genital Tract with Combined Epithelial and Germ Cell or Trophoblastic Components: A Shared Molecular Profile Supports Origin from the Epithelial Component

Andres Acosta[1], Lynette Sholl[2], Christopher Otis[3], Marisa Nucci[1]
[1]Brigham and Women's Hospital, Harvard Medical School, Boston, MA, [2]Brigham and Women's Hospital, Boston, MA, [3]University of Massachusetts Medical School-Baystate, Srpingfield, MA

Disclosures: Andres Acosta: None; Lynette Sholl: *Consultant*, LOXO Oncology; Christopher Otis: None; Marisa Nucci: None

Background: Epithelial malignancies of the gynecologic tract associated with germ cell or trophoblastic components are rare, and their molecular underpinnings remain unknown. Two prevailing hypotheses regarding their ontogenesis propose either divergent differentiation in a single neoplasm, or alternatively, the collision of 2 pathogenetically independent lesions. In this study, we performed a molecular characterization of 5 tumors with different combinations of carcinoma and germ cell or trophoblastic neoplasia to determine 1) the mutational profile of the different components and 2) if the different components have a common origin.

Design: Five cases from 3 institutions were retrieved for the study: Case 1 = ovarian carcinosarcoma (CS) associated with serous borderline tumor-like components + yolk-sac tumor (YST); case 2 = serous carcinoma of endometrium + epithelioid trophoblastic tumor (ETT); case 3 = ovarian CS + YST; case 4 = ovarian HGSC + YST; case 5 = ovarian endometrioid adenocarcinoma + YST. FFPE tissue sections were manually dissected for nucleic acid extraction. In cases 1,2,3 and 5, components of interest present in different blocks were identified, allowing separation before nucleic acid extraction. In case 5 separation was not attempted because the different components were present in the same block and closely intermingled. Sequencing was performed using a targeted sequencing panel (Oncopanel). The current version of this test includes 447 disease-relevant genes and detects single-nucleotide variants, insertions /deletions, copy number alterations and structural variants.

Results: Results are presented in the figure. Briefly, a specific mutational profile was not identified, and the genetic alterations detected are those expected according to the epithelial component of the tumors. Identical insertion-deletions and point-mutations are present in both components. Structural rearrangements were more frequent in the germ cell and trophoblastic components of the tumor.

Figure 1 - 1048

NGS RERSULTS - MISSENSE/NONSENSE MUTATION, REARRANGEMENT, FRAMESHIFT INDEL, IN-FRAME INDEL, DELETION/LOSS, GAIN/AMPLIFICATION (INCLUDING HIGH LEVEL AMPLIFICATIONS), BOTH DELETION/LOSS AND GAIN/AMPLIFICATION. Abbreviations: SBT = serous borderline tumor, CS = carcinosarcoma, HGSC = high grade serous carcinoma, YST = yolk sac tumor, SCE = serous carcinoma of endometrium, ETT = epithelioid trophoblastic tumor, CCC = clear cell carcinoma, EMCA = endometrioid endometrial adenocarcinoma. The components in parenthesis represents the epithelial elements of CS.

Conclusions: Epithelial malignancies of the female genital tract associated with germ cell or trophoblastic components do not show a distinct mutational profile, and show mutations expected according to the epithelial component present. Also, both components share an identical mutational profile, in keeping with a common origin for both components. The most significant difference was the presence of a higher number of structural variants in the germ cell and trophoblastic components.

1049 Differentiated Verruciform Intraepithelial Lesions of the Vulva: Clinico-Pathologic and Molecular Analysis Documenting its Relationship with Verrucous Carcinoma

Amir Akbari[1], Andre Pinto[2], Yutaka Amemiya[3], Arun Seth[4], Jelena Mirkovic[4], Carlos Parra-Herran[4]
[1]University of Toronto, Toronto, ON, [2]University of Miami, Miami Beach, FL, [3]Sunnybrook Research Institute, Toronto, ON, [4]Sunnybrook Health Sciences Centre, University of Toronto, Toronto, ON

Disclosures: Amir Akbari: None; Andre Pinto: None; Yutaka Amemiya: None; Arun Seth: None; Jelena Mirkovic: None; Carlos Parra-Herran: None

Background: Verruciform proliferations of the vulva unrelated to HPV infection are rare. Watkins et al recently coined the term differentiated exophytic vulvar intraepithelial lesion (DEVIL) for these proliferations, which harbor recurrent *PIK3CA* mutations. Verrucous carcinoma (VC), a neoplasm characterized by persistence and local recurrence but nil risk of distant spread, has been associated with *TP53* and *HRAS* mutations. It is still unclear whether DEVIL is related to VC.

Design: Material from cases identified using the words "verruciform" and "verrucous" in our database search was strictly reviewed by 2 gynecologic pathologists. For inclusion, diagnosis of DEVIL required verruciform acanthosis, hyper and/or parakeratosis, hypogranulosis, cytoplasmic pallor and bland nuclei. VC was diagnosed if discontinuous, bulbous, puzzle-like nests of epithelium were seen in the stroma. Lesions with any significant atypia, proliferation or infiltrative borders were excluded. A 9-gene next-generation sequencing panel was performed. Data was compared between samples, looking for shared alterations between VC and previous, concurrent or subsequent DEVIL.

Results: A total of 18 specimens corresponding to 10 patients with DEVIL and/or VC were included (Table). The cohort included 8 women with DEVIL (median age at presentation 66 years), and 7 with VC (median age at presentation 70 years). A similar spectrum of prevalent mutations was found, involving *HRAS* (50% DEVIL, 86% VC), *PIK3CA* (50% DEVIL, 29% VC), *TP53* (25% DEVIL, 43% VC) and *BRAF* (13% DEVIL, 14% VC).

In 3 patients (A-C), DEVIL preceded VC with an interval of 65, 22 and 33 months, respectively. In one (D), DEVIL and VC were diagnosed concurrently. One patient (E) had VC resected and 2 months later developed a DEVIL. In patient A, the same *PIK3CA* mutation was detected in VC, adjacent DEVIL and preceding DEVIL. In patients C and D, VC and concurrent DEVIL shared the same mutations in *HRAS* and *BRAF*, respectively. In patient E, both VC and subsequent DEVIL shared the same *HRAS* mutation.

Patient	Age	Sample	*PIK3CA*	*HRAS*	*BRAF*	*TP53*	*CTNNB1*
A	40	Preceding DEVIL	p.E542K				
		VC (65 months later)	p.E542K, p.E545K			p.R175C	
		Concurrent DEVIL	p.E542K, p.M1043I			p.R175C	
B	71	Preceding DEVIL					
		VC (22 months later)	p.E542K				
		Concurrent DEVIL					
C	61	Preceding DEVIL	p.E542K	p.Q61L			
		VC (33 months later)		p.G12A			
		Concurrent DEVIL		p.G12A			
D	81	Concurrent DEVIL			p.G466R		
		VC			p.G466R	p.R196Q	
E	85	VC		p.Q61R			
		DEVIL (2 months later)		p.Q61R			
F	46	DEVIL	p.E542K			p.R158C	
G	64	DEVIL		p.G12D			
H	64	DEVIL					
I	69	VC		p.G12D		p.R249N	p.M398I
J	54	VC		p.Q61L			

Conclusions: DEVIL is a rare form of squamous proliferation characterized by prevalent *PIK3CA* and *HRAS* mutations. Its temporal relationship with VC and the shared mutational profile between DEVIL and VC in some patients suggest that DEVIL is related to VC, potentially as a precursor. Moreover, given the morphologic and molecular overlap between these two lesions and the nil risk of VC for distant spread, it is conceivable that DEVIL and VC represent a spectrum of the same entity.

1050 Prognostic Significance of Depth and Pattern of Cervical Stromal Invasion in Type 1 Endometrial Carcinoma

Bassam Alkamachi[1], Simeng Zhu[1], Mohamed Elshaikh[2], Ghassan Allo[2]
[1]Henry Ford Health System, Detroit, MI, [2]Henry Ford Hospital, Detroit, MI

Disclosures: Bassam Alkamachi: None; Simeng Zhu: None; Mohamed Elshaikh: None; Ghassan Allo: None

Background: The prognostic significance of cervical stromal invasion (CSI) by endometrial carcinoma is well established, and patients with this form of invasion are offered similar adjuvant therapy. It is not clear whether characteristics of this form of invasion have prognostic implications. We aim in this study to investigate the prognostic significance of depth and pattern of cervical stromal invasion in patients with type 1 endometrial carcinoma.

Design: This is a retrospective study of patients with type 1, FIGO stage 2 endometrial cancer, who were treated at our institution between 1991 and 2019. After IRB approval, we assessed microscopic depth of CSI (measured as distance from cervical surface to deepest point of invasion within cervical stroma), cervical stromal thickness, and pattern of invasion (based on endocervical adenocarcinoma previously described patterns A, B, and C). Clinical data were collected from the medical records. Descriptive analysis and Cox regression models were produced.

Results: Material and data were available on 50 patients. Median age at diagnosis was 65(41-91) years, of which 30 patients had FIGO grade 1, 23 showed <50% myometrial invasion, 11 had angioinvasion, 40 had underwent lymph node dissection, and 42 received adjuvant radiation.

Median depth of CSI was 3.5(0.5-20.0) mm, with median percentage invasion to cervical stromal thickness of 33.3(6.7-100)%. CSI to >2/3 of cervical stroma was found in 8 (16%) of patients, and was associated with worse overall survival (OS) in univariable analysis (HR, 0.22; 95% CI, 0.06-0.75), and after controlling for age, race, grade, depth of myometrial invasion, angioinvasion, peritoneal washings, and adjuvant radiotherapy (HR, 0.08; 95% CI, 0.01-0.53). CSI of 5.0 mm or more, found in 16(32%) patients, was associated with tendency

towards worse OS (HR, 3.1; 95% CI, 0.96 – 10.2), while CSI of 50% cervical stroma or more (n=17, 34%) or patterns of invasion were not associated with different OS on univariable analysis.

Recurrence was present in 5(10%) of patients, significantly higher in those with >1/3 CSI (LH, 7.1; 0=0.008).

Figure 1 - 1050
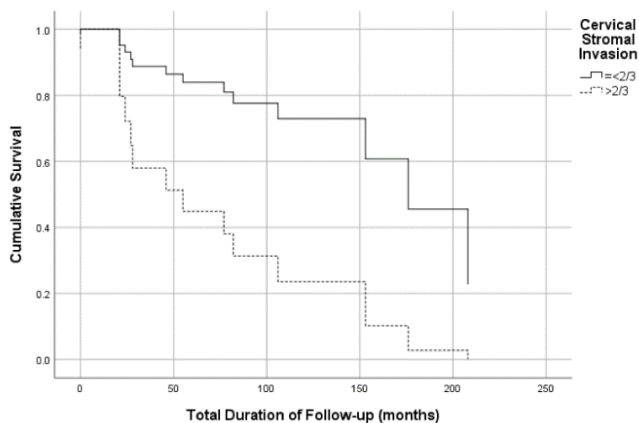
Figure 2 - 1050
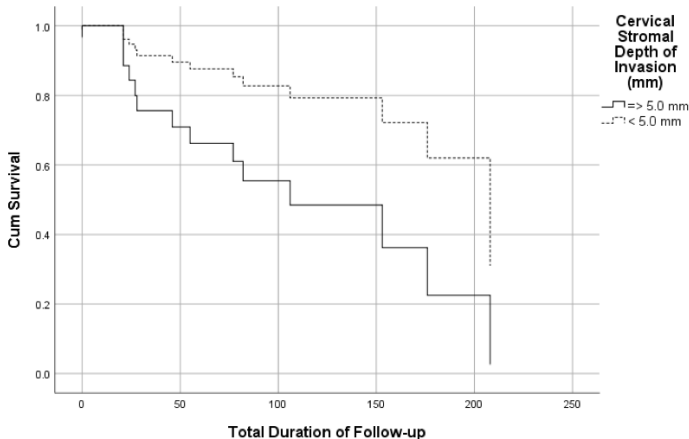
Conclusions: A small subset of type 1, FIGO stage 2 endometrial cancers shows extension to more than 2/3 of cervical stroma and exhibits worse overall survival. Subcategorization of stage 2 and therapy tailoring may be indicated in these patients. Further studies are needed.

1051 Two versus Four Immunohistochemical Stains for Lynch Syndrome Screening in Gynecologic Cancers

Shara-Gaye Allen[1], Amir Akbari[2], Marjan Rouzbahman[3], Gulisa Turashvili[4], Aaron Pollett[4], Alicia Tone[5], Sanaz Sanii[6], Emily Van de Laar[3], Sarah Ferguson[7], Blaise Clarke[2]
[1]Cornwall Regional Hospital, Montego Bay, Jamaica, [2]University of Toronto, Toronto, ON, [3]Toronto, ON, [4]Mount Sinai Hospital, Toronto, ON, [5]Department of Laboratory Medicine and Pathobiology, University of Toronto, Toronto, ON, [6]University Health Network, St. John'S, NL, [7]University Health Network

Disclosures: Shara-Gaye Allen: None; Amir Akbari: None; Amir Akbari: None; Marjan Rouzbahman: None; Gulisa Turashvili: None; Aaron Pollett: None; Sanaz Sanii: None; Blaise Clarke: None

Background: Reflex testing of endometrial cancer and non-mucinous and non-serous ovarian carcinoma is being adopted in many centres. Traditionally, screening using all 4 mismatch repair markers (MLH1, PMS2, MSH2 and MSH6) is performed. These proteins form heterodimers complexes between MLH1 and PMS2 and between MSH2 and MSH6. MLH1 and MSH2 staining is retained in the setting of alteration of PMS2 and MSH6 respectively. However the secondary proteins, PMS2 and MSH6, are not expressed in the absence of MLH1 and MSH2 expression. This allows for a 2 marker (PMS2 and MSH6) screening strategy with associated laboratory cost saving. While this strategy has been validated in colon and endometrial cancer, a recent study highlighted weak MSH6 staining associated with loss of MSH2 as a possible cause of false negative cases.

Design: We reviewed a retrospective series of endometrial and ovarian cancer cases (220 cases) screened with 4 markers and enriched for MSH2/MSH6 deficient cases and cases with subclonal loss of MLH1/PMS2. The two markers (PMS2 and MSH6) were reviewed by three pathologists with variable experience in mismatch repair immunohistochemical screening blinded to the results of the initial four marker clinical screen.

Results: 160 cases were normal (both markers retained). Of the remaining 60 cases, 44 showed PMS2 loss (4 were isolated PMS2 loss) and 16 showed MSH6 loss, (8 were isolated MSH6 loss). All cases were interpreted correctly by 2 pathologists but three cases with MSH6 loss were called equivocal by one pathologist. Subclonal loss was not appreciated by one of the pathologist in one case.

Conclusions: A two marker panel is effective in screening endometrial and ovarian carcinoma for mismatch repair deficiency/ Lynch Syndrome. It behoves us to be aware of the pitfalls of weak MSH6 staining in the setting of MSH2 loss. Also, one is more likely to miss subclonal loss of MLH1/PMS2. While this has no bearing on Lynch syndrome status since these events are secondary to methylation, its role as a predictive marker for immune checkpoint therapy is unclear. Interobserver study suggests that experience with these markers allows one to avoid the misinterpretation of weak MSH6 staining as false negative.

1052   Epigenetic Signatures of Synchronous and Metastatic Endometrioid Adenocarcinomas

Douglas Allison[1], Gulisa Turashvili[2], Jonathan Serrano[3], Britta Weigelt[4], Nadeem Abu-Rustum[4], Matija Snuderl[3], Sarah Chiang[4]
[1]NYU Langone Health, New York, NY, [2]Mount Sinai Hospital, Toronto, ON, [3]New York University, New York, NY, [4]Memorial Sloan Kettering Cancer Center, New York, NY

Disclosures: Douglas Allison: None; Gulisa Turashvili: None; Jonathan Serrano: None; Jonathan Serrano: None; Britta Weigelt: None; Nadeem Abu-Rustum: *Grant or Research Support*, Stryker; *Grant or Research Support*, GRAIL; Matija Snuderl: None; Sarah Chiang: None

Background: Clinicopathologic criteria exist to identify synchronous and metastatic endometrioid carcinomas involving endometrium and ovary. Recent studies utilizing next generation sequencing demonstrated that most clinically suspected synchronous ovarian and endometrial endometrioid tumors are in fact clonally related. We sought to define epigenetic signatures of FIGO grade 1 endometrioid carcinomas of endometrial primary, ovarian primary, synchronous endometrial and ovarian primaries, and endometrial primary with ovarian metastasis.

Design: DNA was extracted from microdissected formalin-fixed, paraffin-embedded tumor tissues from 8 isolated endometrial primaries, 6 isolated ovarian primaries, 5 synchronous endometrial and ovarian primaries and 3 endometrial primaries with ovarian metastasis and subjected to methylation profiling (Illumina MethylationEPIC array). Methylation data were analyzed with the R Bioconductor package minfi, including quality control, data normalization and differentially methylated CpG site analysis. Subsequent filtering was performed using a p-value cutoff = 0.01 and a minimal mean difference of the Beta-value of = 0.1. Copy number alterations were analyzed using conumee package.

Results: Epigenetic profiling revealed that isolated primary endometrial and ovarian tumors formed two distinct methylation clusters according to their site of origin (Fig. 1). Similarly, 4/5 synchronous endometrial and ovarian tumors primary pairs clustered away from each other and by primary site. Both endometrial and ovarian tumors in the remaining synchronous primary pair clustered with isolated primary ovarian tumors. Finally, endometrial and ovarian tumors in all 3 endometrial primaries with ovarian metastasis clustered by disease site. (Fig. 1). Copy number changes largely recapitulated the methylation patterns with some synchronous tumors showing similar profiles and some showing large differences (Fig. 2). Certain copy number alterations (most notably 1q gain) seemed specific to ovarian tumors, a finding observed across both isolated primary and synchronous tumors.

Figure 1 - 1052
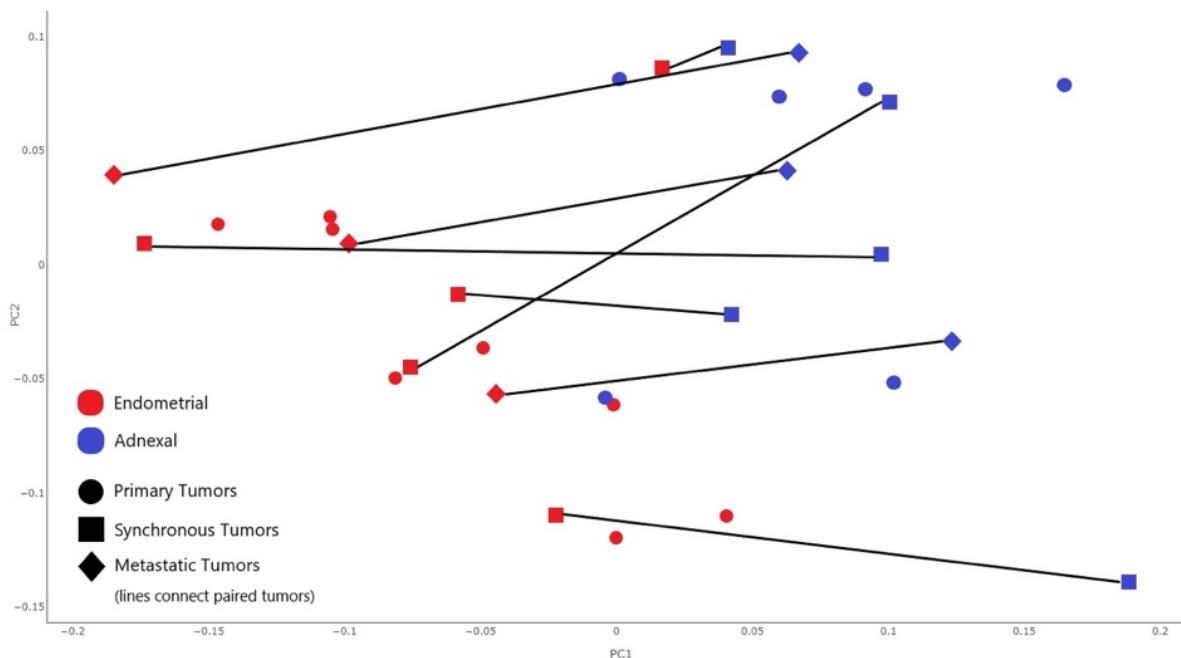
Figure 2 - 1052
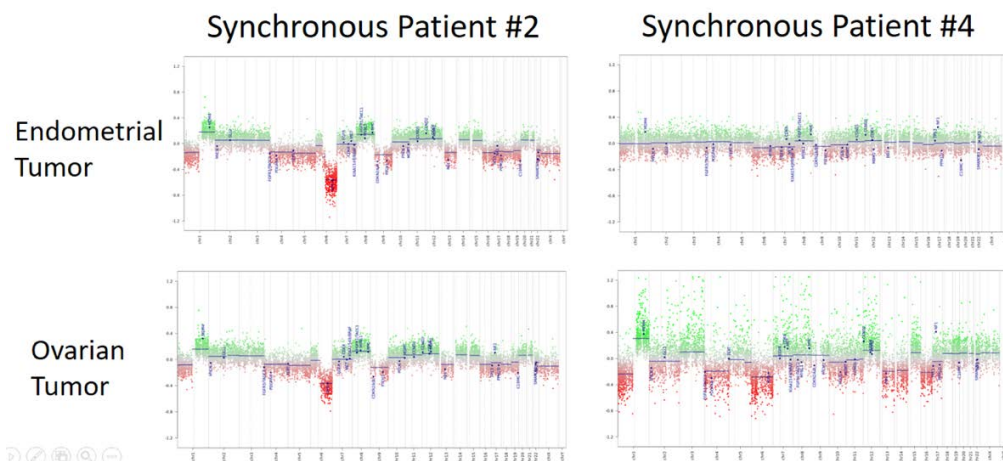
Conclusions: DNA methylation profiles of synchronous endometrial and ovarian tumors and endometrial primaries with ovarian metastasis are similar and cluster by disease site. Copy number changes recapitulate methylation results. These findings suggest site specific effects on tumor development.

1053 B-Catenin and CD10 Expression in Mesenchymal Uterine Tumors: A Canadian Multi-Center Retrospective Study

Noorah Almadani[1], Cecile Le Page[2], C. Blake Gilks[3], Liliane Meunier[4], Lise Portelance[5], Anne-Marie Mes-Masson[6], Cheng-Han Lee[7], Lynn Hoang[7], Kurosh Rahimi[8]
[1]University of British Columbia/Vancouver General Hospital, Vancouver, BC, [2]University of Montréal, Montreal, QC, [3]Vancouver General Hospital, Vancouver, BC, [4]Centre de recherche du Centre hospitalier de l'Université de Montréal (CRCHUM), Montreal, QC, [5]1 Centre de recherche du Centre hospitalier de l'Université de Montréal (CRCHUM) et Institut du cancer de Montréal, Montréal, QC, [6]Centre de recherche du CHUM, Montreal, QC, [7]Vancouver, BC, [8]Université de Montreal, Montreal, QC

Disclosures: Noorah Almadani: None; Cecile Le Page: None; C. Blake Gilks: None; Lise Portelance: None; Anne-Marie Mes-Masson: None; Cheng-Han Lee: None; Lynn Hoang: None; Kurosh Rahimi: None

Background: Beta-catenin has been recently reported in a subset of low-grade endometrial stromal sarcomas (ESS), but few studies thus far have reported the expression patterns of beta-catenin in other uterine mesenchymal tumors, particularly endometrial stromal nodules (ESN), adenosarcomas (AS) and undifferentiated uterine sarcoma (UUS). In this study we evaluate the expression of nuclear beta-catenin as well as CD10, in a variety of uterine mesenchymal tumors to assess their discriminative diagnostic value.

Design: We assessed a retrospective cohort of 74 cases from three institutions in Canada: Vancouver General Hospital (Vancouver), CRCHUM (Montreal) and Ottawa Hospital Research Institute (Ottawa) between 1988 and 2019. We included ESS, ESN, AS, UUS, leiomyosarcomas (LMS) and carcinosarcomas (CS). CD10 and nuclear beta-catenin expression (nuclear or membranous/cytoplasmic) was assessed by immunohistochemistry on tissue microarray and confirmed on whole sections in select cases. Clinical data was extracted from hospital files. Disease-specific survival (DSS) of patients was calculated from the time of diagnosis until death or last follow-up. Progression time (PFS) was calculated from first date of treatment to date of first disease progression.

Results: The immunohistochemical results are summarized in Table 1. Nuclear beta-catenin expression did not significantly correlate with survival (DSS and PFS had p>0.05).

	ESN	ESS	LMS	UUS	AS	CS
beta-catenin M/C (>30% positivity)	1/2 (50%)	31/35 (89%)	5/8 (63%)	5/9 (56%)	11/16 (69%)	3/3 (100%)
beta-catenin nuclear	0/2 (0%)	7/29 (24%)	1/8 (13%)	3/9 (30%)	2/16 (13%)	0/3 (0%)
CD10>30%	2/3 (66%)	12/30 (62%)	2/4 (50%)	3/9 (33%)	4/17 (24%)	2/3 (66%)

Conclusions: Nuclear beta-catenin staining is evident in a portion of LG-ESS, LMS, UUS and AS, but not in ESN and CS. A larger series of ESN, CS as well as HG-ESS will need to be added to substantiate these findings. As expected, CD10 did not discriminate between the different uterine mesenchymal tumors.

1054   ProMisE Molecular Classifier for Endometrial Carcinomas in a Saudi Arabian Population

Noorah Almadani[1], Jawaher Alsahabi[2], Amy Lum[3], Abdulmohsen Alkushi[4], Angela Cheng[5], Jessica McAlpine[6], Philip Clement[7], David Huntsman[8], Lynn Hoang[9], C. Blake Gilks[7]
[1]University of British Columbia/Vancouver General Hospital, Vancouver, BC, [2]King Abdulaziz Medical City - CR, Riyadh, Saudi Arabia, [3]British Columbia Cancer Research Centre, Vancouver, BC, [4]King Abdulaziz Medical City of National Guard, Riyadh, Saudi Arabia, [5]Genetic Pathology Evaluation Centre, Vancouver, BC, [6]University of British Columbia and BC Cancer Agency, Vancouver, BC, [7]Vancouver General Hospital, Vancouver, BC, [8]British Columbia Cancer Research Institute, Vancouver, BC, [9]University of British Columbia, Vancouver, BC

Disclosures: Noorah Almadani: None; Jawaher Alsahabi: None; Amy Lum: None; Abdulmohsen Alkushi: None; Jessica McAlpine: None; David Huntsman: *Stock Ownership*, Contextual Genomics Inc.; Lynn Hoang: None; C. Blake Gilks: None

Background: Endometrial carcinoma (EC) is the most common malignancy of the gynecological tract with increasing incidence and mortality rates world-wide and in Saudi Arabia. Inter-observer variability is a well known obstacle for accurate histopathological subtyping. Furthermore, histomorphological features may not reflect their biological behaviour.

The ProMisE (Proactive Molecular Risk Classifier for Endometrial Cancer) is an emerging, well-established molecular risk stratification system of EC based on The Cancer Genome Atlas (TCGA), and stratifies EC into 4 genomic subtypes: copy number low/p53 wild-type (p53 wt), copy number high/p53 abnormal (p53 abn), ultramutated/polymerase ε exonuclease domain mutated (*POLE* EDM), and hypermutated/mismatch repair deficient (MMR-D).

The molecular subtypes generated by this system can reliably discriminate EC into four different sub-groups that are clinically relevant to prognosis and management. Our goal was to determine if the ProMisE classifier could be applied to an independent population of Saudi Arabian patients.

Design: We assessed a retrospective cohort of 106 women from the King Abdulaziz Medical City diagnosed with EC between 2012 and 2018. Next generation sequencing (NGS) and immunohistochemistry (IHC) for MMR proteins and p53 was performed. Cases were stratified into ProMisE groups: MMR-D, *POLE* EDM, p53 wt and p53 abn, as previously described (PMID: 26172027). Clinical data were extracted from hospital files.

Results: The clinical and molecular findings are presented in Table 1.105 cases had complete IHC and NGS, allowing for ProMisE categorization as follows: MMR-D 24%, *POLE* EDM 8%, p53 wt 45%, p53 abn 22%. The majority of MMR-D cases were MLH1 and PMS2 deficient (24/25, 96%) and minority MSH6 deficient (1/25, 4%). 24 cases had abnormal p53 (23 in the p53 abn group, 1 in the MMR-D group). 9 cases had *POLE* mutations, 6 categorized under *POLE* EDM, and 3 under the MMR-D group. The *POLE* EDM group had the lowest age and lowest BMI. BMI was highest in the p53 wt group. The p53 wt group had the highest proportion of *PTEN*, *KRAS* and *CTNNB1* mutations. Amongst the 4 subgroups, there was a trend towards worse overall survival (Figure 1, *p*=0.47), and significant difference in progression free survival (Figure 2, *p*=0.03).

	N	Age	Body mass index (BMI)	*PTEN*	*KRAS*	*PIK3CA*	*CTNNB1*	Other
MMR-D	25 (24%)	65.7	40.8	5 (22%)	4 (17%)	10 (43%)	4 (17%)	*MAP2K1*=1, *ERBB2*=1
POLE EDM	6 (6%)	51.1	29.8	1 (16%)	0	2 (33%)	1 (16%)	*PDGFRA*=1 *ALK*=1
p53 wt	50 (47%)	62.3	44.4	14 (22%)	15 (23%)	21 (32%)	14 (21.8%)	*GNAS*=1 *MAP2K1*=1 *AKT*=1
p53 abn	24 (22%)	66.2	37.4	2 (25%)	1 (12%)	5 (62%)	0	

Figure 1 - 1054
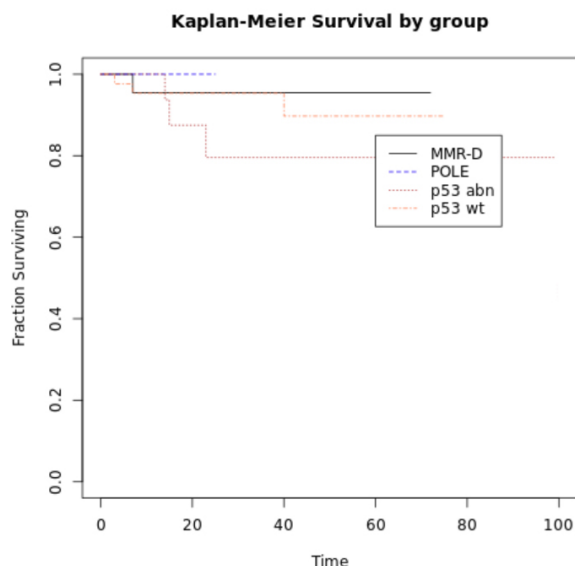
Figure 2 - 1054
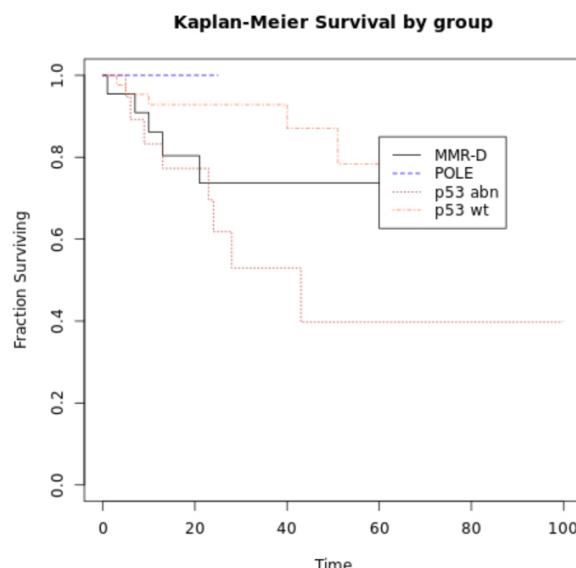
Conclusions: Molecular classification of EC using ProMisE can be applied to a Saudi Arabian population, resulting in comparable distributions and survival curves to that reported previously in North American cohorts.

1055 Invasive Endocervical Adenocarcinoma with Gastric and Intestinal Immunophenotype Correlates with Adverse Clinicopathological Features and Patient Outcome

Shiho Asaka[1], Tomoyuki Nakajima[2], Koichi Ida[3], Ryoichi Asaka[3], Tsutomu Miyamoto[4], Takeshi Uehara[4], Hiroyoshi Ota[5]
[1]Johns Hopkins University School of Medicine, Baltimore, MD, [2]Shinshu University Hospital, Matsumoto, Japan, [3]Shinshu University School of Medicine, Matsumoto, Nagano, Japan, [4]Shinshu University School of Medicine, Matsumoto, Japan, [5]Shinshu University School of Health Sciences, Matsumoto, Japan

Disclosures: Shiho Asaka: None; Tomoyuki Nakajima: None; Koichi Ida: None; Ryoichi Asaka: None; Tsutomu Miyamoto: None; Takeshi Uehara: None; Hiroyoshi Ota: None

Background: A system for classification of invasive endocervical adenocarcinomas (EAs) based on human papillomavirus (HPV) infection has been recently developed (IECC 2018). However, there are limited immunohistochemical markers for subcategorizing EAs, especially EAs with gastric and intestinal differentiation. We have previously shown that EAs in situ (AIS) lesions could be subcategorized into different immunophenotypes using three cell-lineage-specific markers: claudin 18 (CLDN18), gastric cells; cadherin 17 (CDH17), intestinal cells; PAX8, Müllerian epithelial cells. Each AIS immunophenotype showed distinct histopathological characteristics. Here, we subclassified EAs by their immunophenotype and analyzed the patient outcome.

Design: Sixty-six cases of EAs were immunohistochemically analyzed using CLDN18, CDH17, and PAX8. We defined each immunophenotype of EAs as follows: gastric-type (G), diffuse (≥50%) CLDN18 and negative or focal (<50%) CDH17 expression; intestinal-type (I), diffuse CDH17 and negative or focal CLDN18 expression; gastrointestinal-type (GI), diffuse CLDN18 and CDH17 expression; Müllerian-type (M), diffuse PAX8 and negative or focal CLDN18 and/or CDH17 expression, and not otherwise specified (NOS), negative or focal expression of all the three markers. High-risk HPV status was analyzed using RNA-ISH (RNAscope system).

Results: By conventional histology, 66 EAs were classified as 34 usual type (52%), 11 gastric type (17%), 8 iSMILE (12%), 8 mucinous, NOS (12%), and 5 intestinal type (8%). According to the immunophenotype, the cases were categorized as 23 M-type (35%), 15 G-type (23%), 12 NOS (18%), 9 I-type (14%), and 7 GI-type (11%). High-risk HPV was detected in most M- (91%), I- (89%), GI- (57%), and NOS- (83%) types but less frequently in G-type (27%). Compared with M-type, G-type was associated with aging (p=0.0068), negative for high-risk HPV (p<0.0001), concurrent LEGH (p=0.0060), high-grade histology (p=0.0054), advanced FIGO stage (p=0.0001), and lymph node and/or distant metastasis (p=0.0096). Multivariate analysis revealed that G- and GI+I-types were independent predictor of progression free survival (p=0.0007 and p=0.0140, respectively) compared with M-type.

No. of cases [No. of HPV+]	Immunophenotype					Total
Histology	M-type	G-type	GI-type	I-type	NOS	
Usual	16 [15]	4 [1]	3 [2]	6 [5]	5 [3]	34 [26]
Mucinous, NOS	4 [4]	1 [0]	1 [1]	1 [1]	1 [1]	8 [7]
Mucinous, Intestinal	0	1 [1]	2 [1]	2 [2]	0	5 [4]
iSMILE	2 [1]	0	0	0	6 [6]	8 [7]
Gastric	1 [1]	9 [2]	1 [0]	0	0	11 [3]
Total	23 [21]	15 [4]	7 [4]	9 [8]	12 [10]	66 [47]

Figure 1 - 1055

G-type vs. M-type   p = 0.0004
G-type vs. GI+I-type   p = 0.0440
NOS vs. M-type   p = 0.0021

p = 0.0010

Figure 2 - 1055

G-type vs. M-type   p < 0.0001
G-type vs. GI+I-type   p = 0.0034
GI+I-type vs. M-type   p = 0.0446
NOS vs. M-type   p = 0.0003

p < 0.0001
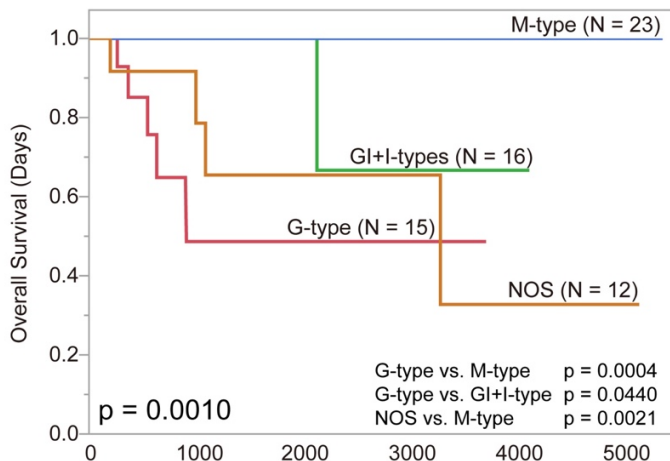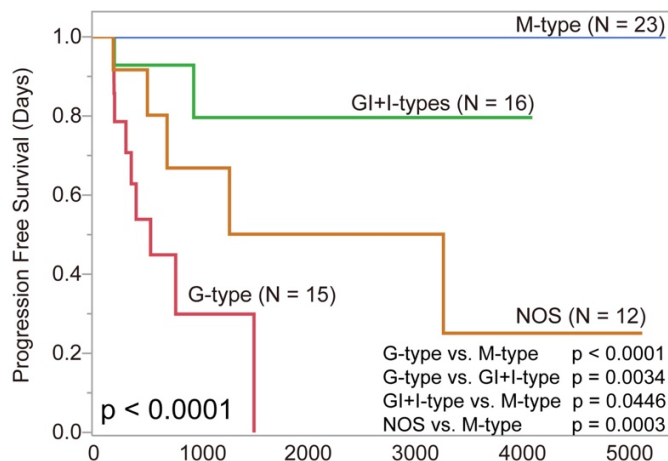
Conclusions: EAs with gastric and intestinal immunophenotype showed aggressive clinicopathological behaviors. Immunohistochemistry for gastric and intestinal phenotype in EAs may improve diagnostic accuracy and prognostic value of EA subtyping and histopathological classification.

1056 Telomere Length Alterations in Adenomyosis and Endometriosis

Shiho Asaka[1], Lihong Li[1], Christine Davis[2], Tian-Li Wang[3], Christopher Heaphy[1], Ie-Ming Shih[4]
[1]Johns Hopkins University School of Medicine, Baltimore, MD, [2]Johns Hopkins School of Medicine, Baltimore, MD, [3]Johns Hopkins Medical Institutions, Baltimore, MD, [4]Johns Hopkins Hospital, Baltimore, MD

Disclosures: Shiho Asaka: None; Lihong Li: None; Christine Davis: None; Tian-Li Wang: None; Christopher Heaphy: None; Ie-Ming Shih: None

Background: Adenomyosis and endometriosis are related gynecologic disorders common in reproductive-age women. Both lesions are characterized by the ectopic presence of normal-appearing endometrial tissue, including glands and surrounding stroma in myometrium and outside the uterine corpus, respectively. Their origins and the biological relationship to eutopic endometrium remains largely unknown. As telomere length can serve as a "molecular clock" and as a marker for the times of (stem) cell division, we analyzed telomere lengths in glandular epithelium and stroma within adenomyosis and endometriosis.

Design: We applied telomere-specific FISH assay to quantitatively measure telomere lengths of epithelial and stromal cells in 30 adenomyotic and 14 endometriotic lesions, and matched eutopic endometria from 42 women. We used the relative telomere length of the lesion compared with the matched eutopic endometrium from the same patient as the study outcome measure. Mann-Whitney test was used to determine the statistical significance (i.e., longer or shorter).

Results: In adenomyosis, 24 (80%) of 30 cases showed significant telomere shortening in epithelial cells, and 21 (70%) showed significant telomere shortening in stromal cells compared with matched eutopic endometria. No adenomyotic lesions showed significantly longer telomere than matched eutopic endometria. In contrast, in endometriosis, 2 (14%) of 14 cases showed significant telomere shortening in epithelial cells and 5 (36%) showed significant telomere shortening in stromal cells. Interestingly, 4 (29%) of 14 endometriotic lesions showed significantly longer telomeres in epithelial cells and 3 (21%) showed significantly longer telomeres in stromal cells. Both epithelial and stromal cells in endometriosis exhibited relatively longer telomere than those in adenomyosis (p=0.0005 and p=0.0678, respectively).

Case No. (%)	Adenomyosis		Endometriosis	
	Epithelium	Stroma	Epithelium	Stroma
Longer*	0 (0%)	0 (0%)	4 (29%)	3 (21%)
No significant change*	6 (20%)	9 (30%)	8 (57%)	6 (43%)
Shorter*	24 (80%)	21 (70%)	2 (14%)	5 (36%)
Total	30	30	14	14
*Telomere length alteration compared with the matched eutopic endometrium from the same patient by Mann-Whitney test (p<0.05 was considered statistically significant).				

Figure 1 - 1056
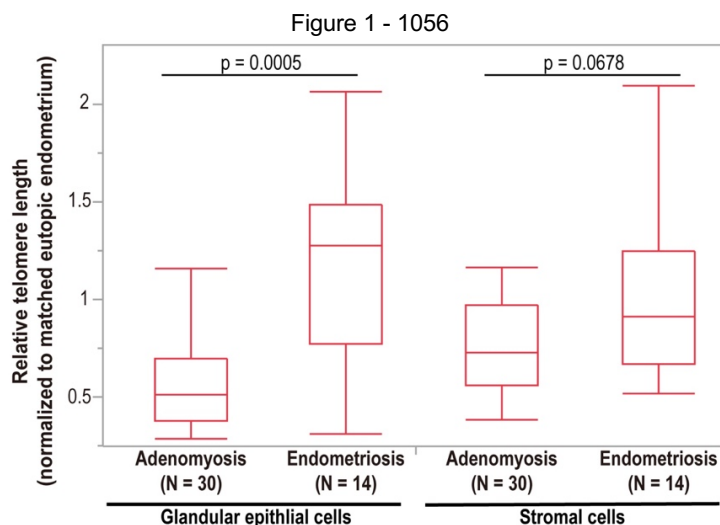
Conclusions: Although adenomyosis and endometriosis are thought to be etiologically related to each other, our new data demonstrate that they are molecularly different at least from the perspective of telomere lengths. The significantly shortened telomeres in adenomyosis as compared to its eutopic endometrium suggests that more cell divisions have occurred in the progenitor or stem cells that are responsible for generating adenomyosis. This new study suggests a new research direction to explore the pathobiology of adenomyosis which has not been well studied in the past.

1057 Minimal Uterine Serous Carcinoma with Concurrent Endometrial Polyp: An Institutional Reappraisal

Hisham Assem[1], Natalia Buza[2], Douglas Rottmann[3], Nana Matsumoto[4], Serena Wong[4], Pei Hui[2]
[1]Yale School of Medicine, New Haven, CT, [2]Yale University School of Medicine, New Haven, CT, [3]Yale School of Medicine, Hamden, CT, [4]Yale New Haven Hospital, New Haven, CT

Disclosures: Hisham Assem: None; Natalia Buza: None; Douglas Rottmann: None; Nana Matsumoto: None; Serena Wong: None; Pei Hui: None

Background: Minimal uterine serous carcinoma (MUSC) includes serous endometrial intraepithelial carcinoma (SEIC) and superficial invasive serous carcinoma. Such lesions frequently involve an endometrial polyp (EMP) in postmenopausal women. While non-invasive or minimally invasive, both types of MUSC can present with extrauterine tumor spread, leading to a dismal clinical prognosis. Recently it was also suggested that a subset of MUSC involving an EMP may represent a distinct subtype of endometrial serous carcinoma capable of aggressive behavior. The aim of this study was to summarize our institutional experience by correlating the morphological features of MUSC involving EMP with extrauterine tumor spread/tumor stage.

Design: Patients who underwent staging hysterectomy with a diagnosis of endometrial serous carcinoma with concurrent presence of an EMP between 2004-2019 were retrospectively identified. Cases with myometrial invasion were excluded. H&E slides were reviewed to confirm diagnosis and to assess the extent of tumor involvement (EMP and endometrium) and the scope of tumor spread. Immunohistochemistry results for p53, p16, WT1 were also retrospectively reviewed.

Results: A total of 84 cases were identified. 83 (98.8%) of these MUSC cases involved an EMP, including 53 cases of polyp confined tumors and 30 cases of tumors involving an EMP combined with SEIC involving the endometrium. Only one case of SEIC with a benign endometrial polyp was identified. Among cases confined to an endometrial polyp, 20.8% (11/53 cases) demonstrated extrauterine involvement compared to 46.7% (14/30 cases) of cases involving both an EMP and the surrounding endometrium (X^2 (1, N = 83) =

6.1, *p* = 0.013). No differences in expression of p53, p16 and WT-1 immunohistochemistry were observed in cases with available immunostains (Table 1).

	MUSC - Polyp Confined (N=53)	MUSC - Not Polyp Confined (N=30)
Extrauterine Disease	11/53	14/30
p53 (mutant)	47/47	18/19
p16 (diffusely positive)	15/15	7/7
WT1 (negative)	7/9	3/5

Table 1: Extrauterine disease and immunohistochemistry observed for p53, p16 and WT1 in cases with available immunostains

Conclusions: This is the largest series examining minimal uterine serous carcinoma presenting with concurrent EMP. An EMP was involved by minimal uterine serous carcinoma in essentially all cases in this study, suggesting that EMP in postmenopausal endometrium may provide a strong microenvironment for the development of uterine serous carcinoma. More importantly, cases of MUSC involving an EMP with simultaneous endometrial involvement have a significantly higher risk to present with extrauterine disease compared to cases of MUSC confined to an EMP, implying careful pathological examination and reporting is essential for risk assessment and prognosis.

1058   MLH1 Loss due to MLH1 Gene Methylation Predicts Worse Survival in Stage I Endometrial Endometrioid Adenocarcinoma

Monica Avila[1], Bryan Fellman[1], Russell Broaddus[2]
[1]The University of Texas MD Anderson Cancer Center, Houston, TX, [2]University of North Carolina School of Medicine, Chapel Hill, NC

Disclosures: Monica Avila: None; Bryan Fellman: None; Russell Broaddus: None

Background: In contrast to other common cancers, the annual mortality from endometrial cancer is increasing. There are few reliable biomarkers to identify early stage patients at risk for recurrence who might benefit from adjuvant therapy. This is a clinically important gap in knowledge, as many endometrial cancer recurrences outside the vaginal cuff are incurable. Mismatch repair deficiency secondary to *MLH1* gene methylation and subsequent loss of MLH1 protein is one of the most common molecular events in endometrioid endometrial carcinoma, occurring in 15-20% of cases. We and others have shown that MLH1 loss is associated with worse survival across all stages. The objective of this study was to determine if MLH1 loss due to *MLH1* methylation is associated with increased risk of recurrence in stage I endometrial cancer patients.

Design: The cohort included 515 endometrial endometrioid carcinoma patients who were screened for Lynch Syndrome by immunohistochemistry testing for mismatch repair deficiency (MMRd). MMRd for this study was defined as loss of MLH1 expression due to *MLH1* gene methylation. Intact mismatch repair (MMRi) was defined as positive expression of mismatch repair proteins. For stage I patients, review of the electronic medical records was performed to determine which received adjuvant radiation therapy. Recurrence-free survival (RFS) and overall survival (OS) were estimated using Kaplan Meier and Cox regression. Median follow-up was 48 months.

Results: Of the 373 stage I patients, 62 (17%) were MMRd and 311 (83%) were MMRi. 32% of stage I patients received some type of adjuvant radiation therapy based on usual clinical and pathological parameters. Multivariate analysis demonstrated that MMRd was associated with significantly worse RFS and OS in the stage I patients. Multivariate analysis did not reveal a survival benefit of adjuvant radiation treatment. The MMRd patients who did not receive adjuvant therapy had the worst RFS (Figure 1).

Figure 1 - 1058

Figure 1A. Recurrence-free Survival by Mismatch Repair and Adjuvant Therapy Status
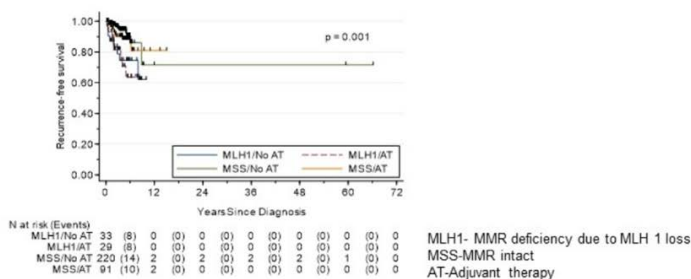
Figure 1B. Overall Survival by Mismatch Repair and Adjuvant Therapy Status
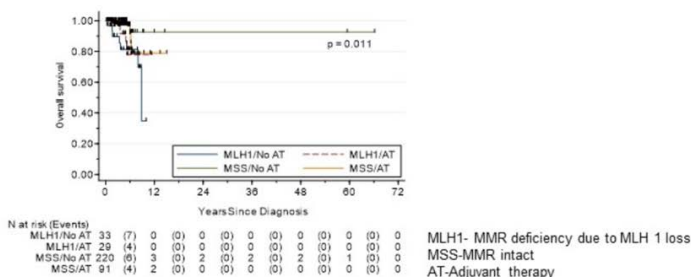
Conclusions: In this stage I cohort, patients with endometrial cancers with *MLH1* hypermethylation had increased risk of recurrence and decreased overall survival regardless of whether or not they received adjuvant radiation therapy. These data suggest that alternative adjuvant therapies should be explored for stage I patients with MLH1 tumor loss. One possibility is prospective trials of checkpoint inhibitors, which are FDA-approved for endometrial cancer patients with advanced disease that is MMR deficient.

1059 Quantification of Primary Tumor-Associated CD3+ Lymphocytes Out-Performs Mismatch Repair Deficiency in Predicting Recurrence in Endometrioid-Type Endometrial Carcinoma

Monica Avila[1], Bryan Fellman[1], Suzanne Crumley[2], Courtney Hudgens[1], Michael Tetzlaff[1], Russell Broaddus[3]
[1]The University of Texas MD Anderson Cancer Center, Houston, TX, [2]Houston Methodist Hospital, Houston, TX, [3]University of North Carolina School of Medicine, Chapel Hill, NC

Disclosures: Monica Avila: None; Bryan Fellman: None; Suzanne Crumley: None; Courtney Hudgens: None; Michael Tetzlaff: *Speaker*, Nanostring; *Advisory Board Member*, Novartis LLC; *Advisory Board Member*, Myriad Genetics; *Advisory Board Member*, Seattle Genetics; Russell Broaddus: None

Background: In contrast to other common cancers, the annual mortality from endometrial cancer is increasing. The reasons for this are multifactorial, but one important knowledge gap is that there are few reliable biomarkers that identify early stage patients at risk for recurrence. Mismatch repair deficient (MMRd) endometrial cancers are associated with higher numbers of tumor-associated lymphocytes, but the clinical significance of this observation is unknown. Our objective was to quantify CD3+ and CD8+ lymphocytes in different regions of MMR intact (MMRi) and MMRd endometrioid-type endometrial carcinomas and determine if these counts were associated with survival.

Design: MMR status was determined by immunohistochemistry. MMRd was defined as endometrial carcinomas with loss of MLH1 expression due to *MLH1* gene methylation. MMRi was defined as positive expression of MLH1, MSH2, MSH6, and PMS2. Immunohistochemistry followed by Aperio image-based quantification was used to assess CD3+ and CD8+ lymphocyte populations in different regions of the primary endometrial carcinomas, including tumor periphery (tumor-myometrial interface), tumor center (bounded on all sides by tumor), and tumor hotspot (area with highest number of lymphocytes). Recurrence-free survival was estimated using Kaplan Meier and Cox regression. Median follow up time was 44 months.

Results: 180 endometrioid grade 2 carcinomas were analyzed, 48 MMRd and 132 MMRi. The MMRd group had significantly higher levels of CD3+ and CD8+ lymphocytes regardless of which tumor region was assessed. Lymphocyte counts in both MMRd and MMRi groups had wide standard deviations such that there was some overlap in counts between the groups (Figure 1). Both MMRd and higher

CD3+ counts were associated with worse recurrence-free survival. However, quantification of CD3+ in the tumor periphery captured 21/23 recurrences which included all of the MMRd cases that recurred and 7 MMRi cases with higher numbers of CD3+ lymphocytes that also recurred. MMRd by itself only captured 14/23 recurrences.

Figure 1 - 1059

Figure 1A. Box Plot of CD3+ & CD8+ Lymphocyte Distribution in MMR Deficient Cohort
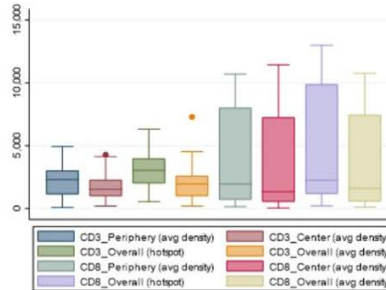
Figure 1B. Box Plot of CD3+ & CD8+ Lymphocyte Distribution in MMR Intact Cohort
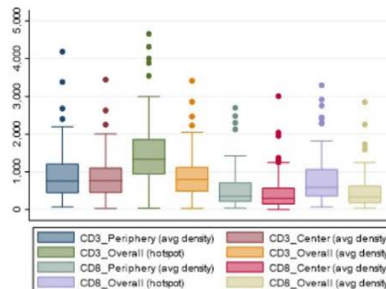
Conclusions: Patients with MMRd endometrial cancers have higher numbers of CD3+ lymphocytic infiltrates within the primary tumor. Irrespective of tumor region, higher CD3+ infiltration is associated with greater risk of recurrence. In predicting tumor recurrence, lymphocytic quantification performed better than assessment of MMR. Thus, quantification of CD3+ lymphocytes should be explored as a clinically relevant biomarker.

1060 Evaluation of Saccharomyces Cerevisiae-Like 1 (SEC14L1) in Gynecologic Malignancies Shows Over-Expression in Endometrial Serous Carcinoma

Natalie Banet[1], Max Masnick[2], M. Ruhul Quddus[3]
[1]Women and Infants Hospital/Brown University, Providence, RI, [2]Geisinger National Precision Health, Rockville, MD, [3]Women & Infants Hospital/Alpert Medical School of Brown University, Providence, RI

Disclosures: Natalie Banet: None; Max Masnick: None; M. Ruhul Quddus: None

Background: Lymph-vascular invasion is a known prognostic factor in varied gynecologic malignancies. Saccharomyces Cerevisiae-Like 1 (SEC14L1), a cytosolic regulator of lipid metabolism, has been identified in breast cancer as a significant gene associated with lymph-vascular invasion, though its precise function in tumorgenesis is unknown. This gene has not been characterized in gynecologic malignancies.

Design: A total of 116 cases from 100 patients were included, to include nine different tumors (see Table 1) and were subjected to immunohistochemical staining for SEC14L1 (Thermo Fisher, PA5-54415). Cytoplasmic expression was scored by intensity and percentage positivity. These results were multiplied to generate an H score. Pertinent clinical variables, including stage and outcome data were collected from the patient files. Slides were reviewed for verification of tumor type and presence or absence of lymph-vascular invasion.

Results: Similar to prior studies, an H score greater than 80 was considered positive; 30% of cases with follow-up were positive. No association was found between positive H score and progression-free survival using the log-rank test for equality in Kaplan-Meier survival estimates. Insufficient follow-up was available to conduct overall survival analysis. No significant relation was noted to lymph-vascular

invasion status, tumor size, patient age, or lymph node status. However, mean H scores were substantially higher in Uterine Serous Carcinoma (mean 181.7; SD 83.0) compared to other 8 tumor types (mean 43.0; SD 61.4; p<0.0001), as noted in Table 1.

Tumor type	# cases	SEC14L1 Expression (H Score)		Positive* (n, %)	
		Mean	SD		
Adenosarcoma	5	24	53.7	1	(20.0)
Clear cell carcinoma	11	42.7	45.4	1	(9.1)
Endometrial Stromal Sarcoma	11	12.7	25.7	0	-
Endometrioid Carcinoma	31	68.7	78.3	8	(25.8)
High-grade serous carcinoma, ovary	21	48.7	60.2	4	(19.1)
Leiomyosarcoma	9	11.7	17.7	0	-
Low-grade serous carcinoma	5	6	8.9	0	-
Malignant Mixed Mullerian Tumor/ Carcinosarcoma	11	41.4	64.2	2	(18.2)
Serous carcinoma, endometrium	12	181.7	83	9	(75.0)
Positive is defined as H Score > 80					

Conclusions: Overall, in this survey of Gynecologic malignancies, SEC14L1 appears to not show a relation to progression-free survival. However, its over-expression in uterine serous carcinoma warrants further investigation in a larger cohort as a potential prognostic or therapeutic target.

1061 Unusual Adnexal Tumors with Recurring STK11 Mutations: A Clinicopathological Study of 11 Cases Including 4 in Patients with Peutz-Jeghers Syndrome

Jennifer Bennett[1], Emily Meserve[2], Brooke Howitt[3], Lauren Ritterhouse[4], John Schoolmeester[5], Sabrina Croce[6], Loes Kooreman[7], Mona El-Bahrawy[8], Gian Franco Zannoni[9], Thomas Krausz[10], W. Glenn McCluggage[11], Robert Young[12], Esther Oliva[4]
[1]The University of Chicago, Chicago, IL, [2]Spectrum Healthcare Partners, Falmouth, ME, [3]Stanford University School of Medicine, Stanford, CA, [4]Massachusetts General Hospital, Harvard Medical School, Boston, MA, [5]Rochester, MN, [6]Institut Bergonié, Bordeaux, France, [7]MUMC, Maastricht, Limburg, Netherlands, [8]Imperial College London, London, United Kingdom, [9]Catholic University of Sacred Heart, Rome, Italy, [10]University of Chicago Hospital, Chicago, IL, [11]The Royal Hospitals, Belfast, United Kingdom, [12]Harvard Medical School, Boston, MA

Disclosures: Jennifer Bennett: None; Emily Meserve: None; Brooke Howitt: None; Lauren Ritterhouse: None; John Schoolmeester: None; Sabrina Croce: None; Loes Kooreman: None; Mona El-Bahrawy: None; Gian Franco Zannoni: None; Thomas Krausz: None; W. Glenn McCluggage: None; Robert Young: None; Esther Oliva: None

Background: *STK11* mutations have recently been described in a small subset of presumed female adnexal tumors of probable wolffian origin (FATWO); however, they lack the classic morphology of FATWOs.

Design: We evaluated the morphology, immunoprofile, and molecular phenotype of 11 tumors identified in part because of an association with Peutz-Jeghers syndrome (PJS) and in part because of uncertainty concerning their specific nature.

Results: Patients, 4 with PJS, ranged from 25 to 66 (mean 44) years. Tumors ranged from 4.5 to 22 (mean 13) cm. Tumors were paratubal (8), ovarian (2), or pelvic (1) with extra-adnexal disease in 5. Follow-up was available for 9 with 2 alive and well, 4 alive with disease, 1 dead of disease, and 2 dead from other causes.

Tumors were comprised of variably anastomosing trabeculae, irregular or regularly disposed cords, and anastomosing nests sometimes associated with tubular (9), papillary (3), or solid (2) growth(s). Tubules were often distended by basophilic (rarely eosinophilic) material. A loose myxoid to edematous background was striking in 9 tumors. Cells were small (n=3) to medium (n=8) with round to ovoid nuclei, minimal pleomorphism, prominent nucleoli, and scattered nuclear grooves. Tumors had clear to eosinophilic, vacuolated cytoplasm. Nuclear to cytoplasmic ratio was increased in 8 tumors and mitoses ranged from 2 to 24 (mean 10) per 10 HPF. Immunohistochemical results are summarized in the table. Pathogenic *STK11* mutations were identified in 8 of 9 tumors with available molecular results, while 1 had a variant of uncertain clinical significance. No other pathogenic variants were identified. No statistical difference in age, tumor size, extra-adnexal disease at presentation, or tumor recurrences was found between PJS-associated and sporadic tumors.

Case	Cytokeratin	Claudin4	EMA	MOC31	Calretinin	Inhibin	SF1	CD10	ER	PAX8	GATA3	*STK11* Variant
1	++	-	+	+	++	+	-	+	+	+	-	p.Y272*
2	++	-	+	-	++	+	-	+	++	-	-	p.L201Cfs*86
3	++	NP	-	NP	++	+	-	++	++	-	-	c.734+1G>A
4	++	NP	+	NP	++	++	-	+	++	-	NP	p.E145Gfs*10
5#	++	NP	-	NP	++	+	NP	+	NP	NP	NP	p.P281Rfs*6
6#	NP	-	+	-	++	+	NP	NP	++	-	NP	p.G163R
7#	++	-	+	-	++	-	-	-	NP	-	+	p.G187S (VUS)
8#	+	-	-	+	++	-	-	++	++	NP	NP	p.K84*
9	NP	NP	-	NP	++	+	NP	+	+	-	-	Pending
10	NP	NP	NP	NP	NP	NP	NP	NP	NP	NP	NP	Pending
11	++	NP	+	-	++	+	+	+	++	-	NP	p.F255Sfs*32

- = negative, + = focal (<50%), ++ = diffuse (>50%), NP = not performed, # = patient has PJS, VUS = variant of uncertain significance

Conclusions: We describe a series of adnexal tumors with *STK11* variants that show characteristic morphological and immunohistochemical features that differ from surface epithelial (negative claudin-4, focal EMA/MOC31), sex cord (negative SF1), typical FATWO (negative SF1), and mesothelial (negative/focal EMA, positive ER/inhibin) tumors. They also lack mutations common to the above entities. Thus, we propose the name *STK11*-mutated adnexal tumor to classify these neoplasms, a subset being associated with PJS. Their histogenesis is elusive at this time.

1062 Embryonal Rhabdomyosarcomas of the Uterine Corpus: A Clinicopathological Study of 13 Tumors

Jennifer Bennett[1], Zehra Ordulu Sahin[2], Andre Pinto[3], Eike-Christian Burandt[4], Leanne de Kock[5], William Foulkes[5], W. Glenn McCluggage[6], Robert Young[7], Lauren Ritterhouse[8], Esther Oliva[8]
[1]The University of Chicago, Chicago, IL, [2]Massachusetts General Hospital, Dorchester, MA, [3]University of Miami, Miami Beach, FL, [4]University Medical Center Hamburg-Eppendorf, Hamburg, Germany, [5]McGill University, Montreal, QC, [6]The Royal Hospitals, Belfast, United Kingdom, [7]Harvard Medical School, Boston, MA, [8]Massachusetts General Hospital, Harvard Medical School, Boston, MA

Disclosures: Jennifer Bennett: None; Zehra Ordulu Sahin: None; Andre Pinto: None; Eike-Christian Burandt: None; Leanne de Kock: None; William Foulkes: None; W. Glenn McCluggage: None; Robert Young: None; Lauren Ritterhouse: None; Esther Oliva: None

Background: Primary embryonal rhabdomyosarcomas of the uterine corpus (ERMS-UC) are rare with fewer than 20 reported. While ERMS are more common in the cervix, where they are often associated with *DICER1* mutations, in both locations, they may be confused with adenosarcomas due to overlapping features including periglandular cuffing and heterologous elements.
While *DICER1* mutations, *HMGA2* amplifications, and alterations in the *PIK3CA* pathway may be seen in adenosarcomas, the molecular landscape of ERMS-UC has not been studied.

Design: We evaluated clinical, morphological, immunohistochemical, and molecular features of 13 ERMS-UC.

Results: Patients ranged from 28-70 (mean 51) years and follow-up was available for 9 with 5 alive and well and 4 dead of disease. Tumors ranged from 4-15 (mean 9) cm and 4 extended to the lower uterine segment, 1 to the serosa, and 1 to the ovary.

On low power, destructive invasion was seen in 9, while 3 had minimal invasion, and 1 was endometrial confined. Alternating hypercellular/hypocellular foci dominated in 7 whereas 6 showed primarily diffuse growth. A cambium layer was noted in 9 and stroma varied from myxoid/edematous to loosely collagenous. Inactive entrapped glands lacking metaplasia were present in 11, focal periglandular cuffing in 10, minimal phyllodes architecture in 3, and rare intraglandular projections in 2. Heterologous elements including fetal-type cartilage in 7 or neuroectoderm in 1 were noted. Most (50-100%) of each tumor was comprised of primitive cells with round to ovoid nuclei, coarse to vesicular chromatin, and scant cytoplasm, while rhabdomyoblasts and tadpole cells were less frequent. Anaplasia was noted in 8 with minor foci resembling spindle cell or alveolar rhabdomyosarcoma in 6 and 2 tumors, respectively. Mitoses ranged from 4-65 (mean 23) per 10 HPF with atypical forms in 3 and brisk apoptoses in 8.

All tumors tested expressed myogenin (3/9 diffuse), myoD1 (1/7 diffuse), and desmin (8/9 diffuse). *DICER1* mutations were detected in 6/9, *TP53* in 5/8, and *KMT2D* in 2/8 (Figure 1). Germline data was available in 2 (45 and 47 years), but neither harbored a *DICER1* mutation. ERMS-UC with *DICER1* mutations were younger (p=0.024) and more commonly had heterologous elements (p=0.048).

Figure 1 - 1062

	1	2	3	4	5	6	7	8	9
DICER1	Missense	Nonsense*	Frameshift*	Missense*		Missense*	Nonsense*	Frameshift	
TP53	Splicing				Missense*	Missense*		Missense*	Missense*
KMT2D							Frameshift	Nonsense	
KRAS				Missense*					
PIK3CA							Missense*		
ARID4A									Frameshift
PPP2R1A									Missense
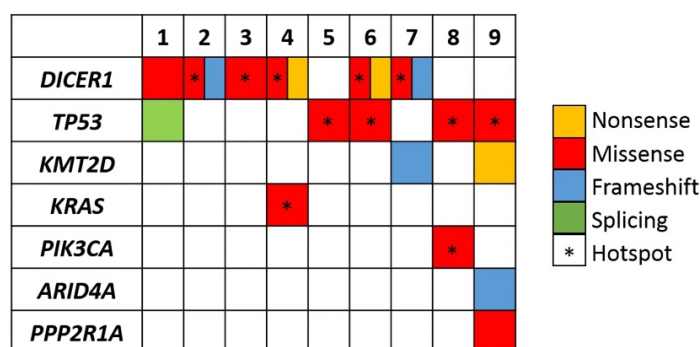
Legend:
- Nonsense (Yellow/Orange)
- Missense (Red)
- Frameshift (Blue)
- Splicing (Green)
- * Hotspot

Conclusions: ERMS-UC show similar clinicopathological features as their cervical counterparts, but typically occur in older females. Although in our small cohort *DICER1* mutations appear sporadic, it is important to recognize this entity and recommend genetics testing.

1063 Inflammatory Myofibroblastic Tumor of the Uterus: An Immunohistochemical Study of 22 Cases

Jennifer Bennett[1], Sabrina Croce[2], Anna Pesci[3], Eike-Christian Burandt[4], Eric Burks[5], Gian Franco Zannoni[6], Joseph Rabban[7], Esther Oliva[8]
[1]The University of Chicago, Chicago, IL, [2]Institut Bergonié, Bordeaux, France, [3]IRCCS Ospedale Sacro Cuore Don Calabria, Negrar, Verona, Italy, [4]University Medical Center Hamburg-Eppendorf, Hamburg, Germany, [5]Boston University Mallory Pathology Associates, Boston, MA, [6]Catholic University of Sacred Heart, Rome, Italy, [7]University of California San Francisco, San Francisco, CA, [8]Massachusetts General Hospital, Harvard Medical School, Boston, MA

Disclosures: Jennifer Bennett: None; Sabrina Croce: None; Anna Pesci: None; Eike-Christian Burandt: None; Eric Burks: None; Gian Franco Zannoni: None; Joseph Rabban: *Employee*, Spouse is an employee of Merck & Co.; Esther Oliva: None

Background: Inflammatory myofibroblastic tumors (IMT) of the uterus often express desmin, caldesmon, and CD10, which may cause diagnostic confusion with smooth muscle and stromal tumors. Transgelin, a new smooth muscle marker, has shown high sensitivity and specificity distinguishing between uterine smooth muscle and stromal tumors while IFITM1, a new endometrial stromal marker, appears to be more sensitive than CD10 differentiating between stromal and smooth muscle neoplasms. In a recent study, abnormal p53 and p16 expression was described in uterine leiomyosarcomas, but not IMTs, and hence, proposed as useful markers in the differential diagnosis. Herein we evaluate a series of uterine IMTs for IFITM1 and transgelin, and further explore their reactivity for p53 and p16.

Design: We stained 22 uterine IMTs, including 4 with aggressive behavior, for IFITM1, transgelin, p53, and p16. IFITM1 was scored for both intensity (0-3) and distribution (0-3) with a combined score >2 considered positive, transgelin as negative, focal (<50% staining), or diffuse (>50%), and p53/p16 as wildtype or abnormal (strong/diffuse or negative).

Results: Patients ranged from 8 to 59 (mean 40) years and tumors from 2 to 20 (mean 7) cm. Follow-up was available in 16 (73%) with 13 (81%) alive and well (1 with a prior recurrence), 2 (13%) alive with disease, and 1 (6%) dead of disease. IFITM1 had a positive combined score in 16 (73%) of IMTs, with most showing no difference in staining intensity or distribution between compact and myxoid patterns. In tumors where CD10 (n=13) was previously performed, it was concordant with IFITM1 in 12 (92%). Transgelin was positive in 21 (95%; 10 focal, 11 diffuse) of IMTs with the staining distribution by histological pattern highly variable. p53 was wildtype in all tumors whereas p16 was abnormal in 9 (43%; 4 negative, 5 strong and diffuse) IMTs. Notably, all 4 aggressive tumors were p16 negative.

Conclusions: Transgelin and IFITM1 are expressed in most IMTs and thus are not useful markers in differentiating these tumors from smooth muscle and stromal neoplasms. Unlike a prior study, we found abnormal p16 expression in 43% of uterine IMTs, which argues against the use of this marker in the distinction from smooth muscle tumors. Interestingly, all aggressive IMTs in this series were negative for p16 in contrast to patchy or diffuse staining in benign tumors, which could potentially be used as a prognostic marker if corroborated by other studies.

1064 ALK Immunoexpression in Vulvar Low Grade Myxoid Mesenchymal Neoplasms is Specific for Inflammatory Myofibroblastic Tumor

Christopher Bowman[1], Ankur Sangoi[2], Fabiola Medeiros[3], Walter Devine[4], Andrew Horvai[1], Joseph Rabban[1]
[1]University of California San Francisco, San Francisco, CA, [2]El Camino Hospital, Mountain View, CA, [3]Cedars-Sinai Medical Center, Los Angeles, CA, [4]University of California San Francisco, Berkeley, CA

Background: Inflammatory myofibroblastic tumor (IMT) of the uterus has recently been acknowledged to be under-recognized in several studies that retrospectively examined ALK immunohistochemistry in smooth muscle tumors of uncertain malignant potential (STUMP) and myxoid smooth muscle neoplasms.   Recognition of uterine IMT is important as some have adverse behavior and targeted therapy is available. In the vulva, a diverse array of mesenchymal tumors may exhibit low-grade morphology and/or myxoid extracellular matrix.   This study used ALK immunostaining to examine the possibility of under-recognized IMT among vulvar mesenchymal tumors.

Design: ALK immunostaining (Leica, Clone 5A4) was performed on 72 primary vulvar mesenchymal tumors with myxoid or low-grade morphology. Cytoplasmic staining for ALK in the tumor cells was considered a positive result. To confirm a positive ALK IHC result, *ALK* gene rearrangement testing was performed by break-apart fluorescence *in situ* hybridization (FISH).

Results: One vulvar mass that was initially suspected to be IMT (3 cm, circumscribed, without atypia, mitosis or necrosis) demonstrated diffuse, strong ALK staining and *ALK* gene rearrangement by FISH. ALK staining was completely negative in all other vulvar tumors: 8 leiomyoma, 2 STUMP, 12 aggressive angiomyxoma, 3 superficial angiomyxoma, 3 superficial myofibroblastoma, 8 angiomyofibroblastoma, 6 cellular angiofibroma, 1 cutaneous angiofibroma, 19 fibroepithelial polyps, 1 myxoid low-grade endometrial stromal sarcoma, 7 neurofibroma, 1 plexiform schwannoma, and 1 vulvar prepubertal fibroma. The sensitivity and specificity of ALK staining for vulvar IMT was 100%.

Conclusions: ALK staining is a sensitive and specific test to distinguish IMT from a diverse spectrum of low-grade myxoid mesenchymal tumors of the vulva. Though primary vulvar IMT is rare (this is the first report of such a case), the diagnosis merits consideration given the availability of targeted therapy for advanced stage or recurrent disease.

1065 Tubal p53 Signatures in Li-Fraumeni Syndrome (LFS) are Geographically Unique, Multi-Clonal and Temporally Dynamic

Jan Brouwer[1], Ju-Yoon Yoon[2], Jingzhong Xie[3], Sarah Hill[4], Wa Xian[5], Christopher Crum[6]
[1]University of Groningen, Groningen, Netherlands, [2]Perelman School of Medicine at the University of Pennsylvania, Philadelphia, PA, [3]University of Houston, Houston, TX, [4]Brigham and Women's Hospital, [5]University of Texas Health Science Center, [6]Brigham and Women's Hospital, Boston, MA

Background: Li-Fraumeni syndrome, with a germ-line TP53 mutation, is susceptible to clonal TP53 inactivating mutations in the FT resulting in p53 signatures. This study addressed three questions relevant to the biology of p53 signatures including 1) their clonality, 2) distribution in the FT and 3) change in frequency over time.

Design: FTs from four cases of LFS were studied. To determine geographic distribution of clonal TP53 mutations events, DNA from p53 signatures in three separate regions from one FT was subjected to ion torrent NGS and the mutational burden analyzed for regional differences. Regional variations in distribution of p53 signatures per se were evaluated by mapping frequency of p53 immuno-positive foci into inner (luminal), middle and outer third of a cross section and fimbria (Fig 1). p53 signatures were recorded and the number(s) of p53+ nuclei counted. An analysis of temporal changes in frequency of p53 signatures was determined in a single case in which right and left tubes were removed at different times over a span of 10 years.

Results: Sequencing of TP53 mutations in one case confirmed the germ-line mutation (c.A643G). Different somatic mutations were identified in sites 1 (c.1083delG & c.254delC), 2 (c.304delA), and 3 (c.1083delG) confirming multiple unique genotoxic events. In the second analysis, the number of p53 signatures per section was markedly higher in the outer 1/3 of the cross sections and in the fimbria. The mean number of cells per p53 signature varied across all regions. However, the number of p53 signatures with high numbers of p53 positive cells was significantly higher in the outer 1/3 relative to all other regions (p = .0001) and to the inner and middle 1/3 of the tubes (p = .0097)(Fig 2). Analysis of two fallopian tubes from the same patient disclosed a dramatically higher number of p53 signatures in the second tube removed 10 years after the first.

Figure 1 - 1065
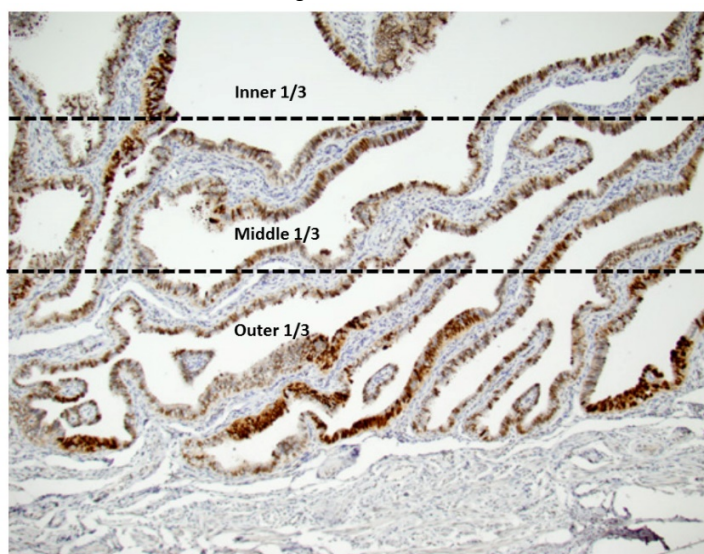
Figure 2 - 1065
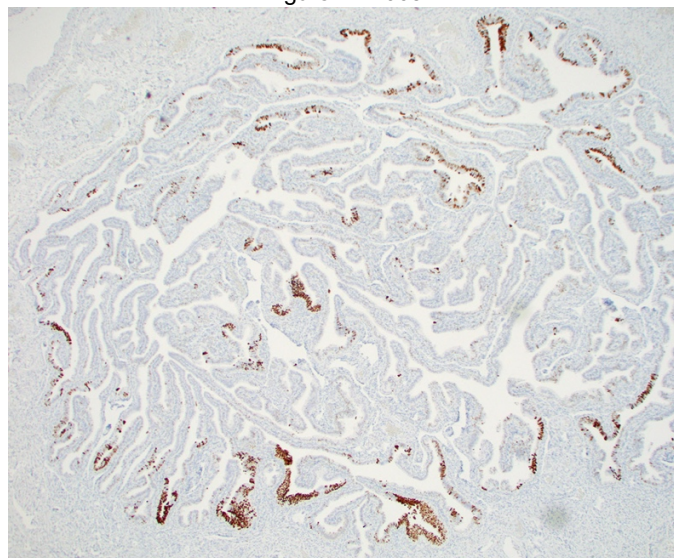
Conclusions: P53 signatures in fallopian tubes of women with LFS are genetically independent events. The outer one third of the fallopian tube as well as the fimbria harbor a significantly higher proportion of p53 signatures. This could reflect a higher proportion of susceptible cells (non-ciliated) as well as the possibility that the peripheral 1/3 of the endosalpinx contains cells with greater capacity for cell division. The higher number of p53 signatures in the second tube years later in one case suggests that genotoxic injury accumulates in the tube over time during the reproductive years.

1066 Assessment of Progestin Therapy Response Potential in Grade 2 Endometrial Endometrioid Carcinoma

Aurelia Busca[1], Ekaterina Olkhov-Mitsel[2], Yutaka Amemiya[3], Jelena Mirkovic[4], Carlos Parra-Herran[4], Arun Seth[4], Bojana Djordjevic[5]
[1]EORLA- University of Ottawa, Ottawa, ON, [2]Sunnybrook Health Sciences Centre, Toronto, ON, [3]Sunnybrook Research Institute, Toronto, ON, [4]Sunnybrook Health Sciences Centre, University of Toronto, Toronto, ON, [5]University of Toronto, Toronto, ON

Disclosures: Aurelia Busca: None; Ekaterina Olkhov-Mitsel: None; Yutaka Amemiya: None; Jelena Mirkovic: None; Carlos Parra-Herran: None; Arun Seth: None; Bojana Djordjevic: None

Background: Progestin treatment is a known fertility sparing strategy for low grade endometrial lesions (LGELs) such as atypical hyperplasia and FIGO grade 1 endometrial endometrioid carcinoma. FIGO grade 2 endometrioid carcinoma (EEC2) is currently treated surgically. There are isolated case reports of successful progestin treatment of patients with EEC2, suggesting that hormonal treatment may be a viable option if the responsive patients could be correctly identified. We have previously demonstrated that LGELs with complete (CR), partial (PR) and no response (NR) to progestin therapy have different genomic and transcriptome profiles. In the current project, we sought to compare the transcriptome profile of CR and NR lesions with that of EEC2.

Design: 20 consecutive cases of EEC2 underwent whole transcriptome profiling (stages T1a=11, T1b=4, T2=4 and T3b=1, LVI in 35%). We previously identified 119 genes which were differentially expressed between pre-progestin treatment samples of CR and NR LGEL cases (P≤0.05, >2-fold change). RNA expression data was subjected to unsupervised hierarchical clustering algorithm to compare the expression of these genes in EEC2 relative to CR (n=6) and NR (n=3) LGELs.

Results: Unsupervised hierarchical clustering of the 119 genes segregated the cohort into two clusters, representing two distinctive gene expression profiles (see heatmap, Figure 1). The first cluster consisted of 4 EEC2 cases (stages T1a=3, T2=1) segregating with all CR cases. The second cluster of the remaining 16 EEC2 cases (stages T1a=8; T1b=4; T2=3; T31b=1) segregated with all NR cases. Compared to EEC2 in the CR-like cluster, EEC2 in the NR-like cluster had higher rates of LVI (0% vs 44%) and greater depth of myometrial invasion (mean 32%, range 0-63% vs mean 44%, range 0-99%, respectively). Some of the genes with the highest difference in expression between the CR-like and NR-like EEC2 clusters were *DKK4, NOTUM, NKD1* (Wnt signaling pathway), *FGF20* and *IGFBPL1* (growth factors), all of which had higher expression in the CR-like cluster.

Figure 1 - 1066
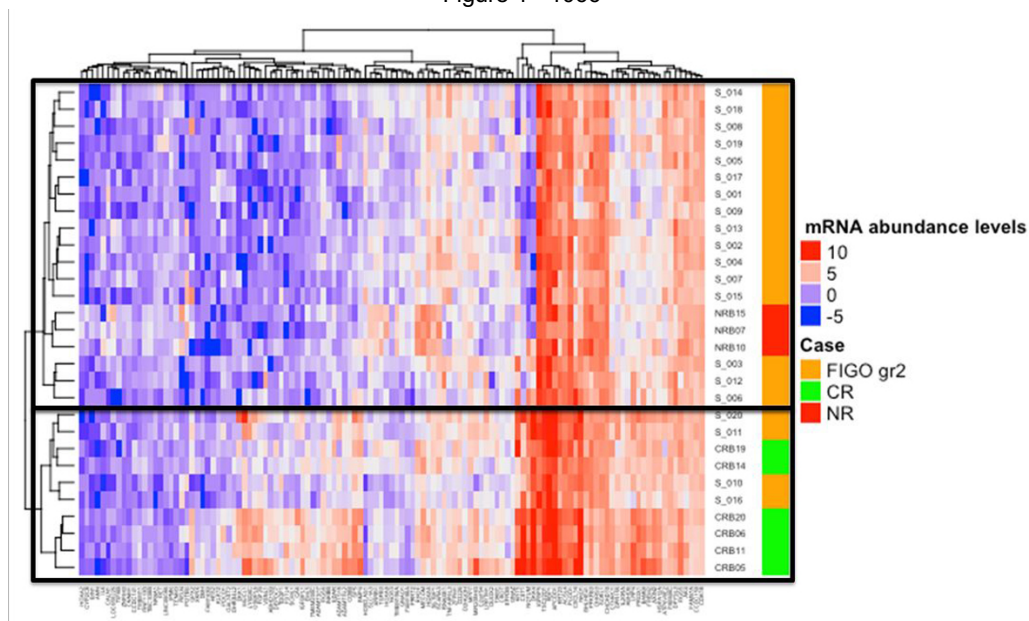
Conclusions: For the first time, we show that a transcriptome profile characteristic of LGELs responsive to progestin therapy exists in a subset of EEC2. This suggests that these tumors may be amenable to a trial of progestin therapy, especially if suspected to be stage T1a on imaging. Further analysis is required to develop sensitive and specific biomarkers of progestin response.

1067 Speckled MLH1 Staining Pattern by Immunohistochemistry in Endometrial Carcinoma

Alain Cagaanan[1], Kristen Karasiewicz[2], Paul Weisman[3], Stephanie McGregor[3]
[1]Madison, WI, [2]University of Wisconsin-Madison, Madison, WI, [3]University of Wisconsin, Madison, WI

Disclosures: Alain Cagaanan: None; Kristen Karasiewicz: None; Paul Weisman: None; Stephanie McGregor: None

Background: Screening for microsatellite instability using immunohistochemistry (IHC) for mismatch repair (MMR) proteins is an effective and cost effective method in endometrial cancers. Misinterpretation of these markers can lead to erroneous reporting and has important prognostic and predictive implications. Speckled (also known as dot-like or punctate) MLH1 staining is common in studies using the M1 clone and has been reported as being associated with MLH1 promoter hypermethylation in colorectal cancers. We characterize MLH1 staining patterns in endometrial cancers with known MLH1 promoter status. We also assess the effect of signal amplification on MLH1 staining.

Design: Endometrial cancer cases (n=34) sent out for MLH1 promoter hypermethylation testing (MLH1HM) were retrieved from our archives. Hematoxylin and eosin-stained and MMR IHC slides were reviewed. Cases were assessed for presence or absence of speckled MLH1 staining. Hypermethylation status and original interpretation of the MMR IHC slides were recorded. In 5 cases with prominent speckled MLH1 staining and positive for MLH1HM, MMR IHC with the anti-MLH1 M1 clone were repeated with and without amplification.

Results: MLH1HM was present in 30 of 34 cases (88%). 23 of 34 cases (68%) showed speckled MLH1 staining ranging from patchy to diffuse tumoral distribution with fine to dense cellular character. Speckled MLH1 staining was present in 22 of 30 (73%) cases with MLH1HM and 1 of 4 (25%) cases without MLH1HM. 1 case with speckled MLH1 staining had been reported as intact but MLH1HM status was positive. Another case with speckled MLH1 was reported as negative but with a comment acknowledging interpretative difficulty due to the speckled extent. In all 5 cases (3 biopsy specimens, 2 resection specimens) with repeat staining, omitting amplification showed overall reduced intensity (Figure 1 without amplification, Figure 2 with amplification). Qualitatively, MLH1 IHC interpretation was easier in the biopsy specimens due to weak internal control staining in resection specimens.

Figure 1 - 1067
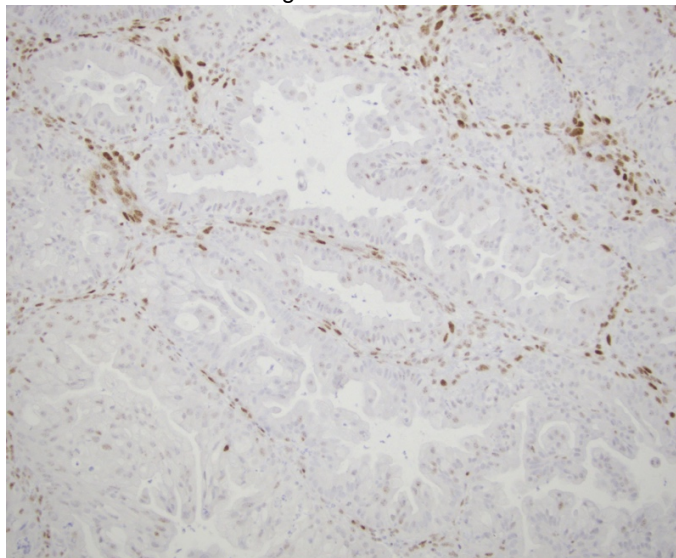
Figure 2 - 1067
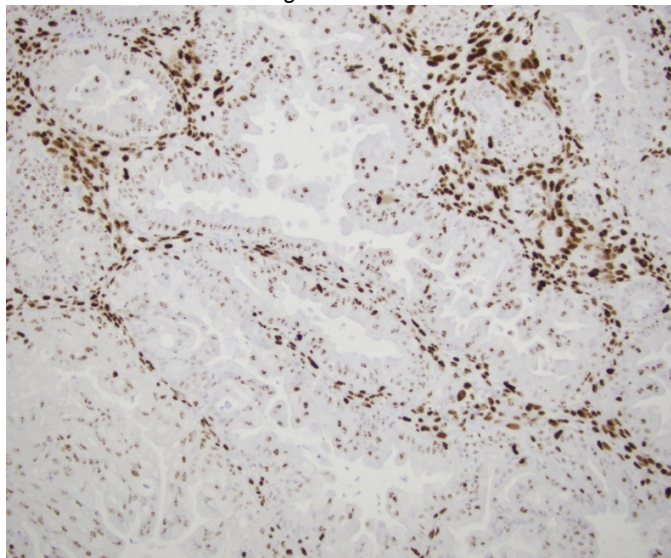
Conclusions: Speckled MLH1 staining is a common phenomenon in endometrial cancer that occurs with and without MLH1HM. This artifact, which appears associated with the M1 clone, can be misinterpreted as intact MLH1 protein expression. Improved MLH1 IHC interpretation can be achieved by changing staining protocols, tissue processing, and specimen selection.

1068 Hypertrophic Lichen Sclerosus: A Putative Precursor to Squamous Cell Carcinoma in the Vulva

Katelynn Campbell[1], Sara Shalin[2], Charles Quick[2]
[1]Little Rock, AR, [2]University of Arkansas for Medical Sciences, Little Rock, AR

Disclosures: Katelynn Campbell: None; Sara Shalin: None; Charles Quick: None

Background: Women with lichen sclerosus (LS) of the vulva have an increased risk for squamous cell carcinoma (SCC), but LS itself has not been implicated as a true precursor. Hypertrophic lichen sclerosus (HLS) is a variant of "classic" LS that may represent a distinct precursor to vulvar SCC. In order to further investigate precursor lesions of vulvar SCC and their oncogenic pathways, we evaluated a series of invasive vulvar SCC for precursor lesions and the expression of p16 and p53 within such lesions and their corresponding invasive cancer.

Design: 36 cases of consecutive vulvar SCCs with sections of adjacent uninvolved epidermis (1998-2015) were identified. Epidermis adjacent to invasive tumor was examined for precursor lesions: differentiated and usual vulvar intraepithelial neoplasia (dVIN, uVIN), differentiated exophytic vulvar intraepithelial lesion (DEVIL), vulvar acanthosis with altered differentiation (VAAD), and HLS. HLS is defined in this study as epidermal acanthosis (without exophytic growth), hyperkeratosis, irregular dermal-epidermal junction (sawtooth or jagged appearance) with a lack of conspicuous cytologic atypia and homogenization of superficial papillary dermis (See Figure 1). All cases were stained for p53 and p16. p16 staining was scored as positive (block positivity) or negative. p53 staining was scored as mutant (positive/null) or wild type (WT).

Results: 19/36 (53%) cases had adjacent uVIN. 4/36 (11%) cases had adjacent dVIN. 10/36 (28%) cases had adjacent HLS. 3/36 (8%) cases were lost to sectioning. No cases of DEVIL or VAAD were identified. Usual VIN and associated SCC were consistently p16 positive and p53 wild type. Differentiated VIN and associated SCC demonstrated mutant p53 staining in all cases, although the sample size was small. HLS more commonly occurs in older women (average age 65 (range 44-87)). IHC results of precursors and their adjacent SCC are shown in Table 1.

Table 1: Immunohistochemical Profile of Vulvar Squamous Cell Carcinomas (n=36) and Adjacent Precursor Lesions

Precursor	Total Cases	p16 Positive Precursor *Cancer*	p16 Negative Precursor *Cancer*	p53 WT Precursor *Cancer*	p53 Mutant Precursor *Cancer*
HLS	10 (28%)	0 (0%) *3 (30%)*	10 (100%) *7 (70%)*	8 (80%) *6 (60%)*	2 (20%) *4 (40%)*
uVIN	19 (53%)	19 (100%) *19 (100%)*	0 (0%) *0 (0%)*	19 (100%) *18 (95%)*	0 (0%) *1 (5%)*
dVIN	4 (11%)	0 (0%) *0 (0%)*	4 (100%) *4 (100%)*	0 (0%) *0 (0%)*	4 (100%) *4 (100%)*

WT= wild type, HLS= hypertrophic lichen sclerosus, uVIN= usual vulvar intraepithelial neoplasia, dVIN=differentiated vulvar intraepithelial neoplasia

Figure 1 - 1068
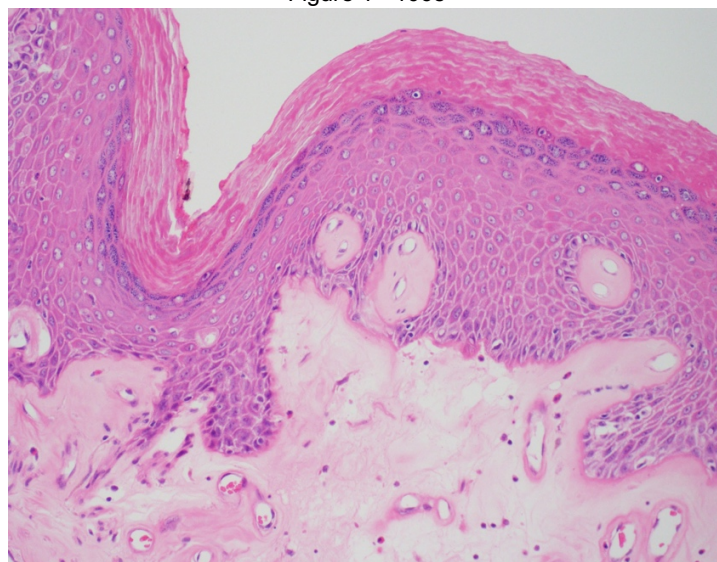
Conclusions: HLS represents a relatively common, putative precursor to invasive SCC of the vulva. Immunostaining with p53 is not predictive of malignant potential in HLS, and p16 is consistently negative. Histologic diagnosis of vulvar HLS warrants increased clinical surveillance of women.

1069   Role of Ki67 Proliferation Index and CD8 Tumour-Infitrating Lymphocyte Counts in Predicting Outcome in High-Grade Serous Tubo-Ovarian Carcinoma (HGSC) Showing No/Partial Response to Neoadjuvant Chemotherapy

Laura Casey[1], Aime Powell[2], Steffen Böhm[3], Ranjit Manchanda[4], Michelle Lockley[5], Martin Kobel[6], Naveena Singh[7]
[1]Royal London Hospital, London, United Kingdom, [2]University of Notre Dame of Australia, Fremantle, WA, Australia, [3]Department of Medical Oncology, London, United Kingdom, [4]Wolfson Institute of Preventive Medicine, Barts CRUK Cancer Centre, London, United Kingdom, [5]Barts Cancer Institute, London, United Kingdom, [6]University of Calgary/Alberta Public Laboratories, Calgary, AB, [7]Barts Health NHS Trust, London, United Kingdom

Disclosures: Laura Casey: None; Aime Powell: None; Steffen Böhm: None; Ranjit Manchanda: *Advisory Board Member*, Astrazeneca and MSD; Michelle Lockley: None; Martin Kobel: None; Naveena Singh: None

Background: We have previously shown the prognostic value of the chemotherapy response score (CRS) for measuring response to neoadjuvant chemotherapy (NACT) in interval debulking surgery specimens of stage IIIC and IV HGSC (CRS1: no or minimal response; CRS2: partial response; CRS3: total/near total response). Its reproducibility, particularly in those with the best response to chemotherapy (CRS3), has been aptly demonstrated and, in this group, the CRS correlates with progression-free and overall survival. However, as currently defined, there is no prognostic distinction between cases showing CRS1 and CRS2, which account for up to 75% cases. It has been shown that the presence and number of CD8 positive tumour-infiltrating lymphocytes (TILs) in HGSC is directly linked to overall survival and, furthermore, that low Ki67 expression is associated with resistance to platinum-based chemotherapy and decreased survival. Our aim was to explore whether Ki67 and/or CD8 TILs predict outcome in HGSC cases showing no/partial response to NACT.

Design: Immunohistochemistry (IHC) was carried out for CD8 and Ki67 on omental sections of HGSC cases showing a partial or no response to NACT. Ki67 was assessed as a percentage of total tumour cells. Cases were classified into i) <30% Ki67 or ii) >/=30% Ki67. CD8 TILs were counted as number/high power field and number/20 tumour cells. Survival analysis was performed using Cox proportional hazards models and the log-rank test.

Results: 39 stage III (n=30) and IV (n=9) HGSC cases were included. Thirty-five patients (90%) had disease recurrence and 20 (51%) had died at study census. Median PFS and OS were 14.1 months (6.3 to 51.6 months) and 31.0 months (14.6 to 66.8 months), respectively. Patients with >/=30% Ki67 were significantly associated with PFS in a multivariate survival model adjusting for age, stage and residual disease (HR 2.9; 95%CI 1.11 – 5.08; p-value 0.025) but not OS (HR 2.1; 95%CI 0.77 – 5.78; p-value 0.144). CD8 TILs were not identified to be a statistically significant predictor for PFS or OS on univariate or multivariate survival models.

Conclusions: Our results indicate that Ki67 predicts PFS in cases of HGSC showing no/partial response to NACT. This simple parameter can easily be incorporated into routine diagnostic practice. Unlike chemo-naive HGSC cases, CD8 TILs do not appear to predict outcome following NACT. Our preliminary findings merit further evaluation in a larger patient cohort.

1070   Next-Generation Sequencing-Based Characterization of Mucinous Ovarian Tumors with Anaplastic Mural Nodules

David Chapel[1], Elizabeth Lee[2], Nathan Teschan[3], Lynette Sholl[1], Panagiotis Konstantinopoulos[2], Marisa Nucci[4]
[1]Brigham and Women's Hospital, Boston, MA, [2]Dana Farber Cancer Institute, Boston, MA, [3]Brigham and Women's Hospital, Brookline, MA, [4]Brigham and Women's Hospital, Harvard Medical School, Boston, MA

Disclosures: David Chapel: None; Elizabeth Lee: None; Nathan Teschan: None; Lynette Sholl: *Consultant*, LOXO Oncology; Panagiotis Konstantinopoulos: *Advisory Board Member*, Tesaro; Marisa Nucci: None

Background: A subset of mucinous ovarian tumors (MOT) harbor anaplastic mural nodules (AMN), which may portend a poor clinical outcome, even in low-stage tumors. Some molecular data indicate a clonal relationship between AMNs and associated MOTs. However, genomic profiling of these tumors remains incomplete, and no molecular determinants of prognosis have been reported.

Design: A next-generation sequencing panel of 447 genes was performed on eight cases of MOT with associated AMN. In 3 cases, two grossly discrete AMNs were sequenced separately. Patient outcomes were compared with clinical, histomorphological, and genomic findings.

Results: Patient were 16-60 years old at diagnosis. Six were stage IA, one stage IC2, and one stage IV, and all received adjuvant chemotherapy. One stage IA patient died of disease 9 months after diagnosis. Seven patients were alive without disease over a follow-up of 6 to 272 months (median, 31 months). The MOT was mucinous borderline tumor (MBT) in 2 patients, MBT with intraepithelial carcinoma in 2, and mucinous adenocarcinoma in 4. The dominant AMN morphology was rhabdoid in 2 cases, sarcomatoid in 3, and pleomorphic in 3 (including 1 with bone formation).

Shared pathogenic mutations were seen in the MOT and AMN in all 8 cases, and grossly discrete AMNs within the same ovary had identical mutational profiles in all 3 tested cases. A shared *KRAS* mutation was seen in 7 cases and a shared *MAP2K1* mutation in 1

case. Additionally, shared *KRAS* amplification was seen in 2 cases and was present in the AMN of a third. A *TP53* mutation was seen in 6 cases (shared in 5 cases; AMN only in 1 case). Shared *CDKN2A* deletion was seen in 5 cases, whereas a shared *CDKN2A* single nucleotide variant was seen in 1, and 2 additional cases had a *CDKN2A* mutation in only the MOT or AMN component. The only patient with *SMARCB1* mutation (AMN component only) died from disease. Mutations in *CDH1* and *PTEN* were not seen.

Figure 1 - 1070

	Case 1		Case 2		Case 3		Case 4		Case 5		Case 6		Case 7		Case 8	
	MOT	AMN	MOT	AMN	MOT	AMN	MOT	AMN	MOT	AMN	MOT	AMN	MOT	AMN	MOT	AMN
Outcome	NED		NED		NED		NED		NED		DOD		NED		NED	
Follow-up time (months)	96		51		31		17		6		9		6		272	
Stage	I		I		I		IV		I		I		I		I	
KRAS																
TP53										★						
CDKN2A										★				★		
MAP2K1																
SMARCB1												★				
Mismatch Repair	MSS		MSS		MSS		MSS		MSS		MSS		MSS		MSS	
TMB (mutations/Mb)	2.281	2.281	3.802	3.802	12.927	13.687	5.323	3.042	5.323	3.802	3.042	4.562	5.323	6.083	3.802	3.802

Legend: Missense | Nonsense | Frameshift | Indel | Splice Site | Deletion | Amplification

★ indicates a non-shared mutation   indicates amplification superimposed on a missense mutation

Figure. Clinical, immunohistochemical, and molecular features of low-grade mucinous neoplasms with anaplastic mural nodules. AMN: Anaplastic mural nodule component; DOD: Dead of disease; IHC: immunohistochemistry; MMR: Mismatch repair; MSS: Microsatellite-stable; MSI: Microsatellite-unstable; MOT: Mucinous ovarian tumor; NED: Alive, no evidence of disease; TMB: Tumor mutational burden

Figure 2 - 1070
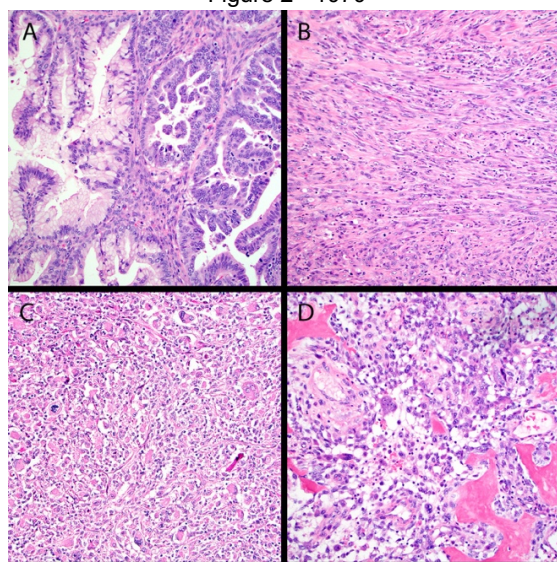
Figure. (A) This mucinous borderline tumor with intraepithelial carcinoma (right half) is associated with an anaplastic mural nodule with a sarcomatoid pattern (B). The morphologic spectrum of anaplastic mural nodules arising in mucinous ovarian tumors also includes rhabdoid (C) and pleomorphic (D) patterns, which may show heterologous elements. (Original magnificiation, 200x)

Conclusions: MOTs and associated AMNs are clonally related lesions with broad genomic overlap, and a single recurrent mutation does not underlie AMN development. RAS pathway mutations appear virtually universal in MOT with AMN, and *TP53* mutations and *CDKN2A* loss are frequent. *SMARCB1* mutation appears to drive AMN development in a minority of cases and may portend a dismal outcome. INI1 immunohistochemistry may be a useful prognostic test in AMNs, as rhabdoid morphology is not specific for *SMARCB1* mutation.

1071 Integrated 5hmC Immunohistochemistry and 5hmC-Modified Genomic Regions as Prognostic Biomarkers in Ovarian Clear Cell Carcinoma

David Chapel[1], Jason Karpus[2], Xiaolong Cui[2], Nida Safdar[3], Ernst Lengyel[2], Esther Oliva[4], Jennifer Bennett[2]
[1]Brigham and Women's Hospital, Boston, MA, [2]The University of Chicago, Chicago, IL, [3]Bedford, MA, [4]Massachusetts General Hospital, Harvard Medical School, Boston, MA

Disclosures: David Chapel: None; Jason Karpus: None; Xiaolong Cui: None; Nida Safdar: None; Ernst Lengyel: None; Esther Oliva: None; Jennifer Bennett: None

Background: Ovarian clear cell carcinoma (OCCC) is an aggressive and chemoresistant tumor, and stage is the only important prognostic factor. 5-hydroxymethylcytosine (5hmC) is an intermediate nucleotide produced in the first step of cytosine demethylation. Preliminary data indicate that 5hmC levels by immunohistochemistry (IHC) have prognostic significance in OCCC, irrespective of tumor stage. However, correlation of 5hmC IHC, 5hmC molecular studies, and clinical outcomes has not been reported.

Design: We applied genome-wide 5hmC-Seal molecular profiling to 40 OCCCs. For each tumor, the total number of genome-wide 5hmC peaks was compared to extent and intensity of 5hmC IHC, tumor stage, and patient outcome--favorable (no evidence of disease) vs adverse (alive with disease/dead of disease). Tumors were sorted by unsupervised clustering to identify differentially hydroxylated genes, and principal components analysis was performed using the identified gene panel and compared to patient outcome.

Results: Clinicopathologic data are summarized in the table. Over a median follow-up of 30 (range 1-150) months, 15 patients had an adverse outcome. On genome-wide analysis, total number of 5hmC peaks positively correlated with 5hmC IHC extent and intensity scores, and negatively with tumor stage. While the number of genome-wide 5hmC peaks was only marginally lower in patients with adverse outcome, clustering and principal components analyses successfully identified panels of differentially hydroxylated genes for stratification based on outcome. The 10 loci showing the greatest discrimination between tumors included 7 microRNAs (MIR6820, MIR92A2, MIR4532, MIR670, MIR572, MIR4685, and MIR5787), as well as SNORD114-28, RN7SK, and GAG12F.

Age (median, years)	56
Outcome Status	**#**
NED	25
AWD/DOD	15
Stage	**#**
IA	3
IC	25
II	1
III	9
IV	2
Tumor 5hmC IHC Extent Score	**#**
1 (<10% staining)	3
2 (10-24%)	6
3 (25-75%)	14
4 (>75%)	17
Tumor 5hmC IHC Intensity Score	**#**
1 (weak)	4
2 (moderate)	23
3 (strong)	13

AWD: Alive with disease; NED: No evidence of disease; DOD: Dead of disease

Figure 1 - 1071
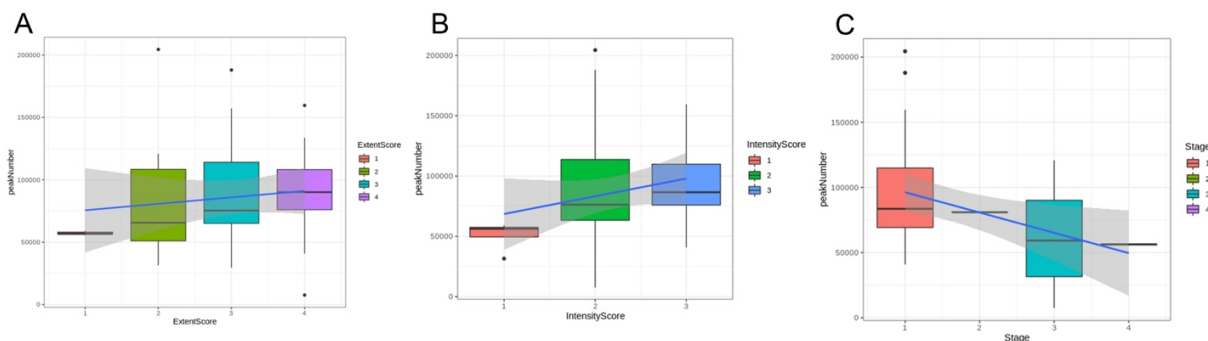
Figure 1. The total number of genome-wide 5hmC peaks correlates positively with 5hmC IHC extent (A) and staining intensity (B), and with tumor stage (C).

Figure 2 - 1071
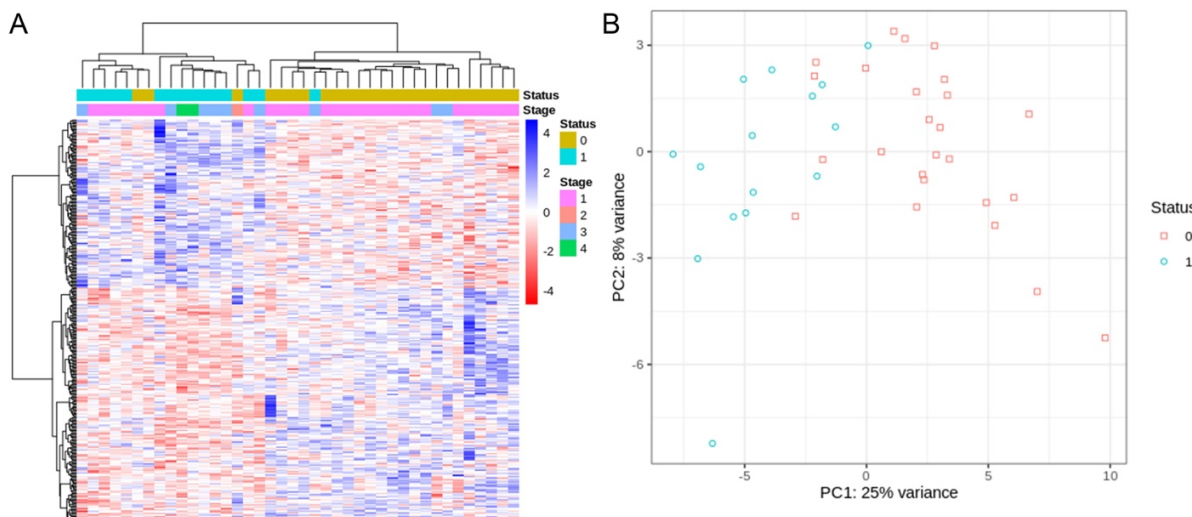
Figure 2. Clustering of genome-wide hydroxymethylation profiles (A) and principal component analysis (B) accurately distinguishes tumors based on patient outcome, pointing to a prognostic role for hydroxymethylation profiling in ovarian clear cell carcinoma. (Status 0: alive, no evidence of disease. Status 1: Alive with disease or dead of disease)

Conclusions: This molecular study of tumor 5hmC profile validates and expands upon previous reports of the prognostic value of 5hmC IHC. A targeted panel of differentially hydroxymethylated genes applied to tumor specimens and circulating DNA, may permit risk stratification of OCCC. MicroRNAs are enriched among prognostically discriminatory loci, further suggesting a critical role for regulation of gene expression in OCCC prognosis. Targeted gene expression profiling, based on the OCCC-specific hydroxymethylation profile, may reveal molecular pathways critical to outcome, opening the possibility of targeted therapies.

1072 Landscape of Putative Precursors to High Grade Serous Carcinoma (HGSC) in the Female Genital Tract

David Chapel[1], Carrie Robinson[2], Emily Goebel[3], Thing Rinda Soong[4], David Kolin[1], Christopher Crum[1]
[1]Brigham and Women's Hospital, Boston, MA, [2]Naval Medical Center San Diego, San Diego, CA, [3]London Health Sciences Centre, Kilworth, ON, [4]University of Washington, Seattle, WA

Disclosures: David Chapel: None; Carrie Robinson: None; Emily Goebel: None; Thing Rinda Soong: None; David Kolin: None; Christopher Crum: None

Background: In the now-widely accepted model of high-grade serous carcinoma (HGSC) development, a serous tubal intraepithelial carcinoma (STIC) develops in the distal tube, and tumor cells spread from the STIC to the peritoneal cavity. A second related model proposes that inconspicuous early serous proliferations (ESPs) exfoliate ("precursor escape"), spread to the peritoneal cavity, and progress to HGSC in a subset of cases. Both models may account for a sizable proportion of extrauterine HGSCs but fail to explain every case. We examined the frequency and histomorphologic features of endometrial ESPs in women with extrauterine HGSC.

Design: The study cohort included two groups. Group 1 comprised consecutive extrauterine HGSCs in which the endometrium and fallopian tubes were entirely submitted for evaluation (11 cases, 129 endometrial and 72 tubal blocks). Group 2 consisted of cases in which exhaustive sectioning of entirely submitted fallopian tubes disclosed no STIC or ESP (from prior work, Soong et al 2018). All endometrial sections from Groups 1 and 2 were immunostained for p53. The frequency of ESPs was recorded and compared to a prior study of benign polyps (Jarboe et al, 2009).

Results: In Group 1, 3 of 11 (27%) endometria contained an ESP, and 2 of 6 (33%) endometrial polyps harbored an ESP, in contrast to 6 ESPs seen in 137 benign polyps by Jarboe et al (P=0.037). A tubal ESP was identified in 4 of 11 (36%) cases. In Group 2, 2 of 11 (18%) cases harbored an endometrial ESP. Across both groups, ESPs included two morphologic types: 1) lesions limited to the surface epithelium (Fig 1) and 2) sub-surface lesions showing endometrioid differentiation (Fig 2).

Figure 1 - 1072
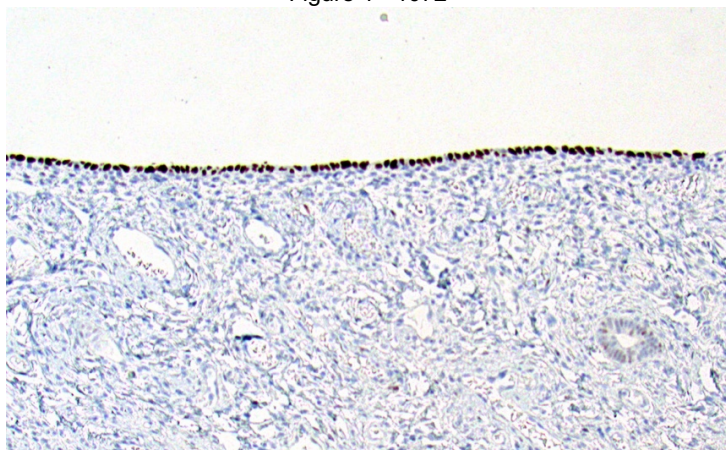
Figure 2 - 1072
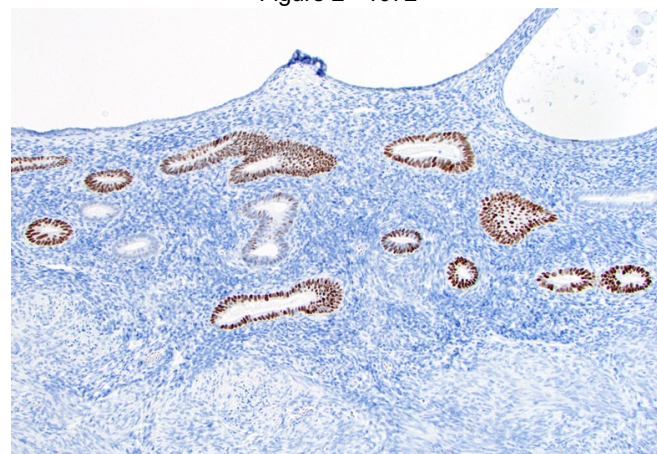
Conclusions: This study indicates that ESPs may be more frequent in the endometria of women with extrauterine HGSC than in healthy women, and that ESPs may be particularly prone to develop in endometrial polyps. Endometrial ESPs show two different morphologic patterns, correlated to surface versus sub-surface location. Molecular studies are in progress to compare the p53 mutations between these ESPs and concurrent HGSCs to elucidate the possible role of the endometrial lining and endometrial polyps in extra-uterine HSGC pathogenesis.

1073 High-Grade Neuroendocrine Carcinoma of the Vulva: A Clinicopathologic Study of 15 Cases

Peter Chen[1], Elizabeth Euscher[2], Preetha Ramalingam[2], Barrett Lawson[2], Anais Malpica[2]
[1]Houston, TX, [2]The University of Texas MD Anderson Cancer Center, Houston, TX

Disclosures: Peter Chen: None; Elizabeth Euscher: None; Preetha Ramalingam: None; Barrett Lawson: None; Anais Malpica: None

Background: High-grade neuroendocrine carcinoma of the vulva (HGNECaV) is rare with most cases reported as Merkel cell carcinoma (MCC). This study presents the clinicopathologic features of the largest series of such cases.

Design: Fifteen cases from 1985-2019 were reviewed for the following: patient (pt) age, clinical presentation, FIGO stage, treatment (tx), follow up (f/u), histological features, immunohistochemistry (IHC) and high risk human papilloma virus (HRHPV) results.

Results: Mean age at presentation was 53 yrs (range, 10-90 yrs), and 33% had presenting symptoms related to metastasis. 13/15 (87%) cases were pure HGNECa, mostly small cell type (10/15, 67%) with only 2/15 (13%) being large cell type. 2/15 (13%) were mixed (squamous Ca or adeno Ca). 43% of the cases were misdiagnosed as non-NECa. All had at least one architectural NECa pattern. All tumors involved the dermis and/or subcutis, 2 were found adjacent to Bartholin/vestibular glands, and 7 had an epithelial component. IHC results were as follows: synaptophysin 14/14 (100%); CD56 7/7 (100%); chromogranin 10/14 (71%); and cytokeratin 20 2/10 (20%)– the "dot-like" pattern was seen in a single case. 2 of 3 cases had signal for HRHPV detected by in situ hybridization. 11/15 (73%) pts. presented with FIGO stage III or IV disease. Tx and f/u information was available for 10 pts. Of these, 8 underwent vulvar excision with adjuvant chemotherapy (CTX) and/or radiation therapy (RTX). 2 pts. received CTX and XRT only. Of the 10 pts. with f/u (6-89 months) 6 (60%) died of disease including 2 stage IB pts. Of the 4 living pts., 1 is alive with stable disease at 56 months, and 1 is disease free at 89 months.

Conclusions: HGNECaV is rare, affects pts. with a wide age range, but mostly peri/postmenopausal, and often presents at an advanced stage. Most cases are small cell type, with an occasional case mixed with another Ca type.Typically, the tumor is in the dermis/subcutis similar to MCC; however, the expression of CK20 with the characteristic dot-like pattern is rare. Synaptophysin and CD56 were the most

commonly expressed neuroendocrine markers. A subset of HGNECaV is HRHPV-related. HRHPV testing may be considered to distinguish HGNECaV from MCC, especially given the lack of CK20 expression in this cohort. Proper recognition of this tumor is essential to ensure its correct treatment as this is an aggressive neoplasm.

1074 TP53-wildtype High-Grade Serous Tubo-Ovarian Carcinomas

M. Herman Chui[1], Robert Soslow[1]
[1]Memorial Sloan Kettering Cancer Center, New York, NY

Disclosures: M. Herman Chui: None; Robert Soslow: *Speaker*, Ebix/Oakstone

Background: High-grade serous ovarian carcinoma is characterized by the near-universal presence of *TP53* mutation (>95% frequency). In this study, we conduct a histopathologic review of tubo-ovarian carcinomas diagnosed as high-grade serous carcinoma (HGSC) and found to be *TP53*-wildtype by molecular analysis.

Design: From retrospective review of targeted exome sequencing data of 938 high-grade tubo-ovarian serous carcinomas, we identified 37 (4%) cases that did not harbor a *TP53* mutation (tp53wt). These cases, along with 33 HGSCs with *TP53* mutation (tp53mut), were subjected to central pathology review performed by 2 gynecologic pathologists blinded to mutation status. Tumor architectural pattern, mitotic count and nuclear atypia (3-point scale) were assessed on representative slides. Immunohistochemical stains for p53, WT-1 and Pax8 are being performed for all cases and are in progress.

Results: Thirty-four of 37 (92%) tp53wt tumors were confirmed to be morphologically consistent with HGSC; the remaining 3 were re-classified as high-grade adenocarcinoma, NOS (n = 2) or with features of serous and endometrioid carcinoma (n = 1). Notable genetic alterations found in tp53wt HGSC include *MDM2* amplification, as well as mutations in *KRAS*, *NRAS*, and *NF1/2*. There were extensive copy number alterations, indicative of genomic instability. Compared to tp53mut HGSC, architectural features of low-grade serous carcinoma - specifically, micropapillary or cribiform architecture or infiltrative nests/inverted micropapillae - were more frequently observed in tp53wt HGSC [tp53mut vs tp53wt: 5/33 (15%) vs 14/34 (41%), p = 0.03]. While most tumors displayed Grade 3 nuclei, there was a trend towards a higher proportion of cases with Grade 2 or Grade 2-to-3 nuclei amongst tp53wt HGSCs [tp53mut vs tp53wt: 2/33 (6%) vs 7/34 (21%), p = 0.15]. No significant difference in mitotic count was observed (tp53mut vs tp53wt: mean, 25 vs 21, p = 0.45). Immunohistochemical staining for p53 on a subset of cases demonstrate wildtype-pattern of expression in most tumors, however some showed complete or near-complete absence of staining.

Conclusions: High-grade "serous" ovarian carcinomas with wildtype *TP53* are rare and constitute a heterogeneous group comprising high grade Mullerian carcinomas with ambiguous morphology, low-grade serous carcinomas that have undergone high-grade transformation, and otherwise conventional HGSC with either intact p53 expression or functionally silenced by non-genetic mechanisms.

1075 The Significance of "Recurrence" in Endometrial Polyps: A Clinicopathologic Analysis

Andreas Ciscato[1], Somaye Zare[2], Oluwole Fadare[2]
[1]University of California San Diego, San Diego, CA, [2]University of California San Diego, La Jolla, CA

Disclosures: Andreas Ciscato: None; Somaye Zare: None; Oluwole Fadare: None

Background: "Recurrence" in endometrial polyps has historically been considered a potentially ominous clinical finding due to the possibility of an undiagnosed adenosarcoma in the original sample. However, the true clinicopathologic significance of endometrial polyp recurrence has never been comprehensively and systematically studied. The current study is a multifaceted examination of the phenomenon of recurrence in endometrial polyps.

Design: We reviewed pathologic material for all patients who were diagnosed with an endometrial polyp in a biopsy, curettage or polypectomy on more than one occasion during a 17-year period (92 patients, 213 polyps). For analytic purposes, we defined a recurrence as a second polyp diagnosed within 12 months of the first (i.e index) polyp, with the latter diagnosed by curettage or polypectomy. Recurrent polyps so defined comprised the study group (28 patients). An age matched control group of patients that were diagnosed with no more than a single polyp by curettage or polypectomy during this period was also established (174 patients). The study and control groups were compared regarding a wide variety of clinicopathologic features, including follow-up.

Results: 27 (96.4%) of the 28 study group patients had only one recurrence, with the last patient recurring twice. The average duration between the index and first recurrent polyp was 4.64 months (range 1 to 11.6). The index and the recurrent polyps for a given patient were generally similar in morphology. A comparison of the study and control groups (n=174) regarding a variety of clinicopathologic features is presented in the table. Some features, including mild stromal atypia, infarction, and numerous polyp fragments harboring thick walled vessels, were more likely to be present in the study group. However, upon review, none of the polyps in the study group were thought to display features diagnostic of adenosarcoma. At an average follow up duration of 14.3 months (range 1 to 112), no malignancy has been diagnosed in the study group, and all patients show no evidence of disease.

Comparison of study ("recurrent") and control ("non-recurrent") groups			
Feature	Study group (n=28)	Control group (n=174)	p value
Patient age (mean)	53.32 years	49.01 years	NS
Follow-up duration and diagnoses	mean 14.37 months (range 1-112): no malignancies	mean 27 months (range 1-204): one endometrioid carcinoma	NA
Polyp size (mean)	2.61 cm	2.52 cm	NS
Stromal infarction	17.85%	6.32%	NS
Mild and focal stromal atypia	7.14%	0%	0.02
Diffuse stromal hypercellularity	35.71%	20.11%	NS
Focal glandular crowding	25%	11.49%	NS
Prominent thick walled vessels in most fragments	53.6%	16.7%	0.000085
Bizarre stromal cells	0%	1.14%	NS
Focal periglandular condensation of stromal cells	3.57%	0.57%	NS
Focal intraglandular stromal papillation	14.28%	1.71%	0.0079
Presence of stromal fragments without epithelium	0%	3.44%	NS
Stromal mitotic index (mean)	1.25	1.10	NS
Clinical history of breast cancer and/or tamoxifen use	7%	4%	NS

Conclusions: Our data shows that patients whose polyps recur within a year, even though the original polyp was removed by an endometrial curettage or polypectomy, are no more likely to be subsequently diagnosed with a uterine malignancy than controls. The precise combination of factors that underlie recurrent potential in endometrial polyps is unclear, but they appear to be mostly unrelated to underlying neoplasia in an unselected population.

1076 Microcystic Stromal Tumor of the Ovary; Additional Morphologic Nuances

Blaise Clarke[1], Anne-Sophie Chong[2], W. Glenn McCluggage[3], Amir Akbari[1], Marisa Nucci[4], Esther Oliva[5], Sarah Alghamadi[6], Asghar Naqvi[7], William Foulkes[2], Barbara Riverapolo[2]
[1]University of Toronto, Toronto, ON, [2]McGill University, Montreal, QC, [3]The Royal Hospitals, Belfast, United Kingdom, [4]Brigham and Women's Hospital, Harvard Medical School, Boston, MA, [5]Massachusetts General Hospital, Harvard Medical School, Boston, MA, [6]McMaster University Medical Centre, Hamilton, ON, [7]McMaster University, Hamilton, ON

Disclosures: Blaise Clarke: None; Anne-Sophie Chong: None; W. Glenn McCluggage: None; Amir Akbari: None; Marisa Nucci: None; Esther Oliva: None; Sarah Alghamadi: None; Asghar Naqvi: None; William Foulkes: None

Background: Microcystic stromal tumors of the ovary are rare neoplasms characterized by a histologic triad of microcysts, solid cellular regions, and hyalinized stroma. These neoplasms have a characteristic immunophenotype with diffuse expression of CD10, WT1, beta-catenin (nuclear), cyclin D1, FOXL2, and steroidogenic factor-1while inhibin and calretinin are usually negative. Molecular analyses have disclosed that these tumors have either a *CTNNB1* or *APC* mutation and that these are mutually exclusive with the former being more common. We sought to further characterize these unusual tumors by studying an additional 7 cases.

Design: Central pathology review of the cases was performed and molecular analysis of *CTNNB1* and *APC* was undertaken.

Results: Four had the typical morphology described above whereas 3 showed additional findings including epithelioid cells with vacuolation imparting a signet ring appearance (2 cases) and a prominent population of spindle cells and cells with bizarre nuclei (one case).

In four of these cases *CTNNB1* mutations were identified in the hotspot in exon 3. A fifth case lacked *CTNNB1* exon 3 mutation and was wild-type for *APC* by next generation sequencing. The rest of the CTNNB1 gene is being interrogated in that case and and the sixth case is currently undergoing molecular analysis.

Case	Morphology	Molecular
1	Signet ring like	CTNNB1
2	Signet ring like	CTNNB1
3	Classic	CTNNB1 hotspot and APC, wild type
4	Classic	CTNNB1
5	Classic	CTNNB1
6	Spindle and bizarre cells	Pending
7	Classic	Pending

Conclusions: While often prototypical in terms of histologic features, an expanded morphologic spectrum including bizarre cells, spindle cells and signet ring cells can occur. Either *APC* or *CTNNB1* mutation is present in almost all cases of ovarian microcystic stromal tumor and this can be a useful diagnostic tool in cases with unusual morphology. Accurate diagnosis is important as these tumors may rarely be an extracolonic manifestation of FAP. Given the presence of signet ring cells and the fact that *CTNNB1* mutations have been demonstrated in occasional ovarian signet-ring stromal tumors, we speculate that these tumors may be pathogenetically related.

1077 Mutations in LRRK2 are Associated with Improved Outcomes and Frequent DNA Polymerase Exonuclease Defects in Endometrial Cancer

Lani Clinton[1], Laurie H Sanders[2], Edgardo Parrilla Castellar[2]
[1]Duke University Medical Center, Mebane, NC, [2]Duke University School of Medicine, Durham, NC

Disclosures: Lani Clinton: None; Laurie H Sanders: None; Edgardo Parrilla Castellar: None

Background: Mutations in *LRRK2* are the most common genetic cause of Parkinson's disease (PD). LRRK2 is a member of the leucine-rich repeat kinases and is functionally implicated in mitochondrial homeostasis and DNA integrity. *LRRK2* mutations were recently described in ER-positive breast cancer. However, the pathophysiologic relationship between LRRK2 and endometrial cancer, a similarly hormone-driven malignancy, is not described.

Design: The Genomic Data Commons Data Portal (https://portal.gdc.cancer.gov) from The Cancer Genome Atlas was searched for *LRRK2* single nucleotide variants and small insertions/deletions in 553 unselected cases of endometrial cancer. Digital histopathology was performed using Slide Image Viewer. Categorical values were compared using the Chi-square test. Overall survival was estimated using the Kaplan-Meier method and tested using the log-rank test.

Results: 144 *LRRK2* mutations were identified in 69 cases of endometrial cancer (median age=59 yrs., median follow up=46 mo.). 53 additional cases had *LRRK2* sequence information without a detectable mutation (median age=64 yrs., median follow up=29 mo.). Inactivating, stop-gain variants (i.e. nonsense, frameshift and splice site) were present in over half of cases (N=38). Endometrioid morphology prevailed among *LRRK2*-mutated tumors (N=89%; OR=4.20; P=0.003), whereas *LRRK2* alterations were rare in serous carcinomas (6%; OR=0.15; P<0.001). 5-year overall survival rates were 93% and 71% among patients with endometrial cancers harboring a *LRRK2* mutation (N=69) versus those without (N=53), respectively (P=0.007; Figure 1), with comparable FIGO stage distribution (P=0.299). Tumors with *LRRK2* mutations had frequent hotspot *POLE* (N=48) or *POLD1* (N=4) exonuclease mutations (OR=10.68, P<0.001), with a mean mutation rate of 13.3 per Mb compared to 1 per Mb in cases without a *LRRK2* mutation (P<0.001). Of note, 87% (N=60) of cases with *LRRK2* mutations had a variant that could not be attributed to the TCT > TAT, TCG > TTG or TTT > TGG mutation patterns.

Figure 1 - 1077
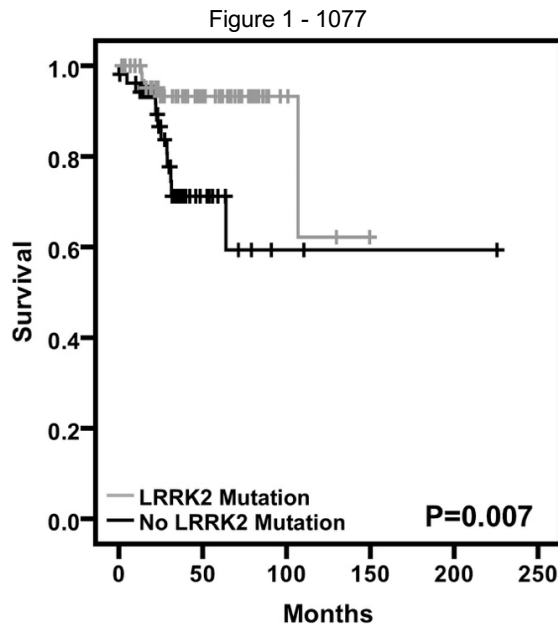
Conclusions: Somatic *LRRK2* mutations occur in endometrial cancer, with frequent loss-of-function alterations and are associated with prognostically favorable disease. The association of polymerase exonuclease defects and *LRRK2* inactivation, seemingly independent of polymerase proofreading errors, suggests an incipient functional relationship between the two that results in the ultra-mutated phenotype of endometrial carcinomas.

1078 Looking Past PD-L1: Expression of Immune Checkpoint TIM-3 and its Ligand Galectin-9 in Cervical and Vulvar Squamous Neoplasia

Jacob Curley[1], Mark Stoler[2], Anne Mills[3]
[1]University of Virginia Health System, Charlottesville, VA, [2]University of Virginia Health System, Earlysville, VA, [3]University of Virginia, Charlottesville, VA

Disclosures: Jacob Curley: None; Mark Stoler: None; Anne Mills: None

Background: Immunotherapies targeting the PD-1/PD-L1 pathway have shown some success in cervical and vulvar squamous cell carcinomas (SCC), but little is known about the potential vulnerability of these tumors to other checkpoint inhibitors. TIM-3 is a checkpoint molecule that exerts immunosuppressive function via its interaction with Gal-9. TIM-3 and Gal-9 have been identified on a variety of malignancies but have not been studied in cervical and vulvar cancers, nor has their relationship to PD-L1 been established.

Design: Sixty-three cervical and vulvar invasive (n=34) and intraepithelial lesions (n=29) were assessed for TIM-3, Gal-9, and PD-L1 in tumor/lesional cells and associated immune cells.

Results: Tumoral TIM-3 expression was identified in 85% of SCC but only 21% of intraepithelial lesions ($p<0.0001$). When immune cells were accounted for, 97% of invasive and 41% of intraepithelial lesions had a TIM-3 combined positive score (CPS) ≥1 ($p<0.0001$). Tumoral membranous expression of Gal-9 was seen in 82% of SCC and 31% of intraepithelial lesions ($p=0.0001$); nearly all cases had Gal-9-positive immune cells. Tumoral PD-L1 was seen in 71% of SCC and 10% of intraepithelial lesions ($p<0.0001$), while the PD-L1 CPS was ≥1 in 82% and 24%, respectively ($p<0.0001$). There were no significant differences in TIM-3-, GAL-9, or PD-L1 expression in cervical vs. vulvar neoplasms, nor was HPV status significantly associated with any of the three markers.

TIM-3, GAL-9, and PD-L1 Co-Expression using the CPS.

	TIM-3+ & GAL-9+ CPS≥1	TIM-3+, GAL-9+, & PD-L1+ CPS≥1
All Intraepithelial Lesions (n=29)	41% (12/29)	7% (2/29)
CIN 3 (n=14)	64% (9/14)	0% (0/14)
VIN 3 (n=13)	23% (3/13)	15% (2/13)
dVIN (n=2)	0% (0/2)	0% (0/2)
All Invasive SCC (n=34)	97% (33/34)	82% (28/34)
Cervical SCC (n=15)	100% (15/15)	87% (13/15)
Vulvar SCC, HPV-Associated (n=16)	100% (16/16)	81% (13/16)
Vulvar SCC, dVIN-associated (n=3)	100% (3/3)	67% (2/3)

Figure 1 - 1078
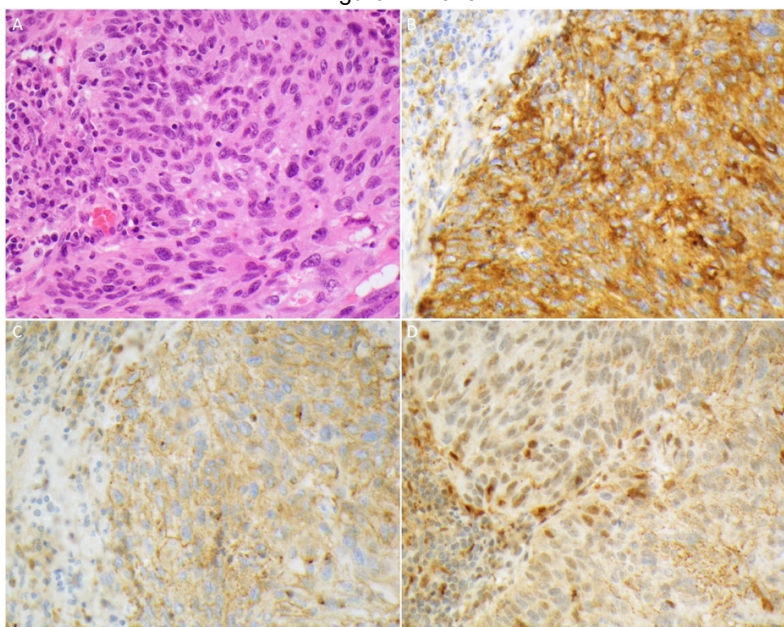
Figure 1
"Cervical SCC (A) with diffuse PD-L1 (B) and TIM-3 (C) expression involving both tumor cells and associated lymphocytes and mixed membranous and nuclear GAL-9 staining (D)."

Conclusions: Dual TIM-3/Gal-9 expression was present in the majority (86%) of PD-L1-positive cases including 100% of PD-L1-positive SCC, suggesting a possible role for TIM-3 checkpoint inhibition in concert with anti-PD-1/PD-L1.

1079 The Chronology of Development of Endometrioid Endometrial and Ovarian Tumors in Patients with Synchronous Disease

Arnaud Da Cruz Paula[1], Lea Moukarzel[2], Nadeem Abu-Rustum[1], Jose Palacios Calvo[3], Xavier Matias-Guiu[4], Jorge Reis-Filho[1], Britta Weigelt[1]
[1]Memorial Sloan Kettering Cancer Center, New York, NY, [2]Department of Surgery, Memorial Sloan Kettering Cancer Center, New York, NY, [3]Hospital Universitario Ramón y Cajal, Madrid, Spain, [4]Hospital U Arnau de Vilanova and Hospital U de Bellvitge, Lleida, Spain

Disclosures: Arnaud Da Cruz Paula: None; Lea Moukarzel: None; Nadeem Abu-Rustum: *Grant or Research Support*, Stryker; *Grant or Research Support*, GRAIL; Jose Palacios Calvo: None; Xavier Matias-Guiu: None; Jorge Reis-Filho: None; Britta Weigelt: None

Background: Sporadic synchronous endometrioid endometrial (EECs) and endometrioid ovarian cancers (EOCs) have been shown to be clonally related and to likely constitute metastases from each other. Here we sought to infer the chronology of the development of EECs and EOCs in patients with sporadic synchronous disease based on bioinformatic approaches.

Design: Sequencing data of 17 previously published sporadic synchronous EECs/EOCs subjected to massively parallel sequencing targeting 341 cancer-related genes were re-analyzed using validated bioinformatics methods. Clonal composition/ cancer cell fractions of somatic mutations were inferred using ABSOLUTE, taking purity, ploidy and copy number into account.

Results: All 17 sporadic synchronous EECs/EOCs were clonally related and were metastases from each other. Based on a clonal composition analysis, the chronology of the development of the EECs and EOCs could be inferred in six cases. In these six synchronous EECs/EOCs, the EOC likely evolved following clonal selection from a subpopulation of the EEC. We observed that either subclonal mutations present in the EEC became clonal in the respective EOC and/ or additional genetic alterations were acquired in the EOC as compared to the EEC. For example, in two of these six cases, subclonal *PIK3CA* hotspot mutations (p.P471L and p.R108H) identified in the EEC became clonal in the EOC. Similarly, in one case, a subclonal *PTEN* hotspot mutation (p.R130G) in the EEC was found to be clonal in the respective EOC. In another case, a subclonal *APC* frameshift mutation (p.D849Efs*11) detected in the EEC was found to be clonal in the EOC, and the EOC harbored an 11q13 amplification, encompassing *CCND1*, not present in the EEC. Of note, in five of the six cases where chronology could be inferred, no endometriosis was present.

Conclusions: Our findings suggest that in a subset of sporadic synchronous EECs/EOCs these lesions are of endometrial origin with the endometrial tumor giving rise to the ovarian tumor.

1080 Concordance of p53 Immunohistochemistry and TP53 Mutation Status in Endometrial Cancer

Arnaud Da Cruz Paula[1], Deborah DeLair[2], Daniel Fix[3], Robert Soslow[1], Kay Park[1], Sarah Chiang[1], Jorge Reis-Filho[1], Ahmet Zehir[1], Rajmohan Murali[1], Vicky Makker[1], Karen Cadoo[1], Jennifer Mueller[1], Mario Leitao[1], Nadeem Abu-Rustum[1], Carol Aghajanian[1], Britta Weigelt[1]
[1]Memorial Sloan Kettering Cancer Center, New York, NY, [2]NYU Langone Medical Center, New York, NY, [3]Hackensack University Medical Center, Hackensack, NJ

Disclosures: Arnaud Da Cruz Paula: None; Deborah DeLair: None; Daniel Fix: None; Robert Soslow: *Speaker*, Ebix/Oakstone; Kay Park: None; Sarah Chiang: None; Jorge Reis-Filho: None; Ahmet Zehir: *Speaker*, Illumina; Rajmohan Murali: None; Vicky Makker: *Consultant*, Eisai; *Grant or Research Support*, Eisai; *Consultant*, Merck; *Advisory Board Member*, Merck; *Grant or Research Support*, Merck; Karen Cadoo: None; Jennifer Mueller: None; Mario Leitao: *Speaker*, Intuitive Surgical; Nadeem Abu-Rustum: *Grant or Research Support*, Stryker; *Grant or Research Support*, GRAIL; Carol Aghajanian: *Advisory Board Member*, Eisai/Merck; *Grant or Research Support*, Astra Zeneca; *Grant or Research Support*, Genentech; *Grant or Research Support*, Abbvie; *Grant or Research Support*, Clovis; Britta Weigelt: None

Background: For the clinical identification of the four molecular subtypes of endometrial cancer (EC), which were originally identified using whole-exome sequencing, surrogates employing immunohistochemistry (IHC) have been implemented. In this surrogate, p53 IHC is used to identify 'copy-number high'/ p53 abnormal ECs. We sought to define the concordance of p53 IHC and *TP53* mutation status in ECs.

Design: Patients with newly diagnosed primary EC were prospectively consented to an IRB-approved protocol. ECs were subjected to p53 and DNA mismatch repair (MMR) protein IHC and to massively parallel sequencing targeting 410-468 cancer-related genes. ECs were classified based on *POLE* mutation status and MMR and p53 IHC into the four molecular subtypes: *POLE* (ultramutated), MMR-deficient, copy-number low (endometrioid) and copy-number high (serous-like). Concordance between p53 IHC and somatic *TP53* mutation status was defined using Cohen's Kappa.

Results: 175 ECs were included in this study (116 endometrioid, 17 serous, 11 carcinosarcoma, 13 mixed, 6 clear cell, 7 dedifferentiated, 5 other). 41 (23%) ECs demonstrated aberrant p53 expression by IHC, and of these 36 (88%) harbored a somatic *TP53* mutation (Table). Of the 134 ECs with normal/ wild-type p53 protein expression by IHC, the majority of ECs (115; 86%) were molecularly concordant and did not harbor a somatic *TP53* mutation (Table). The agreement between the two methods was 151/175 (86%), with a Kappa of 0.726

(good agreement). The sensitivity and specificity of p53 IHC for the detection of pathogenic *TP53* mutations was 66% and 96%, respectively. In total, there were 24 (14%) discrepant cases, which had aberrant p53 IHC in the absence of a *TP53* mutation (n=5) or a *TP53* mutation but normal p53 protein expression patterns (n=19). Of the 19 *TP53*-mutant ECs with normal p53 IHC, 10 harbored non-pathogenic *TP53* mutations, 3 harbored subclonal *TP53* hotspot mutations, 3 had subclonal *TP53* loss of function mutations, and only 3 had clonal *TP53* hotspot mutations (Table). Discrepancies were primarily observed in ECs of MMR-deficient (9/19) or *POLE* (4/19) EC subtypes.

	p53 immunohistochemistry		
TP53		Normal (n)	Aberrant – null expression (n)	Aberrant – overexpression (n)
Sequencing	**Mutation type**			
	TP53 wild-type	115	0	5
	TP53 hotspot	6	0	26
	TP53 loss of function	3	2	6
	TP53 other	10	0	2
	Mutation clonality			
	TP53 clonal	9	1	29
	TP53 subclonal	10	1	5
	Number of hits			
	TP53 bi-allelic	5	1	22
	TP53 mono-allelic	14	1	12

Conclusions: Our findings demonstrate a good concordance between p53 IHC and *TP53* mutation status in EC. p53 IHC is a specific and fairly sensitive surrogate for pathogenic *TP53* mutations. The type and clonality of *TP53* mutations explain the vast majority of discrepancies between sequencing and IHC assessment of *TP53*.

1081 Concordance between Immunohistochemistry for DNA Mismatch Repair Proteins and Next Generation Sequencing for the Identification of Microsatellite Instability in Endometrial Cancer

Arnaud Da Cruz Paula[1], Deborah DeLair[2], Daniel Fix[3], Robert Soslow[1], Kay Park[1], Sarah Chiang[1], Jorge Reis-Filho[1], Ahmet Zehir[1], Diana Mandelker[1], Rajmohan Murali[1], Vicky Makker[1], Karen Cadoo[1], Jennifer Mueller[1], Mario Leitao[1], Nadeem Abu-Rustum[1], Carol Aghajanian[1], Britta Weigelt[1]
[1]Memorial Sloan Kettering Cancer Center, New York, NY, [2]NYU Langone Medical Center, New York, NY, [3]Hackensack University Medical Center, Hackensack, NJ

Disclosures: Arnaud Da Cruz Paula: None; Deborah DeLair: None; Daniel Fix: None; Robert Soslow: *Speaker*, Ebux/Oakstone; Kay Park: None; Sarah Chiang: None; Jorge Reis-Filho: None; Ahmet Zehir: *Speaker*, Illumina; Diana Mandelker: None; Rajmohan Murali: None; Vicky Makker: *Grant or Research Support*, Eisai; *Consultant*, Eisai; *Advisory Board Member*, Merck; *Speaker*, Merck; *Grant or Research Support*, Merck; Karen Cadoo: None; Jennifer Mueller: None; Mario Leitao: *Speaker*, Intuitive Surgical; Nadeem Abu-Rustum: *Grant or Research Support*, Stryker; *Grant or Research Support*, GRAIL; Carol Aghajanian: *Advisory Board Member*, Eisai/Merck; Britta Weigelt: None

Background: The NCCN currently recommends microsatellite instability (MSI) or mismatch repair (MMR) immunohistochemistry (IHC) for patients with endometrial cancer (EC) as a screen for Lynch Syndrome and criteria for immune checkpoint inhibitor therapy. Recently, MSI testing has become available through next generation sequencing (NGS). We sought to compare the concordance of MMR IHC and MSI status obtained via NGS in EC.

Design: Patients with newly diagnosed primary EC were prospectively consented to an IRB-approved protocol. ECs were subjected to MMR IHC and targeted NGS with a panel covering over 400 cancer-related genes. MSIsensor was used to bioinformatically infer the MSI status, with an MSIsensor score ≥10 deemed MSI-high. Tumor cell content was inferred bioinformatically using ABSOLUTE. Concordance between IHC and sequencing results was defined using Cohen's Kappa.

Results: 175 ECs were included (116 endometrioid, 17 serous, 11 carcinosarcoma, 13 mixed, 6 clear cell, 7 dedifferentiated, 5 other). 50 (29%) were considered MMRd based on the loss of at least one MMR protein by IHC, of which 30 (60%) ECs were classified as MSI-high by MSIsensor (Table). Of the 125 ECs with retained MMR expression, the vast majority (123; 98%) was molecularly concordant and was not MSI-high (Table). The overall agreement between MMRd and MSI-high by MSIsensor was 153/175 (87%), with a Kappa of 0.749 (good agreement). Of the 20 MMRd classified as non-MSI-high, 9 were MSI indeterminate and 11 microsatellite stable. Of these 11 discrepant ECs (i.e. MMRd and microsatellite stable), 4 displayed loss of MLH1 and PMS2 expression, 1 PMS2 loss and 6 MSH6 loss of expression (Table). The tumor purity was significantly lower in the 20 MMRd non-MSI-high ECs (median 26%, range 19-60%) compared to the 30 MMRd MSI-high concordant ECs (median 49%, range 20-95%; p<0.001).

MMR IHC Results	MSI Status (MSIsensor)		
	Microsatellite stable (MSIsensor <3) (n)	MSI indeterminate (MSIsensor 3-9.99) (n)	MSI-high (MSIsensor ≥10) (n)
MMR proficient	118	5	2
MMR deficient	11	9	30
MLH1 and PMS2 loss	4	6	29
MSH2 and MSH6 loss	0	1	1
PMS2 only loss	1	1	0
MSH6 only loss	6	1	0

Conclusions: Our findings revealed a good agreement between MMR IHC and MSI status inferred from NGS for EC. Tumor purity may falsely decrease the degree of MSI in EC. However, in addition to MSI status, multi-gene sequencing assays provide information on specific somatic/ germline mutations, copy number alterations and tumor mutational burden in a single assay.

1082 Mesonephric and Mesonephric-Like Carcinomas of the Female Genital Tract: Molecular Interrogation Including Three Cases Mixed with Serous and Mucinous Neoplasms

Edaise M. da Silva[1], Daniel Fix[2], Ana Paula Martins Sebastiao[3], Pier Selenica[1], Ferrando Lorenzo[1], Simon Lee[1], Evan Smith[1], Anthe Stylianou[4], Arnaud Da Cruz Paula[1], Fresia Pareja[1], Sarah Kim[1], Jason Konner[5], Karen Cadoo[1], Nadeem Abu-Rustum[1], Jorge Reis-Filho[1], Jennifer Mueller[1], Britta Weigelt[1], Kay Park[1]
[1]Memorial Sloan Kettering Cancer Center, New York, NY, [2]Hackensack University Medical Center, Hackensack, NJ, [3]Positivo University, Curitiba, PR, Brazil, [4]Department of Surgery, Memorial Sloan Kettering Cancer Center, New York, NY, [5]Department of Medicine, Memorial Sloan Kettering Cancer Center, New York, NY

Disclosures: Edaise M. da Silva: None; Daniel Fix: None; Ana Paula Martins Sebastiao: None; Pier Selenica: None; Ferrando Lorenzo: None; Simon Lee: None; Evan Smith: None; Anthe Stylianou: None; Arnaud Da Cruz Paula: None; Fresia Pareja: None; Sarah Kim: None; Jason Konner: None; Karen Cadoo: None; Nadeem Abu-Rustum: *Grant or Research Support*, Stryker; *Grant or Research Support*, GRAIL; Jorge Reis-Filho: None; Jennifer Mueller: None; Britta Weigelt: None; Kay Park: None

Background: Mesonephric carcinoma (MC) of the cervix is a rare tumor derived from Wolffian remnants. Mesonephric-like carcinomas (MLC) of the ovary (MLCO) and endometrium (MLCE), while morphologically similar, do not have obvious Wolffian origin and possibly represent transdifferentiation of Müllerian tumors. Here, we describe the repertoire of genetic alterations in MC and MLC, including 3 MLCO mixed with Müllerian tumors.

Design: DNA from microdissected tumor and normal tissue from 8 MCs (6 primary and 2 metastatic tumors), 15 MLCOs and 13 MLCEs were subjected to massively parallel sequencing targeting 468 cancer-related genes. The histologically distinct components of three mixed MLCOs were analyzed separately.

Results: Recurrent *KRAS* mutations were present in 100% of MCs, 87% (13/15) of MLCOs and 92% (12/13) of MLCEs (Table). *PIK3CA* mutations were identified in 33% (5/15) of MLCOs, in 23% (3/13) of MLCEs and in two metastases (lung and brain) of MCs. Only MLCs harbored *CTNNB1* (MLCO 1/15, 6%; MLCEs 3/13, 23%) and *PTEN* mutations (MLCEs 3/13, 23%). Copy number analysis revealed frequent gains of 1q in MCs (7/8, 87%), MLCOs (14/15, 93%) and MLCEs (11/13, 85%). Gains of chromosome 12 were more frequent in MLCOs (10/15, 67%) than in MLCEs (2/13, 15%) and MCs (3/8, 37%; *p*<0.05), whereas loss of chromosome 9 was more frequent in MCs (4/8, 50%) than in MLCOs (1/15, 6%) and MLCEs (1/13, 7%; *p*<0.05). Three MLCOs were mixed with other histologies: 2 mucinous borderline tumors (MBT) and 1 serous borderline tumor (SBT). Both MLCO/SBT cases included in this study harbored *NRAS* p.Q61R hotspot rather than *KRAS* mutations. The SBT and MLCO components of one case analyzed separately harbored similar mutation profiles. In both MLCO/MBT cases, the two separately sequenced components shared *KRAS* hotspot mutations. In addition, one of the cases also harbored *PIK3CA* hotspot mutations, whereas in the other case, *CTNNB1* and *AKT* hotspot mutations were found to be restricted to the MLCO component.

		MCs (n=8)	MLCO (n=15)	MLCE (n=13)
Histology	Mesonephric	6 (75%)	-	-
	Mesonephric-like	-	8 (53%)	9 (70%)
	Mixed histologies	1 (12.5%) **A**	6 (40%) **B***	2 (15%) **C***
	Mesonephric MMMT	1 (12.5%)	1 (7%)	2 (15%)
Recurrent Mutations	*KRAS*	8 (100%)	13 (87%)	12 (92%)
	PIK3CA	2 (25%)	5 (33%)	3 (23%)
	CTNNB1	-	1 (6%)	3 (23%)
	PTEN	-	-	3 (23%)
Recurrent Copy Number Alterations	Gain 1q	7 (87%)	14 (93%)	11 (85%)
	Gain chromosome 12	3 (37%)	10 (67%)	2 (15%)
	Loss Chromosome 9	4 (50%)	1 (6%)	1 (7%)

A. Mixed mesonephric and endometrioid (n=1); B. Mixed mesonephric-like and: endometrioid (n=2), MBT (n=2; *both cases had separate components sequenced) and SBT (n=2; *1 case had separate components sequenced); C. Mixed mesonephric-like and: endometrioid (n=1), endometrioid/clear cell carcinoma (n=1)

Conclusions: MLCs are underpinned by somatic *KRAS* mutations akin to MCs but also harbor genetic alterations that are frequently reported in Müllerian tumors, such as *PIK3CA, PTEN* and *CTNNB1*. Our findings suggest that MLCs harbor features similar to those of tumors with mesonephric and Mullerian differentiation. The histologically distinct components of mixed MLCs harbor similar patterns of genetic alterations supporting their clonal relatedness.

1083   Clinicopathologic and Genomic Analysis of Copy Number-High (CN-H) Endometrial Carcinomas

Wissam Dahoud[1], Amir Momeni Boroujeni[2], Chad Vanderbilt[3], Robert Soslow[1]
[1]Memorial Sloan Kettering Cancer Center, New York, NY, [2]Memorial Sloan Kettering Cancer Center, Brooklyn, NY, [3]Memorial Sloan Kettering Cancer Center, Denver, CO

Disclosures: Wissam Dahoud: None; Amir Momeni Boroujeni: None; Chad Vanderbilt: *Consultant*, Paige.AI; *Consultant*, Docdoc ltd.; *Consultant*, OncoKB; Robert Soslow: *Consultant*, Ebix/Oakstone

Background: The TCGA analysis of endometrial carcinomas identified a group of tumors with *TP53* mutations, chromosomal instability and copy number variations (CN-H), The prototypical histotype is serous carcinoma (USC), but there is also a histologically diverse group of endometrial carcinomas with similar genomic characteristics (CN-H non-serous [CN-H-NS]) such as *TP53*-mutated FIGO grade 3 endometrioid carcinoma. We aim to compare the clinicopathologic and genomic features of CN-H-NS versus USC.

Design: All archival USC and CN-H-NSs studied by targeted next generation sequencing were selected and molecular, clinical and pathologic data pertaining to these cases compared. Histotypes were assigned morphologically and in some cases immunohistochemically by a homogeneous group of expert gynecologic pathologists at a single institution.

Results: 129 cases were included in the study: 32 endometrioid (25%), 53 USC (41%), 6 clear cell carcinomas (4%), 28 mixed endometrial carcinomas (22%), and 10 high-grade endometrial carcinomas, unclassified (8%). The median survival was 28.93 months. Histotype did not correlate with survival, but USC was more likely to metastasize to peritoneum and lung. Important predictors of outcome were FIGO stage (p: 0.005) and molecular findings that adversely affect survival (p: 0.0176): namely, chromosome 11q (*FGF* cluster genes) and 8q gains, *ERBB2* and *MAPK3* amplification, and alterations in *CDK12* and *CASP8.*

Figure 1 - 1083

Survival distribution function
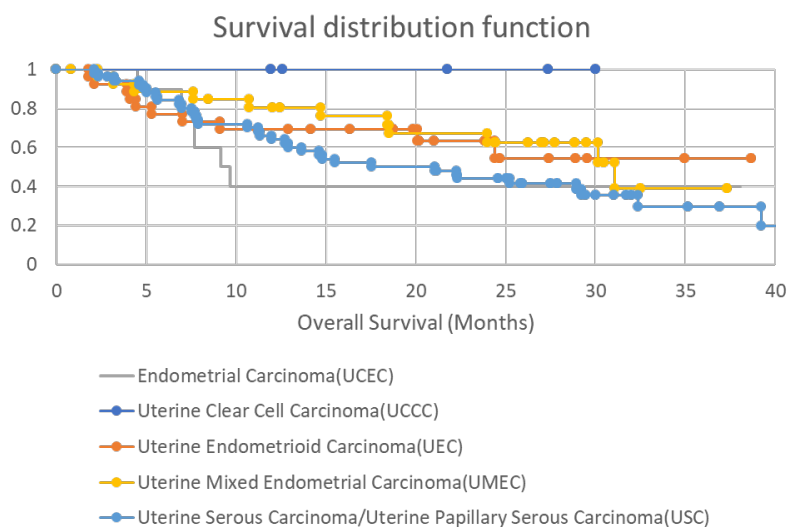
Conclusions: CN-H-NS and USC have similar clinical outcomes regardless of histotype. FIGO stage and molecular findings are the best predictors of outcome overall. This suggests that patients with CN-H carcinomas, regardless of histotype or stage, could be managed similarly to USC, pending studies of chemo- and radio-sensitivity stratified by histotype.

1084 The Prognostic Impact of ARID1A Alteration in a Cohort of Molecular Classified Endometrial Carcinomas

Antonio De Leo[1], Dario de Biase[2], Sara Coluccelli[3], Giulia Dondi[4], Pierandrea De Iaco[1], Anna Myriam Perrone[1], Donatella Santini[1], Giovanni Tallini[5], Claudio Ceccarelli[1]
[1]S.Orsola-Malpighi Hospital, University of Bologna, Bologna, Italy, [2]University of Bologna, Bologna, Italy, [3]Gynecologic Oncology Unit, S.Orsola-Malpighi Hospital, University of Bologna, Bologna, Italy, [4]S. Orsola-Malpighi Hospital, University of Bologna, Modena, Italy, [5]University of Bologna School of Medicine, Bologna, Italy

Disclosures: Antonio De Leo: None; Dario de Biase: None; Sara Coluccelli: None; Giulia Dondi: None; Pierandrea De Iaco: None; Anna Myriam Perrone: None; Donatella Santini: None; Giovanni Tallini: None; Claudio Ceccarelli: None

Background: The Cancer Genome Atlas (TCGA) molecular classification of endometrial carcinomas (EC) into DNA polymerase epsilon mutant (POLEmut), mismatch repair deficient (MMRd), p53 mutant (p53abn) and no specific molecular profile (NS) groups has relevant prognostic impact. Our aim is to investigate the clinicopathologic and prognostic impact of ARID1A alteration in a cohort of ECs classified into TCGA molecular groups.

Design: Clinical and follow-up data, histotype, grade, necrosis, mitoses, Ki-67 proliferation index, pattern of myometrial invasion, lymph vascular invasion, stromal and intraepithelial tumor-infiltrating lymphocytes (sTILs and iTILs), FIGO stage were analyzed in a cohort of 90 ECs. Immunohistochemistry and/or Next-Generation Sequencing (NGS) were used to assign TCGA groups according to ProMisE system and to investigate molecular alterations of multiple target genes including POLE, PTEN, ARID1A, ß-catenin, TP53, MLH1, PMS2, MSH2, MSH6 and L1CAM.

Results: TCGA class assignment: 30 MMRd (33.3%), 7 POLEmut (7.7%), 18 p53abn (20%) and 35 NS (38.9%). TCGA groups are significantly associated with different grade, sTILs, iTILs, mitoses, Ki-67 index, pattern of invasion, L1CAM expression. Each TCGA class was further subdivided based on ARID1A loss/mutation (*A) and on ß-catenin nuclear expression/mutation (*ß) as follows: POLEmut, POLEmut(*A), p53abn, p53abn(*A), MMRd, MMRd(*A), NS, NS(*A), NS(*ß), NS(*ß)(*A). Loss/mutation of ARID1A (*A subgroups) is associated with higher grade (p<0.0001), increase of sTILs and iTILs (p=0.011 and p=0.0006, respectively), necrosis (p=0.018), higher mitotic and Ki-67 proliferation indexes (p<0.0001), MELF pattern of invasion (p=0.048), tumor budding (p=0.004), and L1CAM expression (p<0.0001) in MMRd and NS tumors. ARID1A alteration (*A) is not associated with clinicopathological features or L1CAM expression in POLEmut and p53abn tumors. Seven of 90 (7.7%) ECs recurred (median follow-up 11 months, range 1-99): 4 NS (*A), 1 MMRd (*A), 2 p53abn.

Figure 1 - 1084
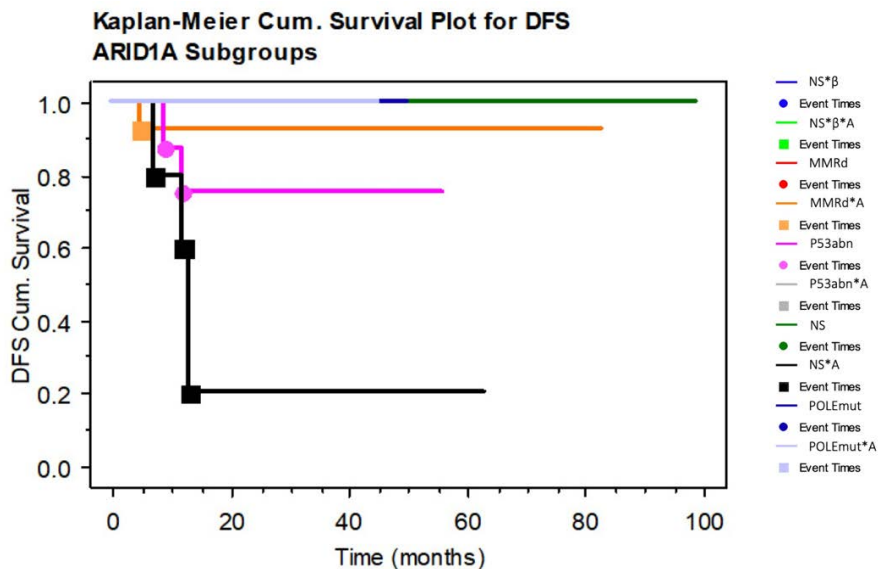
Conclusions: In MMRd and NS groups loss of ARID1A correlates with aggressive clinicopathologic features, including higher grade, increased proliferation, specific invasion patterns (MELF and/or budding), TILs, and worse disease-free survival. ARID1A analysis represents a useful tool to stratify EC risk, and it appears particularly promising for the TCGA NS group.

1085 Exploring the Immune Landscape of Squamous Cell Neoplasia of the Vulva

Hany Deirawan[1], Saivaishnavi Kamatham[2], Joseph Trak[2], Nabil Rahoui[2], Vishakha Pardeshi[3], Mohamad D EL Abdallah[4], Ibrahim Tsolakian[5], Andrew Toma[2], Michael Salloum[6], Kang Chen[7], Rouba Ali-Fehmi[2]
[1]Detroit Medical Center/Wayne State University, Detroit, MI, [2]Wayne State University, Detroit, MI, [3]Westland, MI, [4]Wayne State University, Dearborn Heights, MI, [5]Wayne State University/Detroit Medical Center, Livonia, MI, [6]Wayne State University, Bloomfield Hills, MI, [7]Wayne State University and National Institutes of Health, Detroit, MI

Disclosures: Hany Deirawan: None; Saivaishnavi Kamatham: None; Joseph Trak: None; Nabil Rahoui: None; Vishakha Pardeshi: None; Mohamad D EL Abdallah: None; Ibrahim Tsolakian: None; Andrew Toma: None; Michael Salloum: None; Kang Chen: None; Rouba Ali-Fehmi: None

Background: The overall incidence of vulvar neoplasia has increased multifold, a phenomenon only partially explained by an aging population and improvements in detection rate. The tumor immune microenvironment (TIME) of vulvar cancer is not well studied and has lagged behind because of its exclusion from The Cancer Genome Atlas (TCGA) cohort. The exact sequence of events in the carcinogenesis of vulvar squamous cell carcinoma (vSCC) and the role of the immune response in progression is not fully established. Studying the immune landscape of vSCC offers an opportunity for identifying novel markers of tumor biology and predicting response to immune checkpoint blockade.

Design: We retrospectively identified cases of vulvar intraepithelial neoplasia (VIN3) (n=43) and vSCC (n=46). p53 immunohistochemical labeling was interpreted according to published criteria, and a 1% positivity threshold was adopted for PD-L1. Semi-quantitative assessment of immune fraction and immune cell localization on routine histology with a threshold of 5% to be considered positive was used.

Results: Aberrant PD-L1 expression in tumor cells, defined as staining in more than 1% of cases, was evident in 46.51% and 50% of VIN3 and vSCC cases, respectively. Expression of p53 consistent with non-silent mutations was seen in 23.25% of VIN3 cases and in 21.73% of vSCC cases. There was a strong correlation between p53 mutant vSCC and PD-L1 positivity as shown in Figure 1.

Pattern and extent of immune infiltration was assessed in VIN3 and vSCC. Immune evasion was evident in 47% in VIN3 and 25% of vSCC, respectively. A higher incidence of intraepithelial tumor-infiltrating lymphocytes (TILs[IE]) was observed in PD-L1+ vSCC as illustrated in Table 1. Furthermore, a stromal TIL component was present in 75% of PD-L1+ vSCC vs 31.4% of PD-L1- vSCC cases. Lymphoid aggregates reminiscent of tertiary lymphoid structures were seen more often in PD-L1+ vSCC (62.5% vs. 22.8%) and with plasma cells (≥50%) being a significant component of these aggregates in 60% of vSCC cases. Finally, absence of organized lymphoid structures (OLS) or TILs at the invasive margin in vSCC correlated with an absence of PD-L1 expression as shown in Figure 2.

Table 1. The localization of immune cells in VIN3 and vSCC (expressed as frequency per distinct group)

| Frequency per group	Cases with immune infiltration		
	VIN3	PD-L1+ SCC	PD-L1- SCC
TILs[IE]	13 %	50 %	20 %
Lichenoid/invasive margin TILs	53%	75%	22.8%
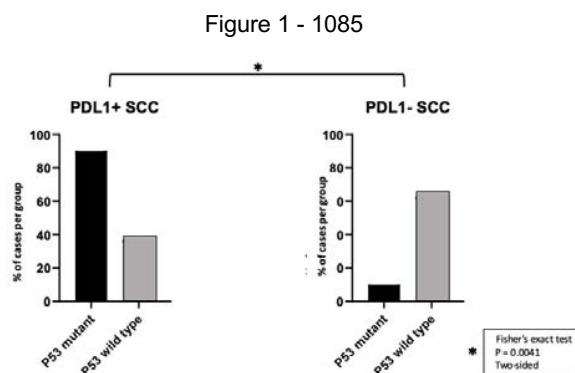
Figure 1 - 1085

Figure 1. Impact of p53 mutations on PD-L1 status in vSCC

Figure 2 - 1085
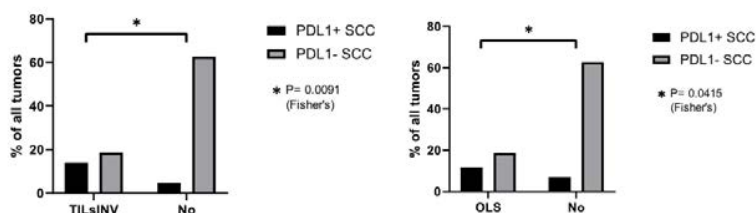
Figure 2. Impact of PD-L1 expression of vSCC on lymphocytes localization to the invasive margin (INV) and organized lymphoid structures (OLS)

Conclusions: The role of HPV status and p53 in evaluating the treatment modalities and the biologic potential of vSCC can be enhanced by a robust cost-effective in-situ assessment of the TIME. This can also help identify novel driver mutations and survival mechanisms of cancer cells.

1086   A Multiplex SNaPshot Assay is a Rapid and Cost-Effective Method for Detecting POLE Mutations in Endometrial Carcinoma

Kelly Devereaux[1], David Steiner[2], Chandler Ho[3], Adam Gomez[4], Linda Gojenola[3], C. Blake Gilks[5], Teri Longacre[6], James Zehnder[1], Brooke Howitt[1], Carlos Suarez[7]

[1]Stanford University School of Medicine, Stanford, CA, [2]Stanford University School of Medicine, Redwood City, CA, [3]Stanford University Medical Center, Palo Alto, CA, [4]Phoenix VA HCS, Phoenix, AZ, [5]Vancouver General Hospital, Vancouver, BC, [6]Stanford University, Stanford, CA, [7]Stanford University School of Medicine, Palo Alto, CA

Disclosures: Kelly Devereaux: None; David Steiner: *Employee*, Google; *Stock Ownership*, Google; Chandler Ho: None; Adam Gomez: None; Linda Gojenola: None; C. Blake Gilks: None; Teri Longacre: None; James Zehnder: None; Brooke Howitt: None; Carlos Suarez: None

Background: *POLE* mutation status in endometrial carcinoma (EC) has important clinical implications, specifically recent evidence suggests that it defines a prognostically favorable subgroup, even amongst high-grade histotypes. Currently, there are no specific morphologic or immunophenotypic features that allow accurate detection of *POLE*-mutated tumors without molecular testing. Consequently, identifying *POLE*-mutated tumors has been challenging without employing costly and time consuming DNA sequencing approaches. Here we developed a novel SNaPshot assay in order to routinely and efficiently test for *POLE* mutations in ECs.

Design: A custom single nucleotide extension SNaPshot assay was optimized on DNA extracted from FFPE tissue. Exonuclease domain *POLE* exons are initially PCR amplified. Hotspot single nucleotide variants are then interrogated by single-base extension, whereby DNA polymerase adds a single fluorescently-labeled dideoxynucleotide (ddNTP) to the 3' end of unlabeled, differentially sized oligonucleotide primers. SNaPshot products are analyzed by capillary electrophoresis and resolved by length and fluorescence.

Results: The SNaPshot assay detects 15 somatic mutation sites within exons 9, 11, 13, and 14 of the *POLE* exonuclease domain. Sites were selected based on evidence of functional impact, association with high tumor mutation burden, and/or mutations reported in clinical outcome studies for ECs. Based on the pathogenic somatic variants previously reported in the literature, the assay is predicted to have a clinical sensitivity of 90-95% for ECs. Validation studies showed 100% specificity and sensitivity for the variants covered, with expected genotypic results for both the positive (n=10) and negative (n=20) patient controls. Analytic sensitivity was conservatively approximated at a 10% variant allele fraction (VAF), with documented detection as low as 5% VAF. As expected, the SNaPshot assay has greater sensitivity than Sanger sequencing, which can only reliably detect variants down to 20% VAF.

Conclusions: We have developed and validated the first SNaPshot assay to detect hotspot exonuclease domain mutations in *POLE*. While NGS and Sanger sequencing-based approaches have also been used to detect *POLE* mutations, a SNaPshot approach was chosen to provide a more optimal balance of analytical sensitivity, cost-effectiveness and efficiency in a high-volume case load setting. This assay is accurate, scalable and may be more suitable for clinical use.

1087 Molecular Classification of Metastatic and Recurrent Endometrial Endometrioid Carcinoma

Kelly Devereaux[1], Stephanie Chow[1], David Steiner[2], Grace Peters-Schulze[3], Chandler Ho[4], Carlos Suarez[5], Ann Folkins[1], Brooke Howitt[1]
[1]Stanford University School of Medicine, Stanford, CA, [2]Stanford University School of Medicine, Redwood City, CA, [3]Stanford University, Stanford, CA, [4]Stanford University Medical Center, Palo Alto, CA, [5]Stanford University School of Medicine, Palo Alto, CA

Disclosures: Kelly Devereaux: None; Stephanie Chow: None; David Steiner: *Employee*, Google; *Employee*, Google; Grace Peters-Schulze: None; Chandler Ho: None; Carlos Suarez: None; Ann Folkins: None; Brooke Howitt: None

Background: Endometrial endometrioid carcinoma (EEC) has variable clinical outcomes. Molecular classification per The Cancer Genome Atlas (TCGA) study may improve prognostication in EEC as well as have treatment implications: *POLE*-mutated, microsatellite instability (MSI), p53 abnormal (p53 abnl), and no specific molecular profile (NSMP). This study classifies metastatic/recurrent ECC into molecular groups to examine the correlation with pattern of disease and outcomes.

Design: EECs metastatic at the time of diagnosis or with documented recurrent/metastatic disease were included. Clinicopathologic features, including clinical status at last follow-up, were recorded. Metastatic/recurrent disease sites were subclassified: vaginal cuff, adnexal, abdominal, lymph node (LN), or distant. Immunohistochemistry (IHC) for PMS2, MSH6, p53 and *POLE* sequencing were performed to establish TCGA molecular classification.

Results: Of 128 patients with EEC, 266 samples (104 primary; 162 metastatic) were included. Primary and matched metastasis was tested in 97 patients. Cases were classified as *POLE*-mutated (8; 6%), MSI (41; 32%), p53 abnl (16; 13%), or NSMP (63; 49%) (Table 1). 66 (53%) presented with metastasis at the time of diagnosis, 44 (35%) had recurrence, and 15 (12%) had both. Discordant classification between primary and metastatic EEC was seen in 4/97 (4%), all related to PMS2/MSH6 IHC. Grade 1 EEC was most likely to be NSMP (80%), while the majority of grade 2 were MSI (54%) and grade 3 was most commonly p53 abnl (42%). Patterns of recurrence compared across TCGA classification are demonstrated in Figure 1. Status at last clinical follow-up revealed the majority of p53 abnl EECs were dead of disease (DOD) or alive with disease (AWD), while the other groups had similar distributions amongst AWD, DOD, and alive with no evidence of disease (ANED) (Figure 2). Notably, the *POLE*-mutated group included 2 patients who were DOD.

Classification	Cases	Grade of Primary EEC			
		1	2	3	Unknown
NSMP	63 (49%)	32 (51%)	19 (30%)	7 (11%)	5 (8%)
MSI	41 (32%)	5 (12%)	26 (63%)	9 (22%)	1 (2%)
POLE MUTATED	8 (6%)	2 (25%)	2 (25%)	3 (38%)	1 (13%)
p53 ABNORMAL	16 (13%)	1 (6%)	1 (6%)	14 (88%)	0 (0%)
Total	**128 (100%)**	**40 (31%)**	**48 (38%)**	**33 (26%)**	**7 (5%)**

Figure 1 - 1087
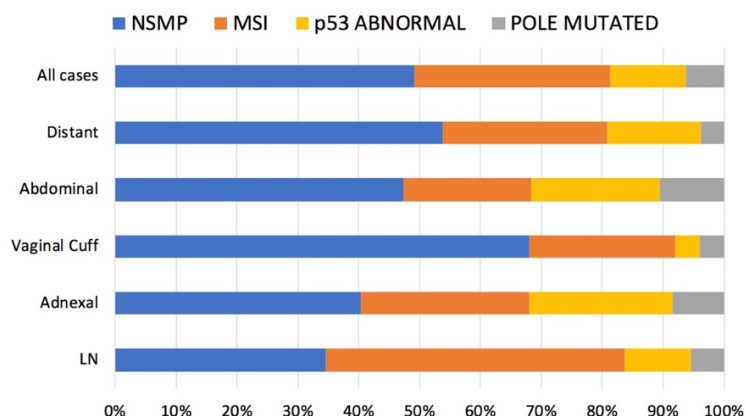
Figure 1. Pattern of disease recurrence based on TCGA molecular classification.

Figure 2 - 1087
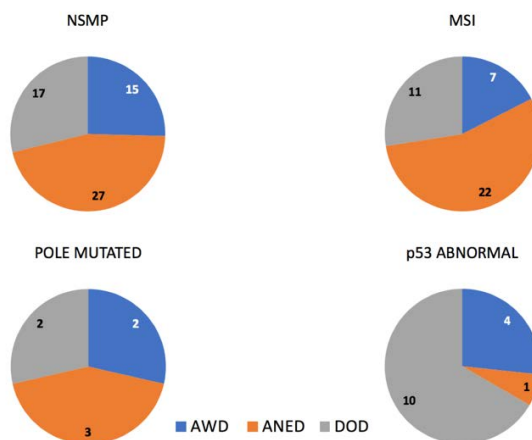
Figure 2. Status at last clinical follow-up grouped by TCGA molecular classification (numbers reflect total number of cases in each category).

Conclusions: TCGA molecular classification in metastatic/recurrent EEC is similar to what is generally reported in EEC.   Discrepant classification between primary and metastatic sites was associated with MSI status, suggesting a relationship with tumor heterogeneity and hypermutation. Molecular studies to assess for tumor mutational burden are underway. Based on classification as MSI/*POLE*-mutated, 38% of metastatic EEC may benefit from immune checkpoint inhibition. Metastatic EEC classified as p53 abnl had the worst clinical outcomes.

1088 Pregnancy-Associated Inflammatory Myofibroblastic Tumors of the Uterus are Clinically Distinct and Highly Enriched for ALK-TIMP3 and ALK-THBS1 Fusions

Kelly Devereaux[1], Megan Fitzpatrick[2], Charles Bangs[3], Sara Hartinger[4], Carol Jones[3], Christian Kunder[1], Teri Longacre[4]
[1]Stanford University School of Medicine, Stanford, CA, [2]Stanford Health Care, Palo Alto, CA, [3]Stanford University, Palo Alto, CA, [4]Stanford University, Stanford, CA

Disclosures: Kelly Devereaux: None; Megan Fitzpatrick: None; Charles Bangs: None; Sara Hartinger: None; Carol Jones: None; Christian Kunder: None; Teri Longacre: None

Background: As ALK-positive inflammatory myofibroblastic tumors (IMTs) have become more widely recognized in the female genital tract, an intriguing subset of tumors associated with pregnancy has emerged. Whether IMTs arising in the setting of pregnancy have a distinct biology and/or disease course compared to non-pregnancy associated IMTs remains unknown. Furthermore, little is known about the clinical and perinatal factors that may influence the development these tumors. Here we report the largest case series of pregnancy-associated IMTs to address these outstanding questions.

Design: A total of eight cases of pregnancy-associated IMTs of uterus were retrospectively reviewed for this study. ALK IHC and fluorescent in situ hybridization (FISH) studies were performed on whole sections. Anchored multiplex PCR and RNA-sequencing techniques were used to identify gene fusions in each tumor.

Results: Pregnancy-associated IMTs occur in association with pregnancy complications, including abnormal implantation, gestational diabetes, pre-eclampsia or coagulopathy. Notably, 7 of 8 IMTs were expelled at the time of delivery as either adherent to placenta or separate, detached tissue. Tumors are small (mean 4 cm), well-circumscribed and histologically show prominent myxoid stroma and a lymphoplasmacytic infiltrate. Granular cytoplasmic and perinuclear ALK IHC staining and a classic *ALK* rearrangement break-apart FISH pattern are seen in 7 out of 8 cases. Of these 7 *ALK*-rearranged tumors, 5 harbor *ALK-TIMP3* and 2 harbor *ALK-THBS1* fusion transcripts. The remaining eighth case has morphologic features of an IMT and is positive by ALK IHC, but lacks *ALK* rearrangement by FISH or a detectable fusion transcript by our methodology. Women with pregnancy associated IMTs do not appear to be at risk of recurrent disease based on short-term follow-up.

Conclusions: Our findings suggest that pregnancy-associated IMTs may arise in association with aberrant endometrial remodeling and placentation during complications of pregnancy. Interestingly, pregnancy-associated IMTs seem to harbor *ALK* rearrangements with genes, such as *THBS1* (thrombospondin-1) and *TIMP-3* (metalloproteinase inhibitor 3), that are known to be transcriptionally active in pregnancy and facilitate endometrial remodeling and implantation. Although the length of clinical follow-up in this study is limited, the fact that the majority of tumors are shed at the time of delivery suggests that these are transient tumors with a particularly indolent clinical course.

1089   Long Interspersed Element-1 (LINE-1) Protein Expression is Present in Clear Cell Carcinomas and Early Endometriotic Precursors

Kyle Devins[1], Sho Sato[2], Lauren Schwartz[3], Ronny Drapkin[4]
[1]Hospital of the University of Pennsylvania, Philadelphia, PA, [2]Perelman School of Medicine, University of Pennsylvania, Philadelphia, PA, [3]Perelman School of Medicine at the University of Pennsylvania, Bala Cynwyd, PA, [4]Perelman School of Medicine at the University of Pennsylvania, Philadelphia, PA

Disclosures: Kyle Devins: None; Sho Sato: None; Lauren Schwartz: None; Ronny Drapkin: *Advisory Board Member*, Repare Therapeutics; *Advisory Board Member*, Siamab Therapeutics; *Consultant*, Mersana Therapeutics

Background: Nearly half of the human genome consists of mobile repetitive DNA elements. The most prevalent is the retrotransposon Long Interspersed Element 1 (LINE-1) which contains over 500,000 copies and constitutes nearly 17% of the genome. LINE-1 is typically suppressed to prevent the deleterious consequences of random LINE-1 element insertion into the genome. However, numerous studies demonstrate LINE-1 reactivation in a variety of epithelial cancers. Herein we demonstrate that LORF1, one of the two open reading frames (ORF) encoded by LINE-1, is expressed in a subset of ovarian clear cell carcinomas (CCOC) as well as endometriotic precursor lesions.

Design: Ten CCOC cell lines were cultured to 80% confluence and investigated for LORF1 expression using Western blotting. A tissue microarray (TMA) was also constructed using archival FFPE tissue from 40 cases of CCOC collected from the institutional pathology department. Three 1.0 mm cores were obtained per tumor. Cases were reviewed to confirm initial diagnosis. Controls consisted of numerous benign and malignant human tissues. TMA slides were investigated with LORF1 immunohistochemistry (IHC). Whole-mount slides of benign endometriosis (BEM) (n=11), atypical endometriosis (AEM) (n=8), ovarian endometrioid carcinoma (OEC) (n=11), proliferative phase endometrium (n=5), and secretory phase endometrium (n=5) were also stained for LORF1. LORF1 expression by IHC was scored as follows: 0 (negative), 1+ (weak cytoplasmic positivity), 2+ (moderate staining in >50% of cells), or 3+ (strong, diffuse)(Figure 1). Scores of 0 and 1+ were considered "LORF1 negative" while scored of 2+ and 3+ were considered "LORF1 positive."

Results: Western blot analysis showed that LORF1 protein was readily detectable in CCOC cell lines, but absent in non-tumorigenic fallopian tube cell lines. LORF1 was positive by IHC in 85% of archived cases (See Figure 2 for scoring distribution). A similar rate of positivity was noted in OEC (8/11). In addition, all 7 cases of AEM and 3/11 cases of BEM stained positive for LORF1. Two cases of proliferative endometrium showed LORF1 expression, but all cases of secretory endometrium were negative.

Figure 1 - 1089
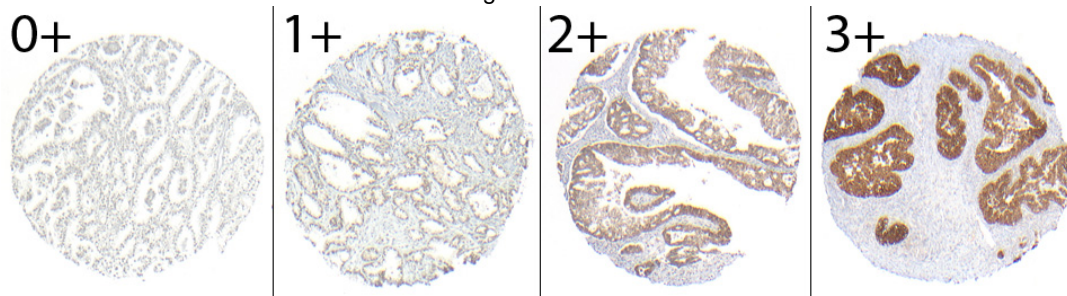
Figure 2 - 1089
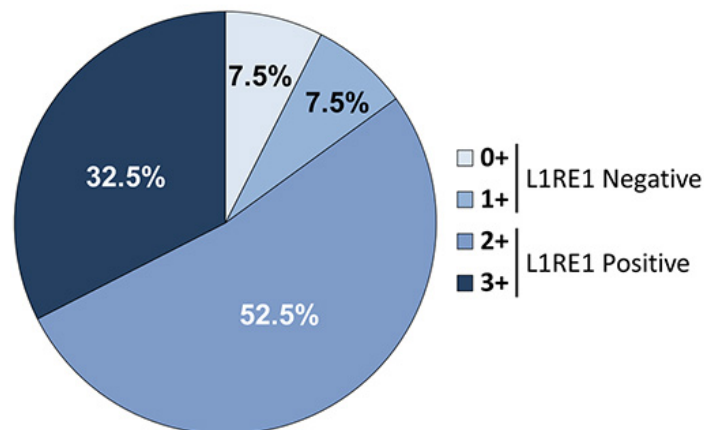
Conclusions: A subset of CCOC and OEC are marked by LORF1 expression, suggesting reactivation of LINE-1 in these tumors. Interestingly, LORF1 expression was also noted in endometrioitic lesions as well as benign endometrium. This suggests LINE-1 reactivation is an early event in the progression from endometriosis to carcinoma.

1090 Comparative Proteomics Identifies EMILIN3 and INA as Novel Markers for Low-Grade Endometrial Stromal Sarcoma

Kyle Devins[1], Dylan Marchione[2], Li-Ping Wang[1], Benjamin Garcia[2], Lauren Schwartz[3], John Wojcik[2]
[1]Hospital of the University of Pennsylvania, Philadelphia, PA, [2]University of Pennsylvania, Philadelphia, PA, [3]Perelman School of Medicine at the University of Pennsylvania, Bala Cynwyd, PA

Disclosures: Kyle Devins: None; Lauren Schwartz: None; John Wojcik: None

Background: Morphologic distinction between LG-ESS and smooth muscle neoplasms, especially highly cellular leiomyoma (HCL), can prove challenging for the pathologist. Detection of gene fusions, most often involving *JAZF1-SUZ12*, can confirm the diagnosis of LG-ESS. However, fusions cannot be detected in all cases due to variant gene partners and availability of testing. Immunohistochemical (IHC) panels to aid in the diagnosis of LG-ESS rely on expression of CD10 and negativity for smooth muscle markers, but IHC is limited by overlapping expression. To improve diagnostic accuracy, we used comparative proteomics to identify novel IHC targets.

Design: Seven cases each of LG-ESS and HCL were selected from archived cases and reviewed to confirm diagnoses. Protein was extracted from FFPE tumor cores using the HYPERsol method and evaluated via liquid chromatography-mass spectrometry. Data was analyzed using Spectronaut Pulsar X.

Tissue microarrays (TMAs) were constructed to test potential IHC markers using cores from FFPE blocks. The TMAs included 9 cases of LG-ESS, 10 HCL, 4 standard leiomyomas, 12 uterine leiomyosarcomas (LMS), and 12 extra-uterine LMS. IHC was performed on a Leica Bond-IIITM instrument using antibodies to EMILIN3 (1:100 dilution, HPA059912, Sigma) and INA (1:200 dilution, HPA008057, Atlas antibodies) and polymer detection per manufacturer protocol (Leica Microsystems RE7230-CE).

Results: An average of 2886 proteins were identified in LG-ESS and 2892 in HCL. Candidate proteins were sorted based on differential expression, focusing on proteins with greater abundance in LG-ESS. NEP/MME (CD10) showed high differential expression in LG-ESS relative to HCL, supporting the utility of our approach. Among novel candidates, elastin microfibril interface-located protein 3 (EMILIN3) and alpha-internexin (INA) were chosen based on expression levels in the tumor samples and tissue expression profiles from the Human Protein Atlas (HPA). IHC testing on TMAs revealed INA to be highly sensitive for LG-ESS (8/8 positive). EMILIN3 was less sensitive (6/8 cases positive) but highly specific for LG-ESS compared to smooth muscle tumors, staining negative in all cases of HCL and LMS. One case of LG-ESS was uninterpretable due to tissue loss.

IHC	Tumor Type	Positive	Total	Percentage
EMILIN3	ESS	6	8	75%
	HCL	0	12	0%
	Uterine LMS	0	12	0%
	EU-LMS	0	12	0%
INA	ESS	8	8	100%
	HCL	1	12	8%
	Uterine LMS	2	12	17%
	EU-LMS	2	12	17%

Figure 1 - 1090   Figure 2 - 1090
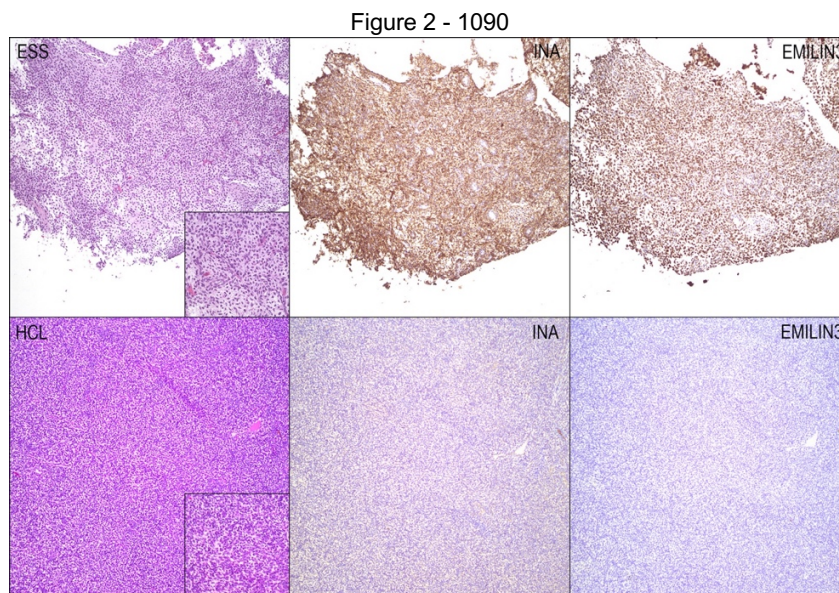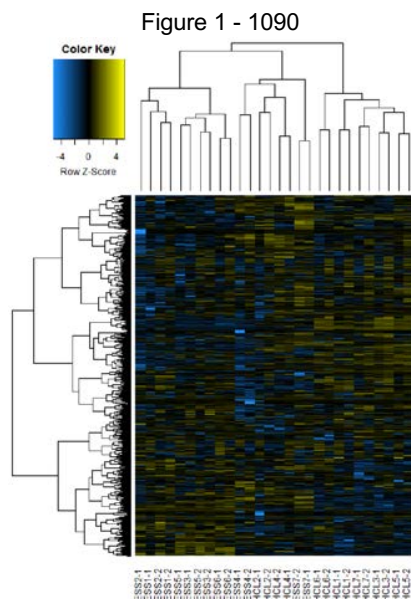
Conclusions: Comparative proteomics of archival specimens identified EMILIN3 and INA as novel diagnostic markers to discriminate between LG-ESS and smooth muscle tumors. These markers have been preliminarily validated on TMAs, and await further validation in larger cohorts.

1091   Ovarian Neuroendocrine Tumors: Pathological and Immunohistochemical Features of a Single-Center Case Series

Doriana Donatella Di Nanni[1], Lucia Domeniconi[2], Francesca Ambrosi[3], Giulia Girolimetti[4], Giacomo Santandrea[1], Donatella Santini[1], Giovanni Tallini[5], Antonio De Leo[1]
[1]S.Orsola-Malpighi Hospital, University of Bologna, Bologna, Italy, [2]Pathology Unit, S. Orsola - Malpighi Hospital, Imola, BO, Italy, [3]S.Orsola-Malpighi Hospital, University of Bologna, Bari, Italy, [4]Department of Medical and Surgical Sciences (DIMEC), Unit of Medical Genetics, University Hospital S.Orsola-Malpighi, Bologna, Italy, [5]University of Bologna School of Medicine, Bologna, Italy

Disclosures: Doriana Donatella Di Nanni: None; Lucia Domeniconi: None; Francesca Ambrosi: None; Giulia Girolimetti: None; Giacomo Santandrea: None; Antonio De Leo: None

Background: Primary neuroendocrine neoplasms (NENs) of the ovary are exceptionally rare entities, mostly arising in mature teratomas. The current pathologic classification of ovarian NENs is morphology-based, a significantly different approach from the standard terminology of gastroenteropancreatic (GEP) NENs. The aim of this study was to analyze the clinicopathological and immunohistochemical features of ovarian neuroendocrine neoplasms and to reclassify this series according to GEP NEN classification.

Design: All cases of ovarian NENs were histologically reviewed according to WHO 2014 Female Genital Tract classification. An immunohistochemical (IHC) panel consisting of Synaptophysin, Chromogranin, Serotonin, Somatostatin Receptor Subtype 2A (SSTR2A), Somatostatin Receptor Subtype 5 (SSTR5), CDX2, TTF-1 and PAX8 was applied. Ki-67 proliferation index was assessed by digital imaging analysis according to the GEP NEN classification. Targeted Next-Generation Sequencing (NGS) analysis was performed in 2 particular cases.

Results: A total of 27 cases was collected, including 12 primary and 15 metastatic neoplasms. Patients median age was 43 years old. According to the WHO 2014 classification, insular carcinoids were 6 cases (50%), trabecular carcinoids 2 (16.7%), strumal-carcinoids 3 (25%), small cell carcinoma of the ovary, pulmonary type (SCCOPT) 1(8.3%). All carcinoids were stage pT1a and were associated with other ovarian neoplasms. The SCCOPT was the only pure NEN, staged as pT3c. Adopting the GEP NEN classification, 7 (58.3%) cases were classified as NET G1, 3 (25%) as NET G2, 1 (8.3%) as NET G3 and 1 (8.3%) as NEC. All cases showed a diffuse positivity for Synaptophysin and Chromogranin. SSTR2A positivity was associated with insular and strumal carcinoids, while SSTR5 and CDX2 was observed in trabecular carcinoids. SCCOPT showed a diffuse positivity for TTF-1, p53 and p16. The molecular analysis demonstrated *TP53* and *IDH1* mutations in one case of NET G3 tumor associated to a Sertoli cell tumor, and *TP53* mutation with mTOR pathway alteration in SSCOPT.

Conclusions: The current WHO 2014 classification showed a consistent immunoprofile for each subtype. The application of GEP NEN classification, including Ki-67 proliferation index, is feasible and better discriminates tumor grade. This approach substantiates the importance of a common classification for NENs reducing inconsistencies and contradictions among the various systems currently in use, allowing a more uniform diagnosis and clinical management.

1092 Loss of MHC Class I Expression in PD-L1-positive HPV-Associated Cervical and Vulvar Neoplasia: A Mechanism of Resistance to Checkpoint Inhibition?

Megan Dibbern[1], Timothy Bullock[2], Linda Duska[2], Mark Stoler[3], Anne Mills[2]
[1]University of Virginia Health System, Charlottesville, VA, [2]University of Virginia, Charlottesville, VA, [3]University of Virginia Health System, Earlysville, VA

Disclosures: Megan Dibbern: None; Timothy Bullock: None; Linda Duska: None; Mark Stoler: None; Anne Mills: None

Background: Decreased expression of major histocompatibility complex class I (MHC I) on tumor cells precludes antigen presentation and therefore prevents immune recognition. Alterations in MHC I expression are thought to compound immune escape and contribute to immunotherapeutic resistance in PD-L1-positive gastric and non-small cell lung carcinomas, but this has not been previously studied in cervical and vulvar cancers. Given the recent FDA approval of anti-PD-1 checkpoint inhibition in PD-L1-positive cervical squamous carcinomas, identifying tumors with loss of MHC I is of clinical interest.

Design: Immunohistochemistry for PD-L1 and MHC I combined A-, B-, and C- heavy chains was assessed in 58 HPV-associated cervical and vulvar lesions, including squamous intraepithelial lesions (SIL) and invasive squamous cell carcinoma (SCC) (15 CIN3, 13 cervical SCC, 12 VIN3, and 18 vulvar SCC cases). PD-L1 expression was classified as present or absent using the combined positive score (CPS) with a threshold of ≥1 required for positivity. MHC I staining was classified as present, clonally lost, or absent.

Results: Although 83.9% of SCC and 22.2% of SIL were PD-L1-positive, 33.5% (11/31) of SCC and 18.5% (5/27) of SIL also showed clonal or complete loss of MHC Class I. Loss of MHC I expression was more common in PD-L1-positive (10/26, 38.5%) vs. PD-L1-negative SCC (1/5, 20%). Among PD-L1-positive SCC, loss of MHC I expression is more common in cervical SCC (5/11, 45.5%) than vulvar SCC (5/15, 33.3%). However, neither of these differences was statistically significant.

	MHC Class I Expression Pattern		
	Intact (%)	**Clonal Loss (%)**	**Complete Loss (%)**
All SCC (n=31)	20 (64.5)	9 (29.0)	2 (6.5)
Cervical SCC (n=13)	8 (61.5)	5 (38.5)	0 (0)
Vulvar SCC (n=18)	12 (66.7)	4 (22.2)	2 (11.1)
All SIL (n=27)	22 (81.5)	5 (18.5)	0 (0)
CIN3 (n=15)	12(80)	3 (20)	0 (0)
VIN3 (n=12)	10 (83.3)	2 (16.7)	0 (0)

PD-L1+ (CPS≥1)					**PD-L1- (CPS<1)**			
MHC Class I Expression Pattern	**Intact (%)**	**Clonal Loss (%)**	**Complete Loss (%)**	**MHC Class I Expression Pattern**	**Intact (%)**	**Clonal Loss (%)**	**Complete Loss (%)**
All SCC (n=26)	16 (61.5)	8 (30.8)	2 (7.7)	*All SCC (n=5)*	4 (80.0)	1 (20.0)	0 (0)
Cervical SCC (n=11)	6 (54.5)	5 (45.5)	0 (0)	*Cervical SCC (n=2)*	2 (100)	0 (0)	0 (0)
Vulvar SCC (n=15)	10 (66.7)	3 (20.0)	2 (13.3)	*Vulvar SCC (n=3)*	2 (66.7)	1 (33.3)	0 (0)
All SIL (n=6)	5 (80.0)	1 (20.0)	0 (0)	*All SIL (n=21)*	17 (81.0)	4 (19.0)	0 (0)
CIN3 (n=2)	1 (50.0)	1 (50.0)	0 (0)	*CIN3 (n=13)*	11 (84.6)	2 (15.4)	0 (0)
VIN3 (n=4)	4 (100)	0 (0)	0 (0)	*VIN3 (n=8)*	6 (75.0)	2 (25.0)	0 (0)

Figure 1 - 1092
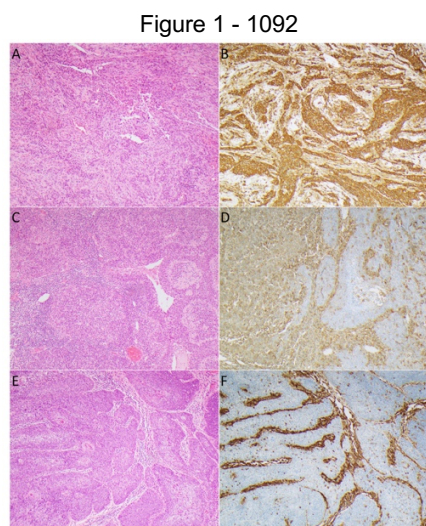
Figure 1: Patterns of MHC Class I Expression in Cervical & Vulvar SCC. MHC Class I expression was scored as intact (Case A-B), clonally lost (Case C-D), or completely absent (Case E-F).

Figure 2 - 1092
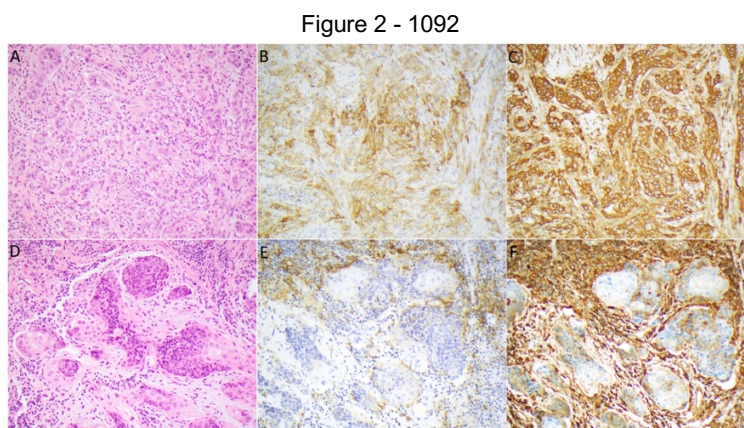
Figure 2: Relationship between PD-L1 and MHC Class I in Cervical SCC. Some tumors, like the case depicted in A-C, demonstrated strong diffuse PD-L1 expression (B) with intact MHC Class I (C), suggesting that this tumor likely remains vulnerable to PD-1/PD-L1 inhibition. Others, like the case shown in D-F, show positive PD-L1 expression (E, positivity seen predominantly in tumor-associated lymphocytes and macrophages) but have loss of MHC Class I (F), suggesting that this tumor may be a poor candidate for checkpoint inhibition targeting the PD-1/PD-L1 axis despite its positive CPS score.

Conclusions: Over one-third of HPV-associated cervical and vulvar SCC show clonal or complete loss of MHC I expression. This suggests that response to therapies targeting the PD-1/PD-L1 axis may be inhibited in a subset of cervical and vulvar neoplasms due to an impaired ability to engage with the immune system related to loss of MHC Class I expression.

1093 Mismatch Repair Deficiency in Endometrial Carcinosarcomas

Jessica Dillon[1], Laura Tafe[2]
[1]Dartmouth Hitchcock Medical Center, Lebanon, NH, [2]Dartmouth-Hitchcock Medical Center, Lebanon, NH

Disclosures: Jessica Dillon: None; Laura Tafe: None

Background: Endometrial carcinosarcoma (ECS) is a rare high-grade, biphasic endometrial carcinoma composed of malignant epithelial and mesenchymal elements derived via divergent differentiation. The carcinoma component is high-grade and may be further classified as serous-like or endometrioid-like based on molecular findings (*PTEN*, *ARID1A*, *PPP2R1A* and/or *TP53* mutations) (PMID: 28292439). The sarcoma component may have homologous or heterologous elements. ECS have aggressive clinical features with high rates of recurrence and a 5-yr progression free survival of 20-35% with advanced stage disease. Identifying therapeutic vulnerabilities in ECS are key to improving patient outcomes.

Design: At our institution, mismatch repair (MMR) immunohistochemistry (IHC) analysis with antibodies against MLH1, PMS2, MSH2, MSH6 was implemented in 2015 as part of Lynch syndrome screening in endometrial cancers. With recent tumor agnostic approval of certain immunotherapy agents with MMR deficiency or microsatellite instability, MMR screening also plays an important role in determining eligibility for immunotherapy. *MLH1* promoter methylation is reflexively ordered on any tumor that shows loss of MLH1/PMS2 by IHC.

Results: From 2015 to present, 31 cases of ECS were identified in the pathology archives. 22 cases had undergone testing for MMR by IHC (3.4% of cases tested; 22/653). The patient age range was 52-82 with the exception on one patient who was 25 at diagnosis. Tumor stage was: IA (6); IB (5); II (1); IIIA (4); IIIC (1); IV (4), and one is not yet staged. Three (13.6%) showed loss of MLH1 and PMS2 in both the carcinoma and sarcoma components. Somatic *MLH1* promoter methylation was identified in all three cases. All three were low stage (IA/IB/IB) and the sarcomatous component was comprised solely of homologous elements. Morphologically, in two cases the carcinomatous component had endometrioid features, one with foci of squamous differentiation. The third had a solid growth pattern not further classifiable by morphology alone. Tumor infiltrative lymphocytes were present in all three cases.

Conclusions: Similar to our findings, the TCGA ECS cohort identified 2/57 cases with loss of MLH1/PMS2 and *MLH1* promoter hypermethylation. Both of these cases were classified as endometrioid-like based on *PTEN* alterations. MMR deficiency is a rare event in a subset of ECS with endometrioid-like features. In addition, identification of MMR deficiency offers a new therapeutic opportunity with available immunotherapies.

1094   Digital Image Analysis for the Diagnosis of Differentiated Vulvar Intraepithelial Neoplasia and Distinction from Benign Mimickers

Soufiane El Hallani[1], Eric Yang[2], Kelly Devereaux[2], Anita Carraro[3], Jagoda Korbelic[3], Arash Javanmardi[3], Alan Harisson[3], Martial Guillaud[4]
[1]University of Alberta, Edmonton, AB, [2]Stanford University School of Medicine, Stanford, CA, [3]BC Cancer Agency, Vancouver, BC, [4]Vancouver, AB

Disclosures: Soufiane El Hallani: None; Eric Yang: None; Kelly Devereaux: None

Background: Differentiated vulvar intraepithelial neoplasia (DVIN) possesses a high oncogenic potential but the high degree of differentiation often results in DVINs being mistakenly diagnosed as benign lesions. The p53 immunohistochemistry marker can be used to support the DVIN diagnosis; however, the characteristic suprabasal p53 overexpression can be encountered in any benign condition in which there is increased epithelial proliferation, and the p53 null-pattern can be subtle and difficult to recognize. A more accurate diagnostic aid tool is needed. We here investigate the role of chromatin-based image analysis in distinguishing DVIN and benign mimickers.

Design: Eighty-two vulva biopsy specimens with 4 major diagnosis categories are selected: Lichen simplex chronicus (n=34); (2) Lichen sclerosis (n=21); DVIN (n=10); squamous cell carcinoma (n=17). All diagnoses are verified by subspecialized gynecologic pathologists based on strict diagnostic criteria and immunohistochemistry. One tissue section is stained with Feulgen-Thionin which binds the nuclear DNA. The regions of interest are delineated manually by pathologist on the digitalized slides and an in-house image analyzer software calculate multiple nuclear features including nuclear shapes and chromatin texture (Figure 1). Statistical stides are performed to compare the performance of combined features to accurately classify the specimens and generate a classifier model.

Results: A total of 44,483 nuclei were individually analysed for over 100 nuclear morphologic and chromatin parameters. The parameter's average per each specimen is included in a stepwise discriminant analysis. The classifyer model has an overall accuracy of 95.5% in distinguishing DVIN versus lichen simplex chronicus (table1), and overall accuracy of 96.8% in distinguishing DVIN versus lichen sclerosis (table 1). The classifier model has a negative predictive value of 96.5% (95% CI: 89% to 99%), positive predictive value of 89% (95% CI: 53% to 98%), sensitivity of 80% (95% CI: 45% to 98%) and specificity of 98% (95% CI: 90% to 99.9%) in distinguishing DVIN from lichen simplex chronicus.

			Observed	
		Accuracy	Lichen simplex	DVIN
Predicted	Lichen simplex	100%	34	0
	DVIN	80%	2	8
	Total	95.50%		
			Observed	
		Accuracy	Lichen sclerosis	DVIN
Predicted	Lichen sclerosis	95.30%	20	1
	DVIN	100%	0	10
	Total	96.80%		

Figure 1 - 1094

A   B
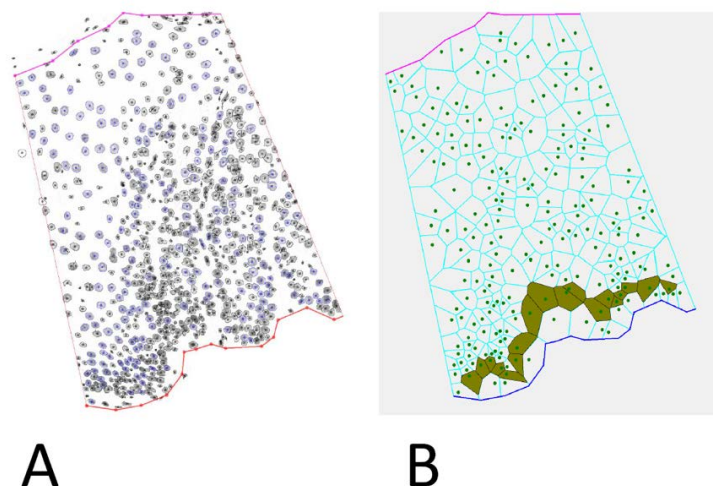
Conclusions: The chromatin-based image analysis is a promising aid tool to reliably rule out benign mimickers when the diagnosis of DVIN is considered based on morphology or p53 immunohistochemistry. In the near future, the integration of such image analysis tools in the pathology practice will be facilitated by further adoption of digital pathology in the workflow environment.

1095 High-Grade Serous Carcinoma (HGSC) of the Ovary: An Immunohistochemical and Molecular Comparative Study of Long and Short-Term Survivors

Gonçalo Esteves[1], Bárbara Mesquita[2], Marta Ferreira[3], Sara Teles[3], Madalena Santos[4], António Guimarães[4], Carla Oliveira[5], Ana Félix[6]

[1]Instituto Português de Oncologia de Lisboa Francisco Gentil, Lisboa, Portugal, [2]Instituto de Investigação e Inovação em Saúde (i3S), Vila do Conde, Porto, Portugal, [3]Instituto de Investigação e Inovação em Saúde (i3S), Porto, Portugal, [4]Instituto Português de Oncologia de Lisboa Francisco Gentil (IPOLFG), Lisbon, Portugal, [5]Institute of Molecular Pathology and Immunology (IPATIMUP)/Instituto de Investigação e Inovação em Saúde (i3S), Porto, Portugal, [6]Instituto Português de Oncologia de Lisboa/CEDOC, Lisboa, Portugal

Disclosures: Gonçalo Esteves: None; Bárbara Mesquita: None; Marta Ferreira: None; Sara Teles: None; Madalena Santos: None; António Guimarães: None; Carla Oliveira: None; Ana Félix: None

Background: HGSC is the most frequent and deadliest ovarian cancer. After surgery and chemotherapy, patients (pts) eventually relapse with chemoresistant disease, dying within 5 years of diagnosis.

Design: We compared a group of 10-year-long survivors (A; n=14pts), who either never relapsed or had multiple chemosensitive relapses, with one of ≤3-year-long survivors (B; n=14pts), to elucidate if transcriptomic profiles and epigenetic markers might explain differences between therapeutic response and survival.

All cases were reviewed and confirmed. HDAC1,2,3,4,6, pHDAC4,5,7 were evaluated in a TMA by IHC. DNA and RNA were extracted from FFPE tissue (14[A]+14[B] primaries + 9[A] relapses). Fusion transcript and differential gene expression analysis were performed using Ion AmpliSeq™/Ion Torrent Proton™ technology and the Oncomine Focus assay, followed by bioinformatics analysis with EdgeR Bioconductor package. *BRCA* genes were studied in 13[A] tumors by targeted NGS. Differentially expressed genes were validated by RT-PCR, and *BRCA* variants by Sanger sequencing.

Results: Complete remission was achieved in 10pts[A] after surgery+chemotherapy. At the end of follow-up, 8pts[A] relapsed up to 8 times; 6[A] were alive without disease and 3[A]+14[B] died of disease. Immunohistochemistry (Table 1) showed HDAC1 expression in all but 2 primaries (pts with more relapses, having died with active disease). HDAC3 negativity was strongly correlated with survival >3 years (*p*=0.0019).

Clustering analysis showed a specific transcriptional profile (25 genes) shared by all relapses and differing from primary cancers (Fig 1). Expression of 16 genes distinguished primaries with multiple relapses from those without/with a single relapse, and 1 gene was specifically upregulated in tumors from non-relapsing patients (*MCMBP*) (Fig 2). Primary tumors from pts with multiple relapses showed downregulation of mitotic cell division and chromosome segregation associated genes, unlike pts without/with a single relapse. The *HLA-AES* fusion transcript was identified in a non-relapsing case. Two *BRCA1* mutations were identified in 2pts[A] showing a similar transcriptomic profile and hinting to *BRCA*-driven tumorigenesis.

	N	HDAC1	HDAC2	HDAC3	HDAC4 (membrane)	HDAC4 (cytoplasm)	HDAC6	pHDAC 4, 5, 7 (cytoplasm)
Primary tumors: Long-term survivors [A]	13	11 (85%)	13 (100%)	6 (47 %)	1 (8 %)	9 (70 %)	9 (70 %)	7 (54 %)
Primary tumors: Short-term survivors [B]	14	12 (85%)	14 (100%)	14 (100 %)	9 (65 %)	13 (93 %)	13 (93 %)	14 (100 %)
Relapses [A]	9	6 (66%)	9 (100%)	4 (44 %)	1 (11 %)	7 (78 %)	7 (78 %)	6 (66 %)
Metastases [A] (As of first surgery)	6	6 (100%)	6 (100%)	4 (66 %)	3 (50 %)	2 (33 %)	6 (100 %)	4 (66 %)
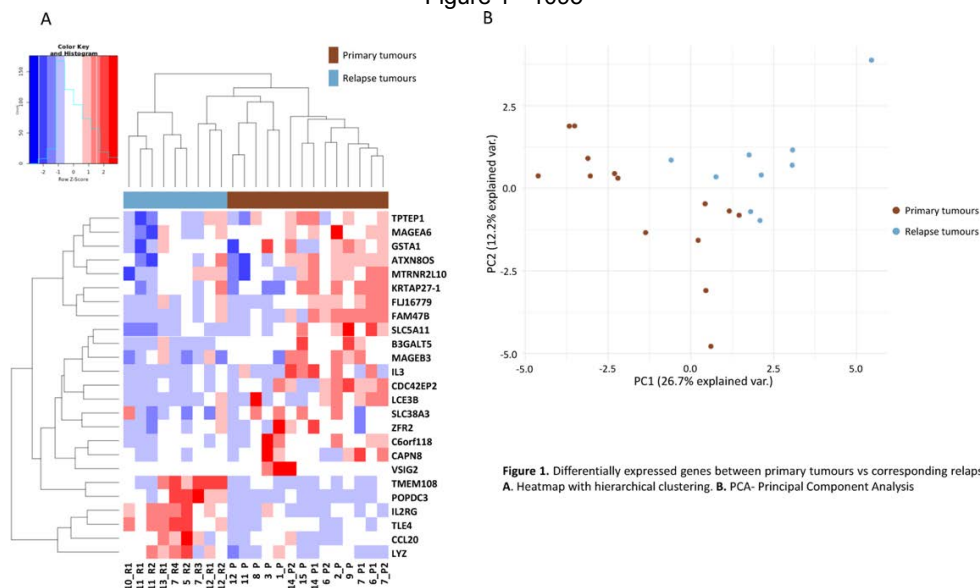
Figure 1 - 1095

Figure 1. Differentially expressed genes between primary tumours vs corresponding relapses.
A. Heatmap with hierarchical clustering. **B**. PCA- Principal Component Analysis

Figure 2 - 1095
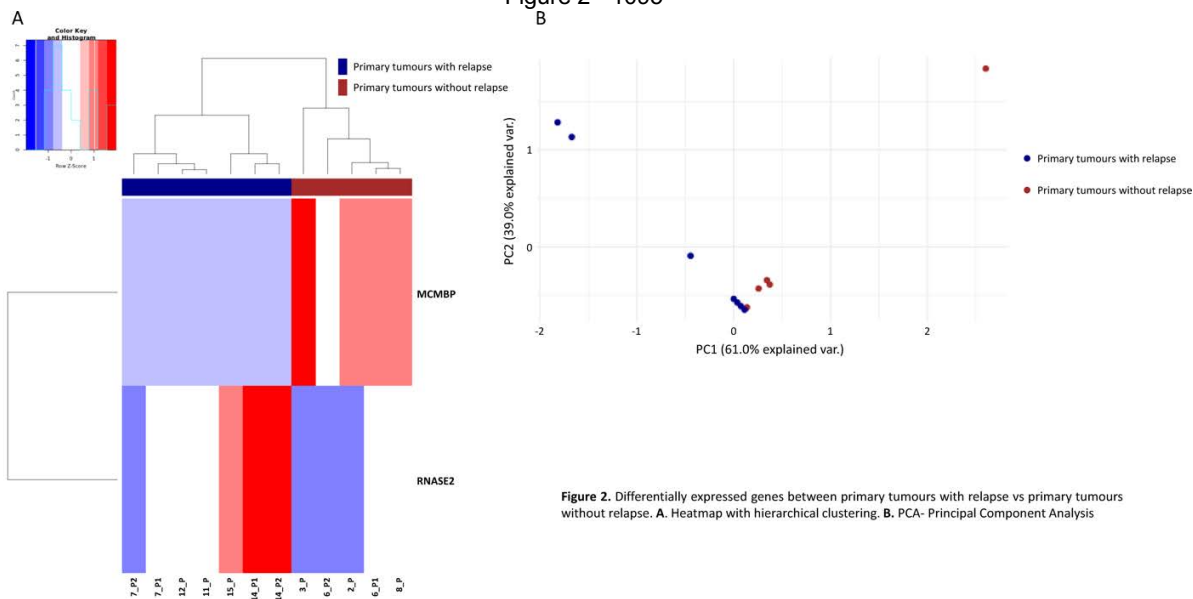
Figure 2. Differentially expressed genes between primary tumours with relapse vs primary tumours
without relapse. **A**. Heatmap with hierarchical clustering. **B**. PCA- Principal Component Analysis

Conclusions: HDAC expression was similar in both cohorts, yet HDAC3 absence was associated with long survival. Particular transcription signatures distinguish long survivors' primary tumors from relapses. Relapse may be predicted based on the expression of a small gene set.

1096   Molecular Characterization of Smooth Muscle Tumors of Uncertain Malignant Potential (STUMP) Using Targeted Next Generation Sequencing

Annacarolina Fabiana Lucia Da Silva[1], Fei Dong[1], Adrian Marino-Enriquez[1], Marisa Nucci[2], Bradley Quade[1]
[1]Brigham and Women's Hospital, Boston, MA, [2]Brigham and Women's Hospital, Harvard Medical School, Boston, MA

Disclosures: Annacarolina Fabiana Lucia Da Silva: None; Fei Dong: None; Adrian Marino-Enriquez: None; Marisa Nucci: None; Bradley Quade: None

Background: Smooth muscle tumors with uncertain malignant potential (STUMP) are a heterogeneous group of uterine smooth muscle tumors (SMT) that cannot be classified as either malignant or benign using currently established morphologic criteria. Although efforts have been made to define the pathogenesis of STUMP, to our knowledge, there are no published studies to date using next generation sequencing.

Design: Our goal was to determine the molecular characteristics of 15 STUMP relative to a cohort of benign but histologically challenging SMT (5 intravascular leiomyomatosis [IVL], 6 atypical leiomyoma [AL] and 4 cellular leiomyoma [CL]) as well as to molecularly annotated uterine leiomyosarcoma (LMS) through the cBioportal public dataset. Tumor sequencing was performed using a hybrid-capture-based, massively parallel sequencing assay (OncoPanel v.3.1). Data was interpreted with attention to potential molecular-histologic correlates, including atypia, mitotic index, atypical mitosis, necrosis, tumor border, LVI and size. Clinical status and follow up were recorded.

Results: 2 of 15 subjects with STUMP had adverse outcome (recurred/metastasized as leiomyosarcoma) but none died of disease. There were no recurrences in other SMT categories. Sequencing data revealed multiple copy number alterations (CNA) in all STUMP. Chromosome losses, some involving tumor suppressor genes known to play a role in LMS (viz., *BRCA2, RB1* and *TP53*) were more frequent than gains. CNA were less frequent in other SMT. Of note, amplification of *RMRP*, which produces a non-coding RNA, was found in 5/15 of STUMP and 2/6 AL. *FH* loss was present in 1 STUMP and 1 AL. We did not identify mutational signatures in any SMT and all were MSS. Occasional mutations in pathogenic genes (*TP53, FH, MEN1, ESR1, ALK*) were present in STUMP. *MED12* mutations were present in LM (1) and IVL (1) but not STUMP. 1 CL showed unusual *KRAS* and *FGFR1* mutations. Sequencing data was available for one subject with adverse outcome (case 10, lung metastasis, 5 years after hysterectomy), which showed additional *ESR1* mutation and losses involving *TET2, APC* and *DMD* compared to the primary.

Conclusions: Like LMS, STUMP show frequent CNA with copy number losses of 1p and 10q and tumor suppressor *RB1* and *TP53*. Amplification of *RMRP*, not previously described in SMT, was common in STUMP and AL. *RMRP* overexpression is seen carcinomas but its role in mesenchymal tumors remains to be determined. No mutations were predictive of behavior or correlated with histologic features.

1097   High Grade Endometrial Stromal Sarcoma with YWHAE Rearrangement: A Detailed Histologic Review of 24 Cases Highlights an Expanded Morphologic Spectrum

Annacarolina Fabiana Lucia Da Silva[1], David Chapel[1], Kyle Strickland[2], Marisa Nucci[3]
[1]Brigham and Women's Hospital, Boston, MA, [2]Duke University Medical Center, Durham, NC, [3]Brigham and Women's Hospital, Harvard Medical School, Boston, MA

Disclosures: Annacarolina Fabiana Lucia Da Silva: None; David Chapel: None; Kyle Strickland: None; Marisa Nucci: None

Background: Uterine endometrial stromal sarcomas are a genetically heterogenous group comprising low grade, high grade and undifferentiated tumors, some of which contain recurrent chromosomal translocations. *YWHAE* rearranged HGESS was reintroduced into the 2014 WHO classification and is now well accepted within the diagnostic lexicon; however, it has become evident with recognition of additional cases that these tumors can show a wider morphologic spectrum. We studied a cohort of primary and recurrent/metastatic tumors for further characterization.

Design: HGESS with *YWHAE* rearrangement were retrieved from our internal and consultation files to include 24 primary tumors, 5 of which also had subsequent recurrence(s)/metastases. Morphologic features were assessed.

Results: Of 24 primary tumors, 16 were biphasic (high- and low-grade components), 2 were conventional/fibromyxoid (low-grade component only), and 6 were high-grade epithelioid component only. Of the biphasic tumors, 12 showed a sharp demarcation to high-grade areas, 12 had intermingling of nests, cords and single cells of the high-grade epithelioid with the low-grade spindle component, and 9 had both patterns. The high-grade epithelioid areas were composed of cells with plump ovoid nuclei with irregular nuclear contour, homogeneously dispersed chromatin and inconspicuous nucleoli with scant (4) to moderate (14) amounts of eosinophilic cytoplasm or combination (4). The average mitotic index per 10 HPF was 18 (range 4-35), 5 (range 2-11) and 9.7 (range 3-27) in high-grade, low-grade and recurrent tumors respectively. LVI was present in 9/24 (37%) primary tumors. Other findings included: pseudo-papillary appearance (7), storiform growth (4), pseudo-glandular spaces (5), sex-cord like foci (SCT) (3), staghorn (5) and chicken wire vessels (2), rhabdoid morphology (2; 1 with severe nuclear pleomorphism) and spindled hyperchromatic cells (2) (Fig1). Of 11 recurrence/metastasis in 5 patients, 6 were biphasic, 6 conventional/fibromyxoid, and 5 high-grade epithelioid component only with concurrent or subsequent metastatic/recurrent sites from the same patient showing any of these three appearances (Fig2).

Figure 1 - 1097
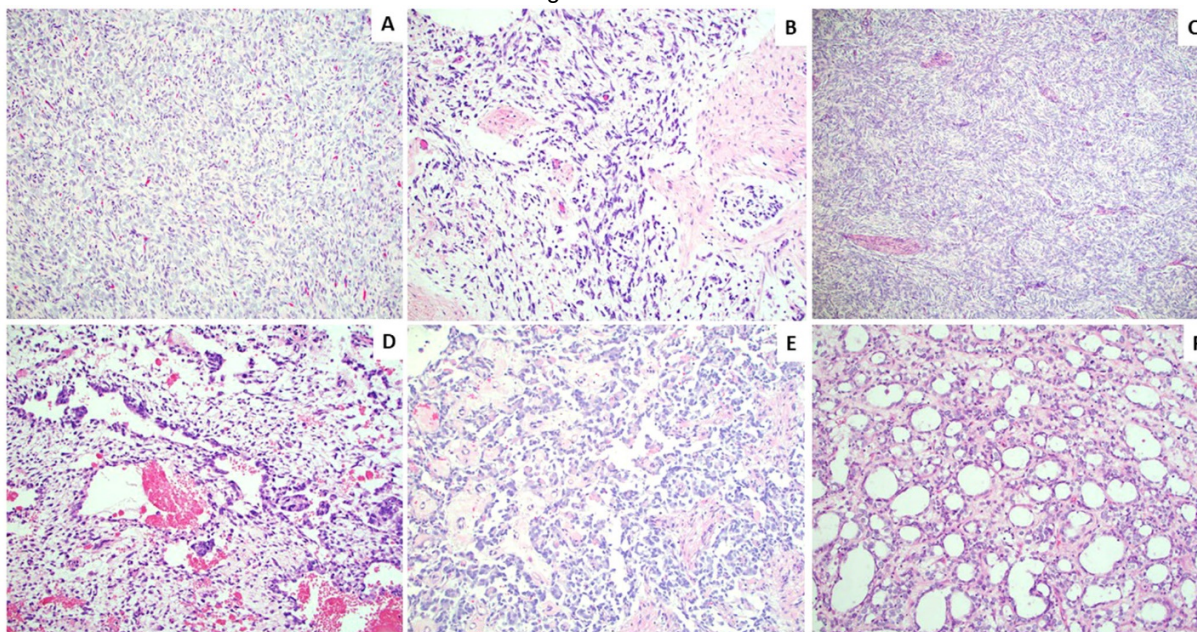
Figure 1. Additional morphologic features of YWHAE-associated HGESS. Fibromyxoid pattern with subtle intermingled isolated epithelioid cells (A). Hyperchromatic spindle cells in myxoid background, (B). Diffuse storiform pattern (C). Pseudo-glandular pattern with epithelioid cells lining dilated spaces (D). Pseudo-vascular spaces with papillary features (E). Micro-cystic pattern (F).

Figure 2 - 1097
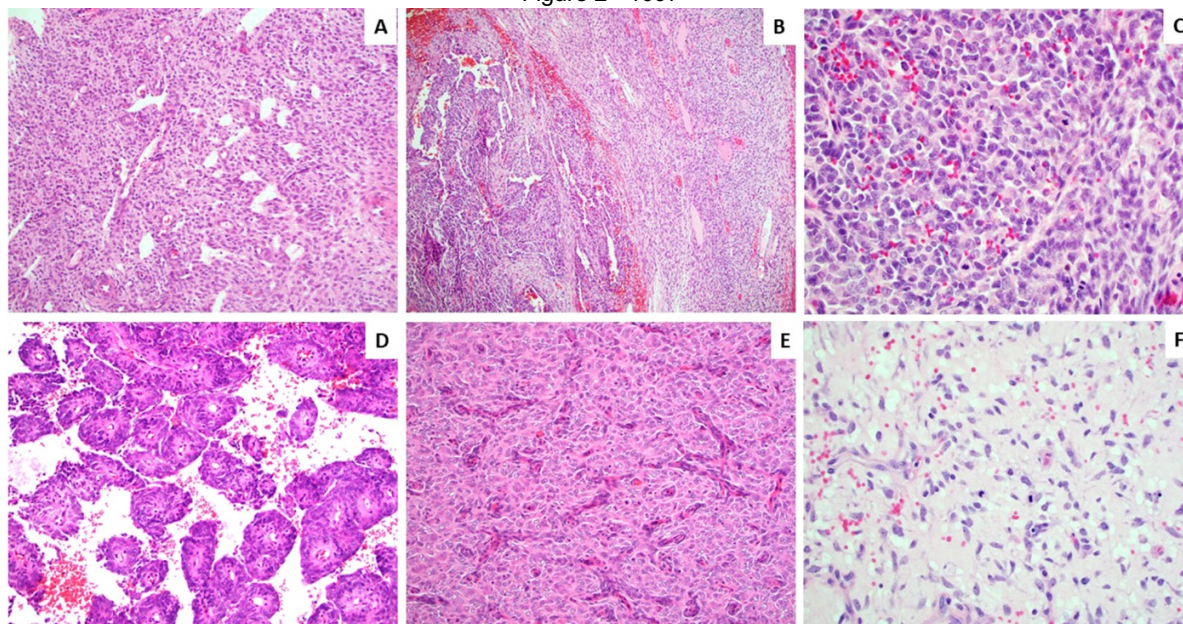
Figure 2. Case 1. Uterine primary and multiple recurrences. Primary uterine tumor, simulating a LGESS conventional type with slightly plump ovoid cells with eosinophilic cytoplasm and staghorn vessels (A). Lung metastasis with biphasic pattern with high grade epithelioid component showing clefted pseudo-vascular spaces (left) and low-grade fibromyxoid pattern (B). High grade epithelioid component with brisk mitotic rate (C). Pseudo-papillary pattern (D). Nested pattern with cells having eosinophilic cytoplasm (E). Chicken wire vessels (F).

Conclusions: YWHAE-rearranged HGESS can show distinctive morphologic features affording its recognition, which is done in combination with confirmatory immunoperoxidase stains or, if needed, genetic studies. Awareness of its expanded morphologic appearance will help in recognizing these unusual and diagnostically challenging tumors.

1098 Primary Peritoneal High Grade Serous Carcinoma Revisited: Precursor Frequency and Implications

Annacarolina Fabiana Lucia Da Silva[1], Christopher Crum[1], David Kolin[1]
[1]Brigham and Women's Hospital, Boston, MA

Disclosures: Annacarolina Fabiana Lucia Da Silva: None; Christopher Crum: None; David Kolin: None

Background: In the current model for high grade serous carcinogenesis (HGSC) a serous tubal intraepithelial carcinoma (STIC) develops in the distal tube and tumor cells spread to the peritoneal cavity. A complementary model proposes that early serous proliferations (ESPs) lead to HGSC via "precursor escape" with HGSC emerging later in he peritoneal cavity. The latter explains "primary peritoneal" HGSC but is not established. Moreover the validity of every STIC as an invariable "launching point" for HGSC has been questioned.

Design: Consecutive cases classified as primary peritoneal high-grade serous carcinoma (HGSC) in which tubes were evaluated by the SEE-FIM protocol were identified from the pathology archives. Diagnosis of PPHGSC based upon the presence of a tumor distribution confined primarily to the extra tubo-ovarian extraovarian tissues, with involvement of the tubes or ovaries limited to the serosal surfaces. where available, all histologic material was reviewed with attention to the presence of STIC or ESPs. Tissue blocks resectioned and immunostained for p53 to maximized identification of any potential precursors. Fallopian tubes from a small group of tumors classified as "ovarian" HGSC were included.

Results: 43 cases classified by pathology report as PPHGSC were identified over a 10-year interval. STIC was reported in 9 cases (21%). In 23 of 43 cases with no STIC reported, blocks were available and sections immunostained for p53. Fourteen associated tumors were strongly p53 positive, 6 displayed a p53 null immunophenotype, one wild type and in two tumors was not available for analysis. 228 tissue sections, including HE and p53 stains were evaluated from the fallopian tubes of the 23 cases. In 2 (9%) a previously unappreciated STIC was identified following sectioning and immunostaining; 6 (26%) contained an ESP, one with a p53 null immunophenotype; 15 (65%) did not display a detectible lesion. Of fallopian tubes from 8 cases with extensive ovarian involvement ("ovarian" distribution) on gross exam 3(38%) contained a STIC and 4 (50%) an ESP.

Conclusions: Although estimates of the frequency of STIC in PPHGSC to approach 50%, this followup study has shown the frequency to be significantly lower (20%). Additional putative precursors (ESPs) were identified in 26% of the remainder but in nearly one-half of PPHGSCs an origin in the fallopian tube is still not evident. This underscores the importance of evaluating other potential origins (?endometrial lining) in the gynecologic tract.

1099 Gastrointestinal Stromal Tumors Presenting as Primary Ovarian or Uterine Neoplasms, Emphasizing Potential Morphological and Immunohistochemical Diagnostic Pitfalls

Daffolyn Rachael Fels Elliott[1], Sanjay Kakar[1], Joseph Rabban[1]
[1]University of California San Francisco, San Francisco, CA

Disclosures: Daffolyn Rachael Fels Elliott: None; Sanjay Kakar: None; Joseph Rabban: *Employee*, Spouse is an employee of Merck & Co.

Background: The clinical presentation of gastrointestinal stromal tumors (GISTs) in women may occasionally simulate a primary ovarian or uterine neoplasm. Epithelioid and myxoid morphologic variants, in particular, may resemble a primary gynecologic epithelial, sex cord-stromal, or mesenchymal neoplasm. The clinico-pathologic features of such GISTs and diagnostic specificity of gynecologic immunohistochemical stains in these cases are not well described.

Design: The study included 155 women with GIST arising at any anatomic site (single institutional database search 1995-2018). Tissue microarrays (triplicate 2 mm cores per tumor) were constructed for 78 GISTs. Immunostains included mullerian epithelial (PAX8, estrogen receptor), sex cord stromal (FOXL2, SF-1, WT-1, calretinin, inhibin), endometrial stromal (CD10, BCOR), malignant germ cell (SALL4), PEComa (HMB-45), inflammatory myofibroblastic tumor (ALK), mesonephric/trophoblast (GATA3), malignant mesothelial (BAP-1) and GIST markers (DOG1 and CD117). Clinical data from an additional 77 GIST was available.

Results: Among 155 women with GIST (median age 63 y), 11% (17) were clinically suspected to be a primary gynecologic neoplasm and 59% of these (10/17) underwent surgery by a gynecologic surgeon. GISTs presenting as gynecologic tumors were larger (10 cm vs. 3.7 cm, p<0.001), higher stage (18% vs. 5%, NS trend), and more likely to metastasize (35% vs. 17%, NS trend) than typical GISTs. Epithelioid morphology was present in 9/17 GISTs, either purely (3) or combined with spindled morphology (6). All 78 GISTs were positive for DOG1 and/or CD117. CD10 was positive in 28%; focal HMB-45 in 10%; focal calretinin in 8%; BAP-1 loss in 6%; BCOR in 1%. All showed diffuse strong cytoplasmic staining for WT-1, but none showed nuclear staining. None stained for FOXL2, SF-1, SALL4, PAX8, inhibin, GATA3 or ALK.

Conclusions: GISTs may occasionally clinically and morphologically simulate primary ovarian or uterine neoplasms; these tumors are often large and may have advanced disease. Although many gynecologic immunohistochemical markers are negative in GISTs, a minority may exhibit focal CD10, HMB-45, calretinin or loss of BAP-1, potentially leading to misdiagnosis if GIST, albeit rare in the pelvis, is not included in the differential diagnosis and pursued with DOG1/CD117 staining.

1100 Whole Genome Copy Number Variant Analysis Identifies Novel Biomarker to Help Distinguish Uterine Smooth Muscle Tumor Types

Brian Finkelman[1], Tingting Gao[1], Xinyan Lu[2], Jian-Jun Wei[3]
[1]Northwestern University Feinberg School of Medicine, Chicago, IL, [2]Chicago, IL, [3]Northwestern University, Chicago, IL

Disclosures: Brian Finkelman: None; Tingting Gao: None; Xinyan Lu: None; Jian-Jun Wei: None

Background: Leiomyoma with bizarre nuclei (LM-BN) is a rare benign uterine smooth muscle tumor with similar histologic and molecular features to leiomyosarcoma (LMS). In clinical practice, diagnosing LM-BN is difficult due to limited knowledge of disease biology and of its relation to LMS. Previous work has suggested that LM-BN can be divided into leiomyoma with fumarate hydratase alteration (LM-FH) and LM-BN based on morphology and FH expression. Our aim was to find novel biomarkers to help distinguish among LM-FH, LM-BN, and LMS.

Design: Whole genome copy number variation (CNV) analysis was performed on 10 LM-FH, 15 LM-BN, and 10 LMS cases to identify candidate tumor suppressor or oncogenes. Tissue microarrays were prepared for 32 LM-FH, 22 LM-BN, and 37 LMS cases, as well as 11 myometrial controls. Semi-quantitative immunohistochemical (IHC) analysis (H-score) was performed for both novel and conventional biomarkers (p16, p53 and FH). Overall biomarker discrimination was assessed via the multi-class area under the ROC curve (AUC), with statistical significance based on the likelihood ratio test of multinomial regression models.

Results: Common CNVs included losses of 1p (80%) and 1q (100%) and gains of 8p (40%) in LM-FH, as well as losses of 1p (67%), 13q (60%), 17p (60%), and 22q (47%) in LM-BN. LMS showed complex CNV changes with some overlap with LM-BN, including losses of 1p, 13q, and 22q. Based on these findings, we identified a set of novel biomarkers (ATAD3, SDCCAG8, PKC, DVL1, COX20, SCO2, and hnRNP U) to analyze by IHC. The multi-class AUCs for the novel biomarker H-scores ranged from 0.54 to 0.75; however, only ATAD3 was significantly associated with tumor type after adjusting for FH, p53, and p16 (P<0.001). IHC results for FH, p16, p53, and ATAD3 are summarized by heatmap with unsupervised hierarchical clustering in Figure 1. A multinomial regression model constructed from FH, p16, p53, and ATAD3 showed excellent overall discrimination among tumor types (multi-class AUC = 0.94), and, importantly, could discriminate well between LMS and LM-BN among FH+ tumors (AUC = 0.82).

Figure 1 - 1100
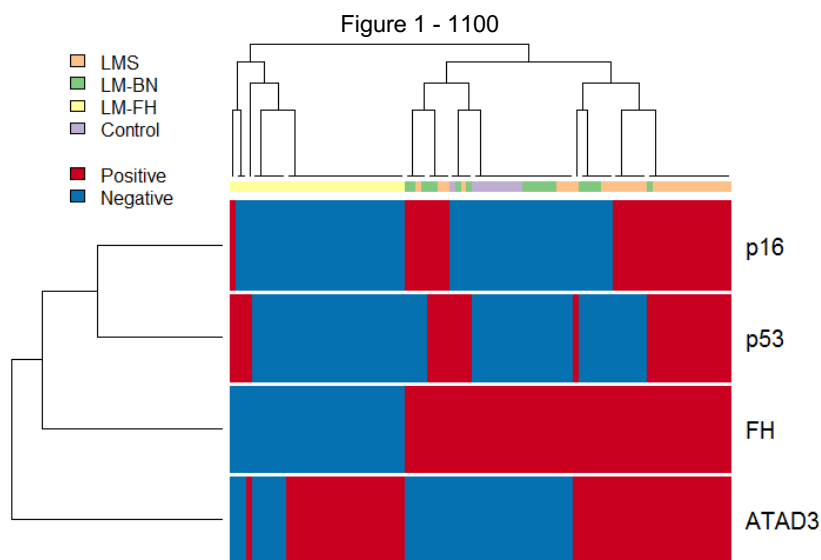
Conclusions: Whole genome CNV analysis of LM-FH, LM-BN, and LMS revealed multiple genomic regions of interest. Of the novel biomarkers, ATAD3, a mitochondrial protein and oncogene, was independently associated with tumor type. A multinomial regression model including FH, p16, p53, and ATAD3 showed good discrimination even between LM-BN and LMS. Independent model validation is necessary before use in clinical practice.

1101   PD-L1 Expression in High Grade Serous Carcinoma of the Female Genital Tract - Experience in a Large Clinical Cohort Reclassified with Immunohistochemistry and NGS

Anna Fischer[1], Nina Neudeck[2], Marcel Grube[3], Irina Bonzheim[4], Jana Pasternak[5], Franziska Otto[1], Karen Greif[6], Christine Beschorner[1], Sara Brucker[5], Diethelm Wallwiener[1], Falko Fend[7], Stefan Kommoss[3], Annette Staebler[8]
[1]University of Tuebingen, Tuebingen, Baden-Wuerttemberg, Germany, [2]University of Tuebingen, Tübingen, Baden-Wuerttemberg, Germany, [3]Tuebingen University Hospital, Tuebingen, Germany, [4]University of Tuebingen, Tübingen, Germany, [5]Tuebingen University Hospital, Tübingen, Germany, [6]Tübingen University Hospital, Tübingen, BW, Germany, [7]University Hospital of Tuebingen, Tuebingen, Baden-Württemberg, Germany, [8]University of Tuebingen, Tuebingen, Germany

Disclosures: Anna Fischer: None; Nina Neudeck: None; Marcel Grube: None; Irina Bonzheim: None; Jana Pasternak: None; Karen Greif: None; Christine Beschorner: None; Sara Brucker: None; Diethelm Wallwiener: None; Falko Fend: None; Stefan Kommoss: None; Annette Staebler: None

Background: High grade serous tubo-ovarian carcinoma (HGSC) is still one of the most lethal carcinomas of the female genital organs. The presence of high numbers of tumor infiltrating lymphocytes (TILs) has been shown to correlate with prolonged overall survival (OS). Recent clinical studies compare single checkpoint-inhibitor therapy to combined immune-targeting therapies and adoptive cell therapy. HGSC may be difficult to distinguish from other histotypes of ovarian carcinoma, specifically high-grade carcinomas. Therefore, we present a large consecutive cohort of HGSC first re-classified via immunohistochemistry and molecular analyses before investigating for PD-L1 expression status using the Combined Positivity Score (CPS).

Design: A consecutive series of 420 cases diagnosed as HGSC and treated at the Womens' Hospital of the University Tuebingen from 2000 until 2016 was reviewed by two independent pathologists. Tissue microarrays (TMAs) were stained for a panel of four markers including WT1, p53, progesterone receptor and Napsin-A. Cases which were unclassifiable via morphology and immunohistochemistry will be analyzed by NGS with a panel of known targets in ovarian carcinomas. PD-L1 via CPS was analyzed by two independent pathologists, one of them accredited for CPS evaluation.

Results: In 89.5% (n= 376/420), diagnosis of HGSC was confirmed (WT1+, p53 aberrant, Napsin-A neg.). 25 cases (5.9%) were reclassified and excluded: 12 (2.8%) low-grade serous, 9 (2.1%) endometrioid, 2 (0.5%) clear cell carcinoma, 2 (0.5%) atypical proliferative serous tumors (APSTs), 3 cases for other reasons (0.8%) (2=metastasis of other primary, 1=technical reasons). 16 cases (3.8%) will be subjected to mutational analysis by NGS. Within the re-classified 376 (100%) HGSC, 131 presented PD-L1 expression (34.8%), 215 were negative (57.2%), 30 cases were not evaluable for technical reasons (8%). For CPS mean value, cut-offs were 0 (n=215, 57.2%), <1 (n=84, 22.3%), 1-25 (n=47, 12.5%), 25 (n=0, 0%).

Conclusions: Within our collective of re-classified HGSC of the female genital tract, PD-L1 expression was found in 34.8%, whereas the majority showed negative results (57.2%). In summary, PD-L1 is expressed in a subgroup of HGSCs suggesting an important role in the tumor microenvironment and providing a potential therapeutic target. Further correlation with clinical data will follow.

1102   Expression Analysis of Selected Biomarkers in Müllerian Adenosarcoma

Jean Fischer[1], Yanli Ban[2], Jian-Jun Wei[3]
[1]McGaw Medical Center of Northwestern University, Chicago, IL, [2]Northwestern University Feinberg School of Medicine, Chicago, IL, [3]Northwestern University, Chicago, IL

Disclosures: Jean Fischer: None; Yanli Ban: None; Jian-Jun Wei: None

Background: Müllerian adenosarcoma (MAS) is a rare biphasic malignant neoplasm for which no reliable diagnostic markers have been reported. Our prior study by whole genome sequencing identified 28 biomarkers within regions of frequent copy number variation (CNV). Expression analysis by immunohistochemistry (IHC) revealed 10 biomarkers with significant upregulation in MAS compared to endometrial (EM) controls. In addition, target validation analysis confirmed several frequently mutated genes in MAS including *KDM6B* and *KMT2C*. In this study, we examined IHC for the selected biomarkers which are highly relevant to MAS, and we correlated with tumor grade, sarcomatous overgrowth (SO), tumor location, and patient age.

Design: A total of 28 MAS were selected after review including 17 low-grade, 11 high-grade, and 15 with SO. Five were from cervix, 19 from endometrium, and 4 from ovary/peritoneum. Seven biomarkers (Cyclin D1, CDK4, KIF14, MDM2, p16, HMGA2, and 14-3-3 ε) from CNV analysis and 2 markers (KMT2C and KDM6B) from mutation analysis were selected for this study. IHC expression was evaluated in stroma and epithelium for intensity (0-3+) and extent (0-100%) and H-scores calculated. IHC was correlated with clinicopathological features using one-way analysis of variance.

Results: Increased stromal expression of the 7 biomarkers from CNV analysis was observed in MAS and demonstrated variation in stromal expression with different clinicopathologic parameters (Table 1). MDM2 had higher expression in ovarian MAS compared to uterine MAS. KIF14 had higher expression in high-grade MAS, MAS with SO, and patients ≥50 years old. CDK4 had higher expression in low-grade MAS as well as MAS without SO. Cyclin D1 was also increased in low-grade MAS. HMGA2 was increased in high-grade MAS

compared to low-grade. Among the markers selected from mutational analysis, KDM6B epithelial expression was significantly decreased in MAS (p=0.02). No other markers showed significant differences in epithelial expression. KMT2C IHC analysis is ongoing.

Table 1. Immunohistochemistry analysis of stromal expression of selected oncogene/tumor suppressor gene products in Müllerian adenosarcoma

	MAS (n=28)	EM (n=14 KDM6B; n=8 all other stains)	MAS vs. EM	MAS Location (Cervix vs. Uterus vs. Ovary)	SO (Present vs. Absent vs. EM)	Tumor Grade (Low vs. High vs. EM)	Patient Age (<50 yo vs ≥50 yo vs. EM)
Markers	Mean (Median)	Mean (Median)	P value	P value	P Value	P Value	P Value
KDM6B	38 (15)	49 (45)	0.46	0.28	0.41	0.65	0.45
Cyclin D1	81 (35)	11 (0)	0.002	0.21	0.10	0.02	0.10
CDK4	69 (30)	10 (5)	0.001	0.73	0.002	0.03	0.06
HMGA2	74 (0)	14 (0)	0.005	0.07	0.09	0.03	0.30
KIF14	107 (80)	31 (40)	<0.001	0.60	0.02	0.02	0.04
MDM2	43 (20)	10 (0)	0.02	0.05	0.28	0.13	0.28
p16	130 (120)	57 (50)	0.04	0.17	0.15	0.11	0.16
14-3-3 ε	164 (180)	98 (95)	0.006	0.91	0.09	0.08	0.06

Conclusions: Cyclin D1 and CDK4 were highly expressed in low-grade MAS, and KIF14 was highly expressed in high-grade MAS. CDK4 was also highly expressed in MAS without SO while KIF14 was highly expressed in MAS with SO. *KDM6B* was frequently mutated in MAS with SO, and IHC revealed decreased expression in the epithelial but not stromal component.

1103 DNA Methylation Profiling of Uterine Sarcomas

Erna Forgo[1], Anna-Lena Lang[2], Vanita Natu[3], Teri Longacre[3], Jennifer Bennett[4], Charles Quick[5], Carlos Parra-Herran[6], Marisa Nucci[7], David Kolin[8], Brooke Howitt[1]
[1]Stanford University School of Medicine, Stanford, CA, [2]Stanford University School of Medicine, Mountain View, CA, [3]Stanford University, Stanford, CA, [4]The University of Chicago, Chicago, IL, [5]University of Arkansas for Medical Sciences, Little Rock, AR, [6]Sunnybrook Health Sciences Centre, University of Toronto, Toronto, ON, [7]Brigham and Women's Hospital, Harvard Medical School, Boston, MA, [8]Brigham and Women's Hospital, Boston, MA

Disclosures: Erna Forgo: None; Anna-Lena Lang: None; Vanita Natu: None; Teri Longacre: None; Jennifer Bennett: None; Charles Quick: None; Carlos Parra-Herran: None; Marisa Nucci: None; David Kolin: None; Brooke Howitt: None

Background: Uterine sarcomas can be difficult to diagnose due to overlapping morphology and immunophenotype. Identification of gene rearrangements can help with classification in some cases. DNA methylation is an epigenetic modification important in the regulation of gene expression. We sought to characterize the epigenetic signatures of uterine sarcomas by DNA methylation profiling in order to determine if subtypes of uterine sarcomas have tumor-defining epigenetic alterations that can be used for classification and prognostication.

Design: Uterine sarcomas derived from formalin-fixed paraffin-embedded tissue from 4 institutions were processed using the Illumina 850k Bead Chip Platform. Cases passing all Q/A parameters were included in the preliminary analysis and comprised endometrial stromal nodules (ESN, n=2), endometrial stromal tumors with limited infiltration (ESTLI, n=2), low-grade endometrial stromal sarcomas (LGESS, n=45; 40 patients), high-grade endometrial stromal sarcomas (HGESS, n=2), müllerian adenosarcomas (MA, n=14), and inflammatory myofibroblastic tumors (IMT, n=5). Gene fusion status for *JAZF1*, *PHF1*, *BCOR* and *YWHAE* was also recorded.

Results: T-distributed stochastic neighbor embedding (t-SNE) dimensionality reduction analysis based on the 20,000 most variable probe sites revealed clustering into 3 main groups which correlated with histologically diagnosed tumor type (Figure 1). Group 1 included ESN, ESTLI, and LGESS; Group 2 included MA, and Group 3 included all 5 IMT cases. Additionally, 5 LGESS from 2 patients, all harboring *JAZF1* rearrangements and all metastatic formed a 4th small, but discrete cluster. Two HGESS clustered on the border of Group 1. Clustering was independent of institutional origin. Within Group 1, LGESS did not appear to form subgroups based on genotype in the t-SNE plot, but additional analyses are pending. Outlier histologic diagnoses are undergoing additional molecular evaluation to confirm or refute the original histologic impression.

Figure 1 - 1103
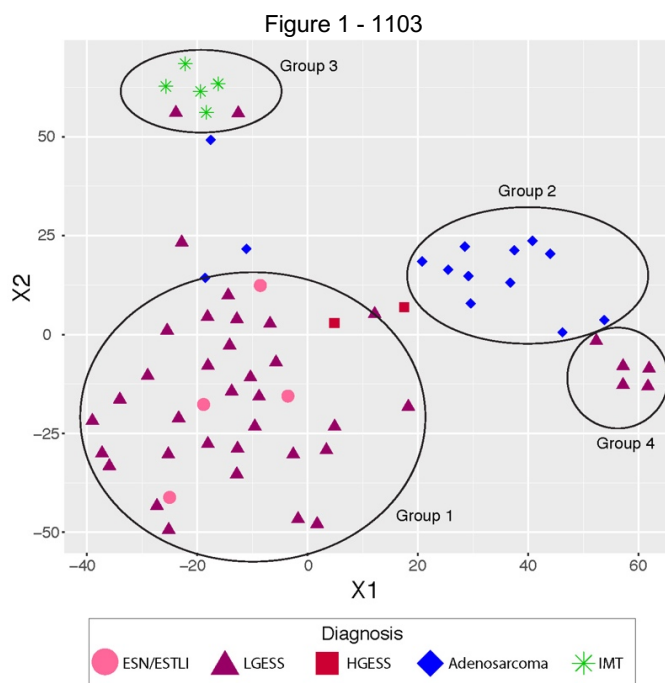
Conclusions: Uterine sarcomas show distinct DNA methylation profiles that generally correlate with histotype. The presence of outliers in the otherwise robust t-SNE clustering observed suggests that some tumors may in fact represent misdiagnosed cases. LGESS with *JAZF1* rearrangement that behaved clinically aggressively formed a distinct cluster. This preliminary data shows the potential for DNA methylation profiling in providing more accurate and clinically relevant diagnostic and prognostic information in uterine sarcomas.

1104 Proportion of Hyperplasia/Carcinoma as a Prognostic Factor for Invasion in Low-Grade Endometrial Carcinomas in Patients Younger than 40 Years Old

Carolina Fraire Vazquez[1], David Cantu de Leon[2], Salim Barquet[1], Isabel Alvarado-Cabrero[3], Guadalupe Moncada[1], Lourdes Peña Torres[1], Maria Delia Perez Montiel[4]
[1]*Instituto Nacional de Cancerologia, Mexico City, Tlalpan, Mexico,* [2]*Instituto Nacional de Cancerologia, Mexico City, Tlapan, Mexico,* [3]*Mexican Oncology Hospital SXXI, IMSS, Ciudad de México, MEX, Mexico,* [4]*Instituto Nacional de Cancerologia, Mexico City, DF, Mexico*

Disclosures: Carolina Fraire Vazquez: None; David Cantu de Leon: None; Salim Barquet: None; Isabel Alvarado-Cabrero: None; Guadalupe Moncada: None; Lourdes Peña Torres: None; Maria Delia Perez Montiel: None

Background: Endometrial carcinoma in young patients is a condition that has been increasing in the past years, many of these women desire fertility preservation but many undergo to hysterectomy. The objective of the study is to determine if the ratio of hyperplasia in relation to adenocarcinoma (H/AC) in the dilation and curettage (D&C) is a prognostic factor that could help in the decision of proposing more conservative treatments in this group of individuals.

Design: A retrospective study was carried out in patients under 40 years of age with a diagnosis of low-grade endometrioid adenocarcinomas in a D&C as diagnostic procedure, the material was reviewed by two pathologists and the percentage of hyperplasia (simple and complex) and the percentage of carcinoma (based on WHO criteria) was estimated in percentage. It was correlated with the findings of a hysterectomy and a ROC curve was performed to determine the cut-off point of the (H/AC) that allows to predict the findings of the hysterectomy specimen.

Results: From January 2006 to December 2018, 119 cases of patients with G1 endometrioid adenocarcinoma under 40 years were identified, of these 66 cases underwent a hysterectomy. Mean age was 34 (range 24-39). The D&C biopsy varied from 1 cc to 10 cc and were included in its entirety. Two patients were re-categorized as G2, by cytologic atypia. The percentage of presence of adenocarcinoma varied from less than 5% to 100% of the biopsy samples. In hysterectomy specimens the diagnosis was: without evidence of tumor 5 (7.5%), 34 intramucosal carcinomas (51.5%), 19 adenocarcinomas with invasion less than 50% (28.7%) of myometrium, 4 carcinomas with invasion greater than 50% (6%) of myometrium, 4 cases with infiltration into the cervical stroma (6%). A total of 31 carcinomas were histologically upgraded (46.97%) in the hysterectomy. When analysis the percentage of adenocarcinoma in the biopsy, we found that patients without residual neoplasia, microscopic foci or without myometrial invasion correlated with a H/AC of 70/30 (AUC=0.78) or

higher in the biopsy. Patients with an upgrade in the hysterectomy correlated with the H/C 40/60 (AUC=0.71) or more. All, except one patient, are alive without recurrence.

Conclusions: Reporting the ratio H/C in patients with low-grade adenocarcinoma seems to be a prognostic factor and help in selecting cases for conservative management. Larger number of cases must be included as well as larger follow-up.

1105 Loss of MHC Class I in Endometrial Carcinoma: A Possible Mechanism of Immunotherapeutic Resistance in Some MMR-Deficient and PD-L1-Positive Tumors

Lisa Friedman[1], Timothy Bullock[1], Emily Sloan[2], Kari Ring[1], Anne Mills[1]
[1]University of Virginia, Charlottesville, VA, [2]University of California San Francisco, San Francisco, CA

Disclosures: Lisa Friedman: None; Timothy Bullock: None; Emily Sloan: None; Kari Ring: None; Anne Mills: None

Background: Major histocompatibility complex (MHC) class I is a membrane-bound protein complex ubiquitously expressed on normal nucleated human cells. MHC class I presents intracellular protein fragments to cytotoxic T cells, allowing these immune cells to detect neoantigens and destroy abnormal cells. MHC Class I loss has been documented in a variety of tumor types and represents a possible mechanism of immunotherapy resistance even among cancers that otherwise appear to be good candidates for checkpoint inhibition, such as mismatch repair (MMR)-deficient and PD-L1-positive malignancies. We herein assess MHC Class I expression in a range of endometrial carcinomas, including MMR-deficient and PD-L1-positive cancers.

Design: Immunohistochemical staining for combined MHC class I A-, B-, and C-heavy chains was performed on 78 cases of endometrial carcinoma [29 MMR-intact, 25 *MLH1*-promoter hypermethylated (*MLH1*-hm) MMR-deficient, and 24 non-hypermethylated (non-hm) MMR-deficient]. The degree of MHC class I staining was classified as present, clonally lost, or absent. Tumoral PD-L1 expression and CD3-positive T lymphocytes were also quantified.

Results: Forty two percent of tumors showed clonal (27%) or complete (15%) loss of MHC class I expression. This included 47% of MMR-deficient and 28% of PD-L1-positive cancers. However, neither loss pattern was significantly associated with stage, grade, MMR status, tumoral PD-L1 expression, PD-L1 CPS, or the CD3+ lymphocyte count. (See table)

	MHC Class I Intact (n=45)	MHC Class I Clonal Loss (n=21)	MHC Class I Complete Loss (n=12)	p-value
MMR-intact (n=29)	19 (66%)	9 (31%)	1 (3%)	0.265
MMR-deficient (n=49)	26 (53%)	13 (27%)	10 (20%)	
MLH1-hm (n=25)	14 (56%)	7 (28%)	4 (16%)	
Non-hm (n=24)	12 (50%)	6 (25%)	6 (25%)	
PD-L1 tumor+ (≥1%) (n=29)	21 (72%)	6 (21%)	2 (7%)	0.380
PD-L1 CPS+ (≥1) (n=67)	37 (55%)	18 (27%)	12 (18%)	0.290
Mean CD3+ tumor-associated lymphocyte count (mean (95% CI))	194 (165-222)	182 (141-224)	158 (103-213)	0.553

Figure 1 - 1105
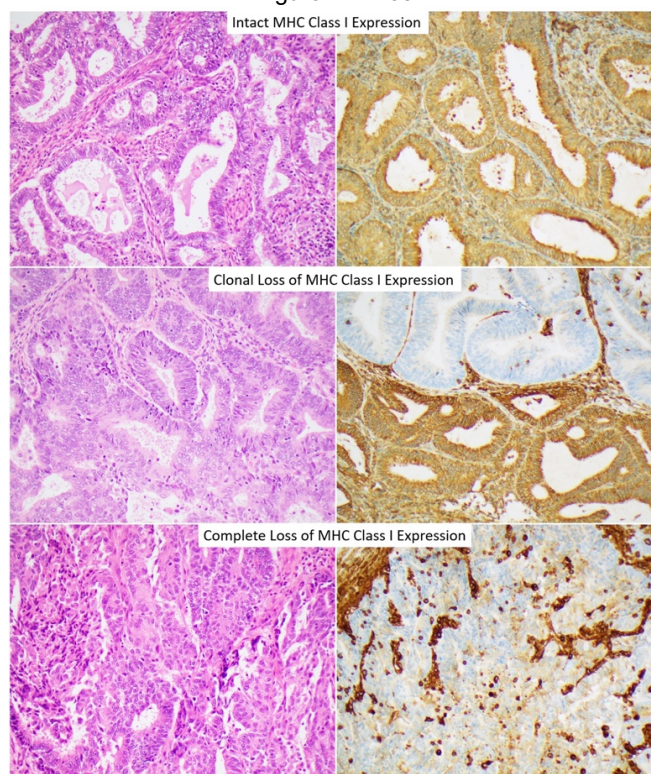
Conclusions: Many endometrial carcinomas demonstrate partial or complete loss of classical MHC class I expression, including 47% of MMR-deficient and 28% PD-L1-positive tumors which might otherwise be considered ideal candidates for immunotherapy. Notably, loss was also commonly observed in MMR-intact tumors and across tumoral grades and stages. These findings suggest that tumoral MHC Class I status may be an important factor to consider when selecting endometrial cancer patients for checkpoint inhibition.

1106   Androgenetic/biparental Mosaic Conception: Histological and Immunohistochemical Analyses of 21 Cases

Masaharu Fukunaga, Shin-Yurigaoka General Hospital, Kawasaki, Kanagawa, Japan

Disclosures: Masaharu Fukunaga: None

Background: Androgenetic/biparental mosaic conception is very rare and always poses a diagnostic challenge both clinically and pathologically. It is generally proven by DNA genotyping.

Design: Twenty-one cases of androgenetic/biparental mosaic conception, all of which were in the first trimester, were retrieved from 690 cases with hydropic placental tissue and were histopathologically analyzed by immunostaining for p57 (Kip2) (p57), which is a product of paternally imprinted, maternally expressed genes. p57-negative cells are generally considered to be androgenetic, while p57-positive cells are biparental.

Results: Androgenetic/biparental mosaic conception is characterized by discordant p57 immunohistochemical expression in different cell types based on the presence or absence of maternal genetic material in these cells. p57 expression was detected in 14 cases of mosaic complete mole (CM) with a placental mesenchymal dysplasia (PMD) component, 4 of mosaic CM with a non-PMD component, in which almost normal villi were observed, 2 of pure PMD, and 1 of mosaic hydropic abortion. p57-positive and -negative cytotrophoblasts and villous stromal cells were observed in mosaic CM cases. PMD villi were histologically characterized by stromal cell hyperplasia and the absence of trophoblastic hyperplasia. A discordant pattern of p57 expression was observed in the PMD component of cases of mosaic CM with PMD and pure PMD, with positive staining in villous cytotrophoblasts and negative stromal cells, indicating a mixture of androgenetic and biparental cells. Fetal parts were observed in 3 cases of mosaic CM with PMD. In 1 case of mosaic hydropic abortion, villi had p57-positive and -negative stromal cells. None of these cases had persistent trophoblastic diseases.

Conclusions: Androgenetic/biparental mosaic conception may be divided into four types: mosaic CM with PMD, mosaic CM with a non-PMD component, pure PMD, and hydropic abortion. Mosaic CM with PMD was the most common type. Mosaic CM is often associated

with PMD and is associated with a risk of persistent disease. Androgenetic/biparental mosaicism may be the etiology for PMD. p57 immunostaining may be a useful screening tool for cytogenetic analyses of androgenic/biparental mosaic conception.

1107 Endometrioid Carcinoma Associated with Atypical Polypoid Adenomyoma

Masaharu Fukunaga, Shin-Yurigaoka General Hospital, Kawasaki, Kanagawa, Japan

Disclosures: Masaharu Fukunaga: None

Background: Atypical polypoid adenomyoma (APA) has been regarded as a benign tumor; however, it is often associated with endometrioid adenocarcinoma (EC), and its histologic diagnosis, biologic potential and patients' management have been controversial.

Design: Thirty-one cases of EC associated with APA were retrieved from 122 cases of APA. Its differential diagnosis, effects of hormonal (medroxyprogesterone acetate) therapy and biologic behavior were studied.

Results: The patients' ages ranged from 28 to 66 (mean: 35) years. Twenty-seven ECs were observed in the APA and 4 were in the adjacent endometrium. Thirty cases were grade 1 EC and 1 was dedifferentiated carcinoma. Eleven patients with APA who were initially treated with curettage or polypectomy followed by hormonal therapy had residual or recurrent APA. Three of them also showed EC. Hysterectomy was performed in 27 patients with APA because a definite diagnosis could not be made preoperatively, the curettages raised the possibility of adenocarcinoma, or because there was a high possibility of residual or recurrent lesions. All showed residual or recurrent APA in hysterectomy specimens and 12 had also EC. Seven had superficial myometrial invasion and 1 showed deep myometrial invasion. The overall residual or recurrent lesion rate of APA patient was high (32 /65, 49%). Thirty patients with EC were alive without evidence of disease at 1 to 225 month and one with dedifferentiated carcinoma developed peritoneal implants and was treated with chemotherapy.

Conclusions: The rate of recurrent or residual APA was high, and the effects of hormonal therapy were limited. The risk EC in women with APA is also high. Almost all of ECs with APA are well differentiated and may have favorable clinical courses, but there is a risk of deep myometrial invasion or developing dedifferentiated carcinoma. The findings indicate a continued risk for the development of EC in patients in whom complete excision of APA cannot be guaranteed. If a definite diagnosis of APA has been made on curettage or polypectomy, hysterectomy is the treatment of choice. However, patients with APA who wish to preserve fertility and managed by local excision should be carefully followed-up. In general, substantial number of EC may arise from APA and APA can be completely replaced by carcinomatous overgrowth. APA areas should be paid attention in cases of EC. APA may be best regarded as analogous to a localized form of atypical complex edometrial hyperplasia.

1108 Morphologic Features Indicating the Mismatch Repair Protein Status in Ovarian Clear Cell Carcinoma and Frequent MSH2/MSH6 Deficient Expression: A Cohort of 176 Patients from China

Huijuan Ge[1], Yaoxing Xiao[2], Guangqi Qin[3], Yanzi Gu[3], Xu Cai[4], Wenhua Jiang[3], Xiaoyu Tu[4], Wentao Yang[4], Rui Bi[3]
[1]Shanghai, China, [2]Department of Pathology, Obstetrics & Gynecology Hospital of Fudan University, Shanghai Red House Obstetrics & Gynecology Hospital, Shanghai, China, [3]Fudan University Shanghai Cancer Center; Shanghai Medical College, Fudan University, Shanghai; Institute of Pathology, Fudan University, Shanghai, Shanghai, China, [4]Fudan University Shanghai Cancer Center, Shanghai, China

Disclosures: Huijuan Ge: None; Yaoxing Xiao: None; Guangqi Qin: None; Yanzi Gu: None; Xu Cai: None; Wenhua Jiang: None; Wenhua Jiang: None; Xiaoyu Tu: None; Wentao Yang: None; Rui Bi: None

Background: Lynch syndrome (LS) is an autosomal dominant tumor syndrome caused by a germline mutation in one of the DNA mismatch repair (MMR) genes (MLH1, MSH2, MSH6 and PMS2), which, after a loss-of-function mutation in the normal allele, increases cancer risk.In the literature, the focus of LS has been predominantly on colorectal carcinoma, but recently, there has been growing recognition of the role that LS plays in the development of gynecologic malignancies.,including ovarian clear cell carcinoma (OCCC). Little is known about the pathological features and MMR expression in OCCC. Hence, we performed MMR staining and assessed the relationship between pathological features and the MMR expression status. We aimed to identify the clinical and histopathological characteristics of ovarian clear cell carcinoma associated with the MMR status and to further examine the element of surveillance for OCCC in LS.

Design: We reviewed specific morphologic features, including histology characteristics (nuclear atypia, necrosis, mitosis, stromal hyalinization, and background precursors) and the host inflammatory response (TILs, PTLs, intratumoral stromal inflammation and plasma cell infiltration), in 176 OCCCs. Immunohistochemistry for MLH1, PMS2, MSH2, MSH6 and ARID1A was performed on sections of a triple-core tissue microarray of 176 OCCCs.

Results: Deficient MMR (dMMR) was detected in 10/176 (5.7%) tumors, followed by MSH2/MSH6 (6/176, 3.4%), MLH1/PMS2 (3/176, 1.7%), and MSH6 (1/176, 0.6%). No case of PMS2 or MSH2 loss alone was observed. The average age of patients with dMMR was 46 years, demonstrating that they were significantly younger than patients with intact MMR (46 years vs. 53 years, P = 0.041). Among the patients with dMMR, 2 had a synchronous malignant tumor, and 2 had a history of HNPCC. Diffuse intratumoral stromal inflammation and

plasma cell infiltration were two unique independent features associated with the dMMR status according to the univariate analysis. ARID1A expression was lost in 8 patients with dMMR (8/10, 80%), but no significant difference between dMMR and ARID1A expression was observed. Diffuse intratumoral stromal inflammation correlated only with the expression of dMMR in the multivariate analysis (P = 0.004).

Table 1 pathologic characteristics of clear cell carcinoma and their association with MMR status			
	MMR-deficient cases （n=10）	MMR-intact cases （n=166）	*P*
Age(y)			0.078
<50	6 （60%）	54 （32.5%）	
≥50	4 （40%）	112 （67.5%）	
Median	46	53	**0.041**
Other tumour	2	39	1.0
HNPCC history	2	20	0.362
Precursor	4 （40%）	61 （36.7%）	0.987
no	1 （10%）	22 （13.3%）	
Adenofibroma	4 （40%）	69 （41.6%）	
Endometriosis	1 （10%）	14 （8.4%）	
both			
Stromal Hyalinizaton			0.671
Focal or absent	8 （80%）	139 （83.7%）	
Diffuse	2 （20%）	27 （16.3%）	
Nuclear Atypia			0.139
High grade	5 （50%）	43 （25.9%）	
Low-medium grade	5 （50%）	123 （74.1%）	
Signet ring cells			0.603
No	10 （100%）	147 （88.6%）	
Yes	0 （0%）	19 （11.4%）	
Peritumoral Lymphocytes			0.127
no	7 （70%）	146 （88%）	
Yes	3 （30%）	20 （12%）	
Intratumoral Stromal Inflammation			**0.001**
Diffuse	5 （50%）	11 （6.6%）	
Focal	5 （50%）	155 （93.4%）	
Plasma Cell Component			**0.037**
≤50%	6 （60%）	145 （87.3%）	
>50%	4 （40%）	21 （12.7%）	
Tumor filtrating Lymphocytes （/10HPF）			0.249
<40	8 （80%）	151 （91%）	
≥40	2 （20%）	15 （9%）	
Mitosis （/10HPF）	5.1	6.4	0.499
Necrosis			0.300
No	3 （30%）	73 （44%）	
Yes	7 （70%）	93 （56%）	
ARID1A			0.203
No	8 （80%） ）	102 （61.4%）	
Yes	2 （20%） ）	64 （38.6%）	
Stage			0.462
I/II	6	110	
III-IV	4	56	

Figure 1 - 1108
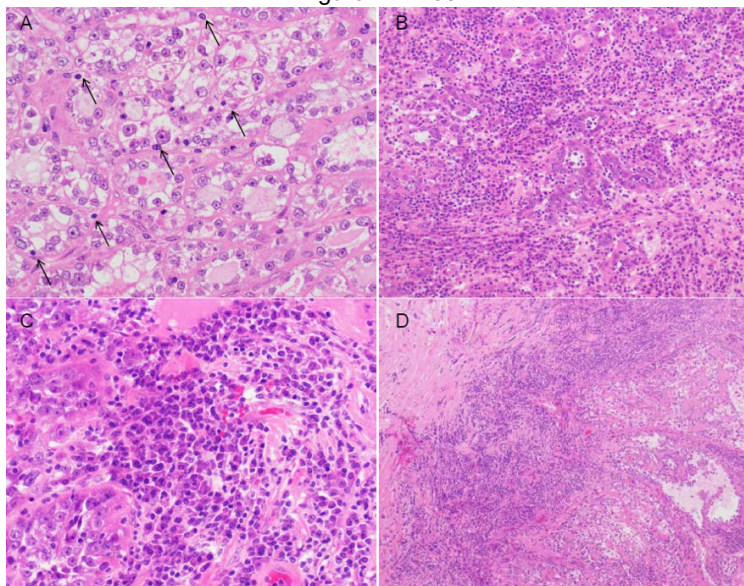
Figure 2 - 1108
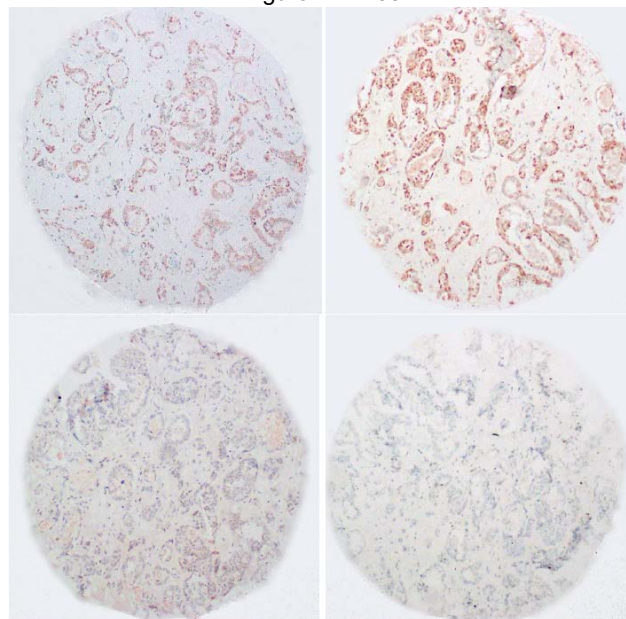
Conclusions: dMMR in OCCC is not highly frequent. Diffuse intratumoral stromal inflammation suggests the use of the MMR status as a unique screening histological feature, and MSH2/MSH6 expression is the most frequently deficient and closely associated with LS.

1109 From Liquid-Based Cytology to Liquid-Based Histology of Pap Smear Samples: Are We Ready to Shift the Paradigm?

Cinzia Giacometti[1], Lucetta Vidotto[2], Sara Ghiretti[1], Mauro Cassaro[1]
[1]ULSS6 Euganea, Camposampiero, Italy, [2]Department of Pathology - ULSS6 Euganea, Camposampiero, Italy

Disclosures: Cinzia Giacometti: None; Lucetta Vidotto: None; Sara Ghiretti: None; Mauro Cassaro: None

Background: Cell block (CB) preparations from residual liquid-based Pap samples (LBPS) have been shown to be of diagnostic value. However, traditional cell block preparation techniques are mostly manual, difficult to standardize, and not feasible for hypocellular samples. Cytomatrix® is a synthetic matrix that counts among its various characteristics the property to capture and store inside its three-dimensional structure, the biological material (micro-macro cells and cell aggregates) from needle withdrawal samples. The matrix is then directly put in formalin and routinely processed to form a paraffin-embedded *ensamble* of matrix and biological material which can be then cut and stained.

Design: In this study, the authors investigated the usefulness of Cytomatrix® cell blocks (CyCB) on residual LBPS to assess all the parameters usually evaluated in Pap samples, according to Bethesda guidelines for interpretation of Pap smears (i.e. adequacy, inflammation, bacterial/fungi, epithelial/glandular lesions etc), blind of previous Pap smear diagnoses.

p16 immunohistochemistry (IHC) was performed on all samples and high-risk HPV (hrHPV) molecular test was performed in suspicious/positive CyCB cases, if not previously available. The results of CyCB interpretation, p16 IHC and hrHPV molecular tests were then compared with the initial diagnoses assessed on LBPS.

Results: One-hundred fifty-nine (159) consecutive Hematoxylin&Eosin-stained CyCB slides prepared from CyCB from residual LBPS (108 normal, 7 ASC-US, 3 ASC-H, 29 LSIL, 6 HSIL, 3 endometrial cells, 2 AGC and 1 unsatisfactory) were analyzed. HrHPV molecular biology was available in 100% of cases. The cellular architecture and morphology were well maintained in all CyCB samples, with excellent consistency.

A total of 18 cases were further categorized/upgraded: 4 cases from normal to LSIL, ASC categories to SIL categories, 2 LSIL to HSIL, 2 AGC and 1 endometrial cells to adenocarcinoma, 1 unsatisfactory to negative (Table 1). HrHPV test were positive in all upgraded cases.

INTERPRETATION/RESULT	LBPS	CyCB
Negative for intraepithelial lesion or malignancies	108	105
ASC-US	7	0
ASC-H	3	0
L-SIL	29	40
H-SIL	6	9
AGC	2	0
Endometrial cells	3	2
Adenocarcinoma	0	3
Unsatisfactory	1	0

Figure 1 - 1109
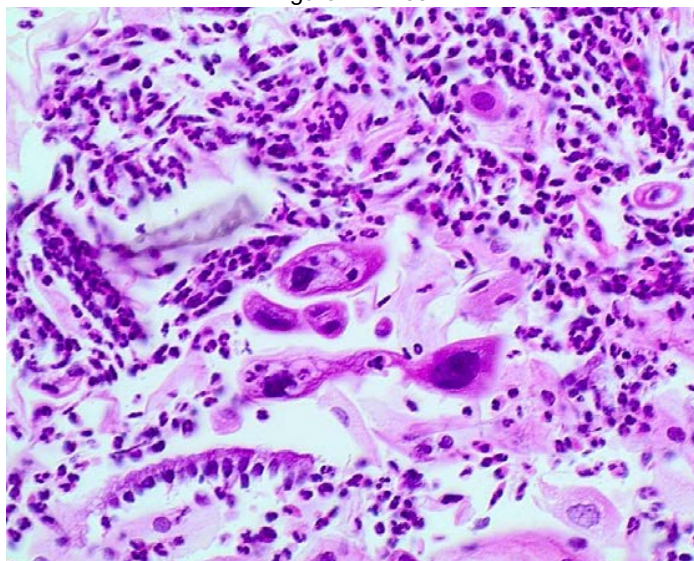
Figure 2 - 1109
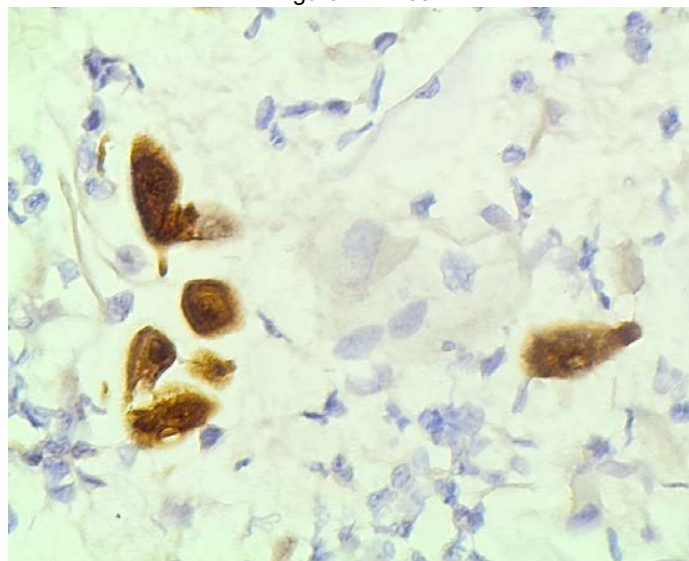
Conclusions: The Cytomatrix® CB system as used in the study allows for the efficient and rapid processing of micro-sized cytology samples minimizing manual handling. It is a useful technique to further categorize both epithelial and glandular lesion, as the pathologist has the ability to improve the diagnostic accuracy of Pap smears using ancillary techniques (i.e. IHC, molecular biology), thus eventually avoiding unnecessary colposcopic evaluation or biopsies.

1110 Detection of TP53 Mutations in the Peritoneal Washings of Women with Germline Mutations in Ovarian Cancer Susceptibility Genes

Emily Goebel[1], Xiaohua Qian[2], Jingzhong Xie[3], David Chapel[2], Sarah Hill[4], Judy Garber[5], Wa Xian[6], Christopher Crum[2]
[1]London Health Sciences Centre, Kilworth, ON, [2]Brigham and Women's Hospital, Boston, MA, [3]University of Houston, Houston, TX, [4]Brigham and Women's Hospital, [5]Dana-Farber Cancer Institute, [6]University of Texas Health Science Center

Disclosures: Emily Goebel: None; Xiaohua Qian: None; Jingzhong Xie: None; David Chapel: None; Christopher Crum: None

Background: Women with germline mutations in the BRCA genes are at increased risk for developing high-grade serous carcinoma (HGSC). The presumed origin for these tumors in many cases is the fallopian tube and the source of the tumor cells is presumed to be exfoliated cells with TP53 mutations from either intra-mucosal serous carcinomas (STIC) or early serous proliferations (via precursor escape). Biologic progression of these cells with TP53 mutations thus can result in "primary peritoneal" HGSC. Recent studies of HGSC cases and controls have confirmed the presence of cells with TP53 mutations in the peritoneal fluid.

Design: The purpose of this pilot study was to determine if healthy women at genetic risk for HGSC harbored cells with TP53 mutations in the peritoneal cavity. Peritoneal washings from women undergoing risk-reduction salpingo-oophorectomy were selected. Discarded samples were centrifuged and cell pellets were processed for DNA extraction. DNA was then subjected to next-generation Ion torrent sequencing and the data were analyzed manually and using the analysis program gatk4 mutect2 (gatkforums.broadinstitute.org). Results were interpreted with the following conclusions: 1) there is a low possibility that the same mutation would be shared by multiple patients, 2) Ion torrent sequencing platform is prone to homopolymer-sequencing-errors (indels), 3) there is a very low possibility that two independent mutation events happened in a single cell.

Results: After excluding mutations that were presumed to be germline variants, 5 samples were identified with unique frameshift mutations in TP53 (Table). One sample contained multiple TP53 mutations, interpreted as likely signifying more than one cell population with a unique mutation.

TP53 mutations in peritoneal fluid of women at risk for HGSC		
Sample	Genetics	TP53 indel
3	BRCA1	chr17: 7579420
4	BRCA1	chr17:7578280
5	BRCA1	chr17:7577031;7036;8280;8464,9547,9861
6	BRIP1	chr17: 7578474
7	BRCA2	chr17: 7579373

Conclusions: Women at increased genetic risk for HGSC frequently harbor cells with TP53 mutations in their peritoneal fluid. The origin of the cell populations with these mutations remains unclear. The possibility that these cells share lineage with endometrial or salpingeal cells with similar mutations is currently under investigation.

1111 Usual Vulvar Intraepithelial Neoplasia with Morphology Mimicking Differentiated Vulvar Intraepithelial Neoplasia and/or Lichen Sclerosus

Laurie Griesinger[1], Richard Lieberman[2], Grace Wang[1], Heather Walline[1], Stephanie Skala[1]
[1]University of Michigan, Ann Arbor, MI, [2]Michigan Medicine, Ann Arbor, MI

Disclosures: Laurie Griesinger: None; Richard Lieberman: None; Grace Wang: None; Heather Walline: None; Stephanie Skala: None

Background: Squamous cell carcinoma (SCC) of the vulva can arise through a human papillomavirus (HPV)-dependent pathway (usual vulvar intraepithelial neoplasia, UVIN) or an HPV-independent pathway (differentiated vulvar intraepithelial neoplasia, dVIN). dVIN is expected to show more rapid progression to SCC. UVIN with superimposed lichen simplex chronicus (LSC) or inflammation has been reported to morphologically resemble dVIN. Such cases of UVIN are block positive for p16 and show parabasal and mid-epithelial p53 staining with sparing of the basal layer. The 11 cases (from 2 studies) with reported HPV genotyping results showed HPV 16. To our knowledge, only 15 cases of UVIN mimicking dVIN have been reported in the literature.

Design: The surgical pathology database of a single large academic institution was searched for vulva specimens with corresponding p53 and p16 immunohistochemical stains, yielding 30 specimens (from 19 patients) resected between 1991 and 2019. In situ hybridization for high-risk HPV and HPV multiplex PCR-MassArray (PCR-MA) to identify high and low risk HPV types (with reflex to L1 consensus PCR for invalid results) were performed on at least one block from each patient (24 blocks from 19 patients for ISH, 21 blocks from 19 patients for PCR).

Results: All cases resembled dVIN morphologically, but with a higher degree of atypia and superimposed chronic inflammation. Nearly all cases showed block positivity for p16 protein by IHC in combination with mid-epithelial p53 staining (see Figure). Nearly all cases had at least patchy positivity by HPV ISH. Thirteen cases yielded valid PCR-MA results with L1 consensus PCR yielding results in 2 additional cases. 9 cases were positive for HPV and 6 cases were negative. Of the positive cases, HPV16 was identified in 5 cases, HPV52 and HPV58 each identified in 2 cases, and HPV31 in 1 case. There was one co-infection with types 16 and 52.

Figure 1 - 1111
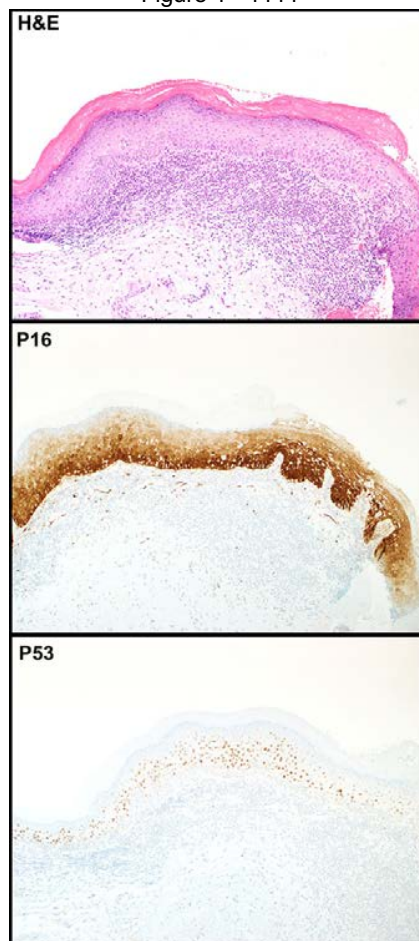
Conclusions: To our knowledge, this is the largest cohort of UVIN mimicking dVIN reported to date. Contrary to prior studies, which reported positivity for HPV16 in all 11 cases tested, we found HPV16 in only 5 cases (33% of total; 63% of HPV positive cases), with other HPV types identified in 3 cases (20% of total; 37% of HPV positive cases), and no HPV identified by PCR in 6 cases (40%). These results add to the small group of reported cases of UVIN mimicking dVIN, and expand the spectrum of associated HPV types.

1112 The Immune Microenvironment in Low-Grade Endometrial Stromal Sarcomas: The Ratio of CD8+ T-Cells/FOXP3+ Tregs (T Regulatory Cells) is a Significant Prognostic Factor

Elin Hardell[1], Jordi Gonzalez-Molina[2], Okan Gültekin[3], Kaisa Lehti[4], Joseph Carlson[5]
[1]Stockholm, Sweden, [2]Department of Microbiology, Tumor and Cell Biology and Department of Oncology-Pathology, Karolinska Institutet, Stockholm, Sweden, [3]Karolinska Institutet, Stockholm, Sweden, [4]Karolinska Institutet and University of Helsinki, Stockholm, Sweden, [5]Karolinska University Hospital, Stockholm, Sweden

Disclosures: Elin Hardell: None; Jordi Gonzalez-Molina: None; Okan Gültekin: None; Kaisa Lehti: None; Joseph Carlson: None

Background: Low-grade endometrial stromal sarcomas (LGESS) are rare malignant tumors of the uterus. They typically affect young and perimenopausal woman and are treated with surgery, possibly in combination with anti-estrogen therapy.

The immune microenvironment has an important role in the development and progress of tumors. The amount of different infiltrating immune cells, including CD8+ T-cells, FOXP3+ Tregs (T regulatory cells) and the ratio of CD8+ T cells/FOXP3+ Tregs has been shown to be prognostic in different tumors. B7H4 and PD-L1 are immune inhibitory proteins overexpressed in a variety of tumors, and have emerged as potential therapeutic targets.

Design: Twenty cases of LGESS were included. All cases had follow-up data and paraffin blocks with formalin fixed tumor material. A tissue micro array was constructed with two core biopsies from each case. Multiplex fluorescent immunohistochemistry in combination with image analysis in QuPath was used to quantitatively assess the expression of different immune markers, including CD8, FOXP3, CD68, CD163, IDO1, B7H4 and PD-L1.

Results: The range of number of detected tumor-infiltrating CD8+ T-cells was 10.13-286.04 cells/mm^2 (mean 77.62). The range of FOXP3+ Tregs was 7.13-584.87 cells/mm^2(mean 122.35). The cases were divided into high and low expression groups using the mean of each marker as cutoff. Kaplan-Meier curves of overall survival showed an improved survival for patients with high numbers of CD8+ T-cells (n=3) compared to patients with low numbers (n=15), figure 1. However, the difference was not statistically significant (p=0.2097). When comparing the group of patients with a high ratio (n=6) of CD8+/FOXP3+ cells with the group with a low ratio (n=12), the group with a low ratio had a significant better survival (p=0.0087), figure 2. A better survival was also seen in the group of patients with high numbers of B7H4+ cells compared to the group with low numbers (range 0-36, mean 5.59, p=0.2358). The quantity of CD68+ macrophages, CD68+CD163+ M2-type macrophages and IDO1 was not prognostic. No expression of PD-L1 was seen.

Figure 1 - 1112
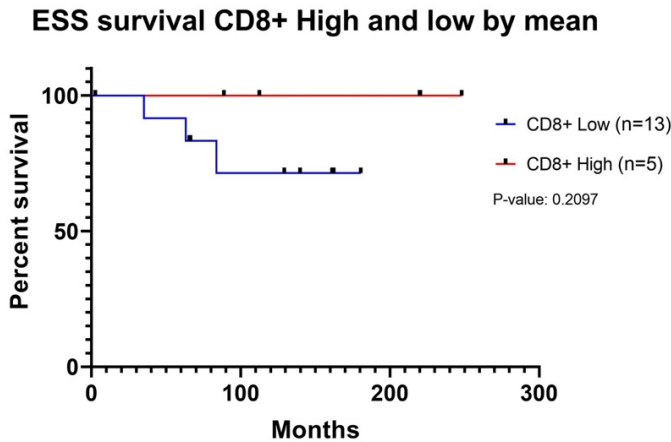
Figure 2 - 1112
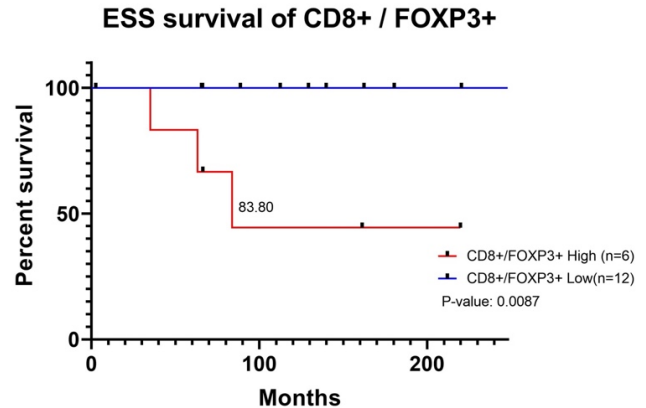
Conclusions: A low ratio of CD8+/FOXP3+ cells is significantly associated with a favorable prognosis in LGESS. For patients with a high quantity of CD8+ T-cells and B7H4, a trend towards better survival was seen. The expression of B7H4 is also a potential therapeutic target.

1113   Clinical and Pathological Features of Vitelline Vasculitis

Yuichiro Hatano[1], Maho Tamada[2], Mikiko Matsuo[2], Hiroyuki Tomita[2], Nami Asano[3], Akira Hara[2]
[1]Gifu University Graduate School of Medicine, Gifu, Japan, [2]Gifu University, Gifu, Japan, [3]Chuno Kosei Hospital, Seki, Gifu, Japan

Disclosures: Yuichiro Hatano: None; Maho Tamada: None; Mikiko Matsuo: None; Hiroyuki Tomita: None; Nami Asano: None; Akira Hara: None

Background: Funisitis is a leading cause of perinatal complications, and in the majority of cases it is caused by chorioamnionitis or umbilical vasculitis. Recently, the vitelline vessel remnant (VVR) was reported to be associated with neutrophilic infiltration (PMID: 30541420), suggesting that even the supernumerary vessel is involved in acute inflammatory processes associated with the umbilical cord. However, the detailed characteristics of this newly proposed microscopic lesion remain unclear. Thus, we conducted the first case series study of vitelline vasculitis to clarify its clinical and pathological features.

Design: In total, 261 obstetric cases were enrolled in this study. CD15 immunostaining was performed to visualize granulocytes in the umbilical cord. Further, a modified version of the revised Blanc classification (PMID: 28691405) was used to assess the severity of funisitis. Clinical data, such as data on perinatal complications, maternal serum C-reactive protein (CRP) levels, cord blood pH, and Apgar score, were obtained from the patients' medical records. Statistical differences were evaluated using Fisher's exact test for categorical variables and Student's t-test, paired t-test, or Welch's t-test for continuous variables.

Results: Of the 261 patients, 22 (8.4%) showed VVR (Figure 1). There were no significant differences in clinical features between patients with and those without VVR. Per the inflammation assessment based on CD15-positive cell distribution, severe funisitis accounted for 16% of the cases and was significantly associated with chorioamnionitis, elevation of maternal serum CRP levels, and weight gain of the placenta. Among patients with VVR, 5 (23%) were assessed as having severe funisitis; CD15-positive cells around the VVR were observed in 20 (91%) patients (Figure 2). Although perivascular granulocytic infiltration corresponds with severe vasculitis per our assessment system, granulocytic infiltration around the VVR was not associated with the abovementioned clinical and pathological characteristics.

Figure 1 - 1113
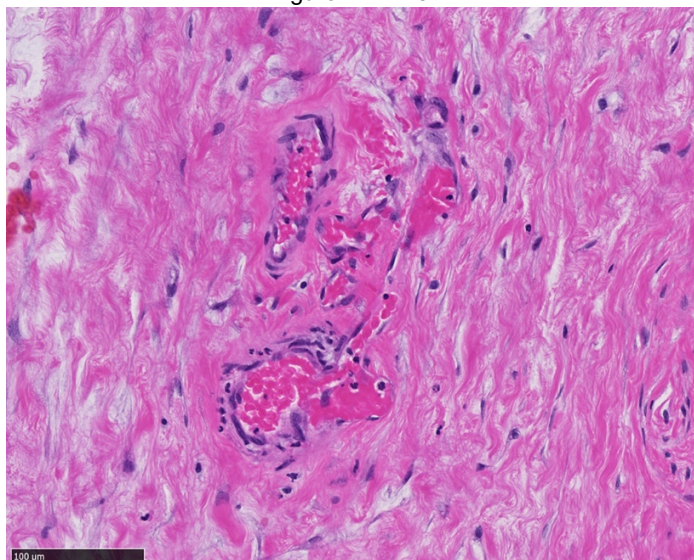
Figure 2 - 1113
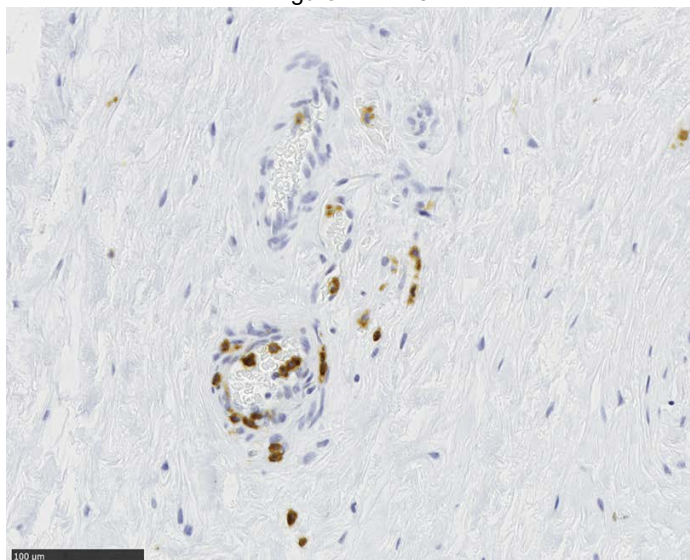
Conclusions: Consistent with previous results, VVR was found to be frequently associated with granulocytic infiltration. Although it is difficult to identify such perivascular inflammation without immunohistochemical analysis, our investigation revealed that vitelline vasculitis itself does not affect the maternal and fetal medical condition.

1114 Gene Fusions Characterize a Subset of Uterine Cellular Leiomyomas

Anjelica Hodgson[1], David Swanson[2], Shangguo Tang[3], Brendan Dickson[4], Gulisa Turashvili[2]
[1]University of Toronto, Toronto, ON, [2]Mount Sinai Hospital, Toronto, ON, [3]Burlington, ON, [4]Mount Sinai Health System, Toronto, ON

Disclosures: Anjelica Hodgson: None; David Swanson: None; Shangguo Tang: None; Brendan Dickson: None; Gulisa Turashvili: None

Background: Uterine leiomyoma, the most common gynecological neoplasm, is a benign neoplasm with smooth muscle differentiation. Studies evaluating the pathogenesis of conventional uterine leiomyoma have shown multiple potential mechanisms including recurrent gene alterations in *MED12* and *HMGA2*. Cellular leiomyoma, a subtype that may be morphologically confused with low grade endometrial stromal neoplasms, remains less well-characterized. Following identification of an index patient with a cellular leiomyoma harboring a *HMGA2-TRAF3IP2* fusion, we undertook a retrospective review of additional cases to better assess the prevalence of fusion events in this tumor type.

Design: A retrospective archival review was performed for cases diagnosed as cellular leiomyoma (2013-2019). Slides were reviewed to confirm the tumor morphology and immunophenotype were concordant with the diagnosis of cellular leiomyoma. Clinicopathologic data from each patient was recorded. RNA-sequencing was performed using formalin fixed paraffin embedded tissue and the TruSight RNA Fusion Panel (Illumina, CA) which evaluates 507 genes for fusions including those typically identified in endometrial stromal neoplasms.

Results: A total of 12 uterine cellular leiomyomas were identified. The median patient age at diagnosis was 52 years (range 35-64). Patients most commonly presented with abnormal uterine bleeding (n=3), symptoms related to tumor bulk (n=2), or both (n=2). Two patients were immediately postpartum and one patient had concurrent grade 3 endometrial endometrioid adenocarcinoma; the remaining 2 patients did not have any pre-operative clinical information available. Myomectomy was performed in 5 patients and hysterectomy in 7 patients. The immunohistochemical and molecular findings are summarized in Table 1. Eleven tumors (92%) had sufficient quality RNA for sequencing. Three tumors harbored gene fusions, two involving the *HMGA2* gene (*HMGA2-NAA11 and HMGA2-TRAF3IP2*) and a novel *TPCN2-YAP1* fusion of uncertain significance. No clinical or pathologic variable was significantly associated with the presence of a gene fusion.

Patient	CD10	Desmin	H-caldesmon	Smooth muscle actin	Estrogen receptor	Progesterone receptor	Fusion
1	Focal, moderate	Focal, strong	Patchy, strong	Diffuse, strong	Diffuse, strong	Diffuse, strong	*TPCN2-YAP1*
2	Focal, strong	Diffuse, moderate	Patchy, moderate	Diffuse, strong	Diffuse, strong	Patchy, strong	Failed sequencing
3	Patchy, strong	Patchy, strong	Patchy, strong	Diffuse, strong	Focal, weak	Patchy, weak	None identified
4	Diffuse, strong	Patchy, moderate	Negative	Diffuse, strong	Diffuse, strong	Diffuse, strong	*HMGA2-TRAF3IP2*
5	Patchy, moderate	Patchy, strong	Patchy, moderate	Diffuse, strong	Diffuse, strong	Diffuse, moderate	None identified
6	Focal, weak	Patchy, moderate	Patchy, weak	Diffuse, strong	Diffuse, strong	Diffuse, strong	None identified
7	Focal, strong	Patchy, strong	Patchy, moderate	Diffuse, strong	Diffuse, strong	Diffuse, strong	None identified
8	Patchy, strong	Diffuse, strong	Patchy, strong	Diffuse, strong	Diffuse, strong	Diffuse, strong	None identified
9	Patchy, moderate	Diffuse, strong	Diffuse, moderate	Diffuse, strong	Diffuse, strong	Diffuse, strong	None identified
10	Patchy, weak	Diffuse, strong	Diffuse, strong	Diffuse, strong	Diffuse, strong	Diffuse, strong	*HMGA2-NAA11*
11	Patchy, strong	Diffuse, strong	Patchy, strong	Diffuse, strong	Patchy, moderate	Diffuse, strong	None identified
12	Patchy, strong	Diffuse, strong	Focal, strong	Diffuse, moderate	Diffuse, strong	Diffuse, strong	None identified

Conclusions: A subset of cellular leiomyomas harbor *HMGA2* rearrangement, suggesting molecular kinship with conventional uterine leiomyomas. The *TPCN2-YAP1* gene fusion may be a novel fusion although additional investigation is required. The results suggest that identification of these fusions may be useful when the diagnosis of cellular leiomyoma is in question.

1115   Clinicopathologic Features of Endometrial Carcinomas with Heterogeneous Loss of Mismatch Repair Protein Immunoexpression. Our Institutional Experience
Yanjun Hou[1], Longmei Zhao[1], Michael Cruise[2], Maria Luisa Policarpio-Nicolas[1]
[1]Cleveland Clinic Foundation, Cleveland, OH, [2]Cleveland Clinic, Cleveland, OH

Disclosures: Yanjun Hou: None; Longmei Zhao: None; Michael Cruise: None; Maria Luisa Policarpio-Nicolas: None

Background: Lynch syndromes (LS) is an autosomal dominant cancer syndrome caused by mutation in one of the mismatch repair (MMR) genes *MLH1*, *PMS2*, *MSH2*, *MSH6* and *EPCAM*. Because of the cost and availability, MMR immunohistochemistry (IHC) is commonly utilized as the initial screening for LS. The common immunoexpression patterns for MMR are either intact or completely lost. Occasionally, heterogeneous staining pattern can be seen and could cause interpretation difficulties. While some previously published literature attributed this heterogeneous expression mostly to technical issues, recent publications attributed this to heterogeneous methylation of the MLH1 promoter or a biological event in tumoral evolution. This study was conducted to review our cases of endometrial carcinoma with heterogeneous immunoexpression of MMR proteins and correlate these results with the clinical findings and MLH1 methylation status.

Design: A pathology archive database search was performed from surgical specimens with diagnoses of endometrial adenocarcinoma and corresponding MMR IHC from 01/2017 to 05/2019. Of the 117 cases, 9 endometrial adenocarcinomas with partial loss/heterogeneous staining pattern of one of or more of the MMR were identified. The slides were reviewed and the partial loss/heterogeneous staining pattern was re-classified based on previously reported patterns by Pai et al (abrupt loss) and Joost et al (intraglandular). The corresponding clinical histories, demographic information and histology were reviewed (Table1).

Results: The patients' age ranged from 43-84 years old (mean=64). Seven of nine (75%) patients were obese. All cases were of endometrioid histologic type (FIGO Grade 1 [7], Grade 2[2]). Regardless of staining pattern (abrupt or intraglandular), it was concordant in 5 cases for MLH1 and PMS2. Four cases showed complete loss of PMS2. MLH1 methylation was present in 89% (8/9) of cases and absent in 1(11%). The latter case was sent for next generation sequencing and showed no alterations of germline or somatic origin.

Table 1. Clinicopathologic Findings, MMR Immunohistochemistry, MLH1 Methylation and NGS Results										
Case	Age	BMI	Histologic type	Procedure	MLH1	PMS2	MSH2	MSH6	MLH1 methylation	NGS
1	52	47	Endometrioid FIGO2	TAHBSO	A/I	A/I	intact	focal A	Present	
2	67	44	Endometrioid FIGO1	curettage	I	Complete loss	intact	intact	Present	
3	84	28	Endometrioid FIGO1	TAHBSO	I	Complete loss	intact	intact	Present	
4	78	55	Endometrioid FIGO1	curettage	A/I	Complete loss	intact	intact	Present	
5	53	44	Endometrioid FIGO1	TAHBSO	A	Complete loss	intact	intact	Present	
6	49	48	Endometrioid FIGO1	curettage	A	A	intact	intact	Present	
7	43	54	Endometrioid FIGO1	TAHBSO	I	I	intact	focal I	Absent	No germline or somatic mutation
8	79	29	Endometrioid FIGO1	curettage	A	A	intact	focal A	Present	
9	67	34	Endometrioid FIGO2	curettage	A	A	intact	intact	Present	
A-abrupt pattern; BMI-body mass index; I-intraglandular pattern, A/I both abrupt and intraglandular pattern, NGS next generation sequencing										
TAHBSO-total abdominal hysterectomy with bilateral salpingo-oophorectomy										

Conclusions: Heterogeneous MMR IHC pattern in endometrial adenocarcinoma is rare (8.0%, 9/117) and often of the endometrioid histologic type (FIGO 1). The patients are usually obese without a family or personal history of Lynch syndrome associated cancer. While our case number is small, our results show that heterogeneous loss of MLH1 is associated with MLH1 promoter methylation. Additional molecular tests will be helpful in supporting our findings.

1116 Malignant Mixed Mullerian Tumors: Does the Epidemiology/Prognosis Differ Based on Histology of Epithelial Component?

K Islam[1], Khadijeh Jahanseir[2], Katrine Hansen[3], C. James Sung[1], Kamaljeet Singh[4], M. Ruhul Quddus[1]
[1]Women & Infants Hospital/Alpert Medical School of Brown University, Providence, RI, [2]Women & Infants Hospital, Providence, RI, [3]Women and Infants Hospital of Rhode Island, Providence, RI, [4]Yale School of Medicine, New Haven, CT

Disclosures: K Islam: None; Khadijeh Jahanseir: None; Katrine Hansen: None; C. James Sung: None; Kamaljeet Singh: None; M. Ruhul Quddus: None

Background: Malignant mixed müllerian tumor (MMMT) also known as carcinosarcoma (CS) is a biphasic tumor with high grade carcinomatous and sarcomatous component. MMMT is known to be an aggressive disease with poor survival even in early stage disease. The epithelium component in MMMT is most often of serous (MMMT SC) type but other müllerian types including endometrioid (MMMT EC) type are rarely seen. The mesenchymal component is either homologous or heterologous which has no influence on disease outcome. In contrast, high-grade serous or clear cell component correlates with a higher frequency of metastasis. The current study is designed to compare prognosis and survival outcome of malignant mixed müllerian tumor with serous (MMMT-SC) versus malignant mixed müllerian tumor with endometrioid (MMMT EC) component.

Design: A total of 57 cases, 51 MMMT-SC and 6 MMMT-EC cases were studied from 1999 to 2019 after IRB approval. The original diagnoses were reconfirmed and the cases were assigned into two groups based on epithelial component of the MMMT. Patient charts were reviewed to obtain clinical information regarding age at diagnoses, tumor stage, and treatment types (surgery and postoperative therapy). Survival outcome was examined in terms of disease-free survival, local and distant recurrence and overall survival. The data was compared to assess for outcome difference between the groups.

Results: The demographic findings are summerized in Table 1 and the findings are presented in Figure 1.

Table 1: Demographics and Characteristics of MMMT SC versus MMMT EC

	MMMT with SC	MMMT with EC
Number (n)	51	06
Age (yr)	53 to 91 Mean: 70.2	56 to 80 Mean: 77
Tumor Location	Endometrial: 39 Ovarian: 9 Fallopian: 2 Vaginal: 1	Endometrial: 6
Follow up (months)	4 to 129	8 to 87
Stage :	Stage I: 30 Stage II: 04 Stage III: 16 Stage IV: 01	Stage I: 04 Stage II: 00 Stage III: 02 Stage IV: 00

Figure 1 - 1116
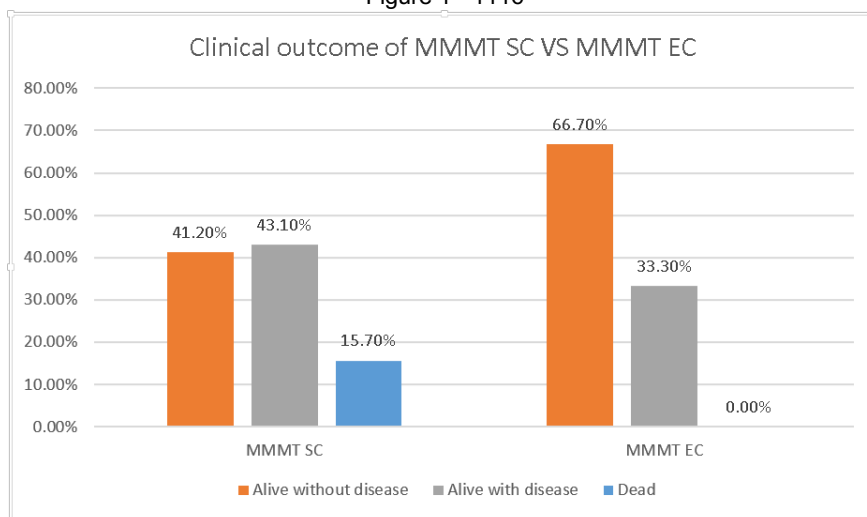
Conclusions: Compared to the other group, MMMT EC is diagnosed in older patients (mean age of diagnosis is 77 yr). Although MMMT EC is diagnosed in older patients compared to MMMT SC, clinical course following treatment is more favorable in MMMT EC (disease free survival in 66.7%) versus 41.2% in MMMT SC. Disease recurrence and metastasis up to 129 months of follow up shows 33.3% recurrence in MMMT EC versus 43.1% in MMMT SC. The clinical course of MMMT appears to vary depending on the epithelial component. Larger multicenter study with additional cases is needed to corroborate our findings.

1117 High Grade Carcinoma of Mullerian Origin with Minor/Focal Sarcoma Component: Are They True Carcinosarcoma?

Khadijeh Jahanseir[1], K Islam[2], Natalie Banet[3], Katrine Hansen[4], Max Masnick[5], C. James Sung[2], M. Ruhul Quddus[2]
[1]Women & Infants Hospital, Providence, RI, [2]Women & Infants Hospital/Alpert Medical School of Brown University, Providence, RI, [3]Women and Infants Hospital/Brown University, Providence, RI, [4]Women and Infants Hospital of Rhode Island, Providence, RI, [5]Geisinger National Precision Health, Rockville, MD

Disclosures: Khadijeh Jahanseir: None; K Islam: None; Natalie Banet: None; Katrine Hansen: None; Max Masnick: None; C. James Sung: None; M. Ruhul Quddus: None

Background: Mullerian carcinonosarcoma (CS) is a malignant biphasic tumor composed of high grade carcinomatous and sarcomatous elements. The current WHO classification of the tumors of the female genital tract, did not address the exact percentage of sarcomatous component require to define CS. On a rare occasion a unique tumor comprising mainly of high grade Mullerian carcinoma with only minor/focal sarcoma (HGC-MS) is encountered. The biological behavior of this subset has not been studied before. Classifying them as high grade carcinoma (HGC) would make these patients eligible for more clinical trials. We intend to explore that question by comparing these tumors with CS and HGC.

Design: Hysterectomy specimens of HGC-MS (n=27; Group 1), CS (n=30; Group 2), and HGC (n=27; Group 3) were retrieved from our archival files, diagnoses confirmed and follow-up recorded from the date of diagnosis to death or last follow-up (2008-2019) after IRB approval. The overall survival and progression-free survival were compared between these three groups using Kaplan-Meier (KM) curves.

Results: Clinicopathologic data is summarized in Table 1. In HGC-MS, follow-up revealed that 12 patients (44%) developed recurrence or metastasis; sites include lung (15%) followed by brain, liver and peritoneum (7%, each). The epithelial component of HGCs were serous (n=18, 62%), endometrioid (n=5, 17%), mixed serous and endometrioid (n=4, 14%), and mixed serous, endometrioid, and clear cell (n=2, 7%). No statistically significant differences of overall or progression free survival between these three groups were identified (p=0.97 and p=0.63; respectively); both tested with long-rank test for equality of survivor functions.

Table 1: Clininicopathological Features of All Three Groups		Group 1 (N=27)	Group 2 (N=30)	Group 3 (N=27)
Age in Yrs.: Range (Median)		53-90 (71)	56-91 (69)	60-92 (70)
Site of tumor: N (%)				
	Uterus	20 (67)	26 (87)	27 (100)
	Ovary	6 (21)	3 (10)	-
	F/tube	2 (7)	1 (3)	-
	Vagina	1 (4)	-	-
FIGO Stage N (%)				
	I	15 (52)	20 (67)	18 (67)
	II	3 (10)	2 (7)	6 (22)
	III	11 (38)	7 (23)	3 (11)
	IV	-	1 (3)	-
Follow/up N (%)				
	Alive w/disease	13 (48)	10 (33)	5 (18)
	Died of disease	3 (11)	5 (17)	5 (18)
	Alive without disease	11 (41)	15 (50)	17 (64)
	Recur/Met	12 (44)	15 (50)	8 (30)

Figure 1 - 1117

Overall survival (failure = death)

Figure 2 - 1117
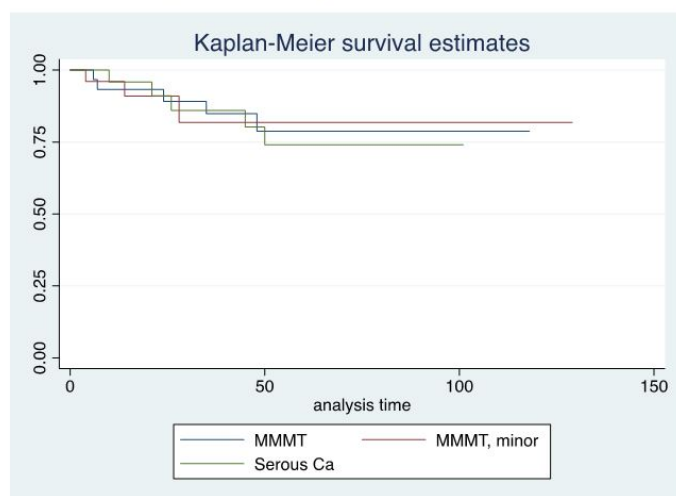
Progression-free survival (failure = recurrence or metastasis)
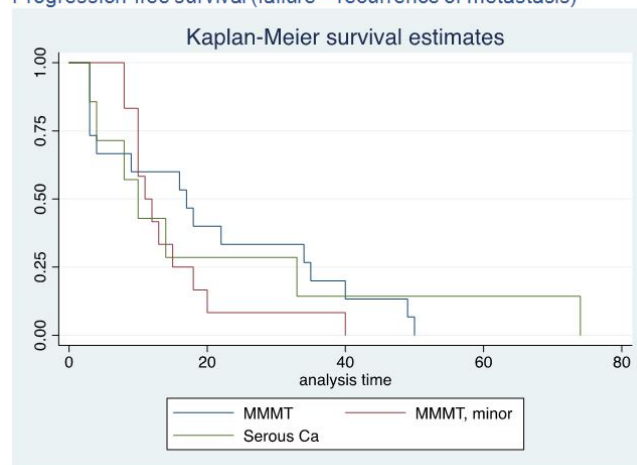
Conclusions: High grade Mullerian carcinoma with minor sarcomatous component had similar biologic behavior to that of CS. Uterine HGCs had a poor prognosis. The overall survival and progression-free survival between these three groups were not statistically significant. Nevertheless, the underlying pathogenesis of this unique group of tumor needs to be further investigated in a multicenter study with more cases. For the time being, we suggest that these tumor should be treated as carcinosarcoma rather that high grade carcinoma.

1118 The Combination of Aberrant p53 and Rb Immunohistochemistry is Highly Specific for Leiomyosarcoma

Tyler Jankowski[1], Sarah Umetsu[1], Nancy Joseph[1], Rebecca Wolsky[1], Nicholas Ladwig[1]
[1]University of California San Francisco, San Francisco, CA

Disclosures: Tyler Jankowski: None; Sarah Umetsu: None; Nancy Joseph: None; Rebecca Wolsky: None; Nicholas Ladwig: None

Background: Uterine smooth muscle tumors are further stratified as leiomyoma (LM), smooth muscle tumor of uncertain malignant potential (STUMP), or leiomyosarcoma (LMS) based on histologic features (tumor-type necrosis, mitotic activity, and nuclear atypia). In some cases, definitive classification of these tumors is challenging due to subjectivity of these features.

Several recent molecular studies, including the adult soft tissue sarcoma TCGA data demonstrated near-universal inactivation of *TP53* and *RB1* with frequent co-inactivation of *ATRX* in LMS. We sought to investigate the utility of IHC for p53, Rb1, and ATRX as a surrogate for the underlying genetic alterations in LMS and compare to other entities in the differential diagnosis.

Design: Rb, ATRX, and p53 IHC was performed on tissue microarrays (2-3 mm cores, in triplicate) and whole slide sections from resection specimens of LMS (n=57, 35 uterine, 22 extra-uterine). Uterine smooth muscle tumors (9 STUMP, 21 LBN, and 49 LM), carcinosarcoma (n=9), low-grade endometrial stromal sarcoma (LGESS) (n=9), high-grade endometrial stromal sarcoma (HG-ESS) (n=4), and undifferentiated endometrial sarcoma (UES) (n=1) were included for comparison.

- Aberrant p53 staining is seen in the majority of LMS (39/57; 70%)
- Aberrant Rb staining is seen in the majority of LMS (38/57; 67%)
- Aberrant p53 staining is seen in STUMP (3/9; 33%) and LBN (5/21; 29%)
- Aberrant Rb staining is seen in STUMP (1/9; 11%) and LBN (3/20; 15%)
- Sensitivity (Sen) and Specificity (Spe) for LMS (as compared to STUMP, LBN, LM, LGESS, HG ESS, Carcinosarcoma, and UES):
    - Individual IHC:
        - p53: Sen = 70%; Spe = 86%
        - Rb: Sen = 67%; Spe = 94%
        - ATRX: Sen = 24%; Spe = 100%
    - Two IHC in combination:
        - p53 and Rb: Sen = 51%; Spe = 98%
        - p53 and ATRX: Sen = 14%; Spe = 100%
        - Rb and ATRX: Sen = 12%; Spe = 100%
    - Three IHC in combination:
        - p53, Rb, and ATRX: Sen = 12%; Spe = 100%

▪	Individual IHC				IHC in Combination			
	Aberrant p53	**Aberrant Rb (Loss)**	**Aberrant ATRX (Loss)**		**Aberrant p53 and Rb**	**Aberrant p53 and ATRX**	**Aberrant Rb and ATRX**	**Aberrant P53, Rb, and ATRX**
LMS (n=57)	39 (70%)	38 (67%)	13 (24%)		29 (51%)	8 (14%)	12 (21%)	7 (12%)
STUMP (n=9)	3 (33%)	1 (11%)	0		1 (11%)	0	0	0
LBN (n=21)	5 (29%)	3 (15%)	0		1 (5%)	0	0	0
LM (n=49)	0	2 (4%)	0		0	0	0	0
LGESS (n=16)	0	0	0		0	0	0	0
HGESS (n=4)	0	0	0		0	0	0	0
Carcinosarcoma (n=9)	7 (78%)	0	0		0	0	0	0
UES (n=1)	0	0	0		0	0	0	0

Conclusions: 1. Aberrant Rb IHC is specific for LMS amongst other uterine mesenchymal tumors. 2. The combination of aberrant p53 and Rb IHC increases specificity for LMS to 98% at the expense of sensitivity, which drops to 51%. 3. The presence of aberrant p53 or Rb IHC in STUMP and LBN may be a sign of their low malignant potential.

1119 PD-L1 and Mismatch Repair Status in Uterine Carcinosarcomas

Taylor Jenkins[1], Mark Stoler[2], Leigh Cantrell[1], Anne Mills[3]
[1]University of Virginia Health System, Charlottesville, VA, [2]University of Virginia Health System, Earlysville, VA, [3]University of Virginia, Charlottesville, VA

Disclosures: Taylor Jenkins: None; Mark Stoler: None; Leigh Cantrell: None; Anne Mills: None

Background: Uterine carcinosarcomas are highly aggressive malignancies with few adjuvant treatment options. Programmed cell death ligand-1 (PD-L1) expression in these tumors may predict response to checkpoint inhibitor therapies. An increase in PD-L1 expression has been shown in endometrial carcinomas with mismatch repair (MMR) deficiencies; however, few studies have evaluated PD-L1 expression in uterine carcinosarcomas. We sought to examine the rate of PD-L1 expression in tumor cells and the immune microenvironment in carcinosarcomas and correlate expression with MMR status.

Design: A 5-year retrospective database search for uterine carcinosarcomas was performed. The histologic diagnoses, MMR immunohistochemistry interpretation, p53 expression, and PD-L1 combined percentage scores (CPS) and tumor percentage scores (TPS) were confirmed by a gynecologic pathologist. In addition to confirming the histologic diagnosis of carcinosarcoma, the epithelial components were also evaluated by three gynecologic pathologists and tumors were stratified based on morphologic resemblance to endometrioid or serous endometrial carcinomas.

Results: 41 cases of uterine carcinosarcomas with available MMR immunohistochemistry were stained for PD-L1 and p53. MMR deficiencies were identified in 7% of cases; all of which were MLH1/PMS2-deficient and *MLH1* hypermethylated. 37 cases (90%) were positive for PD-L1, defined as a CPS score of ≥1 or a TPS score of ≥1%. Only one case, which was MMR intact, showed high expression of PD-L1 using the thresholds of a CPS score of ≥10 or a TPS score of ≥10%. 90% of cases showed aberrant p53 expression, and the majority (83%) had a serous, rather than endometrioid (17%) epithelial component.

Conclusions: The majority of uterine carcinosarcomas show some expression of PD-L1, predominantly in tumor-associated immune cells. Although there was no significant correlation between MMR status and PD-L1 expression, statistical power was limited due to the low rate of MMR loss in this cohort. In addition, our study reveals that the epithelial component in most carcinosarcomas is serous. Given that serous uterine carcinomas are not typically MMR-deficient, this may account for the much lower rate of MMR deficiency in uterine carcinosarcomas as compared to endometrioid and dedifferentiated carcinomas. These findings suggests that for carcinosarcomas, PD-L1 expression may be a more useful predictive biomarker than MMR status in identifying potential candidates for checkpoint inhibitor therapy.

1120 The Utility of Next Generation Sequencing in Advanced Breast and Gynecologic Cancers: Experience of a Large Tertiary Care Women's Hospital

Terrell Jones[1], Somak Roy[1], Rohit Bhargava[2]
[1]University of Pittsburgh Medical Center, Pittsburgh, PA, [2]Magee-Womens Hospital of UPMC, Pittsburgh, PA

Disclosures: Terrell Jones: None; Somak Roy: None; Rohit Bhargava: None

Background: Next generation sequencing (NGS) has the potential to identify genetic alterations that are actionable with targeted or immunotherapies. This is particularly salient in patients who have advanced cancers. However, NGS testing can have a significant cost for patients and is infrequently covered by insurance. Here we review the frequency of NGS testing in advanced breast and gynecologic cancers at our institution and the clinical utility of the results.

Design: A retrospective review identified 108 patients with advanced breast and gynecological cancers who underwent NGS testing between 2015 and 2019 at a single institution. Medical records were reviewed for demographics, pathologic data, sequencing results, treatment, and outcome information. The NGS utilization rate was defined by the presence or absence of clinical action or decision-making documented in the medical records based on NGS results.

Results: The 108 specimens tested included breast (35), cervix (2), endometrium (22), fallopian tube or ovary (47), vagina (1), and vulva (1), with most of the testing performed at Foundation Medicine (90%). The NGS results are summarized in table 1. The overall utilization rate of NGS testing was 38%, with a rate of 41% for breast cancer and 36% for gynecologic cancers. The enrollment in clinical trials based on NGS results was low (5% of cases overall). Overall, 48% patients died, all succumbing to disease. The median survival was 17.2 months for patients with actionable NGS result and targeted treatment, 16.9 months for actionable NGS result but no targeted treatment, and 12.5 months for patients with non-actionable NGS result. The survival difference was not significant (see figure).

Table 1: Next Generation Sequencing results	
Average alterations per case	5
Average variants of unknown significance per case	8
Cases with microsatellite instability	0
Cases with high mutation burden	0
Cases with intermediate mutation burden (>5 to 12 mutations per megabase)	19%
Genes most frequently altered in gynecologic cancers	*TP53* (75%), *KRAS* (21%), *PIK3CA* (21%), *PPP2R1A* (11%), and *CCNE1* (10%)
Genes most frequently altered in breast cancers	*TP53* (57%), *PIK3CA* (37%), *PTEN*, *MYC*, *FGFR1*-all 23%, *CCND1* (17%), *ARID1A*, *CDN2A*, *FGF3*-all 14%, *FGF4* (11%)

Figure 1 - 1120

Overall survival based on NGS test result and subsequent management
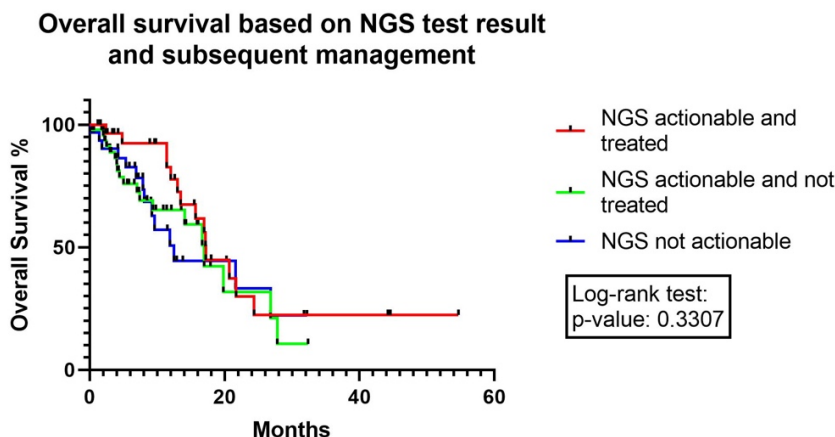
Conclusions: NGS testing for advanced breast and gynecological cancers at our institution has a 38% utilization rate in clinical decision making. However, the utilization rate may be impacted by various factors, including low rate of clinical trial enrollment and availability of clinical trials. Overall, the increased utilization rate over the years did not translate into improved survival.

1121 The Potential Prognostic and Therapeutic Implications of Prolactin Receptor and Growth Hormone-Releasing Hormone Receptor Expression in Uterine Leiomyosarcomas

Terrell Jones[1], Hae-Sun La[2], Rohit Bhargava[3], Mirka Jones[1]
[1]University of Pittsburgh Medical Center, Pittsburgh, PA, [2]Department of Pathology, University of Pittsburgh Medical Center, Pittsburgh, PA, [3]Magee-Womens Hospital of UPMC, Pittsburgh, PA

Disclosures: Terrell Jones: None; Hae-Sun La: None; Rohit Bhargava: None; Mirka Jones: None

Background: The treatment of uterine leiomyosarcomas (uLMS) remains difficult. The rate of recurrence and metastasis is high, with survival reaching only 40-50% in patients with stage I or II disease. Prolactin receptor (ProR) and growth hormone-releasing hormone receptor (GHRHR) have been implicated in carcinogenesis of various tumors in the breast, endometrium, ovary, liver, and prostate. It has also been associated with resistance to chemotherapy. The expression of ProR and GHRHR has not been investigated in uLMS.

Design: Representative sections of twenty-seven uLMS were immunostained with ProR and GHRHR antibodies. Immunoreactivity was calculated as H-score = 1(% of weakly 1+ staining cells) + 2(% of moderately 2+ staining cells) + 3(% of strongly 3+ staining cells). A score of 1 to 100 was classified as weakly positive, 101 to 200 as moderately positive, and 201 to 300 as strongly positive.

Results: All 27 uLMS showed positive immunostaining for ProR and GHRHR (see table). Moderate to strong expression of ProR and GHRHR was observed in 89% and 82% of uLMS, respectively. Patients with tumors showing moderate to strong ProR expression were more likely to die of their disease (p value = 0.0023, unpaired t-test) and showed a higher tumor stage at diagnosis (p value = 0.0373, unpaired t-test). Furthermore, in two patients where the primary and recurrent tumors were tested, there was stronger expression of ProR in the recurrence compared to the primary. This correlation was not found with GHRHR.

Stain	H-score 1-100 (weak)	H-score 101-200 (moderate)	H-score 201-300 (strong)
Prolactin receptor	3/27 (11%)	17/27 (63%)	7/27 (26%)

Growth hormone-releasing hormone receptor	5/27 (18.5%)	17/27 (63%)	5/27 (18.5%)

Conclusions: Both ProR and GHRHR may have tumor promoting effects in uLMS as they have in other neoplasms. In addition, activation of the ProR pathway may contribute to early recurrences and poor survival in patients with uLMS. Frequent ProR expression in uLMS makes these tumors potential candidates for hormonal modulating therapies. GHRHR antagonists that inhibit the in-vitro growth of many human tumors represent a treatment for uLMS that merits further exploration.

1122 RNA Sequencing-Based Immune Signatures Confer Independent Prognostic Value across Molecular Subtypes of Endometrial Cancer

Julia Joseph[1], Corinne Lavasseur[1], Xiaohua Yang[2], Brian Richardson[3], Mark Cameron[3], Stefanie Avril[4]
[1]Case Western Reserve University School of Medicine, Cleveland, OH, [2]Department of Pathology, Case Western Reserve University School of Medicine, Willoughby, OH, [3]Department of Population and Quantitative Health Sciences, Case Western Reserve University School of Medicine, Cleveland, OH, [4]Cleveland, OH

Disclosures: Julia Joseph: None; Corinne Lavasseur: None; Xiaohua Yang: None; Brian Richardson: None; Mark Cameron: None; Stefanie Avril: None

Background: Different surrogate measures of increased anti-tumor immune response have demonstrated prognostic value in solid cancers. A recent publication by Talhouk and colleagues found that molecular subtype was more important than immune response in driving outcomes of 460 endometrial carcinomas. Experience from other solid cancers indicates that the method for measuring immune response can largely impact its prognostic or predictive value in a tissue and organ specific manner. We sought to assess the prognostic value of comprehensive immune-based gene expression signatures across endometrial cancer molecular subtypes.

Design: We analyzed gene-expression based immune signatures of 506 endometrial cancers based on publicly available RNA-sequencing data from The Cancer Genome Atlas (TCGA). The following parameters were evaluated: 4 distinct immune subtypes as defined by TCGA, including C1 'wound healing', C2 'IFN-γ-dominant', C3 'inflammatory', and C4 'lymphocyte depleted' subtype; total leukocyte fraction; abundance of individual immune cell populations by CIBER-SORT algorithm, and molecular subtype. Progression-free survival (PFS) served as reference endpoint.

Results: The 4 different immune subtypes (C1-C4) showed a different distribution across molecular subtypes, with the C1 'wound-healing' subtype predominating in CN-low, MSI, and POLE molecular subtypes, whereas the IFN-γ-dominant C2 subtype was enriched in CN-high. Total leukocyte fraction and abundance of CD4 cells showed no significant difference across molecular subtypes, while CD8 cells were increased in POLE and MSI. Immune subtype was associated with PFS in the entire patient cohort, with C1 and C3 being associated with the best prognosis, C2 with intermediate prognosis, and C4 with the poorest prognosis (p<0.01). Prognostic value of immune subtype was independent of molecular subtype by Cox-regression. In contrast, abundance of individual immune cell populations was not associated with PFS. Interestingly, the prognostic value of immune subtype was molecular subtype dependent, with C1 showing the best prognosis in CN-low, and C2 showing a trend for better prognosis in CN-high, while there was no prognostic difference between C1 versus C2 in MSI or POLE tumors.

Conclusions: Anti-tumor immune response assessed by comprehensive RNA-Seq based immune signatures differs across molecular subtypes of endometrial cancer. Immune subtype conferred independent prognostic value beyond molecular subtype in 506 endometrial cancers from TCGA.

1123 Conventional Cervical Cytology and Primary HPV Test Results Over a Recent 3-Year Period from a Routine Laboratory Setting in Kenya

Ahmed Kalebi[1], Lucy Muchiri[2], Jesca Kirimi[2], Charles Wahome[2], Rabia Mukadam[3]
[1]Lancet Group of Labs - East Africa, Nairobi, Kenya, [2]Pathologists Lancet Kenya, Nairobi, Kenya, [3]pLk, Nairobi, Kenya

Disclosures: Ahmed Kalebi: None; Jesca Kirimi: None; Charles Wahome: None; Rabia Mukadam: None

Background: Cervical cancer is the leading cause of cancer related deaths and the 2nd most common cancer among females in Kenya, after breast cancer, contributing to 13% of the new cancers and 12% of all cancer deaths annually. The Ministry of Health in Kenya released a National Cancer Screening Guideline in February 2019 recommending HPV Testing as the primary screening method and VIA only when HPV Testing is unavailable. Pap smear is scarcely available. Our laboratory is one of the very few in the country that routinely provides Pap smear test and the busiest in terms of annual volumes; we were also the 1st to introduce an FDA-approved HPV genotyping test in the country in 2016. We hereby share our experience considering the dearth of data from Africa, hoping this will add to the body of information available for collaborative exchange and research.

Design: We retrospectively retrieved data from our laboratory information system focusing on conventional cervical cytology done over the recent 3-year period from July 2016 to June 2019 corresponding to the period HPV test on Cobas 4800 platform (Roche) was introduced in our laboratory, which is ISO15189 accredited for both tests.

Results: A total of 27,447 conventional Pap smears were reported in our laboratory between July 2016 and June 2019. The mean age of the women who had Pap smear was 39.5 years and a median age of 38 years; the youngest at 11 years and the oldest at 95 years. A diagnosis of negative for intraepithelial lesions or malignancy (NILM) was rendered in 97.31% of the cases, with a HSIL rate of 1.58%, LSIL at 0.57% and ASC-H at 0.33%. ASCUS was reported in 0.02% and SCC at 0.04%; 43.3% of the cases had significant cervicitis on conventional Pap smear and 13.6% had bacterial vaginosis, while 8.9% had atrophic changes. During the corresponding period, a total of 3523 HPV tests were done, with an over two-fold year-on-year increase in numbers tested. A total of 26.6% of tested positive for HR-HPV, of whom 24.5% tested positive for HPV non-16/18 type, 6.2% type 16 and 3.9% type 18. Infection with multiple HPV types was noted in 6% of cases.

| CONVENTIONAL CYTOLOGY		
Year	*f*	*Months*
2016	5445	Jul-Dec
2017	7990	Jan-Dec
2018	8621	Jan-Dec
2019	5391	Jan-Jun
	27447	
Age		
Mean	39.5	
Median	38.0	
Min	11.0	
Max	95.0	
Diagnosis		
NILM	26129	97.31%
HSIL	423	1.58%
LSIL	153	0.57%
ASC-H	89	0.33%
AGC	37	0.14%
SCC	12	0.04%
ASCUS	5	0.02%
Adenocarcinoma	4	0.02%
Cervicitis	11872	43.25%
Bacterial Vaginosis	3735	13.61%
Atrophic changes	2442	8.90%
Actinomyces	89	0.32%
Trichomomons	68	0.25%
HSV	3	0.01%
HIGH-RISK HPV		
Year	*f*	
2016	235	
2017	434	
2018	896	
2019	1958	
	3523	
	Positive	**Negative**
HPV 16	219	3154
	6.2%	*89.4%*
HPV 18	136	3232
	3.9%	*91.6%*
NON 16/18	866	2504
	24.5%	*71.0%*

Figure 1 - 1123
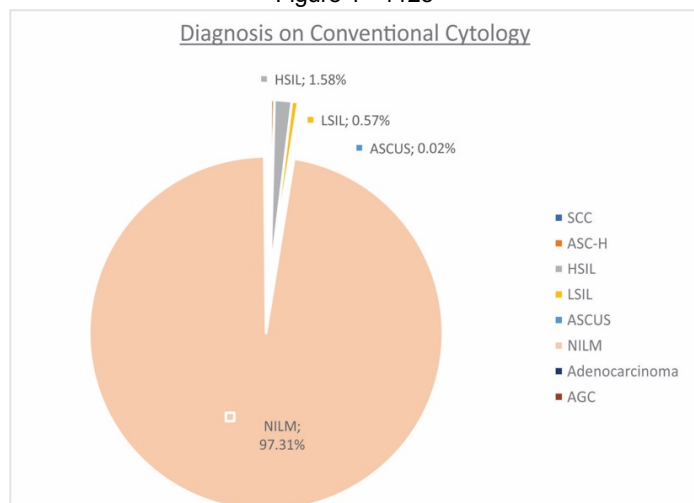
Figure 2 - 1123
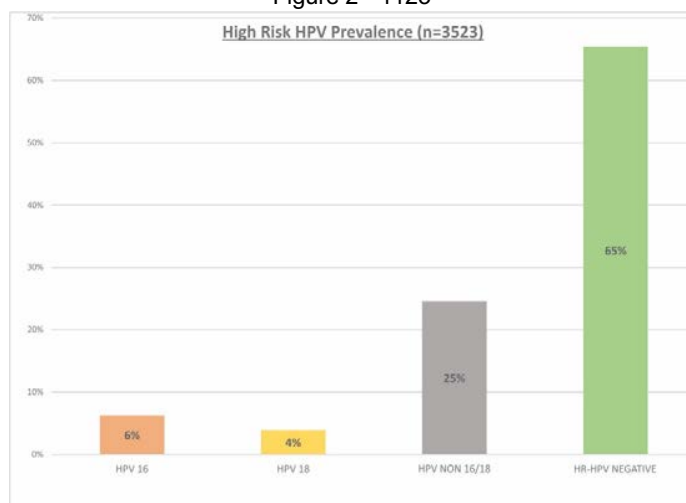
Conclusions: Positivity for HR-HPV is noticeably high in this general population of women tested in a routine setting, non 16/18 HPV types being commonest. HPV Test is gaining popularity in Kenya. The rate of ASCUS observed seems unusually low - likely due to dual reporting by cytologists and pathologists; while HSIL and LSIL rates are comparable to the published literature from Africa and worldwide.

1124 A Refined Cut-Off for p53 Immunohistochemistry Improves Prediction of TP53 Mutation Status in Ovarian Mucinous Tumors: Implications for Outcome Analyses

Eun-Young Kang[1], Dane Cheasley[2], Cecile Le Page[3], Matthew Wakefield[4], Yoland Antill[5], Kylie Gorringe[6], Martin Kobel[1]
[1]University of Calgary/Alberta Public Laboratories, Calgary, AB, [2]Peter MacCallum Cancer Centre, Melbourne, VIC, Australia, [3]University of Montréal, Montreal, QC, [4]Walter and Eliza Hall Institute of Medical Research, Parkville, VIC, Australia, [5]Cabrini Health, Malvern, VIC, Australia, [6]Peter MacCallum Cancer Center, Melbourne, VIC, Australia

Disclosures: Eun-Young Kang: None; Dane Cheasley: None; Cecile Le Page: None; Matthew Wakefield: None; Yoland Antill: None; Kylie Gorringe: None; Martin Kobel: None

Background: *TP53* mutations appear to be implicated in the progression of mucinous borderline tumors (MBOT) to mucinous ovarian carcinomas (MOC), since they are significantly enriched in MOC compared to MBOT. We have recently shown that optimized immunohistochemical staining for p53 is a good proxy for *TP53* mutation detection by sequencing, with 100% specificity and 96% sensitivity in high-grade serous (HGSOC) and endometrioid ovarian carcinomas (EC). We aimed to assess the correlation between optimized p53 immunohistochemistry (IHC) and mutation status by sequencing, and also evaluate the association with outcome in MBOT and MOC.

Design: An initial cohort composed of 12 MBOT and 102 MOC was evaluated with *TP53* mutation screening using whole genome and targeted panel sequencing as previously published [PMID: 31477716]. The cases were stained with optimized IHC for p53 using tissue microarrays (84%) or full sections (16%) and interpreted using established criteria as wild-type or mutant (over-expression, cytoplasmic, or complete absence). Cases were considered concordant if mutant-type IHC staining predicted deleterious *TP53* mutations. Discordant tissue microarray cases were re-evaluated on full sections. An independent expansion cohort of 112 MBOT and 246 MOC was assessed by p53 IHC to infer *TP53* mutation status. Kaplan-Meier survival analyses were performed.

Results: In the initial cohort, 83/114 (73%) cases were concordant when using the established criteria for interpretation. We observed the phenomenon of terminal differentiation in MBOT and some MOC, similar to what has been described in squamous cell carcinomas. Refining the cut-off for over-expression to account for terminal differentiation improved concordance to 95% (108/114 cases). When we then applied IHC with the refined criteria to the expansion cohort, 21% of MBOT showed a mutant-type p53 staining, which was associated with a higher risk of all-cause mortality in univariate analysis (Figure 1; HR=3.08, 95%CI 1.01-8.26, p=0.033). Within MOC, 56% of cases showed a mutant-type p53 staining but this was not associated with overall survival (log-rank p=0.94).

Figure 1 - 1124
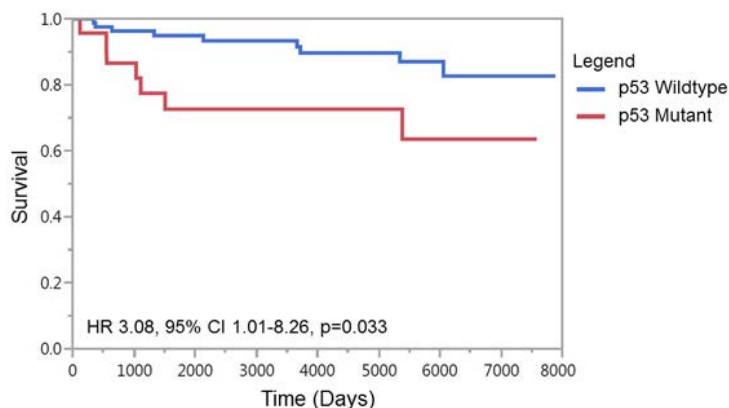
Figure 1. Association of p53 Mutation Status & Overall Survival in Ovarian
Mucinous Borderline Tumors

Conclusions: p53 IHC is an accurate proxy for *TP53* mutation status with refined interpretation criteria accounting for terminal differentiation in MBOT and MOC. *TP53* mutation status inferred by IHC may be a useful biomarker to identify MBOT with a higher risk of mortality; however, it is not prognostic in MOC.

1125 Gastric-Type Mucinous Carcinoma is an Aggressive Subtype of Endometrial Carcinoma

Fumi Kawakami[1], Ken Yamaguchi[2], Tamotsu Sudo[3], Yoshiki Mikami[1]
[1]Kumamoto University Hospital, Kumamoto, Japan, [2]Kyoto University Graduate School of Medicine, Kyoto, Japan, [3]Hyogo Cancer Center, Akashi, Hyogo, Japan

Disclosures: Fumi Kawakami: None; Ken Yamaguchi: None; Tamotsu Sudo: None; Yoshiki Mikami: None

Background: Mucinous carcinoma of the uterine corpus is currently regarded as a variant of low-grade endometrioid carcinoma. However, it appears a heterogeneous group of neoplasm including aggressive tumors showing gastric differentiation, which have not been hitherto well characterized.

Design: We retrieved 7 hysterectomy cases of mucinous carcinoma of the uterine corpus, which fulfilled the histopathologic criteria for gastric-type mucinous carcinoma of the uterine cervix. Cases of synchronous and multifocal mucinous lesions of the female genital tract and Peutz-Jeghers syndrome were excluded from the study.

Results: The median age of the patients was 68 years (range, 52–76 years). Grossly, 6 cases showed predominantly endophytic growth, and one showed exophytic growth. The median tumor size was 32 mm (range, 24-80 mm). Microscopically, all tumors were mucinous carcinoma with voluminous clear or pale eosinophilic cytoplasm and distinct cell border by definition. One case showed focal squamous differentiation. Lymphovascular invasion was identified in all cases and was prominent in 4 cases. Regional lymph nodes metastasis was identified in 4 cases. Intraoperative peritoneal washing cytology was positive in 4 cases. Myometrial invasion was seen in all 7 cases and extended to the outer half in 6 cases. Immunohistochemically, MUC6 was positive in all the cases except 1 and ER was faintly positive in 2 cases with positive rates less than 20% of tumor cells. The pattern of p53 expression was varied. Surrounding non-neoplastic endometrium was atrophic in all cases and mucinous metaplasia was identified in 2 cases. FIGO stage (2018) was I in 2 cases and III in 5 cases. Adjuvant therapy was given in all 7 cases. The median follow-up period was 53 months (range, 14–80 months). Lung metastasis was seen in 3 cases. 3 patients with stage III and 1 with stage IB tumors died of recurrent disease, 1 stage IIIB patient is alive with disease, and 2 patients with stage IA and IIIB disease are alive without disease.

Conclusions: Endometrial mucinous carcinoma with gastric differentiation is characterized by absence of ER expression, higher age, association with atrophic endometrium with or without mucinous metaplasia, advanced stage at diagnosis, frequent lymph node metastasis, occasional distal metastasis, and ominous outcome. Therefore, mucinous histology of endometrial carcinoma does not necessarily mean low-grade and low-stage disease.

1126 Plasminogen Activator Inhibitor 1 (PAI-1) is a Key Driver of Ovarian Cancer Metastasis

Tanya Kelly[1], Mark Ward[2], Bashir Mohamed[3], Cara Martin[4], Cathy Spillane[5], Sharon O'Toole[4], John O'Leary[5]
[1]Trinity College Dublin, Molecular Pathology, CWIUH, Dublin, Ireland, [2]Dublin, Ireland, [3]Trinity College, Dublin, Ireland, [4]Trinity St. James's Cancer Institute, Dublin, Ireland, [5]Trinity College Dublin, Dublin, Ireland

Disclosures: Tanya Kelly: None; Mark Ward: None; Bashir Mohamed: None; Cara Martin: None; Cathy Spillane: None; Sharon O'Toole: None; John O'Leary: None

Background: Ovarian cancer is the 7th leading cause of cancer in women worldwide, and is the deadliest of all gynecological cancers. There are roughly 250,000 new cases diagnosed annually and 140,000 deaths each year. Platelet-cancer cell interactions are intrinsic to ovarian cancer metastasis, and PAI-1 has been identified as a key gene in wound-healing, invasion, and mitosis. This suggests that PAI-1 plays an essential role in ECM remodeling, intravasation/extravasation of tumor cells, and thereby in hematogenous metastasis.

Design: SKOV3 cells were used as an *in vitro* model of metastatic ovarian cancer. Wound-healing assays utilized cells treated with platelets for 24h, or untreated. Wounds were induced at 24h. Untreated cells received fresh medium (FM), one set of cells treated with platelets received FM, and a second set of cells treated with platelets received platelet releasate (obtained by centrifugation of the supernatants from those wells). Cells were observed for 24h, photographed at 0h, 6h, 20h, and 24h, and wound closure was assessed using ImageJ. Flow cytometry was performed to ascertain cell-cycle phase at each time point. Invasion assays were performed using EHS sarcoma gel-coated membrane inserts. Cells were serum-starved and treated with 10nM PAI-1 siRNA or a negative control (siNEG). At 24h, platelets were added to half of both treatment groups. Cells were seeded using FBS as chemoattractant, incubated overnight, fixed, stained, and counted. IF staining was performed using a monoclonal antibody to PAI-1 in cells treated with either PAI-1 siRNA or siNEG, both with and without platelets.

Results: Platelets and their releasate significantly expedite wound healing in SKOV3 cells, and significantly accelerate mitosis. Transiently silencing PAI-1 in SKOV3 cells significantly decreases the wound-healing ability of these cells, even in the presence of platelets. This also significantly impedes their ability to invade (Fig.1). Silencing PAI-1 decreases intracellular PAI-1, and adding platelets increases it (Fig.2).

Figure 1 - 1126
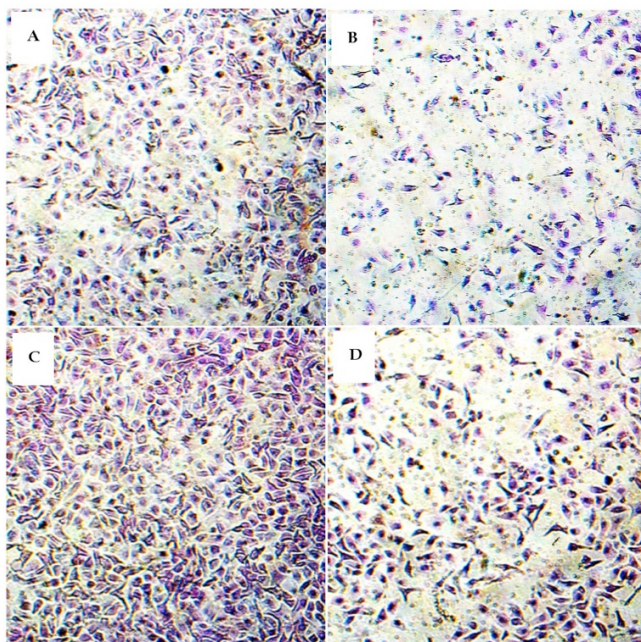
Fig1. SK-OV-3 cells invading through ECM: A. siNEG, B. siPAI-1, C. siNEG with platelets, D. siPAI with platelets

Figure 2 - 1126
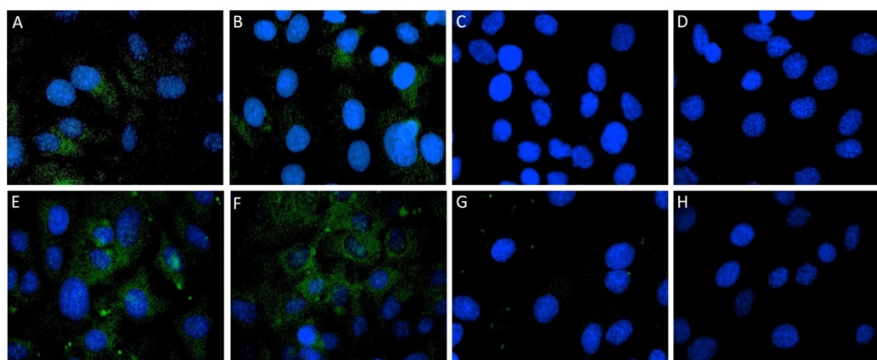
Fig.2 PAI-1 protein in SK-OV-3 cells visualized by fluorescence microscopy. All wells were incubated with a 1:500 dilution of mAb-33H1F7 (monoclonal murine IgG1 against PAI-1) stained with 10µg/mL Höechst and a 1:1000 dilution Alexa Fluor 488 -conjugated goat anti-mouse IgG, with the exception of wells D and H, which received fluorophore-conjugated secondary IgG and Höechst only. **A.** Untreated cells, **B.** Cells treated with siNEG (inert siRNA), **C.** Cells treated with PAI-1 siRNA, **D.** Untreated cells, **E.** Untreated cells incubated with platelets for 24h, **F.** Cells treated with siNEG (inert siRNA) and incubated with platelets for 24h, **G.** Cells treated with PAI-1 siRNA and incubated with platelets for 24h, **H.** Untreated cells incubated with platelets for 24h.

Conclusions: These results show that platelets and PAI-1 are essential to cell motility, wound healing, invasion, and mitosis. Previous work by our team and by others has demonstrated that platelets are fundamental to hematogenous metastasis across multiple types of cancer, and gene expression assays have identified PAI-1 as an integral part of this. Taken together, these experiments suggest that PAI-1 is a key factor in ovarian cancer metastasis.

1127 The Significance of FIGO Grading in MSI-H and POLE-Mutated Endometrioid Endometrial Carcinoma

Elizabeth Kertowidjojo[1], Amir Momeni Boroujeni[2], Robert Soslow[1]
[1]Memorial Sloan Kettering Cancer Center, New York, NY, [2]Memorial Sloan Kettering Cancer Center, Brooklyn, NY

Disclosures: Elizabeth Kertowidjojo: None; Amir Momeni Boroujeni: None; Robert Soslow: *Speaker*, Ebix/Oakstone

Background: With the advancement of diagnostic molecular technology and a move toward precision medicine, the interplay between tumor grading and molecular subtyping has become increasingly complex. The Cancer Genome Atlas studies of endometrial endometrioid carcinoma (EC) reported four molecular subcategories, including: POLE ultramutated, microsatellite instability-hypermutated (MSI-H), copy number low, and copy number high. With the integration of genomic data, it remains to be seen whether tumor grade retains clinical significance in certain molecular subtypes of EC. We studied the significance of FIGO grade in MSI-H and POLE-mutated EC.

Design: All cases of EC with targeted tumor-sequencing indicating MSI-H or POLE somatic exonuclease domain hotspot mutation from a single institution were included in the study. FIGO grade was correlated with various tumor characteristics (i.e. molecular subtype, depth of invasion, FIGO stage, lymphovascular invasion), patient characteristics (i.e. age, BMI), recurrence, and survival.

Results: Of the 319 MSI-H and POLE ECs ascertained, sufficient data were available for analysis in 95 cases, 75 MSI-H (79%) and 20 (21%) POLE. For MSI-H ECs, 24% were FIGO grade 1, 39% FIGO 2, and 37% FIGO 3. There were no statistically significant differences in FIGO stage, patients' age, BMI, mutation count, or percentage of myometrial invasion stratified by FIGO grade. Recurrences were reported in 39%, 45%, and 25% of cases of FIGO grades 1, 2, and 3, respectively. At the time of last follow up (mean of 4 years after initial diagnosis), survival rates were 89%, 79%, and 82%, respectively. Neither recurrence nor survival was statistically different between the three grade groups. For POLE-mutated EC, 40% were FIGO grade 1, 30% FIGO 2, and 30% FIGO 3. Compared to MSI-H ECs, POLE ECs showed similar trends in patient demographics, tumor behavior, and prognosis, though the small number of POLE samples precluded statistical analysis.

Conclusions: In this preliminary analysis of MSI-H and POLE ECs, FIGO grade was not associated with the evaluated parameters, including FIGO stage and prognosis. The intrinsic biology of these tumors may override the significance of FIGO grade.

1128   Immunohistochemical Evaluation of FOXL2 in Sex Cord-Stromal Tumors, Germ Cell Tumors and Normal Tissue of Ovary and Testicle

Patricia Kim[1], Fan Lin[1], Jianhui Shi[1], Haiyan Liu[1], Renuka Malenie[1]
[1]Geisinger Medical Center, Danville, PA

Disclosures: Patricia Kim: None; Fan Lin: None; Jianhui Shi: None; Haiyan Liu: None; Renuka Malenie: None

Background: The *forkhead box L2 (FOXL2)* gene encodes an essential transcription factor in the ovary, and plays an important role in female sex determination and granulosa cell development. Mutation of FOXL2 was reported being fairly specific for sex cord-stromal tumors. Published studies have yielded conflicting results as to FOXL2 expression in sex cord-stromal tumors (SCST). Here, we evaluated FOXL2 expression by immunohistochemistry (IHC) in a series of SCSTs, germ cell tumors (GCT) and normal (NL) tissues of ovary and testis, to assess the diagnostic utility of FOXL2.

Design: IHC evaluation of FOXL2 (HPA069613, Atlas Antibodies) was performed on 56 SCSTs, including ovarian fibroma/thecoma/fibrothecoma (23), Sertoli cell (2), Leydig cell (5), granulosa cell (13) tumors and testicular Leydig cell tumor or hyperplasia (13), 70 cases of testicular GCTs and 98 NL tissues of ovary (63) and testicle (35). The staining intensity was recorded as strong (S) or weak (W); staining distribution was recorded as negative (<5% cell staining), 1+ (5-25%), 2+ (25-50%), 3+ (50-75%), and 4+ (>75%).

Results: The staining results are summarized in Table 1. Strong and diffuse nuclear expression of FOXL2 was identified in 100% of ovarian granulosa cell (13/13) (Fig.1) and Sertoli cell (2/2) tumors on tissue sections (TS). Variable pattern of FOXL2 expression was noted in 95% (22/23) of fibroma/thecoma/fibrothecoma. NL ovarian stromal tissue showed weak to occasional strong expression of FOXL2 in 32.6% (14/43) of cases (Fig.2). No FOXL2 expression was demonstrated in Leydig cell tumor or hyperplasia of the ovary or testicle (0/18), testicular GCTs (0/70) and NL testicular tissues (0/35).

Summary of FOXL2 Expression on 57 SCSTs, 70 GCTs and 98 NL Tissues of Ovary and Testicle.

Tissue/IHC	1+ (w/s)	2+ (w/s)	3+ (w/s)	4+ (w/s)	% Positive
TS, Fibroma/Thecoma/ Fibrothecoma (23)	0	2/2	4/4	6/4	95.7% (22/23)
TS, Sertoli cell tumor (2)	0	0	0/1	0/1	100% (2/2)
TS, Ovarian Leydig cell tumor (5)	0	0	0	0	0% (0/5)
TS, Granulosa Cell Tumor (10) and Mets (3)	0	0	0/1	0/12	100% (13/13)

Testicular Leydig Cell Tumor/Nodule (13)
    TS (3)
    TMA (10)
	0	0	0	0	0% (0/13)

TMA, Testicular GCT (70)
    Mixed GCT (29)
    Seminoma (25)
    Yolk sac tumor (7)
    Embryonal CA (9)
	0	0	0	0	0% (0/70)

NL Ovary (43)
    TS (23)
    TMA (20)
	0	4/2	4/3	1/0	32.6% (14/43)

NL Testicle (35)
    TS (4)
    TMA (31)
	0	0	0	0	0% (0/35)

Figure 1 - 1128
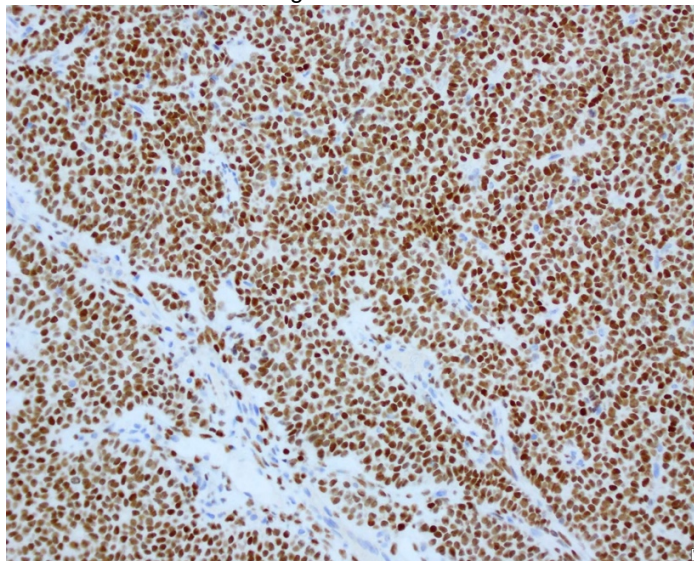
Figure 2 - 1128
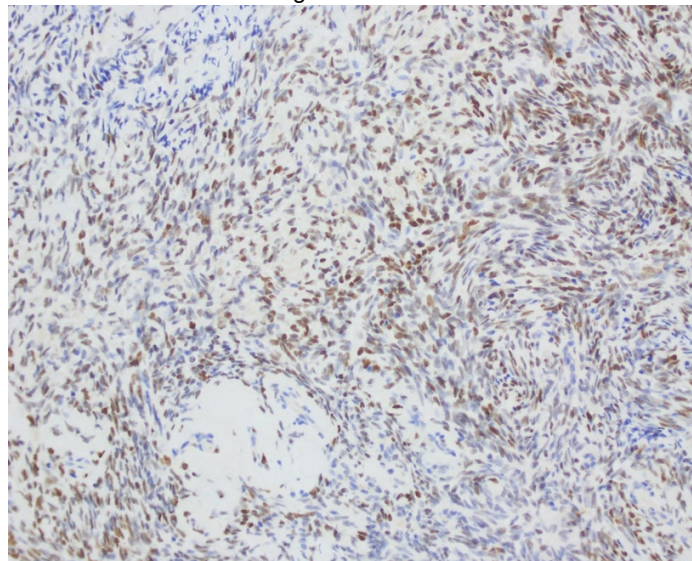
Conclusions: Our data suggested that FOXL2 expression is highly sensitive for characterizing granulosa cell and Sertoli cell tumors of the ovary. It does have significant cross reactivity with fibromas, thecoma, fibrothecoma, as well as NL ovarian stroma. When used in conjunction with morphology, FOXL2 is a useful marker for identifying granulosa cell and Sertoli cell tumors. Additional studies are warranted to validate these findings.

1129 Pathological Chemotherapy Response Score as a Prognostic Marker in Ovarian Cancer: A Retrospective Analysis

Teresa Kim[1], Kari Kubalanza[1], Gottfried Konecny[2], Jianyu Rao[1]
[1]University of California Los Angeles, Los Angeles, CA, [2]David Geffen School of Medicine at UCLA, Los Angeles, CA

Disclosures: Teresa Kim: None; Kari Kubalanza: None; Jianyu Rao: None

Background: Patients with advanced stage ovarian cancer are treated by primary tumor debulking surgery followed by adjuvant chemotherapy and/or neoadjuvant chemotherapy. The addition of neoadjuvant chemotherapy has been shown to improve the completeness of surgery and provide less morbidity and mortality. However, there are no standard biomarkers for treatment response and survival in ovarian cancer. The chemotherapy response score (CRS) is a three tier system that stratifies cases into no or minimal (CRS1), partial (CRS2), and complete or near-complete (CRS3) response to neoadjuvant chemotherapy based on histological examination (Figure 1). This study aims to evaluate the utility of the CRS as a prognostic biomarker for ovarian cancer in response to neoadjuvant chemotherapy.

Design: 28 patients with stage IIIC/IV ovarian cancer who received neoadjuvant chemotherapy and with paired pre- and post-therapy pathological samples were included and information about clinical characteristics, surgical outcome, time to recurrence, and overall survival were collected. After assigning a CRS to each case, the associations between CRS and progression free survival (PFS) and overall survival (OS) were examined.

Results: Pathologic response using the CRS was initially assessed in 28 patients with matched diagnostic biopsy and resection specimens. CRS was significantly associated with OS (Figure 2).

Figure 1 - 1129

Figure 2

CRS 1   CRS 2   CRS 3

Figure 2 - 1129

PFS   OS
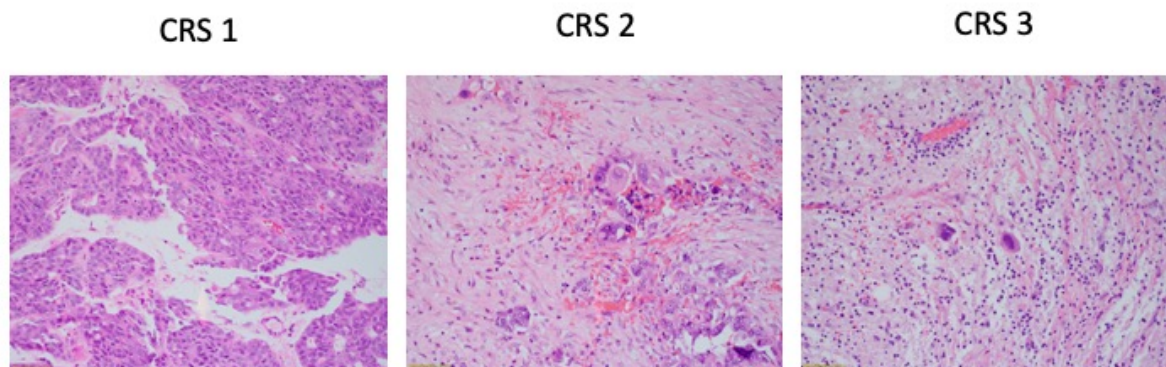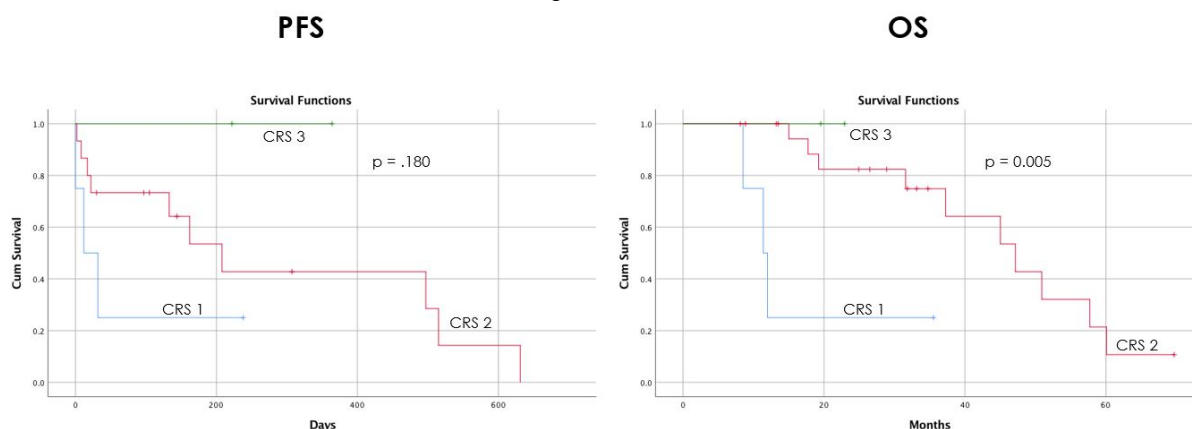
Conclusions: Our study supports prior conclusions that the CRS is an effective biomarker for treatment response and correlates with overall survival. It may help determine prognosis and potentially guide therapeutic decision making in patients with ovarian cancer treated with neoadjuvant chemotherapy. Additional cases are being evaluated to add to the dataset. Currently, we are also characterizing the molecular fingerprints of the initial matched biopsies to identify potential prognostic molecular markers in these tumors.

1130 Evaluation of Claudin-4 in Undifferentiated and Dedifferentiated Endometrial Carcinomas

Kyle Kissick[1], Jefree Schulte[2], David Chapel[3], Andre Pinto[4], Ricardo Lastra[2], Jennifer Bennett[2]
[1]The University of Chicago Medicine, Chicago, IL, [2]The University of Chicago, Chicago, IL, [3]Brigham and Women's Hospital, Boston, MA, [4]University of Miami, Miami Beach, FL

Disclosures: Kyle Kissick: None; Jefree Schulte: None; David Chapel: None; Andre Pinto: None; Ricardo Lastra: None; Jennifer Bennett: None

Background: Endometrial dedifferentiated (DC) and undifferentiated carcinomas (UC) are aggressive tumors that present a diagnostic challenge. Morphologically, they may appear similar to sarcomas and immunohistochemistry is often needed for diagnosis. If epithelial markers (CAM 5.2, AE1/AE3, and EMA) are positive, they are often weakly and focally expressed. Claudin-4 has been proposed as a more specific marker of epithelial differentiation, but only limited studies have been performed assessing its value in UC. Herein we evaluate claudin-4 expression in a series of DC/UC.

Design: Claudin-4 was evaluated for both extent (0=negative, 1+=<5%, 2+=5-24%, 3+=25-50%, 4+=>50%) and intensity (1+=weak, 2+=moderate, 3+=strong) in UC (n=7) and DC (n=6), and its expression was compared to other endometrial tumors including grade 3 endometrioid carcinoma (n=5), carcinosarcoma (n=3), mixed carcinoma (n=2), and serous carcinoma (n=1). The same criteria were applied to previously performed cytokeratin and EMA stains. Any degree of expression was considered positive.

Results: Claudin-4 was expressed in 5/7 (71%) UC and in 3/5 (60%) DC (undifferentiated component). The differentiated foci in DC strongly expressed claudin-4 (all with 4+ extent, 3+ intensity) while the other carcinoma histologic subtypes showed variable claudin-4 expression in extent (range 2+-4+, median 4+) and intensity (range 1+-3+, median 2+).

Type of Tumor	Claudin-4 Extent/Intensity	CAM 5.2 Extent/Intensity	AE1/AE 3 Extent/Intensity	EMA Extent/Intensity	Pan-Keratin Extent/Intensity	BRG-1	INI-1
DC							
1	4+/3+ diff 1+/1+ undiff	4+/2+ diff 1+/2+ undiff	4+/3+ diff 1+/2+ undiff	4+/3+ diff 4+/3+ undiff	NP	Retained	Retained
2	4+/3+ diff 4+/2+ undiff	4+/2+ diff 4+/2+ undiff	4+/2+ diff 3+/3+ undiff	PPR	NP	Lost	Retained
3	4+/3+ diff 3+/2+ undiff	4+/3+ diff 2+/2+ undiff	4+/3+ diff 2+/2+ undiff	NP	NP	Retained	Lost
4	4+/3+ diff 0/0 undiff	NP	0/0	NP	0/0	Lost	NP
5	4+/3+ diff 0/0 undiff	NP	NP	NP	2+/1+	Lost	Retained
UC							
1	4+/2+	1+/1+	1+/3+	NP	NP	NP	NP
2	3+/2+	4+/3+	2+/3+	NP	NP	NP	NP
3	1+/2+	2+/2+	0/0	0/0	NP	NP	NP
4	3+/2+	NP	0/0	NP	0/0	Equivocal	NP
5	0/0	NP	2+/1+	NP	2+/1+	Retained	Pending
6	1+/2+	NP	NP	NP	2+/1+	Lost	Retained
7	0/0	NP	NP	NP	NP	Pending	Pending

NP = not performed, PPR= positive per report, diff = differentiated component, undiff = undifferentiated component

Conclusions: Overall, this study suggests that claudin-4 can be a useful adjunct stain in the differential diagnosis between DC/UC and sarcoma, as some claudin-4 positive DC/UC are negative for cytokeratins and EMA, and vice versa. The stain seems especially helpful in the differential diagnosis between carcinomas and the newly described *SMARCA4*-deficient undifferentiated uterine sarcomas (SDUS), as claudin-4 has been negative in all reported SDUS.

1131 Mullerian Adenosarcoma: Clinicopathologic Features of 78 cases

David Kolin[1], Brooke Howitt[2], Michael Nathenson[3], Marisa Nucci[4]
[1]Brigham and Women's Hospital, Boston, MA, [2]Stanford University School of Medicine, Stanford, CA, [3]Dana-Farber Cancer Institute, Boston, MA, [4]Brigham and Women's Hospital, Harvard Medical School, Boston, MA

Disclosures: David Kolin: None; Brooke Howitt: None; Michael Nathenson: None; Marisa Nucci: None

Background: Mullerian adenosarcoma (MA) is a rare biphasic tumor of the female genital tract composed of malignant stroma and benign epithelium. A subset of patients has an aggressive disease course. We sought to characterize the clinicopathologic features of a large cohort of MA and to determine features which predict patient outcome.

Design: Cases of MA diagnosed at a single centre were retrospectively re-reviewed by at least one gynecologic pathologist to confirm the diagnosis. Tumors were evaluated for FIGO stage, sarcomatous overgrowth, myometrial invasion, stromal cytologic atypia at low power (4X) magnification, mitotic index, necrosis, lymphovascular invasion, and heterologous elements. Immunohistochemical stains for ER, PR, and p53 were performed on a subset of cases. Univariate analysis was used to examine prognostic features.

Results: The clinicopathologic features of the cohort (n=78) are shown in Table 1. Average tumor size was 6.3 (range 0.7-25) cm. Median mitotic index was 5 per 10 HPFs (range 0 to 54). Necrosis was present in 13/73 (18%). MA with either myometrial invasion or sarcomatous overgrowth had a significantly worse overall survival (OS) than those without either feature (Fig 1A, log-rank p<0.005). Similarly, cases with high grade cytologic atypia also had a worse OS than those with only low or intermediate grade atypia (Fig 1B, log-rank p<0.005). Heterologous differentiation (usually rhabdomyoblastic) was associated with a worse OS (log-rank p<0.02). Both ER and PR expression (>10% of tumor cells) were associated with a better OS (p<0.05). However, mutant pattern p53 staining (seen in only 13%) was not associated with a statistically significant difference in OS compared to wild-type staining (p=0.7).

	n (%)	
Patient age (years)	Mean 56 (range 21 to 86)	
Follow up (years)	Median 5.5 (range 0 to 27.4)	
FIGO stage	33 (42%)	
Ia	25 (32%)	
Ib	6 (8%)	
Ic	6 (8%)	
II	4 (5%)	
III	2 (3%)	
IV	2 (3%)	
Not available		
Tumor site	67 (86%)	
Uterine corpus	5 (6%)	
Cervix	3 (4%)	
Ovary	3 (4%)	
Other		
Histologic features	**Present**	**Absent**
Sarcomatous overgrowth	28 (37%)	47 (63%)
Myometrial invasion	34 (50%)	34 (50%)
Heterologous differentiation	17 (29%)	42 (71%)
Lymphovascular invasion	4 (6%)	63 (94%)
Lymph node metastases	1 (3%)	38 (97%)
High grade cytologic atypia	21 (28%)	53 (72%)
Immunohistochemical stains		
ER		
Positive (>10%)	24 (62%)	
Negative (<10%)	15 (38%)	
PR		
Positive (>10%)	21 (55%)	
Negative (<10%)	17 (45%)	
p53		
Mutant	7 (13%)	
Wild-type	46 (87%)	

Figure 1 - 1131

Figure 2 - 1131
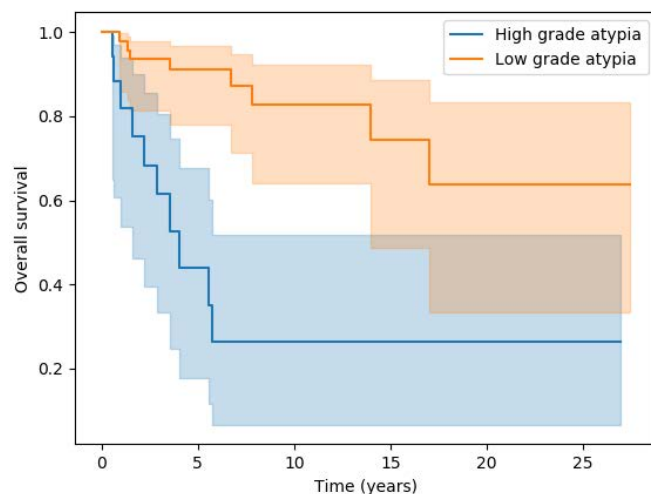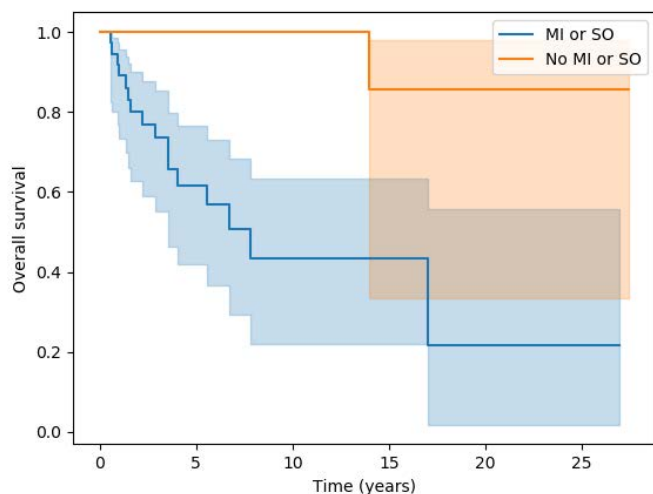
Conclusions: Negative prognostic factors of MA include myometrial invasion, sarcomatous overgrowth, and heterologous differentiation. Those cases without either myometrial invasion or sarcomatous overgrowth are associated with an excellent OS. Tumor grade ("high grade" or "low grade") has traditionally been reported for cases of adenosarcoma, despite limited evidence for its prognostic significance. We demonstrate here, in a large series, that high grade cytologic atypia is a negative prognostic marker, supporting its inclusion as a required reporting element.

1132 Targeted RNA Sequencing Highlights a Diverse Genomic Landscape in Low-Grade Endometrial Stromal Sarcoma, including Novel Fusion Genes

David Kolin[1], Marisa Nucci[2], Sophie Corbett-Burns[3], Martin Chang[4], William Chapman[5], Blaise Clarke[6], Elizabeth Demicco[7], Valerie Dube[8], Marjan Rouzbahman[9], Patricia Shaw[10], Gulisa Turashvili[7], David Swanson[7], Brendan Dickson[11]
[1]Brigham and Women's Hospital, Boston, MA, [2]Brigham and Women's Hospital, Harvard Medical School, Boston, MA, [3]Douglass Hanly Moir Pathology, Sydney, NSW, Australia, [4]The University of Vermont Medical Center, Burlington, VT, [5]University Health Network, Toronto, ON, [6]University of Toronto, Toronto, ON, [7]Mount Sinai Hospital, Toronto, ON, [8]Mississauga, ON, [9]Toronto, ON, [10]Sunnybrook Health Sciences Centre, Toronto, ON, [11]Mount Sinai Health System, Toronto, ON

Disclosures: David Kolin: None; Marisa Nucci: None; Sophie Corbett-Burns: None; Martin Chang: None; William Chapman: None; Blaise Clarke: None; Elizabeth Demicco: None; Valerie Dube: None; Marjan Rouzbahman: None; Patricia Shaw: None; Gulisa Turashvili: None; David Swanson: None; Brendan Dickson: None

Background: Low-grade endometrial stromal sarcoma (LGESS) represents a morphologically and genetically heterogenous mesenchymal neoplasm of the female genital tract. Previous work has shown that approximately half of LGESS are characterized genetically by *JAZF1-SUZ12* fusions, while a smaller proportion involve rearrangement of other genes such as *PHF1*. However, a significant subset of cases has no known genetic abnormalities. We sought to better characterize the genomic landscape of LGESS by examining a modest cohort interrogated with targeted RNA sequencing (RNA-Seq).

Design: A retrospective archival review was performed for cases diagnosed as LGESS. The slides were reviewed to confirm the diagnosis, and representative formalin-fixed, paraffin embedded tissue blocks selected for RNA-Seq. RNA-Seq libraries were created using the TruSight RNA Fusion Panel (Illumina, CA).

Results: 43 cases of LGESS were identified; this included cases that had previously been tested in the course of routine clinical practice (n=28) and a cohort that had not previously been sequenced (n=15). The average patient age was 51 years (range 30-85). Of 43 cases, 39 were successfully sequenced, and 4 failed sequencing due to low quality control metrics. The fusions detected by RNA-Seq are summarized in Table 1. The most commonly detected fusion was *JAZF1-SUZ12*, identified in 17 cases (39.5%), followed by *BRD8-PHF1* (n=3, 7%) and *JAZF1-PHF1* (n=2, 4.7%). Novel translocations were identified in 2 cases, including: MEAF6-PTGR2, and ANP32E-KPNB1 & KAT6B-KANSL1. The latter case, in addition to containing two candidate in-frame fusion products, was notable for an unusual morphology that included areas of sex-cord differentiation.

Fusion	n (%)
JAZF1-SUZ12	17 (39.5)
BRD8-PHF1	3 (7.0)
JAZF1-PHF1	2 (4.7)
ANP32E-KPNB1 and KAT6B-KANSL1	1 (2.3)
EPC1-SUZ12	1 (2.3)
HCFC1-PHF1	1 (2.3)
BCORL1-JAZF1	1 (2.3)
MEAF6-PTGR2	1 (2.3)
EPC1-BCOR	1 (2.3)
EPC1-PHF1	1 (2.3)
PHF1-JAZF1	1 (2.3)
MEAF6-PHF1	1 (2.3)
Negative	8 (18.6)
Failed QC	4 (9.3)

Conclusions: Low-grade endometrial stromal sarcoma is a genetically heterogeneous disease characterized by a variety of gene fusions. The prognostic significance of these translocations, and their associated morphologic features, remain to be fully elucidated. While targeted RNA-Seq represents a practical diagnostic tool in confirming a diagnosis of LGESS in most cases, it is worth noting that approximately 20% of cases had no identifiable fusion using this assay. It is presumed this may be attributable to (1) other fusion products, involving genes that are not covered by the assay and/or (2) other altogether different molecular events (e.g., amplification, SNV/indel, epigenetic).

1133 Genome-Wide DNA Methylation Analysis Reveals Epigenetic Signatures Associated with Molecular Subgroups of Endometrial Carcinoma

Felix Kommoss[1], Basile Tessier-Cloutier[2], Victor Yuan[3], Christian Koelsche[4], C. Blake Gilks[5], David Huntsman[6], Jessica McAlpine[7], Andreas von Deimling[8]
[1]University of Heidelberg, Heidelberg, Germany, [2]University of British Columbia, Vancouver, BC, [3]BC Children's Hospital Research Institute, Vancouver, BC, [4]Ruprecht-Karls-University Heidelberg, Heidelberg, Germany, [5]Vancouver General Hospital, Vancouver, BC, [6]British Columbia Cancer Research Institute, Vancouver, BC, [7]University of British Columbia and BC Cancer Agency, Vancouver, BC, [8]Heidelberg University Hospital, Heidelberg, Germany

Disclosures: Felix Kommoss: None; Basile Tessier-Cloutier: None; Victor Yuan: None; Christian Koelsche: None; C. Blake Gilks: None; David Huntsman: None; Jessica McAlpine: None

Background: Endometrial carcinomas (EC) are complex malignancies with multiple subtypes and a heterogenous survival. Molecular classifiers such as the Proactive Molecular Risk Classifier (PRoMisE) have improved our ability to better stratify EC patients for clinical management, however some limitations remain. We analyzed DNA methylation signatures in molecular subtypes of EC to gain new insights into this disease.

Design: Fifty ECs previously classified according to PRoMisE were selected, including 10 Polymerase-ε exonuclease domain mutated (POLE), 10 mismatch repair deficient (MMR-D), 20 p53 wild-type (p53 wt) and 10 p53 mutated (p53 abn) tumors. Array-based DNA methylation analysis was performed on all cases using the Illumina Infinium MethylationEPIC 850k BeadChip kit. Differentially methylated cytosines (DMCs) for each molecular subtype were identified using linear modeling. DMCs were then tested for functional enrichment using gene ontology analysis.

Results: Of the initial 50 samples, 49 had above 95 % methylation coverage and were included in the analysis. While for POLE tumors 62 DMCs and for MMR-D tumors 1079 DMCs were identified, p53 wt and p53 abn tumors showed 33269 and 70118 DMCs, respectively. Most MMR-D DMCs were hypermethylated (99.4 % hypermethylated DMCs), and included several sites in the MLH1 gene, while for p53 wt and POLE cases hypomethylation was predominant (17.7 % and 29.0 % hypermethylated DMCs, respectively). The DMCs of p53 abn tumors had a more balanced ratio (62.2 % hypermethylated DMCs). The MMR-D differential methylation profile was enriched for genes associated with plasma membrane components, RNA polymerase II-specific DNA-binding transcription factor activity and voltage-gated calcium channel activity (FDR < 0.05). Profiles of p53 wt tumors were enriched for genes associated with extracellular matrix, actin binding and plasma membrane components (FDR < 0.05) and profiles of p53 abn tumors showed enrichment for genes associated with ATP binding (FDR < 0.05). No pathways were found to be significantly enriched among the DMCs of POLE tumors.

Conclusions: Array-based DNA methylation analysis is able to identify epigenetic signatures in EC which are associated with molecular subtypes. These methylation patterns can further inform us on the underlying mechanisms driving tumor biology within molecular subgroups of EC, which may have treatment implication. The presented data will lay ground for further survival-based DNA methylation analysis in EC.

1134 Pattern Based Interpretation of p53 Immunohistoschemistry as a Surrogate Marker for TP53 Mutations in Vulvar Squamous Cell Carcinoma

Kim Kortekaas[1], Basile Tessier-Cloutier[2], Tessa Rutten[1], Mariette Poelgeest[1], Lynn Hoang[3], C. Blake Gilks[4], Tjalling Bosse[5]
[1]Leiden University Medical Center, Leiden, Zuid-Holland, Netherlands, [2]University of British Columbia, Vancouver, BC, [3]Vancouver, BC, [4]Vancouver General Hospital, Vancouver, BC, [5]LUMC, Leiden, Netherlands

Disclosures: Kim Kortekaas: None; Basile Tessier-Cloutier: None; Tessa Rutten: None; Mariette Poelgeest: None; Lynn Hoang: None; C. Blake Gilks: None; Tjalling Bosse: None

Background: *TP53* is the most commonly mutated gene in vulvar squamous cell carcinoma (VSCC) and its prognostic value, particularly in HPV-independent VSCC, is under investigation. In other cancer sites p53 immunohistochemistry (IHC) was shown to be a good surrogate marker for *TP53* mutational status. Here we assess the performance of a pattern-based p53 IHC approach and its interobserver variability.

Design: In a discovery cohort of 61 VSCC with known *TP53* mutational status, we reviewed and defined the different p53 IHC staining patterns. Using a validation cohort of 59 VSCC, two experienced gynaecologic pathologists scored the predefined p53 IHC patterns independently and blinded for the molecular data. A next-generation sequencing (NGS) tumor gene panel was used to initially define the *TP53* gene alterations. All variants with an allelic ratio above 5% were called by a molecular biologist blinded to the p53 IHC results. A chi-square test was used to analyse categorical data, and the agreement was calculated by Cohen's kappa.

Results: From the discovery cohort two wild-type p53-IHC patterns were identified: 1) scattered expression and 2) mid-epithelial overexpression (basal sparing), and four mutant patterns; 3) basal overexpression, 4) parabasal/diffuse overexpression 5) absence of expression with positive internal control and 6) cytoplasmic expression. In the validation set, the agreement of this pattern-based approach between the two observers was high (k=0.71, p<0.001, figure 1). Independent use of the IHC pattern by both observers showed

good concordance to the *TP53* mutation (*k*=0.718 and *k*=0.869). When there was a disagreement (n=12) consensus was achieved between the two pathologists. The final concordance rate, after consensus, between IHC and NGS increased to *k*=0.874 (figure 2), the sensitivity was 93%, the specificity was 100%, positive predictive value and negative predictive value were 100% and 83% respectively. The only two discordant cases had a scattered and mid-epithelial expression pattern of p53 (interpreted as wild-type) and a pathogenic *TP53* mutation (NM_000546.5:c884C>T, c.451C>T).

The pattern-based p53 IHC interpretation accurately reflects *TP53* mutational status in VSCC and is highly reproducible. This study offers guidance to p53 IHC interpretation and provides necessary clarity for resolving the proposed prognostic relevance of p53 status within HPV-independent VSCC.

Figure 1 - 1134

	p53 IHC patterns	Observer 1						
		Scattered	Mid-epithelial	Basal	Parabasal	Absent	Cytoplasmic	
Observer 2	Scattered	13	0	0	0	0	0	13
	Mid-epithelial	0	2	0	1	0	0	3
	Basal	3	0	1	3	0	0	7
	Parabasal-diffuse	0	1	1	23	0	0	25
	Absent	1	0	0	0	5	0	6
	Cytoplasmic	1	0	0	1	0	3	5
		18	3	2	28	5	3	59

Figure 2 - 1134

		P53 IHC pattern		
		wildtype	mutant	
NGS	TP53 wildtype	16	2	18
	TP53 mutant	0	41	41
		16	43	59

Conclusions: A pattern-based p53 IHC interpretation accurately reflects *TP53* mutational status in VSCC and is highly reproducible. This study offers guidance to p53-IHC interpretation and provides necessary clarity for resolving the proposed prognostic relevance of p53 status within HPV-unassociated VSCC.

1135 SATB2 as a Novel Marker of Neuroendocrine Differentiation in the Gynecologic Tract: A Case Series

Vimal Krishnan[1], Cecile Le Page[2], Anne-Marie Mes-Masson[3], Charles Leduc[4], Kurosh Rahimi[5]
[1]Centre Hospitalier de l`Université de Montréal, Montreal, QC, [2]University of Montréal, Montreal, QC, [3]Centre de recherche du CHUM, Montreal, QC, [4]University of Montreal Hospital Centre, Montreal, QC, [5]Université de Montreal, Montreal, QC

Disclosures: Vimal Krishnan: None; Cecile Le Page: None; Anne-Marie Mes-Masson: None; Charles Leduc: None; Kurosh Rahimi: None

Background: Neuroendocrine tumors (NET) of the gynecologic tract are exceedingly rare, with a reported incidence of less than 2%. The diagnosis can often be challenging in poorly differentiated tumors, and determining the site of origin can be problematic. Special AT-rich sequence-binding protein 2 (SATB2) positivity has been recently reported in well-differentiated NETs of the lower gastrointestinal tract and Merkel cell carcinoma. In this study, we characterize for the first time the immunostaining profile of SATB2 in gynecological NETs.

Design: Patients with a diagnosis on surgical specimen of a gynecological tumor with neuroendocrine differentiation, from 2010 to 2019, were included in the study (n=11). Patients diagnosed on biopsy specimen, or without focal staining for at least one neuroendocrine marker (chromogranin, synaptophysin, CD56) were excluded. Diagnosis and SATB2 staining interpretation were performed by a pathologist with expertise in gynecologic pathology. Positive staining was defined as nuclear staining of at least moderate intensity, in >25% of tumor cells. Positive cases were graded as follows : 1+ (>25%), 2+ (50-75%), 3+ (>75%).

Results: A total of 11 gynecologic NETs were included. Median age at diagnosis was 59 years old. No evidence of an extra-gynecologic primary was found on histology or clinical evaluation. Tumor sites were ovarian (n=5), uterine (n=4) and cervical (n=2). Histologic subtypes included small cell (SCNC) (n=2), large cell (LCNC) (n=1) and poorly differentiated neuroendocrine carcinoma (PDNC) (n=4). The remainder of the cases were carcinomas with focal neuroendocrine differentiation (n=4). Overall SATB2 positivity was 6/11. Interestingly, SATB2 was positive in 5/7 high grade NETs. The percentage of tumor cell staining was higher in PDNCs (3+, n=2),

moderate in LCNC (2+, n=1) and lower in SCNC (1+, n=1). SATB2 was negative in a limited number of non-gynecological poorly differentiated NETs, including 2 pulmonary SCNC and 1 intestinal LCNC (data not shown).

Table : SATB2 staining in gynecological neuroendocrine tumors (n=11).				
Patient	Site	Diagnosis	STAB2	Grade
1	Uterus	Endometrioid adenocarcinoma with focal neuroendocrine differentiation	Positive	2+
2	Ovary	Poorly differentiated neuroendocrine carcinoma	Negative	
3	Ovary	Carcinosarcoma with focal neuroendocrine differentiation	Negative	
4	Uterus	Poorly differentiated neuroendocrine carcinoma	Positive	3+
5	Ovary	Poorly differentiated neuroendocrine carcinoma	Positive	3+
6	Cervix	Small cell neuroendocrine carcinoma	Negative	
7	Uterus	Endometrioid adenocarcinoma with focal neuroendocrine differentiation	Negative	
8	Uterus	Endometrioid adenocarcinoma with focal neuroendocrine differentiation	Negative	
9	Cervix	Small cell neuroendocrine carcinoma	Positive	1+
10	Ovary	Poorly differentiated neuroendocrine carcinoma	Positive	1+
11	Ovary	Large cell neuroendocrine carcinoma	Positive	2+

Figure 1 - 1135
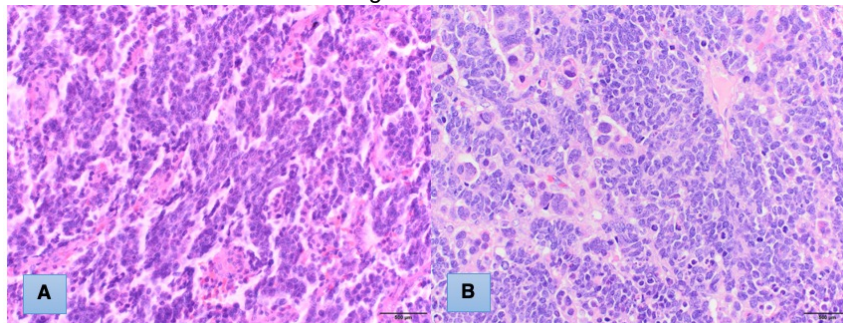
Figure 1 : Histologic subtypes of neuroendocrine tumors in the gynecologic tract. Examples of small cell carcinoma (panel A) and large cell carcinoma (panel B) are shown.

Figure 2 - 1135
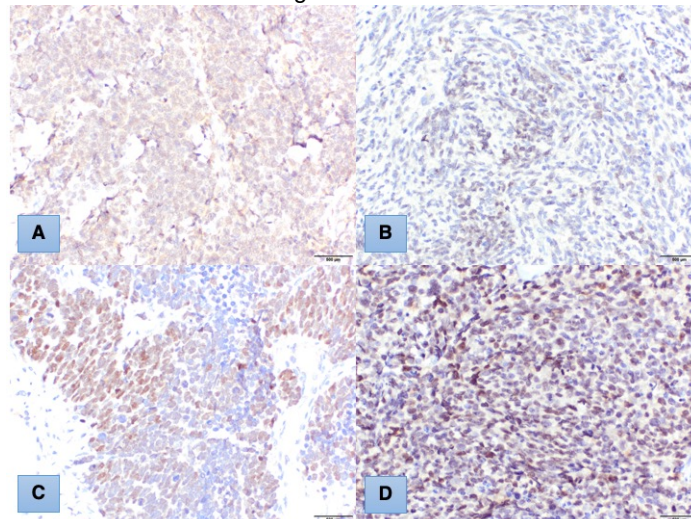
Figure 2 : SATB2 staining. Examples of negative staining (panel A), 1+ staining (panel B), 2+ staining (panel C) and 3+ staining (panel D) are shown.

Conclusions: In this case series, we report for the first time SATB2 positivity in poorly differentiated NETs of the gynecological tract. As the pathogenesis of gynecological NETs have thus far been enigmatic, this could be a stepping stone towards identifying progenitor cells to these neoplasms. Furthermore, SATB2 could potentially be a powerful marker for the diagnosis of poorly differentiated gynecological tumors, as well as in the clinical determination of the site of origin.

1136 MLH1-Hypermethylation and Mutation Status among MLH1/PMS2-Deficient Endometrial Carcinomas: Results from a Universally Screened Population

Brett Kurpiel[1], Kari Ring[1], Martha Thomas[2], Susan Modesitt[1], Anne Mills[1]
[1]University of Virginia, Charlottesville, VA, [2]UVA, Charlottesville, VA

Disclosures: Brett Kurpiel: None; Kari Ring: None; Martha Thomas: None; Susan Modesitt: None; Anne Mills: None

Background: Epigenetic hypermethylation of the *MLH1* promoter region is the most common cause of mismatch repair deficiency (MMRd) in endometrial carcinoma, and in most cases provides reassurance against an associated germline mutation. However, rates of germline mutations have not been well established in this population.

Design: The departmental database of MMRd endometrial carcinomas was searched for all cases with dual MLH1/PMS2 loss, retained MSH2/6 expression, and available *MLH1* promoter hypermethylation (*MLH1*-hm) results. Clinicopathologic variables and germline and somatic tumor testing results were obtained.

Results: 117 MLH1/PMS2-deficient ECAs underwent *MLH1*-hm testing by PCR. *MLH1*-hm testing could not be completed in seven due to sample inadequacy. Of the remaining 110 cases, 100 (91%) were *MLH1*-hm, while three (3%) were low-level/borderline and seven (6%) were not methylated (nm). 16 cases (12 *MLH1*-hm, 3 nm, and 1 insufficient for testing) underwent germline testing, and 6 of these (37.5%) demonstrated germline mutations involving *MSH6, POLD1, BRIP1, RAD51D, PMS2*, and *CHEK2*, all of which were variants of unknown significance (VOUS). The average age among patients with germline mutations was 60 (range 25-72) vs. 65 (range: 52-85) for germline-normal patients. One non-methylated, germline-normal case underwent somatic tumor testing, and demonstrated a somatic mutation in *MLH1*.

Conclusions: In a universally screened population, *MLH1-hm* accounts for the vast majority of MLH1/PMS2-deficient cancers, although rare *MLH1* somatic mutations can occur. Furthermore, germline mutations in other genes implicated in heritable cancer syndromes occur in a subset of *MLH1*-hm carcinomas. However, all germline mutations identified in *MLH1*-hm endometrial cancer patients were variants of unknown significance therefore their contribution to tumorigenesis remains uncertain.

1137 DPC4 Loss in Gynecopathology Related Specimens

DongHyang Kwon[1], Anais Malpica[1], Michael Zaleski[1], Elizabeth Euscher[1], Preetha Ramalingam[1]
[1]The University of Texas MD Anderson Cancer Center, Houston, TX

Disclosures: DongHyang Kwon: None; Anais Malpica: None; Michael Zaleski: None; Elizabeth Euscher: None; Preetha Ramalingam: None

Background: The use of DPC4 in gynecologic pathology is restricted to cases where a pancreatic (Pan) origin in a given neoplasm needs to be excluded. DPC4, which is lost in about 50% of Pan adenocarcinomas (ACas), is part of the battery of immunohistochemical stains used when encountered with mucinous neoplasms (MNs) i0volving the ovary that show worrisome features for metastatic PanACa. Furthermore, we have noted the loss of DPC4 in gastric-type cervical adenocarcinoma (GCxACa). In this study, we present our experience with the loss of DPC4 expression in a cohort of cases referred to a group of gynecopathologists.

Design: A retrospective search of our institutional database was performed to identify tumors that were reported to have a complete loss of DPC4 expression reviewed in the gynecologic pathology service. 28 of such cases were identified from a total of 255 cases with DPC4 immunostain obtained as part of their workup, from 2008-2019. The histologic, clinical and radiographic findings were reviewed to confirm the primary site of origin.

Results: 18 of the 28 cases with loss of DPC4 had clinical information, imaging studies, and follow-up. Median patients' age was 52.2 yrs. (range, 28-86). Additional results are summarized in Table 1. Of the 7 ovarian tumors, 4 were clinically/radiologically or biopsy-proven metastases from the pancreaticobiliary tract, 1 was an ovarian primary, 1 had a Cx origin, and 1 had an unknown primary (no Cx or Pan masses). All 4 primary GCxACa showed loss of DPC4. A pelvic biopsy from a Peutz-Jeghers syndrome patient with CxCA showed loss of DPC4 in the metastatic tumor. The 3 ACas in the vaginal specimens had a urinary tract origin (1), appendiceal origin (1), and unknown origin (1). Of the other 3 metastatic tumors, 1 was Cx primary, 1 was a Pan primary, and 1 remained as unknown.

Table 1. DPC4 Negative Tumors involving the Female Genital Tract Related Cases

Case	Specimen DPC4 staining performed	Primary site	Histotype	Pancreas mass by imaging or biopsy-proven	Cervical mass by imaging or biopsy
1	Ovary	Pancreas	ACa	Y	N
2	Ovary	Pancreas	MCa	Y	N
3	Ovary	Pancreas	MCa	Y	N
4	Ovary	Bile duct	MCa	Y	N
5	Ovary	Ovary	MCa	N	N (remote TAH, LSO)
6	Ovary (B/L)	Unknown	MCa	N	N
7	Ovary	Cervix	ACa	N	Y
8	Cervix and ovary	Cervix	GCxACa	Not available	Y
9	Cervix	Cervix	GCxACa	Not available	Y
10	Cervix	Cervix	GCxACa	IPMN	Y
11	Cervix	Cervix	GCxACa	N	Y
12	Pelvic mass	Cervix	ACa	N	Y
13	Lung	Cervix	MCa	N	Y
14	Vagina	Urethra/bladder	MCa	N	N
15	Vagina	Appendix	ACa	N	N
16	Vagina	Unknown	ACa	N	N
17	Iliac lymph node	Unknown	ACa	N	N
18	Abdominal mass	Pancreatic	ACa	Y	N

ACa: Adenocarcinoma, GCxACa: Endocervical adenocarcinoma, gastric type; IPMN: Intraductal papillary mucinous neoplasm; MCa: Mucinous adenocarcinoma; TAH-LSO: Total abdominal hysterectomy left salpingo-oophorectomy

Conclusions: Loss of DPC4 expression, though typical of pancreaticobiliary tract primaries, can also be seen in a small subset of gynecologic tumors including GCxACa and rarely primary ovarian mucinous carcinoma, as well as, non-pancreatic gastrointestinal tumors. In a female patient, mucinous neoplasms involving the ovary or other metastatic sites with negative DPC4 staining and negative pancreaticobiliary imaging, should raise the possibility of occult GCxACa.

1138   Clinicopathologic and Molecular Investigation of Steroid Cell Tumors: A Series of 18 Cases
Regina Kwon[1], Minghao Zhong[2], Deyin Xing[3]
[1]Johns Hopkins University School of Medicine, Baltimore, MD, [2]Westchester Medical Center, Valhalla, NY, [3]Johns Hopkins Medical Institutions, Ellicott City, MD

Disclosures: Regina Kwon: None; Minghao Zhong: None; Deyin Xing: None

Background: Steroid cell tumors (SCTs) are a rare subset of sex cord-stromal tumors with a propensity for secreting steroid hormones and comprising 0.1% of ovarian tumors and 3% of testicular neoplasms. Although they usually behave in a benign fashion, steroid cell tumors exhibit malignant behavior in approximately 10% to 30% of cases. Little consistent information is available about the molecular profile of steroid cell tumors. Studies and in vitro experiments have implicated a wide range of molecular alterations, often associated with pre-existing syndromes. In this study, we review a series of steroid cell tumors and their molecular characteristics in conjunction with clinical data.

Design: We searched the institutional archives for steroid cell tumors, including Leydig cell tumor, stromal luteoma, hilar cell tumor, and steroid cell tumor not other specified (NOS), diagnosed during the 25-year period from 1994 to 2019. Clinicopathologic data were gathered from the electronic medical record. Slides were assessed for histopathological features, and a subset were submitted for molecular evaluation. The first stage of examination tested nucleic acids extracted from formalin-fixed paraffin tumor samples using the AmpliSeq for Illumina Focus Panel, a targeted next-generation sequencing assay covering hotspot mutations of 52 genes to detect single-nucleotide variants (SNV), insertion/deletions, copy number variations (CNV), and gene fusions.

Results: We identified 50 cases in the institutional archives. The patients ranged in age from 7 to 85 years (median, 63). 22 (44%) of 50 cases were of ovarian origin (female) and 28 (56%) of 50 cases were of testicular origin (male). The most common histopathologic type was Leydig cell tumor (61%), followed by stromal luteoma (22%) and steroid cell tumor NOS (17%). Two cases were malignant: An 85-year-old male with testicular Leydig cell tumor (stage pT2) and a 79-year-old female with ovarian Leydig cell tumor with lymph-vascular space invasion. Two patients (11%) died of unrelated causes, and 33% were lost to follow-up. 18 cases had sufficient tissue for molecular testing. However, the 52-gene hotspot panel failed to detected somatic mutations or apparent copy number changes.

Conclusions: Steroid cell tumors usually behave in a benign fashion, and these tumors do not demonstrate the most frequent mutations found in other solid tumors. Additional molecular studies are needed to further characterize these tumors.

1139 Null Pattern Aberrant p53 Staining is more Frequent in Uterine High-Grade Endometrioid Carcinoma Compared to Serous Carcinoma

Nicholas Ladwig[1], Karuna Garg[1], Amy Joehlin-Price[2]
[1]University of California San Francisco, San Francisco, CA, [2]Cleveland Clinic, Cleveland, OH

Disclosures: Nicholas Ladwig: None; Karuna Garg: None; Amy Joehlin-Price: None

Background: *TP53* gene mutations are among the most common alterations in human cancer and its normal tumor suppressor function can be inactivated by missense, frameshift, or truncating (nonsense/splice site) mutations. Aberrant staining for p53 by immunohistochemistry (IHC) is a reliable surrogate marker for *TP53* mutation with strong diffuse staining seen with missense mutations and complete absence of staining (null) with truncating mutations. Amongst uterine tumors, *TP53* mutations are characteristic of serous carcinoma (USC) but can also be seen in a subset of endometrioid carcinoma, often FIGO grade 3 (EEC3). In our experience, null pattern p53 staining is seen in endometrioid carcinomas or high-grade carcinomas that are difficult to classify. This study was undertaken to formally evaluate and compare the aberrant p53 staining pattern in a cohort of prototypic USC and EEC3. A secondary aim was to correlate p53 staining patterns with clinical outcomes.

Design: p53 IHC was performed on tissue microarray (TMA) or whole slide sections of EEC3 (n=21) and USC (n=49). The staining pattern was reported as "null pattern" or "aberrant positive" when there was complete absence of staining or diffuse strong positive staining (>80% of tumor cells), respectively. Ambiguous IHC results from TMAs were repeated using whole slide sections. A next generation sequencing panel (including coverage of *TP53* and *POLE*) and MMR protein IHC was performed on all EEC3 and a subset of USC. Clinical outcomes were collected from the electronic medical record or California Cancer Registry.

Results: 1. In EEC3 with aberrant p53 IHC, null pattern staining was frequent (38%) (one tumor had POLE mutation, MMR was intact in all cases). 2. USC characteristically shows aberrant positive p53 IHC (92%) and null pattern staining is infrequent (8%). 3. No significant difference in stage or clinical outcomes was associated with the pattern of p53 IHC within EEC3 or USC.

Diagnosis	p53 IHC	Age (yr)	Stage		Clinical Follow up			
			I-II	III-IV	NED	AWD	DOD	LTF
Endometrioid adenocarcinoma, FIGO grade 3 (n = 21)	Null (n=8; 38%)	69.2	5 (63%)	3 (37%)	3 (38%)	0	5 (62%)	0
	Aberrant + (n=13; 62%)	69.0	7 (54%)	6 (46%)	8 (61%)	1 (8%)	4 (31%)	0
Serous endometrial carcinoma (n=49)	Null (n=4; 8%)	64.5	3 (75%)	1 (25%)	2 (50%)	1 (25%)	1 (25%)	0
	Aberrant + (n=45; 92%)	67.7	22 (49%)	23 (51%)	19 (42%)	3 (7%)	15 (33%)	8 (18%)

Conclusions: 1. Amongst uterine high-grade EEC with aberrant p53 IHC, null pattern p53 staining is relatively common. 2. Amongst USC, aberrant positive p53 IHC is common while null pattern staining is uncommon. 3. Aberrant positive p53 staining in USC may relate to hotspot mutations with additional oncogenic biologic implications, as TP53 mutations are often seen in isolation in USC while EEC3 typically harbor additional mutations4. The pattern of p53 staining showed no correlation with clinical outcomes

1140 Chemotherapy Response Score in Extrauterine High Grade Serous Carcinoma and Association with Mutation Status by Next-Gen Sequencing

Barrett Lawson[1], Richard Yang[1], Elizabeth Euscher[1], Preetha Ramalingam[1], Anais Malpica[1]
[1]The University of Texas MD Anderson Cancer Center, Houston, TX

Disclosures: Barrett Lawson: None; Richard Yang: None; Elizabeth Euscher: None; Preetha Ramalingam: None; Anais Malpica: None

Background: Chemotherapy response score (CRS) in extrauterine high-grade serous carcinoma (EHGSCa) has been shown to correlate with disease progression and platinum resistant disease (PRD). The CRS has been included for reporting in the CAP and NCCN

guidelines, though current treatment decisions are not based on the CRS. We seek to determine if the CRS correlates with molecular data.

Design: A retrospective study using a cohort of 151 pts with EHGSCa treated with neoadjuvant chemotherapy, previously scored for the CRS on the omentum, adnexa and as a combined score, of which 35 had Next-Gen Sequencing (NGS) performed. Clinical data recorded included age, date of dx, tumor stage, start and end date of chemotherapy, date of interval debulking surgery, status of optimal tumor reduction, number of chemotherapy cycles, BRCA status, dates of recurrence/progression, date of last follow up and vital status. NGS was performed using a 141 gene Ion AmpliSeq Oncomine panel with the number of somatic mutations and specific variant calls recorded. Fisher exact tests were performed using GraphPad Prism v8.1.2 software.

Results: Median age 61 yrs (42-78). The omental CRS was 1 in 9 cases, 2 in 20, and 3 in 6. Adnexal CRS was 1 in 15, 2 in 15 and 3 in 5. The combined CRS was 2 in 8, 3 in 7, 4 in 12, 5 in 6 and 6 in 2. Of all 35 cases sequenced, all had at least 1 detected mutation (mtn), with 20 cases having 1 mtn, 11 with 2 mtns, 3 with 3 mtns, and 1 with 4 mtns. The most common mtn was *TP53* (34 cases, 97.1%), with 4 cases having mtns for *BRCA2*, 2 with *PIK3CA*, 2 with *ARID1A,* and 1 of each of the
following: *ERBB2, NTRK3, STK11, NTRK2, WT1, ATM, TSC1, PIK3R1, NF1, NOTCH3, CDK2, SMAD4* and *PMS2*. Of the 4 cases with 3 mtns or more, all scored 1 or 2 on the adnexal and omental CRS and scored 4 or less by combined CRS. Using Fisher exact test when combining the CRS1/2 vs.CRS 3 for number of mtns detected, there was no statistically significant association between the number of genes mutated and the omental or adnexal CRS (p=0.56). For the combined CRS, CRS 2 to 4 and CRS 5/6 were combined for comparison with no statistically significant association seen between the combined CRS and number of genes mutated (p=0.55). 11 cases clinically had PRD, of which only 1 case had more than 2 mtns.

Conclusions: While cases with more mtns detected by NGS have low CRS, these findings were not statistically significant, likely due to small sample size. Further studies are warranted to determine the impact of mutational burden on CRS.

1141 Assessment of Indoleamine 2,3-dioxygenase Expression in the Tumor Cells and Tumor Infiltrating Immune Cells in Cervical Carcinomas

Christine Lee[1], Neda Moatamed[2]
[1]University of California Los Angeles, Los Angeles, CA, [2]David Geffen School of Medicine at UCLA, Los Angeles, CA

Disclosures: Christine Lee: None; Neda Moatamed: None

Background: Indoleamine 2,3-dioxygenase (IDO) is an enzyme involved in tryptophan metabolism. IDO has immune-regulating effects in fetal and allograft protection as well as cancer progression. IDO expression in tumor cells promotes immunosuppression and tumor progression. Similarly, dendritic cells that express IDO inhibit T-cells whereas IDO-negative dendritic cells activate T-cells. IDO inhibitors, such as 1-methyltryptophan, may have immunotherapeutic potential. The purpose of this study is to investigate IDO expression in cervical cancer cells and tumor infiltrating immune cells.

Design: We evaluated the expression of IDO immunohistochemical stain in a tissue microarray consisting of 102 cores: 95 cores of squamous cell carcinoma, 5 cores of adenocarcinoma, and 2 cores of benign cervix. IDO rabbit polyclonal antibody was used and a granular cytoplasmic expression was considered a positive reaction. Results for IDO were scored the in tumor infiltrating immune cells (Figure 1) and in the tumor cells (Figure 2).

Results: In cervical squamous cell carcinoma, 92% (87 of 95) of tumor infiltrating immune cells and 31% (29 of 92) of tumor cells showed IDO expression. In cervical adenocarcinoma, IDO was present in 60% (3 of 5) of tumor infiltrating immune cells and 40% (2 of 5) of tumor cells. There was no IDO expression in either infiltrating immune cells or in the tumor cells of benign cervical tissues. Table 1 summarizes these findings.

| **Table 1**. Summary of the IDO expression in tissue microarray of the uterine cervical epithelial neoplasms both in the tumor infiltrating immune and the tumor cells					
Total Cores (n) = 102		**IDO+, Immune cells**		**IDO+ Tumor cells**	
	n	n	%	n	%
Squamous cell carcinoma	95	87	92%	29	31%
Adenocarcinoma	5	3	60%	2	40%
Benign	2	0	0%	N/A	N/A
DO+, IDO positive; **N/A**, not applicable					

Figure 1 - 1141
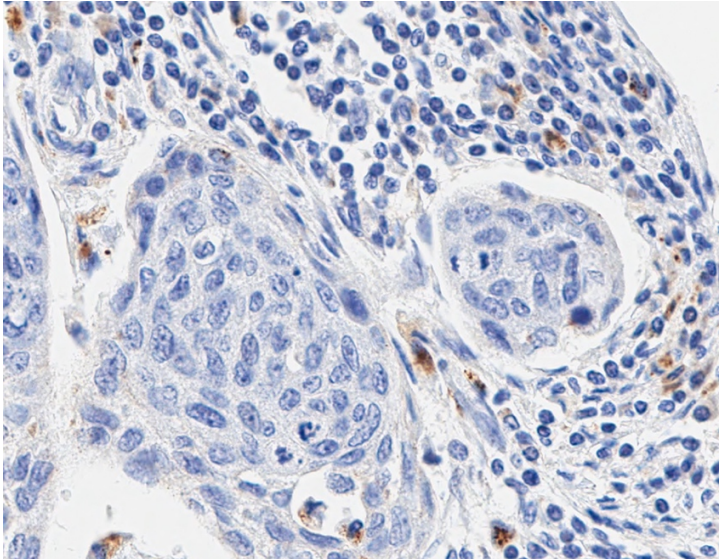
Figure 2 - 1141
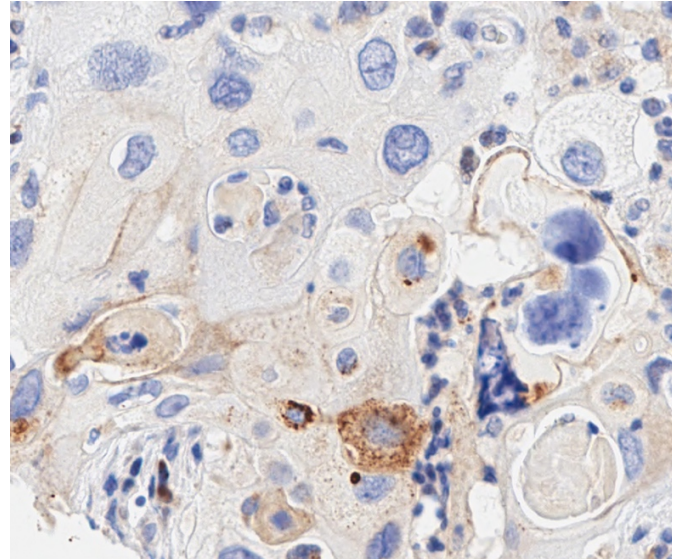
Conclusions: This study shows that the cervical cancers may express IDO both in the tumor cells as well as the tumor infiltrating immune cells. These findings support a possible therapeutic role for IDO inhibitors in a subset of cervical carcinomas.

1142 Ataxia–Telangiectasia Mutated (ATM) Protein Expression in Uterine Smooth Muscle Tumors

Horace Hok-Yeung Lee[1], Kin Long Chow[2], Ho-Shing Wong[3], Tsz Yan Chong[3], Tse Ka-Yu[4], Philip Ip[5]
[1]University of Hong Kong, Hong Kong, Hong Kong SAR, [2]Hong Kong, Hong Kong SAR, [3]Department of Pathology, The University of Hong Kong, Hong Kong, Hong Kong SAR, [4]Obstetrics and Gynaecology, The University of Hong Kong, Hong Kong, Hong Kong SAR, [5]The University of Hong Kong, Hong Kong, Hong Kong SAR

Background: Ataxia-telangiectasia-mutated (ATM) is one of the key kinase involved in cellular response to double-strand DNA damage. When ATM is functional, cells can respond to stress using the DNA damage response pathway. Dysregulation of this pathway in uterine leiomyosarcoma may result in genomic instability. Analysis of ATM protein expression in uterine smooth muscle tumors has not been investigated.

Design: Expression of ATM and phosphorylated ATM (p-ATM) was evaluated on 66 uterine leiomyosarcomas, 18 leiomyomas and 28 myometrium. Immunohistochemistry was performed by using monoclonal antibodies for ATM (Clone Y170, Abcam) and p-ATM (Clone EP1890Y, Abcam) on formalin-fixed paraffin embedded tissue. Staining of the nucleus was considered positive. Lymphocytes served as internal positive controls. Immunohistochemical expression was analysed by using a histoscore, generated by multiplying the intensity (0, 1, 2, 3) with the extent (0, 10%, 25%, 50%, 75% and 100%). The final score ranged from 0 to 300, with 0 being complete loss of staining.

Results: Median age of leiomyosarcoma patients was 50 years (range 33–80). All patients underwent hysterectomy with bilateral salpingo-oophorectomy and without preoperative chemo or radiation therapy. All tumors showed spindle cell differentiation, with diffuse nuclear atypia and >10 mitoses per 10 high power fields (0.55 mm field diameter). Tumor cell necrosis was present in 46 (70%). Thirty-seven (56%) and 36 (54.5%) of leiomyosarcomas had a complete loss of ATM and p-ATM expression, respectively. Although the median score for either marker was 0, the range of expression was 0 to 300. In leiomyomas, there was immunoreactivity for ATM (median 225, range 25-300) and p-ATM (median 300, range 100-300). In the myometrium, there was also positive staining for ATM (median 175, range 25-300) and p-ATM (median 300, range 100-300). There was a significant difference in ATM/p-ATM expression between myometrium and leiomyosarcoma, and between leiomyoma and leiomyosarcoma ($p < 0.05$).

Conclusions: ATM and p-ATM were both expressed in all leiomyomas and normal myometrium. Complete loss of expression for both markers was observed in approximately 55% of leiomyosarcomas. The remaining 45% of cases had retained ATM and p-ATM staining at various intensities and extents. Whether this subset of leiomyosarcoma with retained ATM and p-ATM expression had a better prognosis remains to be further evaluated.

1143 Importance of Histological Subtyping in TP53 Mutant Endometrial Carcinomas

Alicia Leon-Castillo[1], Stephanie de Boer[1], Naveena Singh[2], Linda Mileshkin[3], Anthony Fyles[4], Alexandra Leary[5], Christine Haie-Meder[6], Vincent Smit[7], Godfrey Wilson[8], Remi Nout[9], Nanda Horeweg[1], Carien Creutzberg[1], Tjalling Bosse[10]
[1]Leiden University Medical Center, Leiden, South Holland, Netherlands, [2]Barts Health NHS Trust, London, United Kingdom, [3]Peter MacCallum Cancer Centre, Melbourne, VIC, Australia, [4]University of Toronto, Toronto, ON, [5]Gustave Roussy, Villejuif Cedex, Île-de-France, France, [6]Gustave Roussy, Villejuif, Île-de-France, France, [7]Leiden University Medical Center, Leiden, Netherlands, [8]Manchester, United Kingdom, [9]Erasmus University Medical center, Rotterdam, South Holland, Netherlands, [10]LUMC, Leiden, Netherlands

Disclosures: Alicia Leon-Castillo: None; Stephanie de Boer: None; Naveena Singh: None; Linda Mileshkin: None; Anthony Fyles: None; Alexandra Leary: None; Christine Haie-Meder: None; Vincent Smit: None; Godfrey Wilson: None; Remi Nout: None; Nanda Horeweg: None; Carien Creutzberg: None; Tjalling Bosse: None

Background: The molecular classification of endometrial cancer (EC) based on the TCGA has proven to yield well-defined prognostic subgroups. Interestingly, within the molecularly defined subgroup *TP53* mutant EC (p53mut EC), both endometrioid (p53mut EEC) and serous (p53mut SEC) histologies are identified. In this study we assessed whether this distinction has prognostic relevance.

Design: Available H&E slides were reviewed from collected tissue samples of consenting PORTEC-3 trial participants, identifying 311 EEC and 68 SEC. These EC were molecularly classified by targeted DNA-sequencing for pathogenic *POLE*-exonuclease domain mutations (EDM) and immunohistochemistry for p53 and mismatch repair (MMR) proteins. In addition, 307 EEC and 53 SEC from the TCGA were included. Other histologic subtypes were excluded. P53mut EEC and p53mut SEC were defined as having a p53 mutant staining pattern or a *TP53* mutation, and being MMR proficient or microsatellite stable and without *POLE* EDM. Mann-Whitney, χ^2 and Fisher exact tests were used to compare clinicopathological and molecular features. The Kaplan-Meier method, log-rank test and Cox proportional-hazard model were used for survival analysis.

Results: Comparing histological types, EEC (n=618) and SEC (n=121) had significantly different clinical outcomes: 5-year recurrence free survival (RFS) of EEC 76% versus SEC 55%, *p* log-rank< 0.01; 5-year overall survival (OS) 85% versus 61%, p log-rank < 0.01.

From this cohort, a total of 150 (24%) p53mut EC were identified, 58 (39%) EEC and 92 (61%) SEC. No significant differences in age and stage distribution between the subtypes were found. Mutational data available from TCGA EC (n=59) revealed a significant higher proportion of *PTEN* mutations in p53mut EEC compared to p53mut SEC (23% versus 3% respectively, *p*=0.01), while amplification of Her2/neu was more frequent in p53mut SEC (8% versus 33%, *p*=0.02). 5-year RFS and OS were similar for both groups: RFS of p53mut EEC 51% versus p53mut SEC 55%, *p* log-rank= 0.32; OS was 61% versus 60%, *p* log-rank= 0.82, respectively). Corrected for age and stage by multivariable analysis, histotype did not significantly impact clinical outcome (table 1).

Table 1. Uni- and multivariable analysis of clinicopathological features.									
			Recurrence Free Survival				Overall Survival		
			57 events				49 events		
			Univariable analysis		Multivariable analysis		Univariable analysis		Multivariable analysis	
		Total n	HR (95%CI)	*p*-value	HR (95%CI)	*p*-value	HR (95%CI)	*p*-value	HR (95%CI)	*p*-value
Histo-molecular subgroups										
P53mut EEC	58	1		1		1		1	
p53mut SEC	92	0.77 (0.45-1.29)	0.316	0.71 (0.42-1.21)	0.206	1.07 (0.60-1.92)	0.820	0.89 (0.48-1.63)	0.700
Stage										
I-II	86	1		1		1		1	
III	64	3.38 (1.96-5.81)	<0.001	3.38 (1.96-5.81)	<0.001	2.49 (1.41-4.40)	0.002	2.49 (1.41-4.40)	0.002
Age	150	0,99 (0,95-1,03)	0.494	1.00 (0.96-1.04)	0.986	1.04 (1.00-1.08)	0.057	1.04 (1.00-1.08)	0.056

Conclusions: Despite both histologic and genomic differences, clinical outcome did not show significant differences between p53mut EEC and p53mut SEC. Expanding these findings will be critical in order to define the relative weight of histologic subtyping within the molecular classification.

1144   Genome-Wide Mutation Analysis in Endometrial Atypical Hyperplasia

Lihong Li[1], Pinli Yue[1], Tian-Li Wang[2], Ie-Ming Shih[3], Yan Song[1]
[1]National Cancer Center/National Clinical Research Center for Cancer/Cancer Hospital, Chinese Academy of Medical Sciences and Peking Union Medical College, Beijing, China, [2]Johns Hopkins Medical Institutions, Baltimore, MD, [3]Johns Hopkins Hospital, Baltimore, MD

Disclosures: Lihong Li: None; Pinli Yue: None; Tian-Li Wang: None; Ie-Ming Shih: None; Yan Song: None

Background: Endometrial atypical hyperplasia or endometrial intraepithelial neoplasia (AH/EIN) are widely thought to be the precursor of uterine endometrioid carcinoma (EC) based on clinicopathological features. However, the process of clonal evolution and the molecular alterations that contribute to tumor progression from AH/EIN to EC remains unclear.

Design: We analyzed microdissected paired AH/EIN and EC lesions from 30 hysterectomy specimens by whole-exome sequence (WES). Biospecimens were collected from patients with new EC diagnosis who had not received prior treatment. WES data of matched AH/EIN/EC and normal samples were aligned to the human reference genome and analyzed to identify somatic mutations in AH/EIN and EC.

Results: Among 30 ECs, 9 (30%) had microsatellite instability-high (MSI-H) status. The other 21 cases were microsatellite stable (MSS). Interestingly, 2 (22%) of these 9 MSI-H cases had MSS status in AH/EIN counterparts, indicating MSI developed during tumour progression from AH/EIN to EC. We observed that 18 (60%) of 30 cases had a significant percentage (> 35%) of shared somatic mutations between AH/EIN and matched EC, while the remaining cases harboured fewer shared mutations. This observation suggests that the majority of ECs were derived from extant AH/EINs and both lesions co-developed to acquire their own private mutations. Alternatively, AH/EIN may be genetically heterogeneous and EC subsequently arose from a geographically distinct AH/EIN area. The average cancer driver mutations in AH/EIN and EC were 6.7 and 8.8, respectively. As compared to AH/EINs, 15 (71%) /21 MSS ECs had new cancer driver mutations, among which the most common are *PTEN*, *ARID1A*, *PIK3CA* and *CHD4*. Analysis of mutational signature profile indicated that both AH/EIN and EC shared a similar signature profile except 2 cases exhibiting distinct mutational signatures which also had fewer shared somatic mutations.

Figure 1 - 1144
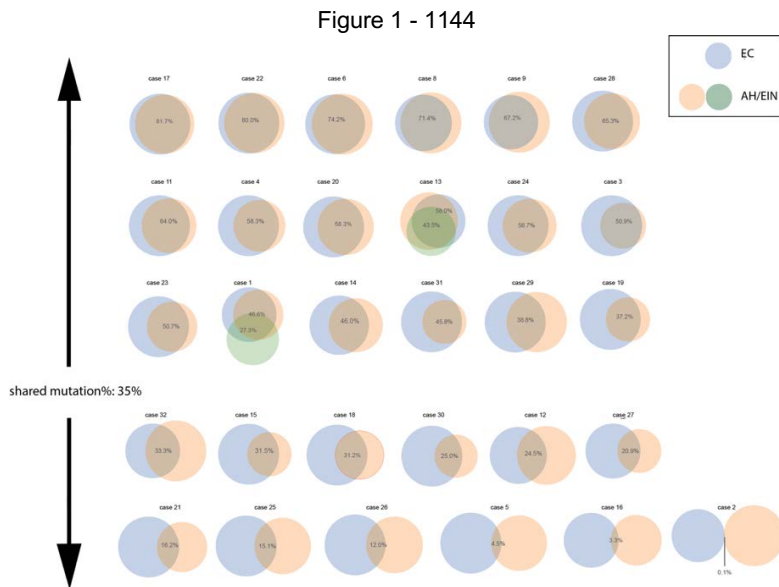
Conclusions: In general, AH/EIN shared several molecular genetic features with EC and the great majority of CAs developed from AH/EIN. Importantly, 71% of MSS ECs harbored new cancer driver mutations which were absent in AH/EIN, suggesting that these genes play a critical role in tumor progression. Our results shed new light into the pathogenesis of tumor progression of EC and have implications in its early detection.

1145 Genomic Profiling of BCOR-Rearranged Uterine Sarcomas Reveals Novel Gene Fusion Partners and Frequent CDK4 Activation

Douglas Lin[1], Amanda Hemmerich[2], Claire Edgerly[2], Eric Severson[2], Richard Huang[3], Shakti Ramkissoon[2], Jonathan Hecht[4], Jeffrey Ross[5], Julia Elvin[1]
[1]Foundation Medicine, Inc., Cambridge, MA, [2]Foundation Medicine, Inc., Morrisville, NC, [3]Foundation Medicine, Inc., Cary, NC, [4]Beth Israel Deaconess Medical Center, Boston, MA, [5]Upstate Medical University, Syracuse, NY

Background: Metastatic high grade endometrial stromal sarcomas (ESS) have a poor prognosis with limited therapeutic options. Genomic alterations of *BCOR* via either gene rearrangement or internal tandem duplication (ITD) define a subset of ESS. However, the molecular landscape of *BCOR*-rearranged ESS has not been established. The goals of this study were to: 1) determine the molecular landscape of *BCOR*-rearranged ESS, 2) to identify the novel *BCOR* fusion gene partners in ESS and associated clinicopathological characteristics, and 3) to potentially unravel targetable genomic alterations in *BCOR*-rearranged ESS.

Design: A retrospective database search of our molecular laboratory was performed for clinically advanced ESS that contained *BCOR* gene rearrangements or *BCOR* ITD. The cases were previously assayed with comprehensive genomic profiling via both DNA- and RNA-based targeted next generation sequencing during the course of clinical care. Clinicopathological and genomic profiling data was centrally re-reviewed.

Results: Here we present the molecular characteristics of the largest cohort of *BCOR*-rearranged ESS to date (n=40), and we compare them to an independent cohort of uterine sarcomas harboring *BCOR* ITD (n=15). This cohort included 31 cases with canonical *ZC3H7B-BCOR* fusion as well as 8 cases with novel *BCOR* gene rearrangement partners, such as *BCOR-L3MBTL2*, *EP300-BCOR*, *BCOR-NUTM2G*, *BCOR-RALGPS1*, *BCOR-MAP7D2*, *RGAG1-BCOR*, *ING3-BCOR*, *BCOR-NUGGC*, *KMT2D-BCOR*, *CREBBP-BCOR* and 1 case with *BCOR* internal rearrangement. Re-review of cases with novel rearrangements demonstrated sarcomas with spindle, epithelioid or small round cell components and varying degrees of fascicular growth pattern, myxoid or collagenous stromal change. Comprehensive genomic profiling revealed high frequency of *CDK4* and *MDM2* amplification in 38% and 45% of *BCOR*-rearranged cases, respectively. Other recurrent targetable alterations included homozygous deletion of *CDKN2A*, which encodes an inhibitor of CDK4 in 28% of cases, and amplification of *PDGFRA* and *ERBB3* in 8% and 5% of cases, respectively. Notably, *CDK4* and *MDM2* amplification was absent in all cases from an independent cohort of 15 ESS harboring *BCOR* ITD (0%, 0 of 15).

Conclusions: Activation of the CDK4 pathway for which targeted therapy is clinically available (i.e. palbociclib), via cyclin D1 overexpression, *CDK4* amplification and *CDKN2A* loss, contributes to the pathogenesis of *BCOR*-rearranged ESS, which may have both diagnostic and therapeutic implications.

1146 Diffuse Intratumoral Stromal Inflammation in Ovarian Clear Cell Carcinoma is Associated with Loss of Mismatch Repair Protein and High PD-L1 Expression

Shih-Yao Lin[1], Jen-Fan Hang[1], Chiung-Ru Lai[2], Teh-Ying Chou[1]
[1]Taipei Veterans General Hospital, Taipei, Taiwan, [2]Taipei, Taiwan

Background: Ovarian clear cell carcinoma (OCCC) is a chemotherapy-resistant cancer with limited treatment options. OCCC is associated with Lynch syndrome. Emerging evidence reveals that deficient mismatch repair (MMR) phenotype brings susceptibility to anti-PD-1/PD-L1 therapy in various types of cancers, and certain histological features are associated with MMR protein deficiency. However, only few studies have addressed this in OCCC. The aims of this study were to evaluate the expression of MMR protein and PD-L1 in OCCC and to correlate the results with histological features.

Design: A retrospective search of OCCC cases from surgical pathology archives between 2009 and 2019 was performed. Clinical histories were collected. All pathologic slides were reviewed to confirm the diagnosis of OCCC and to evaluate the presence of diffuse intratumoral stromal inflammation (brisk inflammation obliterating the tumor-stroma interfaces) and peritumoral lymphocytes (lymphoid aggregates cuffing the tumor edges). Tissue microarray was constructed for immunohistochemistry of MSH2, MSH6, MLH1, PMS2, and PD-L1 (clone SP263). Loss of MMR protein expression (MMR-loss) was determined by loss of nuclear staining for any MMR protein in all tumor cells. PD-L1 staining in tumor (membranous) and tumor-associated immune cells (membranous or cytoplasmic) were scored and grouped to <1%, ≥1-24%, 25-49%, and ≥50%.

Results: A total of 76 OCCC cases were included. None of them met the Amsterdam II criteria for the diagnosis of Lynch syndrome. There were four cases (5.3%) showing diffuse intratumoral stromal inflammation. None of the cases had peritumoral lymphocytes. MMR-loss was seen in two cases (2.6%), loss of MLH1 and PMS2 in one and loss of MSH2 and MSH6 in the other. They both had diffuse

intratumoral stromal inflammation and tumoral PD-L1 expression ≥50%. Among the 74 MMR-intact OCCC cases, only two (2.7%) had diffuse intratumoral stromal inflammation, five (6.8%) showed PD-L1 expression ≥25% in tumor or immune cells, and none had tumoral PD-L1 expression ≥50%. By Fisher exact test, diffuse intratumoral stromal inflammation was significantly associated with MMR-loss (P = 0.021) and tumoral PD-L1 expression ≥25% (P = 0.0006) and ≥50% (P = 0.0001).

Conclusions: Our study demonstrated a small subset of OCCC showing diffuse intratumoral stromal inflammation associated with MMR-loss and high tumoral PD-L1 expression. Histological evaluation is helpful in selecting MMR-loss OCCC for subsequent anti-PD-1/PD-L1 therapy.

1147 Identification of a Hydatidiform Mole in Twin Pregnancy Following Assisted Reproduction

Yan Liu[1], Congrong Liu[1]
[1]Beijing, China

Disclosures: Yan Liu: None; Congrong Liu: None

Background: The aim of this study was to identify a co-existing hydatidiform mole (HM) in twin pregnancy from the abnormal mixed-genomic products of conception (POC) after assisted reproduction by the combination of morphology, immunohistochemistry and molecular genotyping.

Design: A total of 37 patients were collected with suspicion for HM by pathological morphology. They had two embryos individually transferred to their uterus after in vitro fertilization and presented two gestational sacs with undeveloped embryos or one sac with an abnormal area by ultrasonography. The diagnosis of HM was confirmed by histopathological review, evaluation of p57[kip2] immunostaining pattern and short tandem repeat genotyping on the POC and maternal specimens.

Results: Thirty patients were diagnosed as singleton pregnancy, including twenty-two non-molar gestations, six trisomy gestations, one homozygous complete mole and one heterozygous partial mole. Although six patients had ultrasonic imaging of two gestational sacs, the embryonic components in the vacant sac might fade away after transferring. Other seven patients were considered as twin pregnancy by the allelic genotype from two individual conceptions. For the patients with uniform p57[kip2] positivity, excessive paternal alleles indicated the potential partial HM in the twin pregnancy. For the patients demonstrated divergent and/or discordant p57[kip2] immunostaining, twin pregnancy with co-existing complete HM or mosaic conception were confirmed by genotyping of different villi population respectively. These patients were monitored by serum β-HCG, while one twin pregnancy with complete mole suffered invasive mole and received chemotherapy.

Table 1 Diagnosis of 37 patients following assisted reproduction.

Diagnosis	One sac		Two sacs	Total
	without abnormal echogenicity	with abnormal echogenicity		
Singleton pregnancy				
Non-molar gestation	15	2	5	22
Trisomy	5	0	1	6
Hydatidiform mole	0	2	0	2
Twin pregnancy				
Both non-molar gestation	0	0	1	1
Including one complete mole	1	1	0	2
Including one suspected partial mole	0	0	3	3
Including one mosaic pregnancy	1	0	0	1
Total	22	5	10	37

Conclusions: A strategy composed of selective clinicopathological screening, immunohistochemical interpretation and accurate genotyping is recommended for diagnostically challenging mixed-genomic POC of potential twin pregnancy with HM, especially to differentiate a non-molar mosaic conception from a partial mole.

1148 Genomic Signatures and Clinicopathological Correlation in Uterine Smooth Muscle Tumors of Uncertain Malignant Potential, Leiomyosarcoma, and Leiomyoma with Bizarre Nuclei

Ying Liu[1], Jong Kim[2], Fabiola Medeiros[2], Bonnie Balzer[2], Eric Vail[3], Jianbo Song[2], Kevin Baden[2], Gaurav Khullar[4], David Engman[2], Jean Lopategui[3]
[1]University of California Davis Medical Center, Sacramento, CA, [2]Cedars-Sinai Medical Center, Los Angeles, CA, [3]Cedars-Sinai Medical Center, West Hollywood, CA, [4]Sands Point, NY

Background: Differentiating uterine smooth muscle tumors of uncertain malignant potential (STUMP), atypical leiomyoma (LEIO), and leiomyosarcoma (LMS) is challenging. In addition, prognostic genomic biomarkers are not available for these entities. Using copy number variation (CNV) chromosomal microarrays (CMA), we investigated the genomic landscape of these tumors. Our goal was to identify genetic alterations in oncogenes and tumor suppressor genes and evaluate how these genomic signatures may correlate clinicopathologically in patients with STUMP, LEIO, and LMS.

Design: We retrospectively reviewed the pathology and follow up on 20 patients, including 10 STUMP, 5 LMS, and 5 LEIO, and correlated with CMA result. For each patient sample, the results were filtered to only include 720 genes from the COSMIC 2 tier cancer gene census, causally implicated in cancer. The cases were grouped by tumor type (LMS, STUMP, LEIO) and subsequently the net frequency of gene gains and losses within each group was calculated. These lists were then filtered to include genes that were lost or gained only in LMS, only in STUMP, and only in LEIO.

Results: The average age at diagnosis was 66 years for LMS, 50 years for LEIO and 44.9 years for STUMP. The average size of the dominant tumor for LMS was 8.5 cm, 7.3 cm for LEIO and 5.8 cm for STUMP. TSG loss was the predominant CNV in all STUMP. Four of 10 STUMP had a unique 1p loss. Similarly, in LMS, TSG loss was the predominant CNV (CBFB, CTCF, FAT1, KLF6, LARP4B and LRP1B). TP53 loss and gain of oncogenes were only observed in LMS. One case with high nuclear grade, increased mitotic count, and coagulative necrosis had a hybrid genomic fingerprint with loss of 1p only seen in STUMP and loss of TSG CBFB and CTCF also seen in LMS. 17 patients had follow-up ranging from 2 months to 108 months with an average of 37.6 months. Four of 5 LMS patients presented with distant metastases including one who died of the disease. No metastases or death was reported among the STUMP and LEIO patients.

Conclusions: The results of this pilot study suggest that LMS display a unique loss of TP53, loss of other TSG, and gain of oncogenes. STUMP is associated with a unique loss of 1p and loss of TSG. High grade STUMP displays loss of CBFB and CTCF observed in LMS, in addition to 1p loss typically associated with STUMP. Additional studies with a larger cohort and longer clinical follow-up are needed to further ascertain genomic markers of biologic behavior in uterine smooth muscle tumors.

1149 Metastases of Uterine Serous Carcinoma Often Show a HER2 Expression Profile Different from the Biopsy and Hysterectomy Specimens

Valeria Maffeis[1], Carrie Robinson[2], Azra Ligon[3], Beth Harrison[3], Marisa Nucci[4], David Kolin[3]
[1]University of Padova, Padova, PD, Italy, [2]Naval Medical Center San Diego, San Diego, CA, [3]Brigham and Women's Hospital, Boston, MA, [4]Brigham and Women's Hospital, Harvard Medical School, Boston, MA

Background: Uterine serous carcinoma (USC) accounts for approximately half of endometrial carcinoma-related mortality. A subset of USC shows human epidermal growth factor receptor 2 (HER2) amplification, and these patients benefit from treatment with trastuzumab. Therefore, accurate assessment of HER2 status is critical to properly select patients for targeted therapy. However, previous work has shown that there is significant intratumoral heterogeneity of HER2 amplification in USC. This study investigated the potential clinical impact of this heterogeneity by examining HER2 expression in paired endometrial biopsies (B), hysterectomy specimens (H), and metastatic lesions (M) from patients with USC.

Design: Cases of USC were retrospectively identified, for which B, H, and/or M samples were available from the same patient. HER2 status was assessed by IHC (clone SP3) on all samples and scored independently by two pathologists using the updated 2018 ASCO/CAP guidelines for testing in breast cancer as negative (0, 1+), equivocal (2+), or positive (3+). All cases which were scored as 2+, or those with a discordance between paired samples (e.g., 1+ in B and 3+ in H), were tested by FISH.

Results: 59 patients were selected, with 35 B, 58 H, and 73 M (multiple M from the same patient were available in 24 of 42 cases). By HER2 IHC, paired B and H were discordant in 2/35 (6%). Specifically, 2 B were negative (1+) but had a corresponding H with either 3+ or 2+ with amplification by FISH. 7 H with HER2 amplification had at least one negative M, while one case was negative on the B and H, but had three different positive M (Figure 1). H and M pairs showed discordance in 8/39 (20%) of cases. Discordance between multiple M

lesions was found in 5/24 (21%). Heterogeneity in HER2 amplification within a single stained slide was present in 3/35 B (8.5%), 18/58 H (31%) and 2/73 M (3%).

Fig 1. Case #54: (A & B) biopsy (HER2: 0), (C & D) hysterectomy (HER2: 1+), (E & F) lymph node metastasis (HER2: 0), (G & H) omental metastasis (HER2: 3+).

Figure 1 - 1149
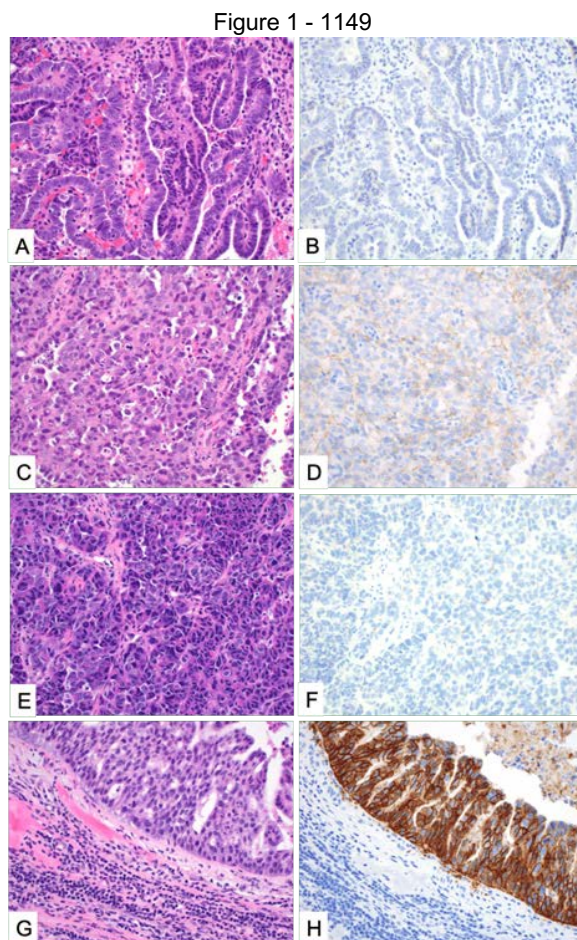
Conclusions: Despite significant HER2 overexpression heterogeneity in over 30% of slides from hysterectomy specimens, there was excellent overall agreement (94%) in HER2 scores between biopsy and hysterectomy specimens. However, HER2 overexpression is discordant in up to 20% of hysterectomy-metastasis pairs, suggesting that testing should be performed on a site of metastatic disease prior to the initiation of targeted therapy.

1150 Frequency of Molecular Alterations Using a Targeted RNA Sequencing Approach in Uterine Mesenchymal Tumors

Leonel Maldonado[1], Amir Momeni Boroujeni[2], Ryma Benayed[1], Martee Hensley[1], Marc Ladanyi[1], Kay Park[1], Robert Soslow[1], Sarah Chiang[1]
[1]Memorial Sloan Kettering Cancer Center, New York, NY, [2]Memorial Sloan Kettering Cancer Center, Brooklyn, NY

Disclosures: Leonel Maldonado: None; Amir Momeni Boroujeni: None; Ryma Benayed: None; Martee Hensley: None; Marc Ladanyi: None; Kay Park: None; Robert Soslow: *Speaker*, Ebix/Oakstone; Sarah Chiang: None

Background: Recurrent translocations resulting in gene fusions underpin a wide variety of uterine mesenchymal tumors, particularly endometrial stromal sarcomas (ESS) and some leiomyosarcoma (LMS) variants. We aimed to determine the frequency and types of fusions detected by targeted RNA sequencing performed as part of the diagnostic evaluation of various uterine mesenchymal tumor subtypes.

Design: Fusion status of all uterine endometrial stromal and smooth muscle tumors, malignant PEComas, uterine tumor resembling ovarian sex cord tumor (UTROSCT) and inflammatory myofibroblastic tumors (IMT) submitted for targeted RNA sequencing as part of their diagnostic evaluation in 2015-2019 was retrospectively reviewed. Re-review of pathology slides was performed when sequencing results and diagnosis were discordant.

Results: Targeted RNA sequencing results were available in 69 uterine mesenchymal tumors, including 1 endometrial stromal nodule (ESN), 10 low-grade ESS (LGESS), 15 high-grade ESS (HGESS), 5 ESS not otherwise specified (NOS), 2 smooth muscle tumors of uncertain malignant potential (STUMP), 12 LMS, 11 myxoid LMS, 2 epithelioid LMS, 6 malignant PEComa, 3 intravenous leiomyomatosis (IVL), 1 IMT and 1 UTROSCT. Fusions were detected in 100% of ESN and IMT; 93% of HGESS; 90% of LGESS; 60% of ESS NOS; 9% of LMS and 36% of myxoid LMS; no fusions were detected in STUMP, epithelioid LMS, PEComa and UTROSCT (Table 1). Sequencing results permitted reclassification of 1 myxoid LMS and 1 LMS, as IMT and fibrosarcoma-like uterine sarcoma, respectively, as well as upgrade of 1 LGESS and 1 ESS NOS found to have *ZC3H7B-BCOR* and *YWHAE-NUTM2B* fusions. Novel *JAZF1-RADIL*, *EPC1-CXorf67*, *AEBP2-ETV6* and *FOXO1-ATP7B* fusions were detected in 3 HGESS and 1 myxoid LMS, respectively.

Tumor type	Fusion frequency, %	Gene fusion	Reclassification	
ESN	100 (1/1)	*JAZF1-SUZ12*		
LGESS	90 (9/10)	*JAZF1-SUZ12* *JAZF1-PHF1* *YWHAE-NUTM2*	HGESS	
HGESS	93 (14/15)	*YWHAE-NUTM2A/B* *ZC3H7B-BCOR* *JAZF1-PHF1* *MEAF6-PHF1* *EPC1-PHF1* *JAZF1-RADIL* *EPC1-CXorf67* *AEBP2-ETV6*		
ESS NOS	60 (3/5)	*JAZF1-SUZ12* *MEAF6-PHF1* *ZC3H7B-BCOR*	HGESS	
LMS	9 (1/12)	*NTRK1-LMNA*	Fibrosarcoma-like uterine sarcoma	
Myxoid LMS	36 (4/11)	*TRPS1-PLAG1* *FAM110B-PLAG1* *FN1-ALK* *FOXO1-ATP7B*	IMT	
IMT	100 (1/1)	*IGFBP5-ALK*		
Epithelioid LMS	0 (0/2)			
PEComa	0 (0/6)			
IVL	0 (0/3)			
UTROSCT	0 (0/1)			
STUMP	0 (0/2)			

Conclusions: Targeted RNA sequencing confirmed fusion status in most ESS and a large subset of myxoid LMS. This method allowed modification of tumor classification or grade in rare lesions diagnosed LMS or its morphologic variants and ESS that are difficult to grade.

1151 Prevalence of Lynch Syndromein Synchronous Endometrial and Ovarian Carcinoma Patients

Tibiletti Maria Grazia[1], Di Lauro Eleonora[2], Ghezzi Fabio[3], Anna Chiaravalli[1], Nicoletta Donadello[4], Fausto Sessa[5]
[1]Ospedale di Circolo ASST Settelaghi Varese, Varese, Italy, [2]Dept. of Pathology ASST Settelaghi, Varese, Varese, Italy, [3]Dept. of Obstetrics and Gynecology Ospe. Del Ponte ASST Settelaghi, University of Insubria, Varese, Varese, Italy, [4]Dept. of Obstetrics and Gynecology Ospedale del Ponte ASST Settelaghi, Solbiate Arno, Varese, Italy, [5]Dept. of Pathology ASST Settelaghi, University of Insubria, Varese, Varese, Italy

Disclosures: Tibiletti Maria Grazia: None; Di Lauro Eleonora: None; Ghezzi Fabio: None; Anna Chiaravalli: None; Nicoletta Donadello: None; Fausto Sessa: None

Background: Synchronous endometrial and ovarian carcinomas (SEO) represent approximately 5% of endometrial and 10-20% of ovarian carcinomas, respectively. Few data are available in literature about the involvement of SEOs in inherited cancer syndromes; recently two SEOs showing germline pathogenetic BRCA variant identified on tumor tissue were described.

Design: Here we describe 28 SEOs from 28 patients (mean age 50.1) studied for Mismatch repair (MMR) defects using both Immunohistochemical and molecular approach and for germline mutations of MMR and BRCA genes.

Results: Interestingly 14 out of 28 SEOs (50%) were MMR defective and 11 out of 28 patients carried MMR pathogenetic germline mutations. Seven out of 11 MMR defective SEOs displayed endometrioid endometrial and ovarian cancers. Patients with proficient MMR SEOs were tested for BRCA germline mutations and 2 carriers of BRCA1 and 2 pathogenetic mutations were identified. SEOs of BRCA mutated patients were endometrioid endometrial/ovarian cancers and endometrioid endometrial and serous ovarian cancers.

Conclusions: Somatic testing including Immunohistochemical and microsatellite instability analyses on SEOs are useful to identify patients affected by inherited cancer syndromes. Our data demonstrate a high incidence of Lynch syndrome in SEOs patients. SEOs patients could benefit from PARP-inhibitor therapy when BRCA mutated and from immunotherapy when MMR mutated.

1152 Comparative Assessment of p53 Immunohistochemistry and TP53 Mutation Status by Next Generation Sequencing in High Grade Endometrial Carcinomas

Nana Matsumoto[1], Douglas Rottmann[2], Hisham Assem[3], Serena Wong[1], Pei Hui[4], Natalia Buza[4]
[1]Yale New Haven Hospital, New Haven, CT, [2]Yale School of Medicine, Hamden, CT, [3]Yale School of Medicine, New Haven, CT, [4]Yale University School of Medicine, New Haven, CT

Disclosures: Nana Matsumoto: None; Douglas Rottmann: None; Hisham Assem: None; Serena Wong: None; Pei Hui: None; Natalia Buza: None

Background: Evaluation of *TP53* mutation status by p53 immunohistochemistry (IHC) is frequently used in the diagnostic work-up of high grade endometrial carcinomas to aid the distinction between histologic subtypes and help predict clinical outcome. Although p53 IHC has been regarded as a reliable surrogate marker, studies validating its concordance with *TP53* mutations, particularly by Next Generation Sequencing (NGS) methods, have been limited in endometrial carcinomas. We aimed to evaluate the correlation between different p53 IHC patterns and *TP53* mutations by NGS in high grade endometrial carcinomas.

Design: High grade endometrial carcinomas diagnosed between 2011 and 2019 with available NGS data were retrospectively identified in our departmental archives. H&E slides were reviewed and a representative tissue block was selected for IHC. P53 IHC (DO7 clone) was performed in each case and categorized into one of four staining patterns: (1) normal/wild-type, (2) "all" (strong, diffuse) (3) "null" (complete absence) (4) cytoplasmic with variable nuclear staining. *TP53* sequencing results were retrieved from the NGS reports in the patients' electronic medical records.

Results: A total of 44 endometrial tumors were included in the study: 22 pure serous carcinomas, 9 mixed carcinomas with a serous component, 3 carcinosarcomas with a serous component, and 10 FIGO grade 3 endometrioid carcinomas. *TP53* mutation was identified by NGS in all tumors with a serous component and in 2 of 10 high grade endometrioid carcinomas. Aberrant p53 IHC staining pattern was observed in 33 of 34 (97%) tumors with a serous component showing "all" pattern in 27 cases, "null" pattern in 2 cases, and cytoplasmic and strong nuclear staining in 4 cases. Among endometrioid carcinomas, one of the 2 tumors with *TP53* mutation showed a "null" IHC pattern, all other tumors displayed wild-type p53 IHC (Table 1).

Table 1. Correlation between p53 IHC pattern and *TP53* mutation type

P53 IHC pattern (All tumors, n=44)	TP53 mutation type by NGS
"All" (Diffuse, strong nuclear) n=27	Missense, loss of function n=25 Splice site n=2
"Null" (Complete absence) n=3	Splice site n=1 Deletion, frameshift n=1 Nonsense, premature truncation n=1
Aberrant cytoplasmic/nuclear n=4	Nonsense, premature truncation n=2 Missense, loss of function n=2
Wild-type n=10	No mutation n=8 Nonsense, premature truncation n=1 Deletion, frameshift n=1

Conclusions: Our results showed a 95% overall concordance rate between p53 IHC and *TP53* mutation in high grade endometrial carcinomas. The concordance was highest among tumors with a serous component (97%), while grade 3 endometrioid carcinomas showed a 90% concordance rate, confirming that p53 IHC is a reliable surrogate for assessing the *TP53* mutation status in endometrial carcinomas. The most common aberrant p53 IHC pattern ("all") resulted from missense, loss of function mutations in most tumors, while less common p53 staining patterns ("null", cytoplasmic/nuclear) showed association with splice site and truncating mutations.

1153 The Impact of the LAST Recommendations on Cervical Biopsy Diagnoses at a Tertiary Care Academic Center
Chelsea Mehr[1], Amrom Obstfeld[2]
[1]Dallas, PA, [2]The Children's Hospital of Philadelphia, Philadelphia, PA

Disclosures: Chelsea Mehr: None; Amrom Obstfeld: None

Background: In 2012, the Lower Anogenital Squamous Terminology Standardization Project (LAST) guidelines were published providing consensus recommendations regarding the evaluation and reporting of squamous lesions. Recommendations regarding the use of p16 immunostaining were a significant part of the LAST recommendations. Since LAST publication, concerns about misdiagnosis due to overinterpreation of the p16 stain have been raised. The goal of this study was to examine the use of the p16 immunostain and to evaluate changes in rates of diagnoses associated with immunostain usage, potentially identifying trends suggesting p16 misuse.

Design: Pathology reports for cervical biopsy diagnoses rendered between 2006 and 2017 were extracted from a local pathology report database. The statistical programming language R was used to parse this text and analyze the findings. The diagnoses made as well as the presence or absence of the term p16 were determined for each year. Rates of diagnoses (no CIN lesion, low-grade, or high-grade dysplasia) were subgrouped by year as well as presence or absence of p16 immunostaining. Findings for the years before 2012 and after 2012 (2012 was used as a washout period) were compared using chi-squared testing.

Results: Within the study period 20,646 cervical biopsy diagnoses were analyzed prior to 2012 and 15,491 were analyzed after 2012. After the publication of the LAST criteria, there was a 6% decline in the rate of low-grade diagnoses and a 5.4% increase in non-CIN diagnoses (p<0.001 for both) with no significant change in high-grade diagnoses (Figure 1). The fraction of high grade diagnoses did not increase with p16 use following the publication of the LAST criteria (Figure 2).

Figure 1 - 1153

Figure 2 - 1153

Figure 1: Cervical Biopsy Diagnoses by Year (2006-2017)

Figure 2: Diagnoses Associated with p16 Use
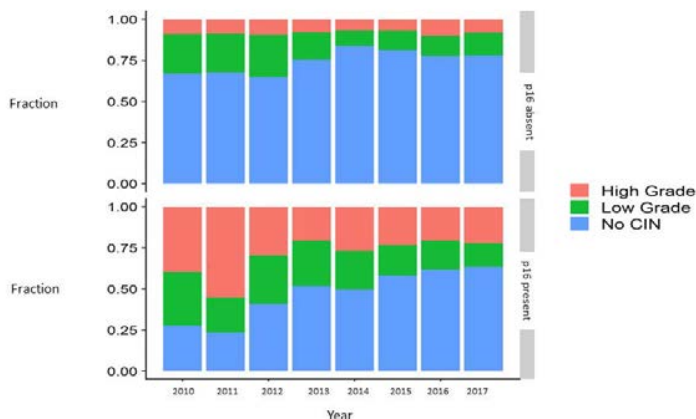
Conclusions: Given the LAST criteria recommendations, changes in the diagnoses and habits of pathologists are expected. Our data suggest significant changes in the frequency of diagnoses following the publication of the LAST criteria. Immunostaining for p16 does not seem to be associated with an increase in high grade diagnosis, arguing against overdiagnosis facilitated by misinterpretation of the immunostain. Finally, this study demonstrates the potential utility of using warehoused pathology data and a robust statistical programming language to provide insight into the day to day workflows and diagnostic trends of a pathology service.

1154 African-American Women with Cervical Cancer have a Predominance of Non-Vaccine Targeted HPV Type 35 which is Associated with Their Poor Survival

Rachelle Mendoza[1], Elmer Gabutan[1], Tahmineh Haidary[2], Mouyed Alawad[1], Raag Agrawal[3], M. Haseeb[1], Raavi Gupta[1]
[1]SUNY Downstate Medical Center, Brooklyn, NY, [2]Great Neck, NY, [3]SUNY Downstate, Brooklyn, NY

Disclosures: Rachelle Mendoza: None; Elmer Gabutan: None; Tahmineh Haidary: None; Mouyed Alawad: None; Raag Agrawal: None; M. Haseeb: None; Raavi Gupta: None

Background: Infection with high-risk human papilloma virus (HPV) is one of the definitive events linked to cervical carcinogenesis. Since the introduction of the HPV vaccine 2006 there has been marked reduction in the incidence and mortality of cervical cancer. As the vaccine targets nine high-risk HPV types, the non-targeted types continue to spread and cause disease. Here, we aimed to investigate the prevalence of high-risk HPV types in cervical cancer in our patient population.

Design: Forty-nine patients with squamous cell carcinoma of cervix were identified and their clinicopathological data were recorded. DNA was extracted from formalin-fixed paraffin-embedded tissues and subjected to multiplex PCR using 33 HPV primers, and gel electrophoresis. Correlations between different parameters were determined by Pearson's Chi-squared or Fisher's exact test. Cumulative 5-year disease-free (DFS) and overall survival (OS) were calculated by Kaplan-Meier method and analyzed by log-rank test.

Results: Forty-five of the 49 patients were American-American (83%). 34 of 49 were diagnosed at an early clinical stage (69%) and 24 of 49 had poor histologic grade (48%). HPV non-16/18 types were present in 38 (78%) patients and HPV 16/18 were present in 11 (22%). Most frequently isolated HPV types were 35 (13.3%), and 18 and 16 (12% each). Mixed HPV infections (>2 types) were found in 11 (22%) patients. 19 (39%) patients were infected with at least 1 non-vaccine targeted HPV type. Patients infected with HPV type 35 (87.5%) and HPV type 18 (85.7%) were diagnosed in early clinical stage, but most had poor tumor histologic grade (p=0.036). Patients with non-16/18 infections had shorter mean DFS (26.9 months) and OS (31.3 months) than those with HPV 16/18 (29.5 and 35 months) among those diagnosed at an early stage. Also, patients with HPV type 35 had shorter mean OS (14.8 months) compared to those infected with other types (35.9 months) in early clinical stage (p=0.021) (Figure).

Figure 1 - 1154
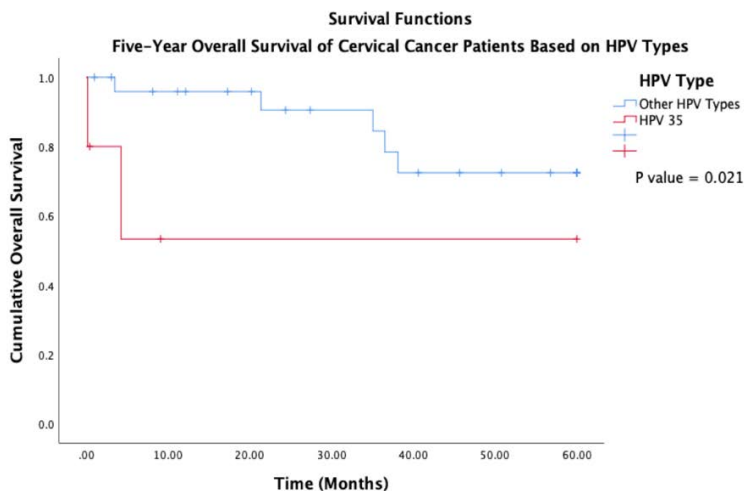
Conclusions: HPV 35 was the most common genotype isolated in our predominantly African-American study population. This finding is remarkable as HPV type 35 is not included in the HPV vaccine in use in the U.S. HPV non-16/18 types were predominant in this cohort and many had mixed HPV infection. Patients diagnosed at an early stage with non-16/18 types and HPV 35 infection had shorter mean DFS and OS. These results warrant expanding HPV targets in the HPV vaccine in current use.

1155   Immunohistochemical Expression of SOX10 in Ovarian Epithelial Malignant Tumors

Jelena Mirkovic[1], Dina Bassiouny[1], Fang-I Lu[1], Bojana Djordjevic[2], Carlos Parra-Herran[1], Sharon Nofech-Mozes[1]
[1]Sunnybrook Health Sciences Centre, University of Toronto, Toronto, ON, [2]University of Toronto, Toronto, ON

Disclosures: Jelena Mirkovic: None; Dina Bassiouny: None; Fang-I Lu: None; Bojana Djordjevic: None; Carlos Parra-Herran: None; Sharon Nofech-Mozes: None

Background: Immunohistochemistry expression of SOX10, a marker of peripheral neural tumors, melanocytic tumors and neural crest-derived tumors, has also been reported in several carcinomas, notably in a significant proportion of triple negative breast cancers. SOX10 immunohistochemical expression in ovarian epithelial malignant tumors was previously evaluated in small cohorts with variable results. Our aim was to comprehensively analyze SOX10 immunohistochemical expression in a large cohort of ovarian epithelial malignant tumors.

Design: Tissue microarrays consisting of 1 mm tissue cores in duplicate per case were stained for SOX10. We included high grade serous (HGSC), low grade serous (LGSC), high grade endometrioid (HGEC), low-grade endometrioid (LGEC), clear cell (CCC), and mucinous (MC) carcinomas. Nuclear staining intensity (weak, moderate, strong) and percentage of tumor cells staining was recorded. Any moderate or strong staining, as well as weak staining in ≥10% of cells, was considered positive.

Results: Cohort consisted of 405 ovarian epithelial malignant tumors including 186 HGSC, 33 LGSC, 51 HGEC, 37 LGEC, 58 CCC, and 40 MC. Overall, 30/405 (7%) of cases demonstrated SOX10 expression, all with focal distribution. Moderate expression was seen in a total of 17/405 (4%) cases in up to 15% of tumor cells, predominantly in high-grade carcinoma categories. Only 2/405 cases showed strong staining in up to 5% of tumor cells, both in HGSC category.

Table 1. SOX10 immunohistochemistry expression in ovarian epithelial malignant tumors: Intensity and percentage of tumor cells staining

Diagnosis	Weak (≥10%)	% of cells (up to)	Mod.	% of cells (up to)	Strong	% of cells (up to)	Total
HGSC (n=186)	6	35%	11	15%	2	5%	19 (10%)
LGSC (n=33)	0	-	0	-	0	-	0
HGEC (n=51)	1	10%	2	8%	0	-	3 (6%)
LGEC (n=37)	1	10%	0	-	0	-	1(3%)
CCC (n=38)	3	15%	3	10%	0	-	6(10%)
MC (n=40)	0	-	1	2%	0	-	1(2.5%)
All (n=405)	11	35%	17	15%	2	5%	30 (7%)

Conclusions: SOX10 is uncommonly expressed in ovarian epithelial malignancies (only 7% of the cases in our cohort). Positive cases showed focal, predominantly weak or moderate staining. Diffuse, moderate to strong SOX10 immunohistochemical expression is not compatible with primary ovarian epithelial malignancy, and could be a useful marker when differential diagnosis includes SOX10 positive carcinomas, such as triple negative breast cancer.

1156 Frequent NTRK Expression in High-Grade Endometrial Stromal Sarcoma Harboring BCOR/BCORL1 Genetic Alterations

Nissreen Mohammad[1], Robert Wolber[2], Stephen Yip[1], Martin Kobel[3], Brendan Dickson[4], Cheng-Han Lee[5]
[1]University of British Columbia, Vancouver, BC, [2]University of British Columbia, North Vancouver, BC, [3]University of Calgary/Alberta Public Laboratories, Calgary, AB, [4]Mount Sinai Health System, Toronto, ON, [5]Vancouver, BC

Disclosures: Nissreen Mohammad: None; Stephen Yip: *Advisory Board Member*, Bayer; Pfizer; Roche; *Speaker*, Roche; Martin Kobel: None; Brendan Dickson: None; Cheng-Han Lee: None

Background: NTRK-associated genetic fusions were recently reported in a subset of uterine sarcomas with features of fibrosarcoma, and pan-Trk immunohistochemistry appears to be a sensitive method for identifying these tumors. These cellular spindle cell sarcomas exhibit morphologic overlap with high-grade endometrial stromal sarcomas showing predominantly, or exclusively, a spindle cell morphology, such as those with *BCOR/BCORL1* rearrangement. The purpose of this study was to examine NTRK expression, using pan-TRK immunohistochemistry, in a series of molecularly confirmed spindle cell endometrial stromal sarcomas with *BCOR/BCORL1* alterations, to confirm whether expression is restricted to NTRK-associated tumors.

Design: We performed Pan-Trk immunohistochemistry (Abcam, clone EPR 17341) on hysterectomy whole sections of 9 high-grade endometrial stromal sarcomas that were molecularly confirmed by either RNA-sequencing (TruSight RNA fusion panel, Ilumina, CA) or by Sanger sequencing for exon 15 of BCOR. Staining intensity and percent tumor cell staining were evaluated (NM, CHL).

Results: All 9 high-grade endometrial stromal sarcoma exhibited a pure monomorphic spindle cell morphology, with at least focally cellular and mitotically active areas that resembled fibrosarcoma. RNA-sequencing identified *ZC3H7B-BCOR* fusions in 5 cases, *EPC1-BCOR, ECP1-BCORL1* and *JAZF1-BCORL1* fusion in 1 case each. The remaining case (#1) did not harbor demonstrable fusion by RNA-sequencing, but was found to harbor internal tandem duplication in exon 15 of *BCOR* (93 base duplication). None of these 9 tumours demonstrated concurrent genetic fusions involving *NTRK1/2/3*. By pan-Trk immunohistochemistry, 8 of 9 tumours showed NTRK expression, ranging from weak focal staining in 10% of tumor cells to moderate-to-strong staining in 80-100% of tumor cells (Table 1).

Case	Fusion	NTRK	Intensity	Percent
1	*BCOR* ITD	Positive	2	30
2	*EPC1-BCOR*	Positive	1	60
3	*EPC1-BCORL1*	Positive	3	30
4	*JAZF1-BCORL1*	Positive	1	10
5	*ZC3H7B-BCOR*	Positive	3	80
6	*ZC3H7B-BCOR*	Negative	0	0
7	*ZC3H7B-BCOR*	Positive	2	80
8	*ZC3H7B-BCOR*	Positive	1	80
9	*ZC3H7B-BCOR*	Positive	2	100

Conclusions: We identified frequent NTRK immunoexpression in high-grade endometrial stromal sarcoma with a spindle cell morphology harboring *BCOR* or *BCORL1* alterations. This is in keeping with a recent report of NTRK expression in 3 of 5 high-grade endometrial stromal sarcoma with *ZC3H7B-BCOR* fusion (PMID: 31375766). Together, these findings highlight a potential diagnostic pitfall and underscore the need for further molecular characterization of pan-Trk immunopositive uterine spindle cell sarcomas.

1157 HER2 Expression in Endometrial Serous Carcinomas

Ioana Moisini[1], Huina Zhang[1], Alexandra Danakas[2], David Hicks[1], Bradley Turner[1]
[1]University of Rochester Medical Center, Rochester, NY, [2]University of Rochester Medical Center, Greece, NY

Disclosures: Ioana Moisini: None; Huina Zhang: None; Alexandra Danakas: None; David Hicks: None; Bradley Turner: None

Background: Uterine papillary serous carcinomas (UPSC) are type II endometrial carcinomas associated with advanced stage, poor overall survival and more importantly, chemo resistance to known therapies, with response rates of only 20-50% to standard chemotherapy regimens. Addition of Transtuzumab to carboplatin-paclitaxel in UPSC has been shown to increase progression-free survival. The human epidermal growth factor receptor 2 (HER2) has been reported to be overexpressed in over 30% of UPSC and addition of HER2-targeted therapy Transtuzumab to carboplatin-paclitaxel in UPSC has been shown to increase progression-free survival; however, the concordance of HER2 protein expression by immunohistochemistry (IHC) and HER fluorescence in-situ hybridization (FISH) continues to be a subject of debate. Our goal in this study is to further evaluate the concordance of HER2 protein expression and HER FISH.

Design: The database at the University of Rochester Medical Center was searched for all cases of UPSC since 2016. A total of 34 cases with available tissue were retrieved (27 cases of pure UPSC carcinoma and 7 cases of mixed serous/endometrioid or clear cell). HER2 IHC and HER2 FISH were performed on all cases. In cases showing tumor heterogeneity, multiple areas were counted on FISH. HER2 IHC was evaluated based on the ASCO/CAP 2007 criteria, while HER2 FISH was evaluated based on the more current ASCP/CAP 2018 criteria.

Results: HER2 was positive in 17.6% of our cases when evaluated by IHC and/or FISH. 23/24 (96%) cases of HER2 negative (score 0 or 1+) or HER2 positive (score 3+) IHC cases were concordant with FISH (Table 1). 100% of IHC positive cases were also concordant with FISH. One IHC negative (score 1+) case was FISH amplified and only 2/8 (25%) of HER2 equivocal cases were FISH amplified.

Table 1: Correlation of HER2 IHC and HER FISH

		HER2 FISH	
Type of carcinoma	Cases (n)	Non- amplified (n)	Amplified (n)
Uterine papillary serous carcinoma			
HER2 IHC score			
0	5	5	0
1+	11	10	1
2+	8	6	2
3+	3	0	3
Mixed serous/other type carcinoma			
HER2 IHC score			
0	1	0	0
1+	3	0	0

Conclusions: Our study supports that there is an overall concordance between HER2 protein expression and HER FISH based on the ASCO/CAP 2007 and the ASCO/CAP 2018 criteria. Additional studies on larger populations are currently being pursued. We are currently developing an algorithmic approach for evaluation of HER2 by FISH based on the ASCO/CAP 2018 FISH criteria which can be reliably applied in pure or mixed UPSC.

1158 Molecular Subclassification of Copy Number-Low Endometrial Carcinomas

Amir Momeni Boroujeni[1], Bastien Nguyen[2], Britta Weigelt[2], Chad Vanderbilt[3], Robert Soslow[2]
[1]Memorial Sloan Kettering Cancer Center, Brooklyn, NY, [2]Memorial Sloan Kettering Cancer Center, New York, NY, [3]Memorial Sloan Kettering Cancer Center, Denver, CO

Disclosures: Amir Momeni Boroujeni: None; Bastien Nguyen: None; Britta Weigelt: None; Chad Vanderbilt: *Consultant*, Docdoc ltd. (Singapore); *Consultant*, Paige AI; *Consultant*, OncoKB; Robert Soslow: *Speaker*, Ebix/Oakstone

Background: Molecular genomic studies of endometrial carcinomas (ECs) have identified a group of copy number-low (CN-L) tumors lacking hyper/ultramutation, chromosomal instability or *TP53* mutation. The aim of this study was to define the molecular characteristics of CN-L ECs and their association with outcome.

Design: CN-L ECs subjected to clinical next generation sequencing were analyzed, and clinico-pathologic data pertaining to these cases assessed. All ECs were reviewed and histologically typed by expert gynecologic pathologists at a single institution. Non-linear dimensionality reduction using T-SNE on non-negative matrix factorized (NMF) copy number and mutation data followed by K-means unsupervised clustering was used to cluster tumors into 3 molecular subgroups.

Results: In total, 394 CN-L ECs were studied, including 375 endometrioid (95%), 13 mixed (3%), 6 high-grade carcinomas and unclassified (1.5%) carcinomas. The median survival was 34.59 months. Based on clustering of copy number and mutational data, three molecular subgroups were identified: C1, with *PTEN* and *PIK3R1* mutations; C2, with *PTEN* and *PIK3CA* mutations; and C3, with *AKT1* mutations and 1q and 8q gains in absence of *PTEN* mutations. Log-rank analysis showed significant differences between the clusters, with C1 having the best outcomes (>90% survival at 4 years), C2 with intermediate outcomes and C3 with the worst outcomes (p=0.0001).

Figure 1 - 1158
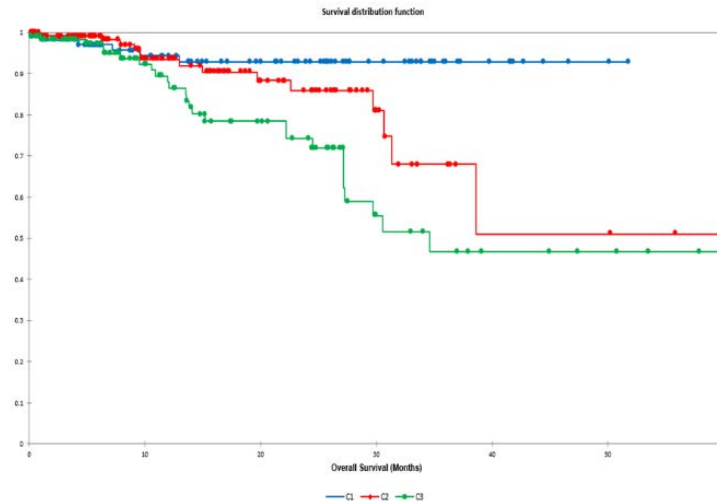
Conclusions: CN-Ls form the largest group of ECs and are heterogenous at the genetic and clinical level. CN-L ECs can be subclassified into 3 molecularly distinct subgroups with important outcome differences. This approach can potentially be used in risk-stratification of patients for therapeutic and management purposes.

1159 Alterations in Chromatin Remodeling Genes in Endometrial Epithelial Tumors are Associated with Prognosis

Amir Momeni Boroujeni[1], Chad Vanderbilt[2], Rajmohan Murali[3]
[1]Memorial Sloan Kettering Cancer Center, Brooklyn, NY, [2]Memorial Sloan Kettering Cancer Center, Denver, CO, [3]Memorial Sloan Kettering Cancer Center, New York, NY

Background: Chromatin remodeling genes (CRG) are components of epigenetic regulatory mechanisms and alterations in these genes have been identified in several tumor types, including gynecologic tumors. In this study, we sought to investigate the prevalence and clinicopathological associations of CRG alterations in epithelial tumors of the endometrium (ETs) and adnexa (ATs).

Design: We performed a retrospective analysis of ET and AT specimens sequenced using a targeted clinical next generation sequencing panel targeting up to 468 genes, including the CRGs: ARID1A, ARID1B, ARID2, ATRX, BAP1, CREBBP, CTCF, EP300, IKZF1, KMT2A, KMT2B, KMT2C, NCOR1, RAD54L, RB1, SMARCA4, and SMARCD1. Cases with microsatellite instability or POLE mutation were excluded. We analyzed associations of CRG alterations with clinicopathologic findings.

Results: A total of 1147 ETs and 1114 ATs consisting of various diagnoses including endometrioid, serous, clear cell, mesonephric, and carcinosarcoma were evaluated. Up to 45% of ET and 37% of AT harbored at least one pathogenic CRG alteration, the most common being *ARID1A* (ET: 25%, AT: 11%) followed by *CTCF* in ET (7%) and *RB1* in AT (7%). In ETs, some CRG alterations (*ATRX, SMARCA4, RB1*) were associated with higher FIGO stage (~50% stage III or IV) and poor overall survival, regardless of presence or absence of other CRG alterations (p=0.006) (G1). Conversely, alterations in the other CRGs (*ARID1A, ARID1B, ARID2, BAP1, CREBBP, CTCF, EP300, IKZF1, KMT2A, KMT2B, KMT2C, NCOR1, RAD54L* and *SMARCD1*) without alterations of *ATRX, SMARCA4* and *RB1* was associated

with lower stage at presentation (~70% stage I) and improved survival outcomes (p=0.007) (G2) even compared to the group without any CRG alterations (G3). While similar trends were observed in ATs, these failed to reach statistical significance.

	Endometrial (n=516)		Adnexal (n=412)	
	Tumors with at least 1 CRG alteration (n, %)	Most common CRG mutations (n, %)	Tumors with at least 1 CRG alteration (n, %)	Most common CRG mutations (n, %)
Endometrioid adenocarcinoma	262 (51%)	ARID1A (196, 75%) CTCF (66, 25%) KMT2D (19, 7%)	19 (5%)	ARID1A (12, 63%) CREBBP (3, 16%) RB1 (2, 11%)
Serous carcinoma	71 (14%)	ARID1A (16, 23%) SMARCA4 (8, 11%) EP300 (7, 10%)	235 (59%)	ARID1A (30, 13%) KMT2C (29, 12%) RB1 (28, 12%)
Clear cell carcinoma	17 (3%)	ARID1A (4, 24%) KMT2C (4, 24%) EP300 (3, 18%)	60 (15%)	ARID1A (54, 90%) ARID1B (5, 8%) KMT2C (5, 8%)
Carcinosarcoma	56 (11%)	ARID1A (12, 21%) CREBBP (6, 11%) RB1 (6, 11%)	22 (6%)	RB1 (5, 23%) ARID1A (5, 23%) KMT2C (2, 9%)

Figure 1 - 1159
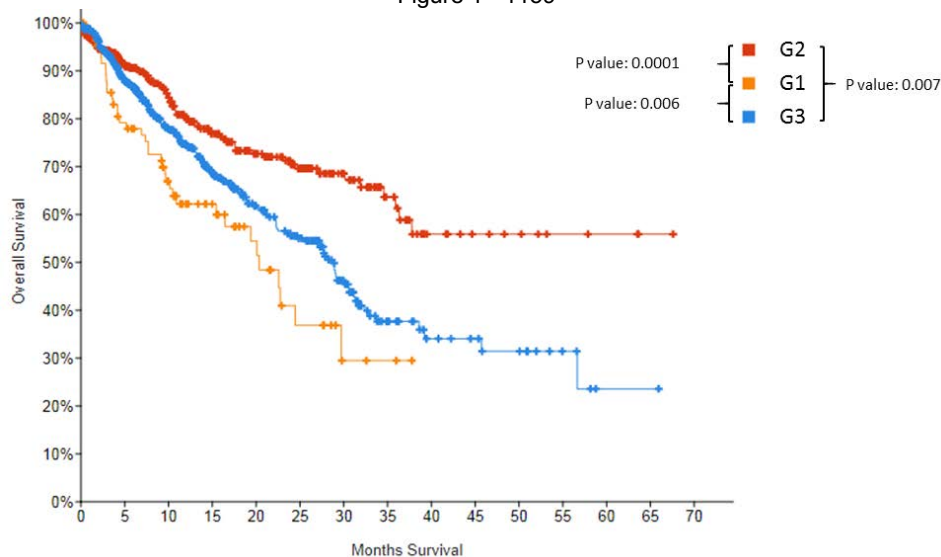
Conclusions: CRG alterations are common in ETs and ATs and are associated with clinicopathologic features and survival. Our data suggest that CRG alterations modulate the behavior of tumors, likely through epigenetic mechanisms.

1160 High NTRK3 Expression in High-Grade Endometrial Stromal Sarcomas with BCOR Abnormalities

Amir Momeni Boroujeni[1], Ryma Benayed[2], Martee Hensley[2], Cristina Antonescu[2], Marc Ladanyi[2], Sarah Chiang[2]
[1]Memorial Sloan Kettering Cancer Center, Brooklyn, NY, [2]Memorial Sloan Kettering Cancer Center, New York, NY

Disclosures: Amir Momeni Boroujeni: None; Ryma Benayed: None; Martee Hensley: None; Cristina Antonescu: None; Marc Ladanyi: None; Sarah Chiang: None

Background: A subset of high-grade endometrial stromal sarcomas harbor rearrangements involving the BCL-6 corepressor (*BCOR*) gene, manifesting as *ZC3H7B-BCOR* fusion or *BCOR* internal tandem duplication (ITD) involving exon 15. *BCOR* plays a role in suppressing gene transcription and maintaining tissue homeostasis and gene silencing through epigenetic mechanisms. NTRK3 mRNA upregulation was previously reported in soft tissue sarcomas harboring *BCOR-CCNB3* fusion and *BCOR* ITD. Here, we aim to evaluate NTRK expression in high-grade endometrial stromal sarcomas with *BCOR* genetic alterations.

Design: Pan-NTRK immunohistochemistry targeting *NTRK1, NTRK2* and *NTRK3* was performed on paraffin-embedded, formalin-fixed tumoral tissue sections of 8 high-grade endometrial stromal sarcomas with *BCOR* rearrangement (7 *ZC3H7B-BCOR* fusion, 1 *BCOR* ITD) previously confirmed by fluorescence in situ hybridization or a targeted RNA capture fusion assay. An *RBPMS-NTRK3* fusion-positive uterine sarcoma served as a positive control. NTRK RNA expression data from the RNA capture fusion assay was extracted from 5 *ZC3H7B-BCOR* and 1 *RBPMS-NTRK3* fusion-positive uterine sarcomas and compared.

Results: Strong cytoplasmic pan-NTRK staining in ≥95% of cells was seen in the tumor harboring *BCOR* ITD. Cytoplasmic staining in ≥50% of cells was moderate in 4 and weak in 3 *BCOR* fusion-positive tumors. Significant mRNA upregulation of *NTRK3* was seen in all tested tumors with either conventional gene fusion or ITD, the latter comparable with that seen in the *NTRK3* fusion-positive tumor. mRNA Expression of *NTRK1* and *NTRK2* was not increased.

Figure 1 - 1160
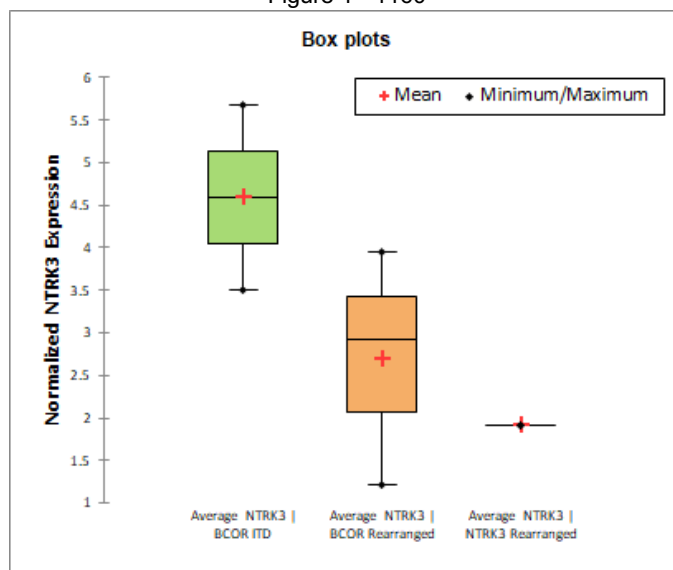
Conclusions: *BCOR* genetic alterations lead to upregulation of *NTRK3* at mRNA and protein levels in high-grade endometrial stromal sarcoma. Further investigation of *NTRK3* overexpression serving as a potential therapeutic target in these tumors is required.

1161 FOXL2 Mutation Status in Ovarian Adult Granulosa Cell Tumors with an Extensive Fibrothecomatous Component

Paloma Monroig-Bosque[1], Erika Walker[2], Donna Coffey[3], Suzanne Crumley[2], Michael Deavers[4], Randall Olsen[5], Ramya Masand[6], Ekene Okoye[2]
[1]Houston Methodist Hospital, Pearland, TX, [2]Houston Methodist Hospital, Houston, TX, [3]The Methodist Hospital, Houston, TX, [4]Houston Methodist, Houston, TX, [5]Houston, TX, [6]Baylor College of Medicine, Houston, TX

Disclosures: Paloma Monroig-Bosque: None; Erika Walker: None; Donna Coffey: None; Suzanne Crumley: None; Michael Deavers: None; Randall Olsen: None; Ramya Masand: None; Ekene Okoye: None

Background: Nearly all adult granulosa cell tumors (AGCT) harbor a mutation in the FOXL2 gene, whereas most fibromas/thecomas do not. Accurate classification of AGCT with an extensive fibrothecomatous component (AGCT-FTC; 10-50% granulosa cells), referred to as "mixed granulosa theca cell tumors" can be challenging by histology and reticulin stain. We sought to characterize FOXL2 mutation status in these diagnostically challenging tumors.

Design: Retrospective review of AGCT-FTC and molecular testing for FOXL2 was performed (largest series to date, n=15). Diagnostically challenging fibrothecomas with sex cord elements (granulosa cell proliferation) (FT-SCE) were included. Reticulin stains were reviewed. FFPE tissue microdissection was performed, and FOXL2 mutation status was tested in both components independently.

Results: We identified 15 cases classified as AGCT-FTC and 3 classified as FT-SCE. Mean patient age was 54 yrs; 11 were Stage IA & 4 were Stage IC. Follow-up data was available for 12/18 patients, all of whom had no evidence of disease at last follow-up (mean follow-up time 51.8 mo.). Reticulin stains were reviewed in 13/15 AGCT-FTC and showed loss of fibers in areas of GCT and preservation in areas of FTC. Three cases of FT-SCE showed preserved reticulin with only focal loss. FOXL2 mutation was detected in 8/15 AGCT-FTC (53.3%), and 1/3 FT-SCE (33.3%), with concordance in both granulosa and fibrothecomatous components. FOXL2 mutation was

detected in 6/8 (75 %) cases with ≥35% granulosa cells in AGCT-FTC, and in 2/7 (28.5%) of AGCT-FTC cases with < 35% granulosa cells (Table 1).

Figure 1 - 1161

Table 1:
Correlation between the % of granulosa cells in the tumor and FOXL2 mutation status in the granulosa cell component and the fibrothecomatous component.

Case type	% of granulosa cells	Granulosa cell component	Fibrothecomatous component
FT-SCE	Indeterminate	*Not detected*	*Not detected*
FT-SCE	Indeterminate	*Not detected*	*Not detected*
FT-SCE	Indeterminate	*Mutation detected*	*Mutation detected*
AGCT-FTC	10	*Not detected*	*Not detected*
AGCT-FTC	15	*Not detected*	*Not detected*
AGCT-FTC	15	*Not detected*	*Not detected*
AGCT-FTC	20	*Mutation detected*	*Mutation detected*
AGCT-FTC	25	*Not detected*	*Not detected*
AGCT-FTC	30	*Not detected*	*Not detected*
AGCT-FTC	30	*Mutation detected*	*Mutation detected*
AGCT-FTC	35	*Mutation detected*	*Mutation detected*
AGCT-FTC	35	*Mutation detected*	*Mutation detected*
AGCT-FTC	40	*Mutation detected*	*Mutation detected*
AGCT-FTC	40	*Mutation detected*	*Mutation detected*
AGCT-FTC	45	*Mutation detected*	*Mutation detected*
AGCT-FTC	45	*Mutation detected*	*Mutation detected*
AGCT-FTC	50	*Not detected*	*Not detected*
AGCT-FTC	50	*Not detected*	*Not detected*

Conclusions: FOXL2 mutation status is concordant in both granulosa and fibrothecomatous components of AGCT-FTC, suggesting that the FTC represents a variant histologic pattern in AGCT. Although there is a rough correlation between the percentage of granulosa cells and the presence of a FOXL2 mutation, the % granulosa cells do not reliably predict FOXL2 mutation. AGCT-FTC appears to present at an early stage and behave indolently.

1162   The Targetable Immune Checkpoint VISTA is Highly Expressed in a Subset of Endometrial Carcinomas, Particularly Those Exhibiting Mismatch Repair Deficiency and PD-L1 Expression
Margaret Moore[1], Lisa Friedman[1], Kari Ring[1], Emily Sloan[2], Anne Mills[1]
[1]University of Virginia, Charlottesville, VA, [2]University of California San Francisco, San Francisco, CA

Disclosures: Margaret Moore: None; Lisa Friedman: None; Kari Ring: None; Emily Sloan: None; Anne Mills: None

Background: Mismatch repair-deficient (MMRd) endometrial carcinomas (ECs) possess higher neoantigen loads than mismatch repair-intact (MMRi) ECs, and targetable immune modulatory molecules —including PD-L1, IDO-1, LAG-3, and TIM-3—exhibit differential expression across mismatch repair groups. V-domain Ig suppressor of T cell activation (VISTA) is a B7 protein that represents another immunosuppressive checkpoint molecule which may have immunotherapeutic value in these tumors. However, little is known about VISTA expression in ECs or its relationship to MMR status and PD-L1 expression.

Design: Immunohistochemistry for VISTA, CD3, and PD-L1 was performed on representative whole sections of 78 ECs [29 intact carcinomas, 25 MLH1-hypermethylated MMRd carcinomas, and 24 unmethylated MMRd carcinomas]. VISTA-positive (VISTA+) and CD3-positive (CD3+) lymphocytes were separately enumerated. Membranous tumoral PD-L1 staining was scored using a semi-quantitative scale (<1%, 1-5%, 6-10%, 11-25%, 26-50%, and >50%). Due to the therapeutic significance of a combined positive score (CPS) [CPS=(#PD-L1+ tumor cells, lymphocytes, & macrophages)/(# tumor cells) x 100] of ≥ 1 in some tumor types, cases with a CPS ≥ 1 were also identified.

Results: No statistical difference in age, stage, or grade at presentation was identified between MMR groups. VISTA+ lymphocytes were observed in all cases; no tumoral expression of VISTA was seen. MMRd ECs demonstrated higher levels of VISTA expression than MMRi ECs ($p=0.00004$), with both hypermethylated and unmethylated ECs demonstrating increased expression relative to intact ECs ($p=0.001$, $p=0.001$). Greater numbers of CD3+ lymphocytes were present in the MMRd subset ($p=0.00005$). The VISTA:CD3 ratio was significantly higher in MMRd versus MMRi ECs ($p=0.04$). Tumoral PD-L1 expression was not significantly correlated with VISTA expression, however a PD-L1 CPS ≥ 1 was significantly associated with increased VISTA expression ($p=0.0002$), greater numbers of CD3+ lymphocytes ($p=0.0001$), and an increased VISTA:CD3 ratio ($p=0.04$).

	Median VISTA+ lymphocytes/HPF	Mean CD3+ lymphocytes/HPF	Median VISTA: CD3 Ratio (VISTA+lymphocytes/HPF)/ (CD3+lymphocytes/HPF)
MMR Status			
MMRd	12.9	217	0.065
MMRi	2.6	131	0.022
p value	0.00004	0.00005	0.04
PD-L1 Status			
PD-L1 CPS≥ 1	9.2	201	0.056
PD-L1 CPS <1	1.3	82	0.013
p value	0.0002	0.0001	0.04

Conclusions: VISTA+ lymphocytes are common in endometrial carcinomas. VISTA and CD3 expression are more robust in MMRd ECs than MMRi ECs, and in cases with a PD-L1 CPS ≥ 1 versus <1. The increased VISTA:CD3 ratio in MMRd ECs suggests that increased VISTA expression is not merely attributable to the higher absolute number of inflammatory cells in these cancers. These findings suggest that MMRd ECs may be good candidates for therapeutic agents targeting VISTA.

1163 Five Year Experience of Pathologic Ultrastaging of Endometrial Cancer Sentinel Lymph Nodes: A Focus on Prevalence, Treatment and Outcome of Patients with Isolated Tumor Cells

Samaneh Motanagh[1], Jessica Dillon[2], Kristen Muller[3], Jorge Gonzalez[2], Laura Tafe[3]
[1]Lebanon, NH, [2]Dartmouth Hitchcock Medical Center, Lebanon, NH, [3]Dartmouth-Hitchcock Medical Center, Lebanon, NH

Disclosures: Samaneh Motanagh: None; Jessica Dillon: None; Kristen Muller: None; Jorge Gonzalez: None; Laura Tafe: None

Background: Endometrial cancer is the most frequent uterine malignancy in the United States, with prognosis largely dependent on stage. Sentinel lymph node (SLN) mapping is an established technique for identifying low volume nodal disease in endometrial carcinomas. At this time, few studies have provided follow-up data to assess the utility of SLN biopsies and clinical management of low volume disease, particularly isolated tumor cells (ITCs). We report follow-up data examining the prevalence of low volume disease in our patient cohort, the clinical treatment of all SLN cases with ITCs and patient outcome.

Design: From 2014 to August 2019, the gynecologic oncologists at our institution performed SLN mapping on 451 women with newly diagnosed endometrial carcinoma. Of those, 437 cases underwent pathologic examination using the MSKCC protocol for lymph node ultrastaging consisting of two additional deeper recuts and paired pancytokeratin stains (PMID: 23694985).

Results: Of 437 cases, a total of 14 macrometastases (3%, 14/437) and 2 micrometastases (<1%, 2/437) were identified on the initial H&E slides. An additional 2 micrometastases and 37 ITCs (8.5%, T1a – 11; T1a – 20; T2 – 3; T3a – 2; T3b - 1) were identified on cytokeratin stain using pathologic ultrastaging. 40 patients with micrometastases and ITCs had endometrioid histology (grade I/II – 33, grade III – 7), 1 with mixed. In patients with ITCs, treatments were rendered as follows: 9 brachytherapy, 13 radiotherapy (RT), 1 chemotherapy (CT), 4 (CT+RT) and 6 patients did not receive further care (T1a – 3; T1b – 2; T2 – 1). Four patients were lost to follow up. To date, only one ITC patient (FIGO grade III, T1b) (2%, 1/37) experienced a recurrence in the omentum at 11 months post-surgery despite hormone and brachytherapy.

Table. The pathologic features and treatment of the 37 patients with ITCs. All tumors were endometrioid histology.

PATIENT	TUMOR SIZE (CM)	GRADE	STAGE	LVI	TREATMENT	RECURRENCE	F/U (2019)
1	4.0	II	T1A	NO	None	NONE	NED
2	1.5	II	T1A	NO	Brachy	NONE	NED
3	3.7	II	T1A	NO	Brachy	NONE	NED
4	5.5	II	T1A	NO	RT	NONE	NED
5	7.1	I	T1A	NO	Brachy	NA	NA
6	7.7	II	T1B	NO	CT + RT	NONE	NED
7	4.0	I	TIB	NO	Brachy	NONE	NED
8	3.0	II	T1B	NO	Brachy	NONE	NED
9	3.0	III	T1B	NO	Brachy	NA	NA
10	8.0	II	T1B	NO	Brachy	NONE	NED
11	10.5	II	T1B	NO	RT	NA	NA
12	3.0	III	T1B	SUSP	Brachy + hormonal	POS; 11 mos., omental mass	DOD
13	3.7	III	T2	NO	CT + RT	NONE	NED
14	4.5	I	T1B	NO	RT	NONE	NED
15	7.0	I	T1B	NO	RT	NA	NA
16	1.8	I	T1A	NO	None	N/A	RECENT
17	6.5	I	T3A	POS	NA	N/A	RECENT
18	9	III	T1B	POS	NA	N/A	RECENT
19	4.5	III	T1B	POS	RT	N/A	RECENT
20	3.7	I	T1A	POS	RT	N/A	RECENT
21	3	II + undiff	T1B	POS	CT + RT	N/A	RECENT
22	6	III	T1B	POS	None	N/A	N/A
23	6	II	T1B	POS	RT	NONE	NED
24	8.5	II	T3B	POS	CT	NONE	NED
25	4.1	II	T2	POS	None - declined	NA	NA
26	10	II	T2	NO	NA	NA	NA
27	5.5	I	T1B	NO	RT	NONE	NED
28	4.5	I	T1A	NO	RT	NONE	NED
29	8	I	T3A	POS	NA	NA	NA
30	4.5	I	T1B	POS	RT	NONE	NED
31	5.3	III	T1B	POS	None	NONE	NED
32	1	II	T1B	NO	RT	NONE	NED
33	5	I	T1A	POS	RT	NA	NA
34	3.3	I	T1A	NO	None	NONE	NA
35	5.1	II	T1B	NO	Brachy	NA	NA
36	5.3	II	T1B	NO	RT	NA	NA
37	1.5	I	T1A	NO	CT + RT	NONE	NED

Conclusions: SLN mapping decreases the morbidity and mortality associated with lymphadenectomy and our surgeons are appropriately selecting patients for SLN with low-risk of bulky lymph node disease. However SLN ultrastaging is resource intensive and, the predominant finding is ITCs. Clinical treatment of ITCs remains variable without a consensus in the oncologic community, which is reflected in our data. Our results further question the utility of SLN ultrastaging, given the continued controversy of clinical management of ITCs and low yield of detecting micrometastatic disease and predicting tumor recurrence.

1164 Evaluation of Histologic Size of High Grade Squamous Intraepithelial Lesion (HSIL) with Preceding Abnormal Cytology versus HSIL with Preceding Negative Cytology

Shima Mousavi[1], Dina Mody[1], Suzanne Crumley[1], Ekene Okoye[1]
[1]Houston Methodist Hospital, Houston, TX

Disclosures: Shima Mousavi: None; Dina Mody: None; Suzanne Crumley: None; Ekene Okoye: None

Background: HSIL can be preceded by a negative (neg) Papanicolaou (Pap) test, usually with a concurrent positive HRHPV test. The purpose of this study was to assess if there is a histologic size difference between HSIL cases with preceding neg cytology (NILM) vs those with preceding abnormal cytology (ASCUS and above), and to evaluate the significance of HRHPV genotype on the size of HSIL seen on histology.

Design: We retrospectively reviewed our Laboratory database for liquid-based Pap tests performed on a low risk screening population over a period of one year (2017). Of 189,243 pap tests, 6,755 had follow up biopsy, with 294 having a HSIL diagnosis. 245 of HSIL cases had a preceding abnormal pap test (ASCUS and above), and 49 of HSIL cases had a neg preceding Pap test (NILM). Histologic review of 72 HSIL cases, with slides available, (combination of cervical biopsies and LEEPs), including 27 with preceding NILM Pap/positive HRHPV (NILM arm) and 45 patients (pts) with ASCUS and above cytology (ASCUS+ arm) was conducted. HSIL size was measured using a calibrated microscope camera. Statistical analysis was performed using the *t-test*.

Results: Mean age of pts with preceding neg cytology was 45 yrs (24- 66) vs. 33 yrs (21-57) in those with preceding abnormal cytology; (p < 0.0004). The average size of HSIL in the NILM arm was 4.53 vs 6.22 mm in the ASCUS+ arm; (p < 0.311). In the NILM arm, the majority of cases were HR HPV 16 positive (17/27; 62.9%); and 22/27;81.5% were HPV 16 and/or 18 positive. The remaining 5/27 cases were HRHPV non-16/18 positive. The size of HRHPV 16/18 positive HSILs was larger than the HRHPV non-16/18 positive HSILs (5.42 vs. 0.78 mm); (p < 0.004). However, in the ASCUS+ arm there was no significant difference between size of HRHPV16/18 positive HSILs and HPV non16/18 positive group HSILs, 5.84 vs. 5.17mm (p < 0.77).

Conclusions: Negative cytology more frequently precedes the biopsy diagnosis of HSIL in an older population. The size of HSIL in cases with preceding negative versus positive cytology did not show a significant difference. However, the size of the HRHPV 16/18 HSILs was smaller as compared to the HR HPV non-16/18 HSILs in the NILM arm. These findings suggest that the non-16/18 HR HPV types may induce smaller lesions, and have important implications for screening in the HPV vaccination era with an anticipated decrease in HRHPV 16/18-related cases. In these cases, the smaller HSIL lesions associated with HR HPV non-16/18 types may be more challenging to detect.

1165 Comparison of the New CAP-ACP Consensus Guidelines for Endometrial Biopsy Reporting to Current Practice in Ethiopia: Are Guidelines From High Income Countries Applicable in Low- and Middle-Income Countries?

Zewditu Nigatu[1], Zemen Asmare[2], Dana Razzano[3], Joseph Rabban[4]
[1]St. Paul's Hospital Millennial Medical College, Addis Ababa, Gulele, Ethiopia, [2]SPHMMC, Addis Ababa, Ethiopia, [3]New York Medical College, Valhalla, NY, [4]University of California San Francisco, San Francisco, CA

Disclosures: Zewditu Nigatu: None; Zemen Asmare: None; Dana Razzano: None; Joseph Rabban: *Employee*, Spouse is an employee of Merck & Co.

Background: Standardized classification and reporting of endometrial pathology is essential for optimal patient management. Recently, consensus recommendations from high-income countries have been published for endometrial biopsy reporting (CAP-ACP guidelines, PMID: 29369922) and for endometrial cancer reporting (ISGyP guidelines, PMID: 30550479). The feasibility of applying these guidelines in low-middle income countries (LMIC) has not been evaluated. As the first of a multi-step evaluation, this study examined endometrial biopsy reporting practices in one of the largest centers in Ethiopia and correlated with the new CAP-ACP reporting guidelines.

Design: Endometrial biopsy, polypectomy and curettage reports from Jan 2014 to Feb 2018 from one of the largest centers in Ethiopia (patient catchment population over 5 million) were reviewed for the submitted clinical history and final diagnosis, then correlated with the CAP-ACP reporting guidelines.

Results: 1,590 endometrial biopsy reports were evaluated. Abnormal uterine bleeding (65%) was the leading indication; clinical history was not provided for 20%. The diagnoses were 81.4% benign, 0.4% atypical hyperplasia, 2% carcinoma, 10% trophoblastic disease, and 6.2% inadequate for diagnosis. The leading benign diagnoses were normal functioning endometrium (32%), polyps (30%) and retained products of conception (29%) while 1% were acute or granulomatous endometritis. The diagnostic sub-categories aligned well with those of the CAP-ACP guidelines with minor exceptions: 1.) diagnoses of hormonal imbalance were not sub-classified as disordered proliferative pattern, irregular secretory pattern or progestin-treatment effect. 2.) non-diagnostic specimens were not stratified as to the cause for inadequacy. 3.) extra-uterine tissues were not noted in any case.

Conclusions: Current endometrial biopsy reporting practices for benign disease in Ethiopia align well with new CAP-ACP guidelines. Minor opportunities exist for fine-tuning classification of hormonal alterations, describing reasons for a non-diagnostic biopsy, and recoqnizing extra-uterine tissue. The next step is to evaluate our endometrial cancer reporting practices in comparison to the new ISGyP recommendations to identify further opportunities for optimization. We recommend that other LMIC also perform similar correlations as awareness of regional variations between LMIC may be of value in designing future international guidelines.

1166 Expression of B7-H4 and IDO1 is Associated with Drug Response and Prognosis of High Grade Ovarian Serous Carcinoma

Na Niu[1], Yanping Zhong[1], Amir Jazaeri[1], Anil Sood[1], Jinsong Liu[1]
[1]The University of Texas MD Anderson Cancer Center, Houston, TX

Disclosures: Na Niu: None; Yanping Zhong: None; Amir Jazaeri: *Grant or Research Support*, Iovance; *Grant or Research Support*, AstraZeneca; *Grant or Research Support*, BMS; *Grant or Research Support*, Aravive; *Grant or Research Support*, Pfizer; Anil Sood: None; Jinsong Liu: None

Background: High grade ovarian serous carcinoma (HGOSC) is the most lethal gynecologic malignancy. Immune checkpoint inhibitors against PD-L1 and CTLA-4 have shown significant efficacy in multiple tumor types, however, the effectiveness of these drugs in treating HGSOC has been limited. This is probably due to the intrinsic immune suppressive status of ovary and low expression of PD-L1 and CTLA4 in HGOSC. Therefore, alternative targets or markers are needed to guide therapeutic strategies.

Design: 24 drug (paclitaxel and carboplatin) sensitive and 24 resistant samples were selected from 660 archived HGSOC cases in Department of Pathology in MDACC and clinical information was extracted. Nanostring including 33 immune-related genes was used to determine the immune status between the sensitive and resistant groups. 4 genes of most significant difference in expression were selected and verified further with multiplex immunohistochemical staining on 222 HGSC samples obtained from primary surgery between 2009 and 2015 at MDACC. The relationship between different checkpoint inhibitors and clinicopathologic features and the inter-variates correlation were analyzed.

Results: Intrinsic drug resistant HGSOC samples had higher levels of B7-H4 and IDO1, in addition to inflammatory factors such as IL-6 and IL-8 (Figure 1). B7-H4 (68.5%) and IDO1 (71.6%) were diffusely expressed in tumor cells in HGSOC samples, respectively, and their overexpression in tumor cells was associated with higher Tim3 positivity in stromal components, advanced pTNM stage and significantly impaired overall survival and disease free survival (Figure 2), while the expression of PD-L1 (3.8%, locally) in tumor cells and CTLA4 (2.2%, in stromal cells) is low and does not correlate with survival. Co-expression of B7-H4 and IDO1 was found in 49.1% studied cases, suggesting their important role in immune suppressive microenvironment.

Figure 1 - 1166
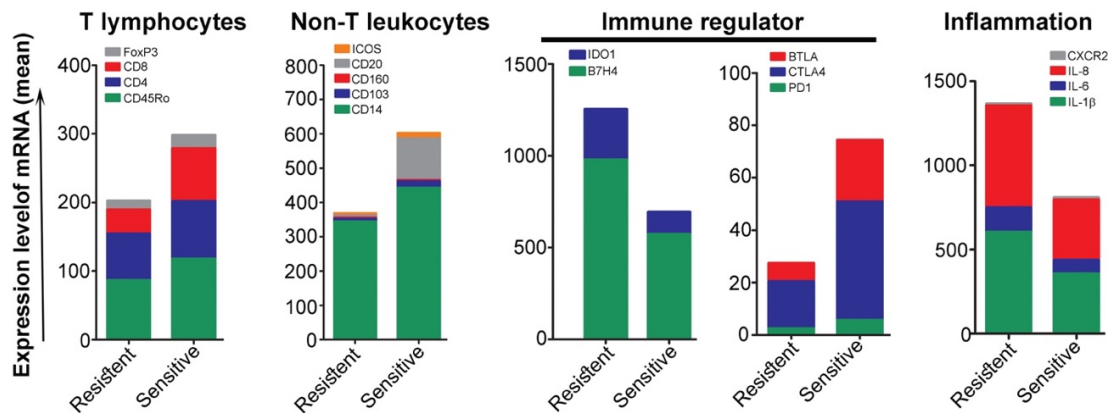
Figure 2 - 1166
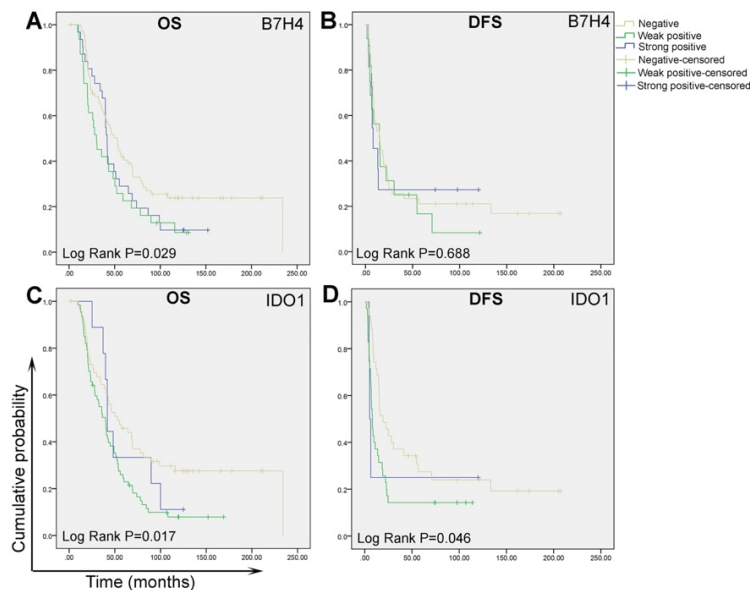
Conclusions: B7-H4 and IDO1 may present novel targets for immune therapy in ovarian cancer.

1167   Comprehensive Genomic Characterization of Primary Ovarian Mucinous Carcinoma

Carlos Parra-Herran[1], Sharon Nofech-Mozes[1], Jasmina Uzunovic[2], Fabien Lamaze[2], Ilinca Lungu[2], Carolyn Ptak[2], Bernard Lam[2], Paul Krzyzanowski[2], Aurelia Busca[3], Dina Bassiouny[1], Jane Bayani[2], Philip Awadalla[2], John Bartlett[2]
[1]Sunnybrook Health Sciences Centre, University of Toronto, Toronto, ON, [2]Ontario Institute for Cancer Research, Toronto, ON, [3]EORLA- University of Ottawa, Ottawa, ON

Background: Compared to other types of ovarian cancer, primary ovarian mucinous carcinoma (pOMC) is rare and underrepresented in molecular ovarian cancer studies. Our main goal was to study the genetic profile of pOMC using next generation sequencing in order to integrate this entity into our current molecular-based classification and pathogenesis models for ovarian cancer.

Design: Whole exome sequencing of tumor and normal tissue was performed in 40 cases with confirmed diagnosis of pOMC after secondary review of archival material and clinical information (pre- and post-surgery) to exclude metastases. Patient outcome was recorded. Through a multi-step bioinformatics approach, prevalent single nucleotide variations (SNVs), insertions and deletions (indels) and affected pathways were identified.

Results: Median patient age was 54 years (range 17-86). Most cases were FIGO stage I (33, 82%) at presentation; remaining were stage II (4, 10%) or III (3, 7%). A high spectrum of mutations was identified (Figure 1). Mutational burden was on average 94 mutations / case (range 19-300). Prevalent mutations included *KRAS* (70%); *TP53* (60%); *FLG* (15%); *CDKN2A, TNN* and *MYO15A* (12% each); *RNF43, RNF213* and *POLE* (10% each). *KRAS* and *TP53* mutations coexisted in 14 (35%) lesions. A total of 311 genes, mutated in 2 or more tumors, were used for pathway network analysis. Pathways recurrently affected included NCAM, cadherin and Wnt signaling, extracellular matrix organization, DNA damage and Beta1 integrin cell surface interactions. Around 60% of the genes identified in these pathways are known to be involved in oncogenesis. With a median follow-up of 40 months (mean 47, range 1-169), adverse events were documented in 4 (10%) patients. None of the SNVs identified correlated with adverse outcome.

Figure 1 - 1167
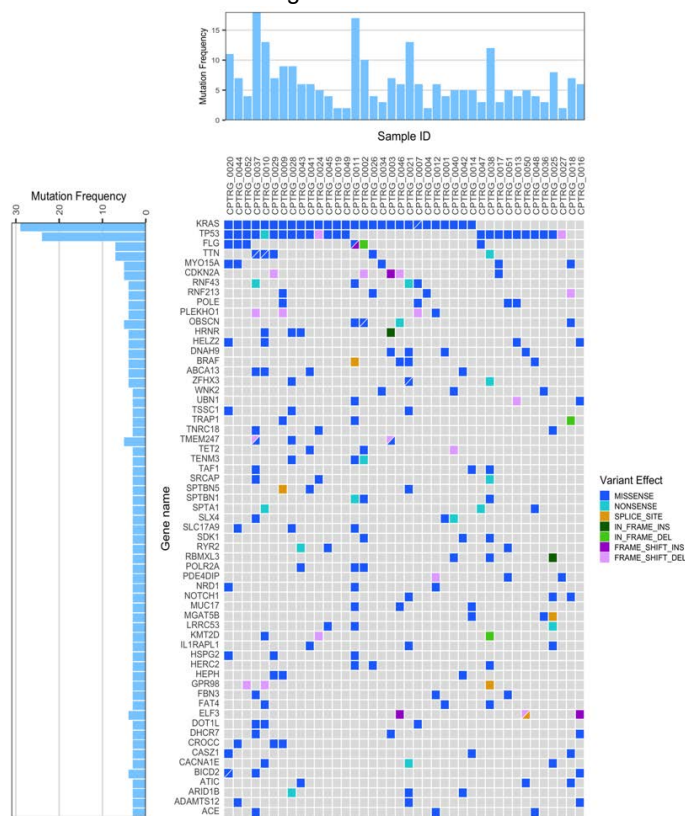
Conclusions: The mutational landscape of pOMC is heterogeneous, with predominance of *KRAS* and *TP53* mutations as peviously reported by other groups. Although no single mutation of oncogenic pathway was predominant in our sample, we identified several alterations that can help elucidate the pathogenesis of pOMC and potentially separate this tumor from its mimickers. It provides a rationale to examine the role of new targeted therapies against *KRAS* in advanced mutated pOMC. The prognostic and predictive role of gene sequencing in this tumor type remains to be fully characterized.

1168 Immunohistochemical Predictors of Aggressive Endometrial Adenocarcinoma from Low Grade Biopsy Specimens

Danielle Petty[1], Omer Hassan[1], Harrison Martin[1], Antonio de las Morenas[1]
[1]Wake Forest Baptist Medical Center, Winston-Salem, NC

Disclosures: Danielle Petty: None; Omer Hassan: None

Background: International Federation of Gynecology and Obstetrics (FIGO) grades for endometrial adenocarcinoma are based on % solid tumor and are used along with measures such as myometrial invasion >50% for surgical planning (grade 3 or >50% invasion generally undergo extensive pelvic and/or para-aortic lymph node dissection). Though a morbid procedure, thorough sampling provides prognostic and therapeutic guidance. Low-grade biopsies lead to limited nodal sampling, though resection specimens sometimes reveal a higher grade or more invasive lesion than anticipated. Quality predictors for aggressive lesions would improve patient care.

Increased immunohistochemical (IHC) human epididymis protein 4 (HE4) expression has been associated with increased clinical stage in endometrial adenocarcinoma. High Ki67 is also generally associated with more aggressive neoplasms. We hypothesized these markers would help predict high-grade processes for proper surgical intervention.

Design: Ten years of CoPath records were searched to identify FIGO graded endometrial biopsy specimens diagnosed as endometrioid adenocarcinoma. Extent of myometrial invasion and biopsy and resection grades were recorded. Many biopsies were consult cases; as such, obtainable cases that were upgraded and/or had >50% myometrial invasion were selected for the study group, and obtainable cases that remained grade 1 with minimal invasion were controls. Biopsy slides for both groups were examined by 4 pathologists using IHC for HE4 and Ki67. Membranous/cytoplasmic staining was considered positive for HE4; intensity was scored 1-5 (pale focal=1, moderate focal=2, moderate diffuse=3, dark focal=4, dark diffuse=5). Ki67 was scored by % nuclear positivity in neoplastic cells.

Results: 301 H&E diagnoses of FIGO graded endometrial adenocarcinoma on biopsy with corresponding resection were identified. HE4 and Ki67 IHC for 13 controls and 13 study cases were scored as outlined. Of 138 cases that remained grade 1 on resection, 23 had >50% myometrial invasion. Using univariate analysis of variance, increased HE4 staining was associated with a higher level of % invasion ($p=0.0008$) and higher resection grade ($p=0.036$). Ki67 was similarly significant with $p=0.023$ for higher % invasion and $p=0.015$ for higher resection grade.

Table 1. Biopsy and Resection FIGO Grades n (%)

		Resection Grade		
		1	2	3
Biopsy Grade	1	138 (46)	46(15)	6(2)
	2	10(3)	62(21)	14(5)
	3	0	1(0)	24(8)

Conclusions: Intensity of HE4 staining of endometrial glands and elevated Ki67 on endometrial biopsy specimens can aid in predicting that a FIGO grade 1 endometrial adenocarcinoma may exhibit more aggressive features than anticipated.

1169 Nodal Metastasis Detection in Endometrial Carcinoma with Microcystic, Elongated, and Fragmented Pattern is Markedly Increased by Cytokeratin Immunostaining

Kimmie Rabe[1], Sayak Ghatak[2], Irina Stout[2], Britt Erickson[2], Mahmoud Khalifa[1]
[1]University of Minnesota - Twin Cities, Minneapolis, MN, [2]University of Minnesota, Minneapolis, MN

Disclosures: Kimmie Rabe: None; Sayak Ghatak: None; Irina Stout: None; Irina Stout: None; Britt Erickson: None; Mahmoud Khalifa: None

Background: While there is growing acceptance of sentinel lymph node biopsy in the staging and management of endometrial carcinoma, there are currently no universal guidelines for processing and pathologic examination of lymph nodes in this setting. The microcystic, elongated, and fragmented (MELF) pattern of myoinvasion in endometrial carcinoma has been associated with an increased risk of lymph node metastasis. Our aim is to assess the need for cytokeratin immunohistochemical (IHC) stains in detecting nodal metastasis, sentinel and non-sentinel, in the MELF setting with a focus on isolated tumor cells (ITCs).

Design: From the 2009-2019 pathology database of our institution, we recovered 18 cases of FIGO grade 1 endometrial carcinoma with a MELF pattern of myoinvasion. Three cases were excluded from the study since no lymphadenectomy was performed. A total of 15 hysterectomy specimens with lymphadenectomy, 3 sentinel, 1 sentinel and non-sentinel, and 11 non-sentinel, were identified. Lymph nodes removed were pelvic and para-aortic. All H&E stained slides from lymph nodes were reviewed and negative nodes were subjected to cytokeratin AE1/AE3 IHC stains. All cytokeratin-positive lymph nodes were subsequently stained for calretinin to exclude the possibility of mesothelial inclusions.

Results: Of the 15 cases of endometrial carcinoma, 5 cases (33%) had positive lymph nodes based on H&E stained sections at the time of their initial diagnosis. With the addition of IHC stains, 4 previously negative cases were found to have positive non-sentinel lymph nodes. This included 3 cases with newly discovered ITCs and one case with ITCs and a micro-metastasis. Therefore, this cohort went from 5/15 (33%) positive lymph nodes to 9/15 (60%) with the addition of IHC. Additionally, IHC staining revealed more areas of non-sentinel metastases in 2 cases that were initially node-positive. In one of these patients, 3 additional micro-metastases were found.

Figure 1 - 1169
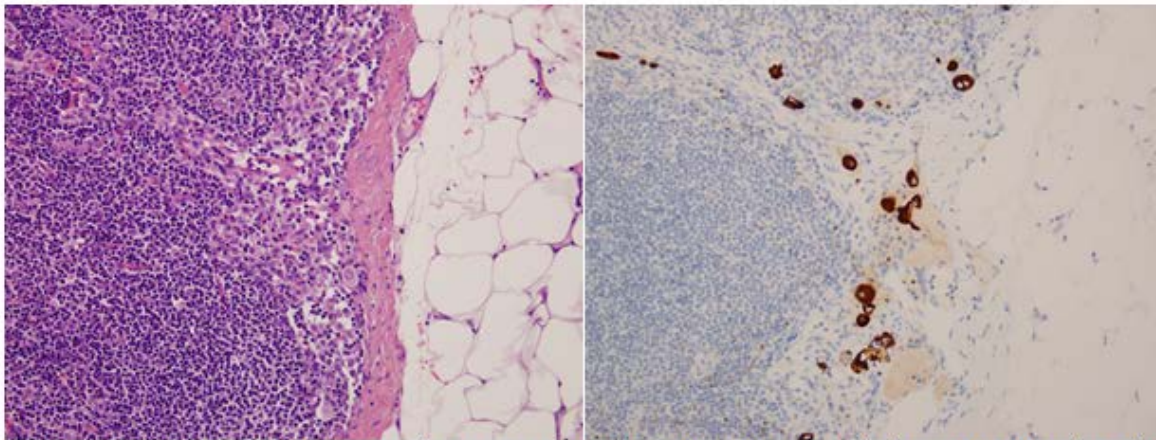
Figure 1 H&E stain of lymph node (left) and isolated tumor cells in the subcapsular sinus highlighted by cytokeratin AE1/AE3 immunohistochemical stain (right).

Conclusions: Cytokeratin IHC staining of lymph nodes is important since it nearly doubled the detection rate of lymph node metastases in our sample of women with MELF pattern of myoinvasion. While we work toward accepted guidelines for lymph node sampling and handling in endometrial carcinoma, immunohistochemical stains should be routinely performed on MELF positive cases in order to detect occult lymph node metastases.

1170 ConCerv: A Prospective Trial of Conservative Surgery for Low-Risk Early Stage Cervical Cancer-Assessment of Pathologic Parameters

Preetha Ramalingam[1], Rene Pareja[2], Aldo Lopez[3], Jose Fregnani[4], Andre Lopes[5], Myriam Perrotta[6], Audrey Tsunoda[7], Lois Ramondetta[1], Tarinee Manchana[8], David Crotzer[9], Orla McNally[10], Martin Riege[11], Julian Di Guilmi[12], Gabriel Rendon[13], Bryan Fellman[1], Maria Delia Perez Montiel[14], Jose Manuel Carvajal[15], Giovanni Scambia[16], Robert Coleman[1], Kathleen Schmeler[1]
[1]The University of Texas MD Anderson Cancer Center, Houston, TX, [2]Clinica de Oncologia Astorga, Esmeraldal, Antioquia, Colombia, [3]Instituto Nacional de Enfermedades Neoplásicas, Lima, Peru, [4]A.C.Camargo Cancer Center, Liberdade, Sao Paulo, Brazil, [5]Instituto Brasileiro de Controle do Cancer, São Paulo, SP, Brazil, [6]Hospital Italiano de Buenos Aires, Buenos Aires, Argentina, [7]Hospital Erasto Gaertner, Curitiba, PR, Brazil, [8]Chulalongkorn University, Bangkok, Bangkok, Thailand, [9]Nebraska Methodist Hospital, Omaha, NE, [10]Royal Women's Hospital, Parkville, VIC, Australia, [11]Instituto de Ginecologia, Rosario, Santa Fe, Argentina, [12]Hospital Britanico de Buenos Aires, Buenos Aires, Argentina, [13]Instituto de Cancerologia, Medellin, Antioquia, Colombia, [14]Instituto Nacional de Cancerologia, Mexico City, DF, Mexico, [15]General Hospital Doctor Alfredo Punarejo H., Matamoros, Tamaulipas, Mexico, [16]Policlinico Gemelli, Rome, Italy

Disclosures: Preetha Ramalingam: None; Rene Pareja: None; Andre Lopes: None; Audrey Tsunoda: *Speaker*, Roche; *Speaker*, Astra Zeneca; Tarinee Manchana: None; Gabriel Rendon: None; Bryan Fellman: None; Maria Delia Perez Montiel: None; Kathleen Schmeler: None

Background: The standard of care for early stage cervical cancer is radical hysterectomy (RH) or radical trachelectomy (RT) in women desiring future fertility. A multi-institutional study was performed to prospectively evaluate the safety, feasibility and oncologic outcomes of conservative surgery in women with early stage cervical cancer. The aim of this analysis is to characterize the pathologic features by central review of this cohort, and determine its impact on eligibility and outcomes.

Design: A prospective, multicenter study evaluated conservative surgery (either cone or simple hysterectomy with lymph node (LN) assessment) in 100 eligible women with FIGO (2009) stage IA2 or IB1 cervical cancer. Pathologic parameters that would result in ineligibility include 1) high grade non-squamous cell carcinoma (SCC) or adenocarcinoma histology; 2) lymphovascular invasion (LVI); 3) change in pathologic stage, 4) absence of invasive carcinoma. Initial pathology review was performed at participating sites with central pathology review (CR) determining final eligibility.

Results: Of the 100 cases 48 were SCC and 52 were adenocarcinoma. Discrepancy in one or more pathologic parameters was noted in 45 cases (26%) of 169 enrolled patients (24 opted out for other reasons). Discrepancies altered eligibility in a subset of patients. Histologic discrepancy (1 adenosquamous carcinoma; 1 mixed SCC and neuroendocrine carcinoma, 1 adenoid basal carcinoma (ABC) and 5 CIN-3), and definite/suspicious for LVI (15 cases, 8%) made pts ineligible. 5 cases were downgraded from SCC (3 IB1, 1 1A1, 1 1A2, to CIN-3), 8 had pathologic stage downgraded to IA1 (5 from IB1 and 3 from IA2) and making pts. ineligible for study. 4 cases were downgraded from 1B1 to 1A2 and 5 cases were upgraded from IA2 to IB1 but neither excluded eligibility.

Conclusions: Pathologic review is critical to determine eligibility for conservative surgery. CR altered eligibility of ~20% of the total cases enrolled for conservative surgery in cervical cancer. The most important reasons for discrepancies of pathologic review from participating centers and CR included 1) distinguishing LVI from retraction artifact, 2) identifying non-squamous histology or unusual tumors such as ABC, and 3) overcalling CIN-3 involving endocervical glands as invasive carcinoma. Differences in measurement of horizontal extent due to presence of CIN3 involving glands or AIS and/or depth of invasion did not affect eligibility.

1171 Next Generation Sequencing in Peritoneal versus Pleural Mesotheliomas-Commonalities and Differences

Preetha Ramalingam[1], Richard Yang[1], Barrett Lawson[1], Elizabeth Euscher[1], Anais Malpica[1]
[1]The University of Texas MD Anderson Cancer Center, Houston, TX

Background: Peritoneal and pleural mesotheliomas (MM) are typically high grade malignancies with tendency for poor outcomes. In the current targeted therapy era, few molecular targets have thus far been identified in these tumors. The aim of this study is to elucidate the spectrum of molecular changes in a cohort of pleural and peritoneal MM with emphasis on differences in these two patient populations and correlation with outcomes.

Design: 70 cases of pleural (37) and peritoneal (33) MM, who had molecular testing were identified (2008 to 2019). All cases were confirmed by immunohistochemical staining at the time of original diagnosis. The following data was collected: patient (pt) age, gender, histologic subtype, next generation sequencing (141 gene Oncomine AmpliSeq panel) and outcome. Follow up was available in 68 pts. Kaplan Meier curves and Fisher's exact tests were performed in GraphPad Prism v8.1.2.

Results: Pleural MM: 26 (70%) male (M) and 11 (30%) female (F); mean age at presentation (AAP) 67yrs (range, 26-84). Peritoneal MM: 20 F (60%), 13 (40%) M; AAP 55 yrs (range, 3-77). 56 were epithelioid MM (80%), 9 sarcomatoid (13%) and 5 (7%) biphasic. Molecular alterations (MA) in pleural MM: NF2 16/37 (43%), TP53 12/37 (32%), BAP1 11/37(30%), miscellaneous (FANCD2, SETD2, SF3B1, FANC1 FGFR1, NOTCH3M ERBB4, FBXW7) 14/37(38%), no mutations (muts) 7/37 (19%); 67% of pts. with no muts. died of disease (DOD) and 50% of pts. with muts. DOD. 50% of F pts. DOD in 5 yrs. compared to 54% of M pts. Pleural pts showed higher rates of NF2 muts. (p<0.0001). MAs in peritoneal MM: no muts. 19/33 (58%); TP53 4/33 (12%), BAP1 4/33(12%), NF2 0/33 (0%), miscellaneous (VHL, CSF1R, MAX, PIK3CS, FGFR3, MET, MDM2, TET2); 14/37(38%). Only 21% of pts. without muts. DOD, however, 69% of pts. with muts DOD. 32% of F pts. DOD within 5 yrs. compared to 46% of M pts. Peritoneal MM had improved overall (OS) (p=0.0084) and disease free survival (DFS) (p=0.0006).

Characteristics	Pleural	Peritoneal
Number of cases	N=37	N=33
Age, mean (range)	67 (26-84)	55 (3-77)
Male: Female	2.36:1	1.53:1
No mutation	7 (19%)	19 (58%)
NF2	16 (43%)	0 (0%)
TP53	12 (32%)	4 (12%)
BAP1	11 (30%)	4 (12%)
Misc. mutations	14 (38%)	8 (24%)
>1 mutation	13 (35%)	3 (9%)
Dead of Disease with mutations	50%	69%
Dead of Disease without mutations	67%	21%

Figure 1 - 1171

Figure 1

A

Hazard Ratio (Mantel-Haenszel)	A/B	B/A
Ratio (and its reciprocal)	2.851	0.3507
95% CI of ratio	1.309 to 6.212	0.1610 to 0.7640

OS peritoneal vs pleural

Pleural (n=36)
Peritoneal (n=33)

P value 0.0084

B

Hazard Ratio (Mantel-Haenszel)	A/B	B/A
Ratio (and its reciprocal)	2.656	0.3765
95% CI of ratio	1.521 to 4.636	0.2157 to 0.6573

DFS peritoneal vs pleural

Pleural (n=36)
Peritoneal (n=33)

P value 0.0006

Figure 2 - 1171

Figure 2

Test	Fisher's exact test
P value	<0.0001
P value summary	****

NF2 vs Site

Pleural
Peritoneal

NF2 Mutated   NF2 Wildtype
NF2 Mutation Status

Conclusions: NGS testing showed important difference between pleural and peritoneal MM. Pleural MM has a high frequency of somatic muts. with NF2 being the most common; however, there was no association of mut. status with clinical outcome. In contrast peritoneal MM has a much lower mut. rate however, pts. with muts. are more likely to DOD within 5yrs. Pleural MM have worse OS and DFS compared to peritoneal MM, independent of mut. status. There appears to be no significant gender differences in either pleural or peritoneal MM.

1172   Evaluation of HPV RNA In-Situ Hybridization (ISH) and p16 Immunohistochemistry (IHC) Concordance in Endocervical Adenocarcinomas

Hezhen Ren[1], Jennifer Pors[2], Christine Chow[3], Monica Ta[3], Simona Stolnicu[4], Robert Soslow[5], David Huntsman[6], C. Blake Gilks[7], Lynn Hoang[1]
[1]University of British Columbia, Vancouver, BC, [2]Vancouver, BC, [3]Genetic Pathology Evaluation Centre, Vancouver, BC, [4]University of Medicine, Pharmacy, Sciences and Technology, Targu Mures, Mures, Romania, [5]Memorial Sloan Kettering Cancer Center, New York, NY, [6]British Columbia Cancer Research Institute, Vancouver, BC, [7]Vancouver General Hospital, Vancouver, BC

Background: The concordance between high-risk human papillomavirus (HR-HPV) infection and p16 (a cyclin dependent kinase inhibitor and surrogate biomarker for HR-HPV) has been well-documented in squamous neoplasms of the uterine cervix and head and neck. Few studies, however, have assessed the concordance in glandular neoplasms of the uterine cervix. Recent studies have shown 5 cases of

p16 positive gastric-type cervical adenocarcinomas but most were HPV negative by DNA testing. Therefore, the study aims to examine the concordance of p16 with HPV RNA ISH in endocervical adenocarcinoma, including a larger set of gastric-type.

Design: p16 and HPV-ISH concordance was assessed in endocervical adenocarcinomas using a tissue microarray, and equivocal staining was repeated using whole sections. p16 IHC was scored as positive if there was diffuse, strong cytoplasmic and nuclear staining. HPV RNA in-situ hybridization was performed using ACD RNAscope and scored positive if there was dot-like nuclear staining.

Results: We included 113 endocervical adenocarcinomas, grouped by the IECC: 94 HPVA (HPV-associated) cases (63 usual-type, 4 intestinal, 4 villoglandular, 1 iSMILE, 22 mucinous NOS), 18 NHPVA (non-HPV-associated) cases (9 gastric, 4 minimal deviation, 5 mesonephric), and 1 adenocarcinoma NOS. p16-HPV-ISH was concordant in 107 (95%) cases and histotype was concordant with HPV status in 100 (88%) cases. In the discordant cases, 5 were initially diagnosed as HPVA mucinous NOS by morphology, but were p16+/HPV- or p16-/HPV- and therefore re-classified as NHPVA mucinous NOS. On review, these cases did not exhibit classic features of HPVA (i.e. apical mitoses, apoptotic bodies). 1 other case was initially diagnosed as NHPVA gastric but was p16+/HPV+. Histology of this case showed hybrid features and it was re-classified as HPVA mucinous NOS. 3 cases of NHPVA gastric-type had equivocal HPV-ISH (exhibited odd background stromal staining), and p16 was negative in 1 and patchy in 2. These 3 cases were likely HPV negative (HPV-PCR pending). 5 HPVA were p16-/HPV-, despite classic HPV histology.

	Number of Cases	IECC Classification	
P16+/HPV+ (concordant)	87	86 HPVA	61 Usual-type 3 Mucinous, intestinal-type 17 Mucinous NOS 4 Villoglandular 1 iSMILE
		1 NHPVA	1 Gastric
P16-/HPV- (concordant)	20	5 HPVA	2 Usual-type 1 Mucinous, intestinal-type 2 Mucinous NOS
		14 NHPVA	5 Gastric-type 5 Mesonephric 4 Minimal deviation
		1 Adenocarcinoma NOS	
P16+/HPV- (discordant)	3	3 HPVA	3 Mucinous NOS
P16-/HPV+* (discordant)	3	3 NHPVA	3 Gastric-type
Excluded	16	12 Post-treatment	
		1 Metastasis	
		2 Adenosquamous	
		1 Technical/Missing	
Total	129 (113 included)		
*Odd background staining, likely HPV negative by PCR			

Conclusions: Most p16-ISH and histotype-HPV discordant cases were mucinous (mucinous NOS and gastric-types). In HPVA and NHPVA mucinous cases, pathologists should exercise caution in looking for classic HPV-related histologic features. Ambiguous cases may warrant referral for HPV-ISH or PCR (in equivocal HPV-ISH cases, such as gastric-types). Histology alone accurately predicts IECC group in 100/113 (88%) of cases.

1173   International Endocervical Adenocarcinoma Criteria and Classification (IECC): An Independent Cohort with Clinical and Molecular Relevance

Hezhen Ren[1], Noorah Almadani[2], Jennifer Pors[2], Julie Ho[3], Christine Chow[4], Kay Park[5], Simona Stolnicu[6], Robert Soslow[5], David Huntsman[7], C. Blake Gilks[8], Lynn Hoang[1]
[1]University of British Columbia, Vancouver, BC, [2]Vancouver, BC, [3]Vancouver Coastal Health, Vancouver, BC, [4]Genetic Pathology Evaluation Centre, Vancouver, BC, [5]Memorial Sloan Kettering Cancer Center, New York, NY, [6]University of Medicine, Pharmacy, Sciences and Technology, Targu Mures, Mures, Romania, [7]British Columbia Cancer Research Institute, Vancouver, BC, [8]Vancouver General Hospital, Vancouver, BC

Background: The IECC was a multi-institutional collaborative effort published in 2018 to provide a morphologic, etiologic (HPV-status) and clinically meaningful classification framework for endocervical adenocarcinomas. In this study, we re-examine the IECC using an independent cohort of cases and provide further molecular insights using targeted next generation sequencing (NGS).

Design: Consecutive cases of endocervical adenocarcinomas were collected from a single institution and classified into the IECC categories using morphologic, p16 immunohistochemistry (IHC) and HPV in-situ hybridization (ISH) data. Clinical information was collected and NGS was performed encompassing 33 known cancer genes.

Results: We included a total of 112 cases, 90 HPVA (HPV-associated: 64 usual, 4 intestinal, 4 villoglandular, 1 iSMILE, 17 mucinous NOS) and 22 NHPVA (non-HPV-associated: 12 gastric/minimal deviation, 5 mesonephric, 5 mucinous NOS). Patients in the NHPVA group had worse progression free survival (PFS, HR: 10.86; p<0.001) and worse overall survival (OS, HR: 14.65; p<0.001), compared to the HPVA group (Figures 1 and 2). 71 cases had sufficient tissue for NGS. The HPVA group had a higher number of somatic mutations (29/55, 53%) compared to the NHPVA (6/16, 38%). *STK11* was unique to the NHPVA group, while *PIK3CA* and *GNAS* were confined to the HPVA group. NHPVA had more frequent *TP53* mutations. *KRAS* and *PIK3CA* were not identified in any of the gastric/minimal deviation carcinomas. *ERBB2* was seen in a minor portion of HPVA and NHPVA, which may have therapeutic implications.

| IECC	Subtype	KRAS	PIK3CA	TP53	GNAS	ERBB2	STK11	BRAF	MET	AKT1	ROS1	IDH2
HPVA (n=91)	Usual (n=40)	10* (25%)	10* (25%)	2 (5%)	5 (13%)	2* (5%)		1 (3%)	3 (8%)	1 (3%)	1 (3%)	1 (3%)
	Intestinal (n=2)				1 (50%)							
	Villo-glandular (n=4)	2 (50%)	1 (25%)		1 (25%)				1 (25%)			
	Mucinous NOS (n=9)	1 (11%)				2 (22%)						
NHPVA (n=19)	Gastric/ Minimal Deviation (n=10)			2 (20%)		1 (10%)	1 (10%)					
	Mesonephric (n=5)	1 (20%)		2 (40%)								
	Mucinous NOS (n=1)											
*One case had multiple mutations in the same gene												

Figure 1 - 1173
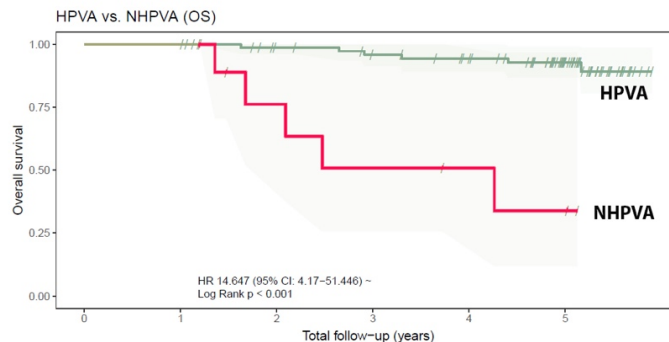
Figure 2 - 1173
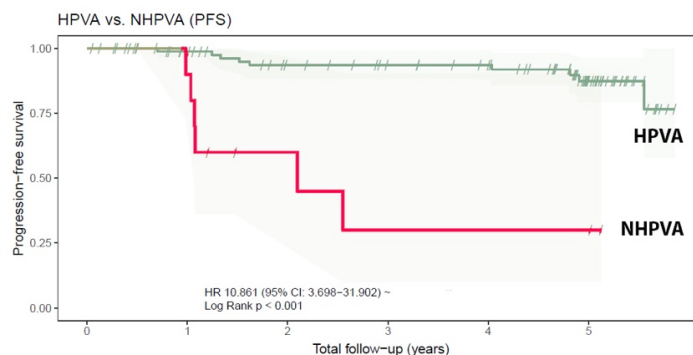
Conclusions: Our study reconfirms the clinical relevance of the IECC framework, with NHPVA tumors having worse OS and PFS compared to the HPVA. While the molecular landscape of the HPVA and NHPVA did mostly overlap, there were some differences: HPVA

had a higher number of somatic mutations, *STK11* mutations were confined to NHPVA, *PIK3CA* and *GNAS* were confined to HPVA. While *KRAS* mutations are common in mucinous carcinomas in general, our limited number of NHPVA gastric types did not harbor *KRAS* mutations.

1174 SATB2 Overexpression in a Subset of High-Grade Endometrial Stromal Sarcomas

Armando Reques[1], Ursula Acosta[2], Luisa Sofía Silva Alcoser[1], Ana Aula Olivar[3], Santiago Ramon Y Cajal[1], Ángel García[1], Josep Castellvi[1]
[1]Vall d'Hebron University Hospital, Barcelona, Spain, [2]Hospital Universitari Vall d'Hebron, Barcelona, Spain, [3]Vall d'Hebron University Hospital (HUVH), Barcelona, Spain

Background: Endometrial stromal sarcoma (ESS) accounts for <10% of uterine sarcomas. Nowadays, it can be classified according to the degree of differentiation in two grades: low grade (LG-ESS) and high grade (HG-ESS). In some high-grade cases it is not possible to demonstrate its differentiation and are classified as undifferentiated uterine sarcoma (UUS). The identification of molecular alterations is fundamental in the classification of sarcomas including ESS. Rearrangements of BCOR fusions have been identified in some types of sarcomas such as small round cell tumors, and classify ESS in a specific subtype. In the same way, SATB2 detection is useful for classification of some sarcomas and its overexpression correlates with BCOR in some of them.

Design: We have reviewed 37 consecutive cases of ESS diagnosed in our hospital between 2001 and 2019, and tissue microarrays were constructed. The grade of the ESS, lymphovascular invasion, lymph node metastasis, the presence of recurrences and the survival time were recorded. Immunohistochemistry for CD10, cyclin D1, SATB2 and BCOR was performed.

Results: In our series, we found 19 LG-ESS (51%), 4 of them showed endometrioid-type glands, and 18 HG-ESS (49%). In the immunohistochemical study, 3 HG-ESS cases showed BCOR nuclear overexpression (16%) and 5 HG-ESS cases (28%) had SATB2 nuclear expression [Figure 1]. None of these SATB2 positive cases showed overexpression of BCOR, but in 4 of them, cytoplasmic expression of BCOR was observed. None of the LG-ESS cases, showed BCOR or SATB2 expression. Aside from the relation with BCOR and SATB2 expression with high-grade ESS, we have not found any correlation with other clinico-pathological features.

Figure 1 - 1174
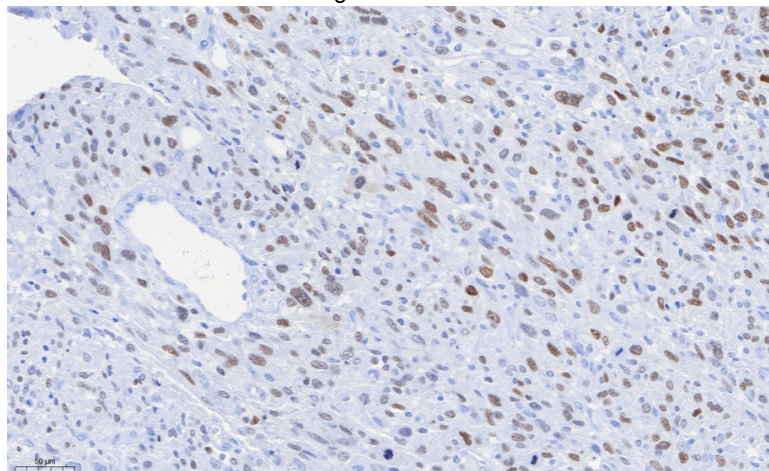
Conclusions: We have identified a subgroup of high-grade ESS with SATB2 expression that has not been described previously, and it accounts for the 28% of cases in our series. Interestingly, we have found no correlation with BCOR expression and, surprisingly, a BCOR cytoplasmic immunoreactivity was observed in these cases, that it has not been described previously. More studies are needed to elucidate the clinical and prognostic relevance of this subgroup of ESS.

1175 Digital Quantification of PHH3 and KI-67 in Characterization of Uterine Smooth Muscle Tumors

Jesus Rico Castillo[1], Joanna Chan[1], Dan DeCotiis[2], Connie Cao[1]
[1]Thomas Jefferson University Hospital, Philadelphia, PA, [2]Einstein Medical Center

Disclosures: Jesus Rico Castillo: None; Joanna Chan: None

Background: Uterine smooth muscle tumors (USMT) are the most common lesion of the female genital tract and occur in nearly 40% of women older than 35 years of age. USMT are classified as leiomyosarcoma (LS), smooth muscle tumors of uncertain significance (STUMP), symplastic leiomyoma (SYM) or benign leiomyoma (LM) based on atypia, necrosis, and mitotic count. Visual assessment of mitotic count is time consuming and subject to misinterpretation. In this study we correlate classification of USMT and mitotic count to digital quantification of mitosis specific marker PHH-3 and proliferation marker KI-67.

Design: 17 LMS, 5 STUMP, 8 SYM, 2 atypical leiomyoma (AL) and 7 LM were reviewed. 50 high powered fields ($5mm^2$) were visually analyzed for mitotic count (MC). Standard staining for PHH3 and Ki-67 was done on one section from each case. Three $65mm^2$ areas were selected for digital analysis of PHH3 and Ki-67 in each case. The PHH3 and Ki-67 counts were correlated to each other, to MC, and to the diagnosis. Data was analyzed with R statistical programing language. Correlation analysis was done using Pearson correlation tests, group analysis was done using one way ANOVA.

Results: Digital quantification of PHH3 is significantly different between LMS compared to STUMP and SYM (p=0.006). Digital quantification of Ki-67 is significantly different between LMS, STUMP, SYM, and LM (p<0.01). Using ROC curves, KI-67 is a more sensitive and specific discriminator than MC. There is no statistically significant correlation between MC and PHH3 or between MC and Ki-67. On a total sample basis, there is also no significant correlation between digital quantification of PHH3 and Ki67.

Conclusions: Accurate assessment of proliferation is crucial in diagnosis of USMT. Visual analysis of mitotic index is time consuming and subjective. Fast, objective measurement of proliferation can be done using digital quantification of proliferation markers such as PHH3 and Ki-67. This study suggests that digital quantification with PHH3 or Ki-67 may be a viable alternative to visual assessment of counting mitoses. Visual analysis of mitotic figures and digital quantification with Ki-67 can discriminate between all classifications of USMTs, however digital quantification of KI-67 is more sensitive and specific. Digital quantification of PHH3 can reliably detect LMS compared to other USMT with atypia such as STUMP and SYM. Further studies include correlating digital quantification of PHH-3 and Ki-67 with clinical outcomes.

1176 Associations between Patterns of Intraluminal Tumor Cell Involvement in SEE-FIM Examined Tubes and Endometrial Carcinoma Characteristics and Outcomes

Monica Rodriguez[1], Ashley Felix[2], Mary Anne Brett[3], Goli Samimi[4], Mark Sherman[5], Maire Duggan[3]
[1]Cumming School of Medicine, University of Calgary, Calgary, AB, [2]The Ohio State University, Columbus, OH, [3]University of Calgary, Calgary, AB, [4]National Cancer Institute, Bethesda, MD, [5]Mayo Clinic, Jacksonville, FL

Disclosures: Monica Rodriguez: None; Mary Anne Brett: None; Maire Duggan: None

Background: Endometrial carcinoma cells in the fallopian tube lumen (Intraluminal Tumor Cells-ILTCs) are associated with non-endometrioid histotypes and higher stage. In the absence of mural invasion (FIGO stage 3A), their prognostic role is controversial. The impact of SEE-FIM examination on the detection of ILTCs and associations with clinico-pathological features and outcomes are unknown.

Design: Glass slides of tubes from 50 non-endometrioid and 222 endometrioid carcinomas were independently reviewed by 2 pathologists to categorize ILTCs as; 1) floating in the lumen, 2) attached to the mucosa, 3) size, 4) stroma present, and 5) mural invasion. Disagreements were reviewed by a third pathologist and final status was based on agreement between any 2. Clinical, pathological, and outcome variables were extracted from the cancer centre data base. Chi-square tests compared characteristics of women stratified by ILTC categories (floating vs. attached to the mucosa). Significant variables (p<0.05) were included in a multivariable logistic regression model. Kaplan–Meier estimates and log-rank tests compared survival distributions according to ILTCs. Cox proportional regression estimated multivariable-adjusted hazard ratios (HRs) and 95% confidence intervals (CIs).

Results: ILTCs were present in 56 (15.1%); 55 floating, 24 attached to the mucosa, 36 had more than 50 cells, 24 had stroma, and 35 (62.5%) had mural invasion. ILTCs floating in the lumen or attached to the mucosa were non-significantly more common among women age ≥ 55 years, and being overweight or obese. Detection of carcinoma cells in tubes was significantly associated with FIGO stage 3/4, LVI, myometrial invasion of 50% or more, and a non-endometrioid histotype. Of 345 women with follow-up, 34 (9.8%) died of their disease. Identification of ILTCs was non-significantly associated with higher mortality {HR1.64 (95% CI= 0.74-3.63)} and the association was further attenuated when adjusted for stage and histotype. There was insufficient data to analyze outcome by category of ILTCs.

Conclusions: Approximately 15% of SEE-FIM examined tubes demonstrated ILTCs and similar to other studies, ILTCs were associated with higher stage and non-endometrioid histotypes. A prognostic effect independent of stage and histotype was not found in this limited dataset. Analysis of larger series is needed to more definitively assess whether ILTCs are an independent prognostic factor.

1177   A First and Second Line Marker Panel for the Distinction of Clear Cell from Endometrioid Carcinoma of the Ovary: Implications for Mismatch Repair Deficiency Testing

Monica Rodriguez[1], Jonathan Slack[2], Martin Kobel[3]
[1]Cumming School of Medicine, University of Calgary, Calgary, AB, [2]Alberta Health Services, Calgary, AB, [3]University of Calgary/Alberta Public Laboratories, Calgary, AB

Disclosures: Monica Rodriguez: None; Jonathan Slack: None; Martin Kobel: None

Background: Distinction between ovarian clear cell carcinoma (CCC) and endometrioid carcinoma (EC) is critical because CCCs have poor response to platinum-based therapies and ECs are universally screened for Lynch syndrome. Recent studies have identified problems with reproducibility in cases with ambiguous morphology. Our goal was to establish an efficient and accurate immunohistochemical (IHC) panel for the distinction of CCC from EC.

Design: Cases with a confirmed diagnosis of EC (N=183) or CCC (N=164), each represented by 3 cores in four tissue microarrays (TMAs), were obtained from the Alberta Ovarian Tumor Type (AOVT) tumor bank. From the literature, we identified 8 markers with discriminatory potential. IHC expression was categorized dichotomously (absent vs. present); except for HNF1B (>50% moderate intensity), and CTNNB1 (only nuclear staining was considered positive). Nominal logistic regression modeling (NLMR), hierarchical clustering and recursive partitioning were used to evaluate marker combinations.

Results: Using NMLR, 5 markers (HNF1B, PR, Napsin A, CDX2, and AMCAR) contributed significantly to the prediction with an area under the curve of 0.995, correctly classifying 95% of cases. Using the top 3 markers (HNF1B, PR, Napsin A), supervised hierarchical clustering of the 8 possible combinations demonstrated that the 2 prototypical combinations, combined accounting for 76% of total cases, were 100% accurate in predicting either CCC (Napsin A present, HNF1B diffuse, PR absent, N=132, 38%) or EC (Napsin A absent, HNF1B non-diffuse, PR present, N=129, 38%). The remaining 83 cases (24% of total), had equivocal IHC combinations and as such required additional workup. Recursive partitioning in this group was further able to correctly classify 69/83 cases using the hormone response marker KIAA1324, CDX2 and AMACR. Mismatch repair deficiency (MMRd) was lower in cases of CCC with a prototypical IHC profile (2%) than in prototypical EC (12%) or cases with equivocal immunohistochemistry (13%).

	CCC N=163	EC N=183	Difference
PR present	6.1%	86.8%	80.7%
Napsin A present	92.1%	11.5%	80.6%
HNF1B diffuse	92.7%	13.3%	79.4%
KIAA1324 present	14.2%	89.4%%	75.2%
ER present	15.4%	87.4%	72%
CDX2 present	3.7%	56.4%	52.7%
CTNNB1 nuclear	1.2%	46.5%	45.3%
AMCAR present	83.3%	42.2%	41.1%

Conclusions: A first line panel consisting of Napsin A, HNF1B, and PR can accurately distinguish CCC and EC in three-quarters of cases. The remaining equivocal combinations required additional, second-line biomarkers. MMR deficiency in prototypical CCC is low; universal testing is not warranted. However, carcinomas with non-prototypical Napsin A, HNF1B and PR combinations had a similar rate of MMR deficiency as prototypical EC, and should also be tested for Lynch syndrome.

1178   Ovarian Clear Cell Carcinoma: Analysis of POLE Mutations, p53 and DNA Mismatch Repair Protein Expression

Juan Rong[1], Charles Quick[2], Krisztina Hanley[3], Farnaz Hasteh[1], Somaye Zare[1], John Thorson[1], Oluwole Fadare[1]
[1]University of California San Diego, La Jolla, CA, [2]University of Arkansas for Medical Sciences, Little Rock, AR, [3]Emory University, Atlanta, GA

Disclosures: Juan Rong: None; Charles Quick: None; Krisztina Hanley: None; Farnaz Hasteh: None; Somaye Zare: None; John Thorson: None; Oluwole Fadare: None

Background: The Cancer Genome Atlas (TCGA) molecular classification of endometrial carcinoma has provided a valuable framework for prognosticating patients with endometrial cancers, and may ultimately direct management. The aim of this study is to determine, using a TCGA surrogate classifier, whether TCGA-like subgroups are discernible in ovarian clear cell carcinoma (OCCC).

Design: 47 archived cases of OCCC were retrieved from three institutions. Cases were required to show characteristic morphology as well as Napsin A immunoreactivity. Representative formalin-fixed paraffin-embedded blocks that harbored at least a 40% tumor load were selected for DNA extraction. PCR for *POLE* exons 9 and 13, which cover the hotspot mutations (P286R and V411L) in endometrial carcinoma, was performed; PCR amplicons were confirmed by gel electrophoresis, followed by direct Sanger sequencing. Immunohistochemical studies for p53, MSH6, MSH2, MLH1 and PMS2 were performed on the corresponding sections.

Results: The mean age at diagnosis for the 47 patients was 55 years (range: 31 to 84 years, median 55 years). 49% had accompanying endometriosis. Mean tumor size at excision was 12 cm (range: 1-25). 26, 3 and 18 cases were FIGO stage I, II and III respectively. None of the 30 cases wherein *POLE* sequencing was completed demonstrated mutations in exon 9 or 13. A single nucleotide variance (rs56367014) with no known functional significance was detected in one case. None of the 47 cases showed loss of MSH6 or MSH2 expression; one case showed loss of PMS2 and MLH1 expression. This case was p53-wild type. A p53 mutation-type staining pattern was present in 6 (12.8 %) cases (4 null and 2 overexpression). At a mean follow-up of 44 months (range: 0-181, median 31 mo), both p53 mutation-type staining and FIGO stage were significantly associated with worse overall survival on multivariate analysis (Cox regression: p53, p=0.025; Stage I vs II/III, p=0.007).

Conclusions: In this cohort of OCCC, we identified no case with a hotspot *POLE* mutation, and the group showed a low (2.1%) frequency of DNA MMR deficiency. p53 mutation-type staining was found in 12.8% and may be of adverse prognostic significance. Therefore, the full quartet of TCGA-like molecular subclasses of endometrial carcinoma are not present in OCCC, and surrogate classifiers may not be ideally applicable to this histotype. Future studies may help to define whether the improved prognostication in OCCC is achieved by simply subclassifying them based on p53 status.

1179 Does Specimen Type Have an Impact on HER2 Status in Endometrial Serous Carcinoma?
Douglas Rottmann[1], Nana Matsumoto[2], Hisham Assem[3], Serena Wong[2], Pei Hui[4], Natalia Buza[4]
[1]Yale School of Medicine, Hamden, CT, [2]Yale New Haven Hospital, New Haven, CT, [3]Yale School of Medicine, New Haven, CT, [4]Yale University School of Medicine, New Haven, CT

Background: A recent clinical trial showed prolonged progression-free survival in HER2-overexpressing endometrial serous carcinomas (ESC) when trastuzumab was added to traditional cisplatin-based chemotherapy. Approximately one third of ESC are HER2 positive, and recent studies identified significant intratumoral heterogeneity of HER2 overexpression and/or amplification in over 50% of HER2 positive cases. We aimed to evaluate the concordance of HER2 status between endometrial curettage and subsequent hysterectomy specimens in ESC.

Design: Patients diagnosed with ESC between 2014-2018 at our institution with available tumor tissue from endometrial curettage and hysterectomy specimens were included. H&E slides were reviewed to confirm the diagnosis and select representative tissue blocks. HER2 immunohistochemistry (IHC) (EP3 clone) was performed on a selected block from both specimen types in each case. HER2 FISH has been evaluated on a subset of cases. HER2 immunostaining was evaluated for intratumoral heterogeneity and HER2 scores were assigned using a modified version of the 2007 ASCO/CAP breast cancer guidelines. The HER2 immunohistochemical score and HER2 status were compared between the two specimen types.

Results: A total of 42 cases were included in the final analysis. Fourteen cases (14/42, 33%) were HER2 positive on the hysterectomy, including eight cases of 3+ IHC and six cases with 2+ IHC and amplification on FISH. The HER2 status of the curettage and hysterectomy was concordant (both HER2 positive or negative) in 95% of cases (40/42), with identical HER2 IHC scores in 64% (27/42) of tumors. The two cases with discordant HER2 status were both positive on the curettage (3+ IHC, and 2+ IHC with FISH amplification) and negative on the hysterectomies (1+ IHC in both cases). Intratumoral heterogeneity of HER2 staining was appreciated in 10 tumors (23%), including one of the two discordant cases.

HER2 IHC Score	Curettage/Biopsy (n=42)	Hysterectomy (n=42)
0	7	6
1+	8	15
2+	18	13 (6 FISH amplified)
3+	9	8

Table. HER2 IHC of biopsy/curettage and hysterectomy specimens.

Conclusions: The concordance rate of HER2 status between the two specimen types of ESC is high (95%). All discordant cases in our cohort were HER2 positive on endometrial curettage and HER2 negative on hysterectomy, while no reverse change in HER2 status was noted. Given the frequent heterogeneity of HER2 expression in ESC, the potential for a spatially more heterogeneous sampling of endometrial cavity in curettage may provide a possible explanation for our findings. HER2 testing of ESC performed on endometrial curettage may help identify a greater proportion of patients eligible for trastuzumab therapy.

1180 Molecular Landscape of HPV Negative Vulvar Squamous Cell Carcinoma including NOTCH Alterations

Abeer Salama[1], Amir Momeni Boroujeni[2], Chad Vanderbilt[3], Robert Soslow[1]
[1]Memorial Sloan Kettering Cancer Center, New York, NY, [2]Memorial Sloan Kettering Cancer Center, Brooklyn, NY, [3]Memorial Sloan Kettering Cancer Center, Denver, CO

Disclosures: Abeer Salama: None; Amir Momeni Boroujeni: None; Chad Vanderbilt: *Consultant*, Docdoc. ltd. (Singapore); *Consultant*, Paige AI; Chad Vanderbilt: *Consultant*, Docdoc. ltd. (Singapore); *Consultant*, Paige AI; *Consultant*, OncoKB; Robert Soslow: *Speaker*, Ebix/Oakstone

Background: Vulvar squamous cell carcinoma can be HPV driven or alternatively can occur independently of HPV (HPV Neg VSCC) and in the setting of differentiated vulvar intraepithelial carcinoma. The latter often harbors TP53 mutations, however, there is only limited information about other molecular alterations. The aim of this study is to characterize the molecular landscape of HPV Neg VSCC.

Design: All HPV Neg VSCC cases from a single institution that underwent targeted hybrid capture next generation sequencing panel were evaluated; HPV status was determined using mRNA ISH for high risk HPV as well as bioinformatically through off-target capture DNA sequenced by the NGS panel. Clinicopathologic data were evaluated.

Results: 14 HPV Neg VSCC cases were sequenced. The most common genomic alterations were TP53 mutations (93%, n=13), TERT promoter mutations (85.7%, n=12), NOTCH pathway alterations (71%, n=9), CDKN2A (deep deletion or mutation) (50%, n=7), FAT1 mutations (43%, n=6), JAK3 (21%, n=3), and PIK3CA mutations (14%, n=2). 11q gain was also seen (2 cases) but only in the setting of NOTCH alterations. All patients suffered a recurrence. Overall survival was adversely affected by NOTCH alterations (P value 0.04), even in the setting of FIGO stage I disease.

Figure 1 - 1180

Overall Survival Kaplan-Meier Estimate
- Cases with Alteration(s)
- Cases without Alteration(s)
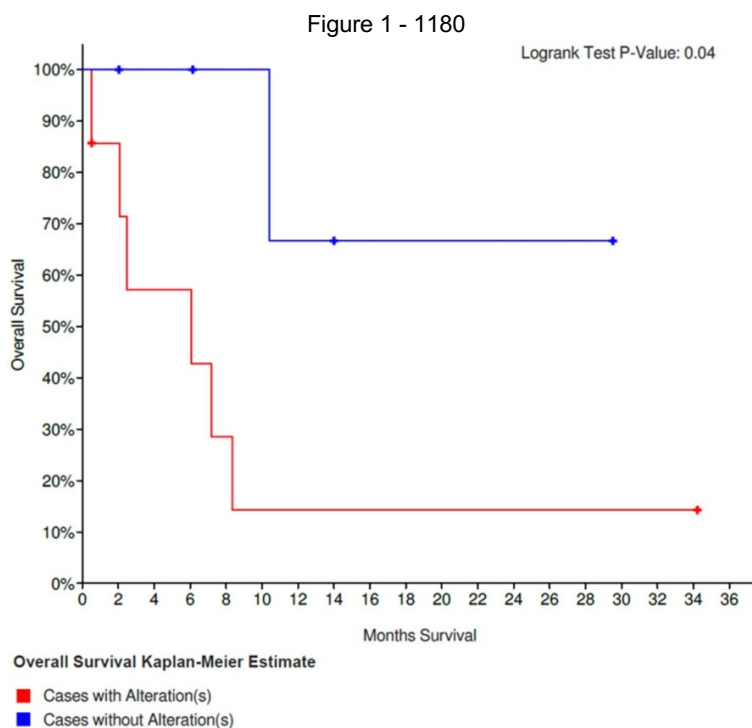
Conclusions: HPV Neg VSCC tumorogenesis differs from HPV driven vulvar squamous cell carcinomas with TP53 and TERT alterations being the main drivers. However, it appears NOTCH pathway alterations play an important role in tumor progression with tumors harboring these alterations having worse clinical outcomes. This is a novel finding.

1181 Clinicopathologic Analysis of Necrosis in Ovarian Fibromas: Frequency, Pathology, and Clinical Outcomes

Christine Salibay[1], Somaye Zare[2], Oluwole Fadare[2]
[1]University of California San Diego Health, La Jolla, CA, [2]University of California San Diego, La Jolla, CA

Disclosures: Christine Salibay: None; Somaye Zare: None; Oluwole Fadare: None

Background: Most fibromas of the ovary display characteristic macroscopic and morphologic features, and accordingly pose minimal to no diagnostic difficulty. However, we have encountered occasional fibromas that display necrosis, with associated alterations that deviate from the typical appearances of the neoplasm. In this study, we report findings from an institutional review of necrosis in ovarian fibromas.

Design: A review of clinicopathologic records was performed on 95 fibromatous ovarian neoplasms, including 75 ovarian fibromas, 15 fibrothecomas, 4 cellular fibromas, and 1 mitotically active cellular fibroma (MACF). Clinical and pathologic data were collected from cases showing necrosis of any extent or type.

Results: Necrosis was identified in 15% (14/95) of all cases, including 13%(10/75) of typical fibromas. Infarcted and non-infarcted fibromas showed no significant differences in patient age and tumor size. Torsion was clinically suspected in 2%. Grossly, the cut surfaces of infarcted fibromas were described as solid (93%), pedunculated (29%), cystic (43%), white or yellow (64%) and reddish (14%). As determined microscopically, the proportion of tumor that was necrotic ranged from 12 to 97% (mean 54.6%). Necrotic zones showed complete devitalization of tumor cells and lesional vessels (7%), "ghost" outlines of tumor cells (21%) or both. The demarcation between the necrotic and viable areas were sharp (14%), indistinct (57%) or in some tumors, both. The areas adjacent to necrosis showed no increased mitotic activity, and infarcted fibromas as a group were no more mitotically active than non-infarcted fibromas. None showed cytologic atypia. Other common features in infarcted fibromas include edema (72.2%), hemorrhage (55.6%), hemosiderin (72.2%), calcifications (66.7%), hyalinization (66.7%), and histiocytic aggregates (33.3%). Only 2 cases showed coagulative necrosis of the type that is characteristic of malignant smooth muscle neoplasia: one fibrothecoma [associated with Meigs syndrome] and a MACF. None of the patients with follow-up have experienced a recurrence.

Conclusions: A subset of otherwise typical fibromas show necrosis. Although the necrosis may distort the gross and microscopic appearances of fibromas, they typically retain their characteristic features in the viable areas. Awareness of the potential for fibromas to display necrosis may prevent their misclassification as "atypical" or even malignant, especially during intraoperative assessments.

1182 Expression of Immune Checkpoint Regulators, Cytotoxic T Lymphocyte Antigen 4 (CTLA-4), Programmed Death-Ligand 1 (PD-1/PD-L1), and Indolaimine-2, 3-Deoxygenase (IDO) in Uterine Mesenchymal Tumors

Alireza Samiei[1], Itsushi Shintaku[2], Jennifer Katzenberg[3], Neda Moatamed[4]
[1]Department of Pathology and Laboratory Medicine, David Geffen School of Medicine at UCLA, Los Angeles, CA, [2]University of California Los Angeles, Los Angeles, CA, [3]San Diego, CA, [4]David Geffen School of Medicine at UCLA, Los Angeles, CA

Disclosures: Alireza Samiei: None; Itsushi Shintaku: None; Jennifer Katzenberg: None; Neda Moatamed: None

Background: Immune checkpoint inhibitors such as cytotoxic T lymphocyte antigen 4 (CTLA-4) and programmed death 1/ programmed death-ligand 1 (PD-1/PD-L1), in combination with the immunosuppressive molecule indolaimine-2, 3-deoxygenase (IDO), have recently emerged as effective candidate treatments against a range of human malignancies. Here, we have investigated their expression in the uterine mesenchymal tumors.

Design: We assessed CTLA-4, PD-1, PD-L1, and IDO expression on paraffin embedded tissue blocks, comprising of 11 uterine leiomyomas, 17 uterine leiomyosarcomas (LMS), 8 recurrent/ metastatic uterine LMS, and 8 endometrial stromal sarcomas (ESS). Immunohistochemical (IHC) staining with PD-L1 (SP142), PD-1 (Nat105), CTLA-4 (F8) and IDO (ab106134) antibodies were performed. The IHC was classified as positive when staining was present in the following pattern: PD-L1: cell membrane of the tumor (Figure 1A), PD-1: cell membrane of peri/intra tumoral lymphoid cells (Figure 1B), CTLA-4 and IDO: strong granular cytoplasmic reactions of the tumor cells (Figure 1C & 1D, respectively).

Results: Table 1 summarizes the frequency of PD-L1, PD-1, CTLA-4, and IDO positivity in uterine mesenchymal tumors. PD-L1 was positive in 29% (5/17) of uterine LMS, 63% (5/8) of recurrent/metastatic LMS, and 13% (1/8) of ESS. PD-1 was positive in 24% (4/17) of uterine LMS, 38% (3/8) of recurrent/metastatic LMS, and 13% (1/8) of ESS. CTLA-4 was positive in 18% (3/17) of uterine LMS, 38% (3/8) of recurrent/metastatic LMS, and 13% (1/8) of ESS. IDO was positive in 6% (1/17) of uterine LMS, 38% (3/8) of recurrent/metastatic LMS, and none of ESS. Leiomyomas had no expression of the aforementioned molecules.

Table 1. Summary of the immunohistochemistry reactions in the tumors					
	n	PD-L1	PD-1	CTLA-4	IDO
Uterine leiomyoma	11	0 (0%)	0 (0%)	0 (0%)	0 (0%)
Uterine leiomyosarcoma	17	5 (29%)	4 (24%)	3 (18%)	1 (6%)
Uterine leiomyosarcoma, recurrent/metastatic	8	5 (63%)	3 (38%)	3 (38%)	3 (38%)
Endometrial stromal sarcoma	8	1 (13%)	1 (13%)	1 (13%)	0 (0%)

Figure 1 - 1182
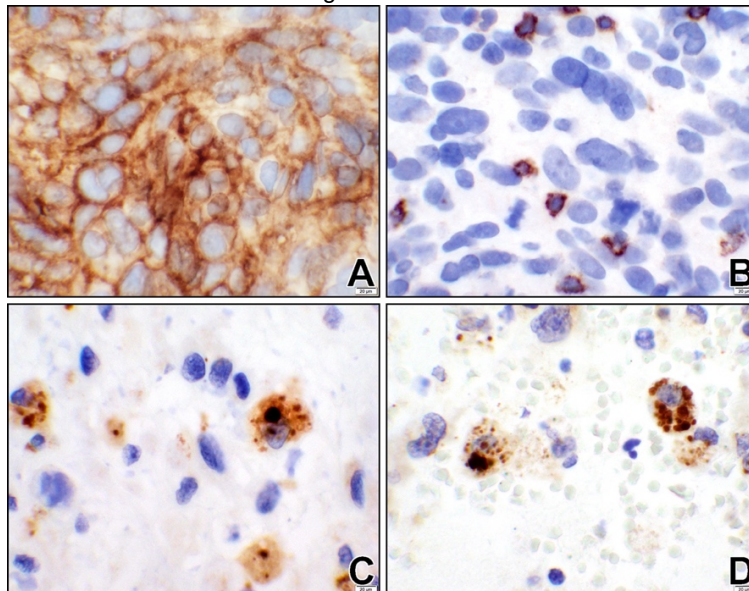
Conclusions: We report that a noticeable number of uterine and recurrent/metastatic LMS, as well as a small percentage of ESS, demonstrate PD-L1, PD-1, and CTLA-4 expression. A smaller percentage of uterine and recurrent/metastatic uterine LMS also express IDO. The highest expression was seen in metastatic/recurrent LMS. Our findings provide support for the use of immune checkpoint inhibitors in the malignant uterine mesenchymal tumors.

1183 Clear Cell Carcinoma of Uterine Cervix: A Clinicopathologic Review and Molecular Characterization

Sanaz Sanii[1], Niki Esfahanian[2], Blaise Clarke[3], Joerg Schwock[4], Liat Hogen[5], Kathy Han[5], Stephanie Lheureux[5], Nicole Park[5], Tracy Stockley[6], Marjan Rouzbahman[7]
[1]University Health Network, St. John's, NL, [2]McMaster University, Hamilton, ON, [3]University of Toronto, Toronto, ON, [4]University Health Network, University of Toronto, Toronto, ON, [5]University Health Network, Toronto, ON, [6]Genome Diagnostics University Health Network, Toronto, ON, [7]Toronto, ON

Disclosures: Sanaz Sanii: None; Niki Esfahanian: None; Blaise Clarke: None; Joerg Schwock: None; Liat Hogen: None; Kathy Han: None; Nicole Park: None; Tracy Stockley: None; Marjan Rouzbahman: None

Background: Clear cell carcinoma of uterine cervix (CCCUC) is a rare variant of cervical adenocarcinoma unrelated to Human Papilloma Virus (HPV) unlike most primary malignancies of cervix. With a global trend towards HPV testing instead of cytology for the purpose of cervical cancer screening, prevention and/or early detection of the less common HPV-unrelated cervical cancer variants requires better understanding of their underlying biology.

Design: Ten CCCUCs were identified during a 15-year period. Clinicopathological characteristics were studied. Immunohistochemistry (IHC), Linear Array HPV Genotyping, and next generation sequencing (NGS) was performed in 6 cases with available material.

Results: Mean age of patients was 39.6 (range of 18-82). All presented with vaginal bleeding. Six out of ten cases were diagnosed at FIGO stage IB. Eight patients had initial surgery, with lymph nodes dissection in 7. Adjuvant therapy followed in 5 cases. One patient had neoadjuvant radiation therapy followed by surgery. One patient had only brachytherapy. Median follow up period was 38 months. Clinicopathologic findings are presented in table 1.

In 6 cases with available material, Linear Array HPV Genotyping proved negative HPV status and IHC showed wild type p53 expression, positive PAX8 and HNF1β, and negative ER/PR. MMR protein expression in IHC was intact in 4 cases. Two cases had lost/equivocal MSH2/MSH6 expression, one of which as well as other 4 cases proved negative for microsatellite instability in NGS. According to both breast cancer and gastric adenocarcinoma scoring guidelines for Her2 expression by IHC, all 6 cases showed score 2+.

NGS identified 70 gene variants across 6 CCCUC samples. Two cases had null (nonsense) variants in ATM, CHEK2, KDM5C, and KMT2C. One case had an SPOP M117V variant which has been previously reported in endometrial cancer. Overall, variants in genes with roles in apoptosis, DNA repair, cell cycle, PI3K-AKT signaling, and transcriptional regulation were identified in this data set.

Clinicopathological characteristic of clear cell carcinoma of the uterine cervix			Number of cases (total = 10)
Age	Range: 18-82 years	Age <=30	5
Distribution		Age >30	5
	Mean: 39.6 years		
	Median: 31 years		
Pap test result prior to diagnosis		Normal	2
		Abnormal (AGC)	3
		Unknown	5
Stage (FIGO)		IB	6
		IIA1	1
		IIB	2
		Unknown	1
Lymphovascular space invasion		Positive	4
		Negative	6
Lymph node metastasis at presentation		Positive	2
		Negative	8
Recurrence during follow up		Pelvic	1
		Distant	1
		Pelvic & Distant	2
		Negative	6
Patient status at the end of follow up period		Alive without disease	5
		Alive with disease	2
		Expired of disease	3
AGC: atypical glandular cells; FIGO: International Federation of Gynecology and Obstetrics			

Conclusions: Our study further elucidates the clinicopathological features of CCCUC and is the first to investigate its molecular characteristics. Potentially actionable molecular alterations were detected. Further study of CCCUC molecular profile is required to better characterize this rare malignancy and to allow development of novel diagnostic and therapeutic techniques.

1184   Massively Parallel Sequencing Analysis of Gastric-Type Cervical Adenocarcinomas Reveals Mutations in Cell Cycle-Related Genes and Rare Potentially Targetable ERBB2 Mutations

Pier Selenica[1], Barbara Alemar[1], Karen Talia[2], W. Glenn McCluggage[3], Yoshiki Mikami[4], Takako Kiyokawa[5], Britta Weigelt[1], Kay Park[1], Rajmohan Murali[1]
[1]Memorial Sloan Kettering Cancer Center, New York, NY, [2]The Royal Women's Hospital, Melbourne, VIC, Australia, [3]The Royal Hospitals, Belfast, United Kingdom, [4]Kumamoto University Hospital, Kumamoto, Japan, [5]The Jikei University School of Medicine, Minato-ku, Japan

Disclosures: Pier Selenica: None; Barbara Alemar: None; Karen Talia: None; W. Glenn McCluggage: None; Yoshiki Mikami: None; Takako Kiyokawa: None; Britta Weigelt: None; Kay Park: None; Rajmohan Murali: None

Background: Gastric-type cervical adenocarcinoma (GCA) is a clinically aggressive subtype of endocervical mucinous adenocarcinoma characterized by gastric-type mucin, lack of association with human papillomavirus (HPV) and resistance to chemo/radiotherapy. Here,

we sought to characterize the landscape of genetic alterations in a large cohort of GCAs, and to compare it to those of usual-type HPV-associated endocervical adenocarcinomas (UEAs) and adenocarcinomas of gastric and pancreatic origin, which show some morphologic overlap with GCAs.

Design: GCAs (n=79) were subjected to massively parallel sequencing targeting 410-468 cancer-related genes. Somatic mutations and copy number alterations (CNAs) were determined using validated bioinformatics methods, and statistical comparisons were evaluated with a two-tailed Fisher exact test. Mutational data for UEAs (n=21), pancreatic adenocarcinomas (PAs, n=178) and intestinal gastric adenocarcinomas (IGAs, n=148) from The Cancer Genome Atlas (TCGA) were obtained from cBioPortal.

Results: GCAs harbored a median of 4 non-synonymous somatic mutations (range 0-23) with the most frequent somatic mutations affecting *TP53* (38%), *CDKN2A* (20%), *KRAS* (18%) and *STK11* (11%). Rare, potentially targetable mutations in *ERBB2* (9%) were identified. All GCAs displayed low levels of CNAs with no recurrent high-level amplifications or homozygous deletions detected. In comparison to UEAs, GCAs harbored a higher frequency of mutations affecting cell cycle related genes including *TP53* (38% vs 4%, p<0.01) and *CDKN2A* (20% vs 0%, p=0.01); however fewer mutations in *PIK3CA* (6% vs 25%, p=0.01) were detected. In contrast, *TP53* mutations were found to be less prevalent in GCAs compared to both PAs (38% vs 56%, p<0.01) and IGAs (38% vs 57%, p<0.01). GCAs also showed a higher frequency of *STK11* mutations than PAs (11% vs 2%, p<0.01) and IGAs (11% vs 1%, p<0.01). Additionally, mutations in *ERBB2* and *ERBB3* (9% vs 1%, and 10% vs 0.5%, both p<0.01) were enriched in GCAs compared to PAs whereas *CDKN2A* and *KRAS* mutations (20% vs 1%, p<0.01, and 18% vs 6%, p<0.01) were enriched in GCAs compared to IGAs.

Conclusions: Our findings suggest that GCAs are underpinned by somatic mutations in cell cycle-related genes and in potentially targetable genes (e.g. *ERBB2*). Importantly, certain genes that are enriched for somatic mutations in GCAs such as *CDKN2A* and *STK11* could be used as biomarkers to distinguish them from other tumor types with similar histologic features.

1185   Rare Driver Mutations in the Intermediate Trophoblastic Tumors

Maryam Shahi[1], Rena Xian[1], Brigitte Ronnett[2], Deyin Xing[3]
[1]Johns Hopkins Medical Institutions, Baltimore, MD, [2]Johns Hopkins Hospital, Baltimore, MD, [3]Johns Hopkins Medical Institutions, Ellicott City, MD

Disclosures: Maryam Shahi: None; Rena Xian: None; Brigitte Ronnett: None; Deyin Xing: None

Background: Intermediate trophoblastic tumors, which include placental site trophoblastic tumor (PSTT) and epithelioid trophoblastic tumor (ETT), are uncommon, with nearly all assumed to be gestational in origin. Most occur in the uterus and those in extra-uterine sites are considered metastatic or ectopic gestational trophoblastic tumors but rare non-gestational types have been encountered. Since these tumors are relatively resistant to chemotherapy and because gestational and non-gestational types have different pathogenesis and require different therapy, identification of genetic alterations that might be amenable to pathway/molecule-based therapeutic approaches would be useful.

Design: Next-generation sequencing using a large (637) gene panel was performed using genomic DNA extracted from paraffin-embedded tumor tissues of 8 intermediate trophoblastic tumors (4 ETT, 3 PSTT, 1 ETT with choriocarcinomatous (CC) differentiation). DNA genotyping was performed on 4 ovarian tumors to determine their gestational versus non-gestational status. Clinicopathologic features were analyzed.

Results: In 6 tumors, copy number variations (CNVs) were identified, including gains of 5p,7,8q,11q,12,14,20 and losses of 2,7,8p,9,16p,19. Somatic mutations (from 2-6) were identified in 5 tumors, including oncogenic driver mutations involving EGFR, HRAS, and ERBB4 in individual tumors; however, recurrent somatic mutations were not identified (see table)

Age	Diagnosis	Site	Genotyping	Aneuploidy	CNVs	Notable mutation
25	ETT	Uterus	Presumed gestational (molar pregnancy)	Absent	None	SUFU PIK3C2B FANCC ARID1A
41	ETT	Uterus	Presumed gestational	Present	(+20)	GSK3B ECT2L TRAF5
39	ETT	Ovary	Non-gestational	Present	(+5p, maybe also +20p)	Not available
36	ETT	Ovary	Gestational	Absent	None	None
55	ETT-CC	Ovary	Gestational	Present	(+1q, +3p, CTNNB1 amp, +7, +8q, +11q, +12, +14)	HRAS CD22 PPP2R1A MLH1 PHF6 BRD4
31	PSTT	Uterus	Presumed gestational (missed abortion)	Present	(-8p,-16)	EGFR LRP1B
37	PSTT	Uterus	Presumed gestational (recent normal term pregnancy)	Present	(-2, -16p, -19)	GSK3B ECT2L TRAF5
30	PSTT	Ovary	Non-gestational	Present	possible -9p	None

Conclusions: The finding of genetic alterations involving EGFR, HRAS, and ERBB4 in some intermediate trophoblastic tumors offers the potential for individualized management strategies using pathway/molecular-based targeted therapies for treatment of these chemoresistant tumors.

1186   IDO Expression in Uterine Smooth Muscle Tumors: Implications for Immunotherapy

Elisheva Shanes[1], Lisa Friedman[2], Anne Mills[2]
[1]Northwestern University, Chicago, IL, [2]University of Virginia, Charlottesville, VA

Disclosures: Elisheva Shanes: None; Lisa Friedman: None; Anne Mills: None

Background: Immunotherapies targeting the IDO checkpoint axis have recently become available. Given the poor prognosis of uterine leiomyosarcoma (LMS) and the paucity of available therapeutic options, the potential impact of immunotherapy in this patient population may be significant. IDO expression patterns in uterine LMS, as well as in lower grade uterine smooth muscle tumors (USMT), have not been investigated.

Design: 50 USMT comprised of 22 LMS, 8 smooth muscle tumors of uncertain malignant potential (STUMP), 10 atypical leiomyomas (AL), and 9 benign leiomyomas (BL) were immunostained for IDO, CD8, and FoxP3. Tumoral IDO expression was semi-quantitatively scored by extent (negative, 1-5%, 6-10%, >10%) and IDO-positive tumor-associated immune (TAI) infiltrates were scored as absent, focal, moderate, or brisk. Endothelial cell staining with IDO was scored as absent, focal, moderate, or extensive. CD8-positive and FoxP3-positive lymphocytes were manually enumerated and averaged across 5 to 10 high-power fields. Follow-up status and therapeutic history was recorded where available.

Results: Tumor IDO expression was not seen in any smooth muscle tumors. IDO positivity was seen in TAI in 32% of LMS, 25% of STUMP, 50% of AL, and 22% of BL. IDO positivity in endothelial cells within the tumor was seen in 82% of LMS, 63% of STUMP, 70% of AL, and 67% of BL.

Tumor Type	TAI IDO+	Endothelial IDO+	Average CD8+/HPF (range)	Average FoxP3+/HPF (range)
LMS	Overall: 7 (32%) Focal: 7 (32%) Moderate: 0 (0%) Brisk: 0 (0%)	Overall: 18 (82%) Focal: 6 (27%) Moderate: 1 (5%) Extensive: 11 (50%)	90 (0 – 300)	9 (0 – 45)
STUMP	Overall: 2 (25%) Focal: 1 (13%) Moderate: 1 (13%) Brisk: 1 (13%)	Overall: 5 (63%) Focal: 1 (13%) Moderate: 3 (38%) Extensive: 2 (25%)	10 (1 – 41)	1 (0 – 8)
AL	Overall: 5 (50%) Focal: 4 (40%) Moderate: 0 (0%) Brisk: 1 (10%)	Overall: 7 (70%) Focal: 1 (10%) Moderate: 1 (10%) Extensive: 5 (50%)	10 (2 – 30)	2 (0 – 9)
BL	Overall: 1 (11%) Mild: 1 (11%) Moderate: 0 (0%) Brisk: 0 (0%)	Overall: 6 (67%) Focal: 4 (44%) Moderate: 0 (0%) Extensive: 2 (22%)	29 (2 – 165)	0 (0 – 2)

Conclusions: A significant percentage of uterine smooth muscle tumors demonstrate IDO expression in the endothelial cells of intratumoral vessels, including 82% of LMS. While 32% of LMS have IDO expression within TAIs, this is limited to only focal expression. USMTs do not express IDO in tumor cells. These data suggest that directed therapy towards IDO may have limited utility in the treatment of LMS.

1187 Low-Grade, Low-Stage Endometrioid Endometrial Adenocarcinoma: A Morphological and Molecular Study of 19 Cases

Aarti Sharma[1], Angelica Moran[1], Sahana Somasegar[1], David Chapel[2], Ricardo Lastra[1], Nita Lee[1], Lauren Ritterhouse[3], Jennifer Bennett[1]
[1]The University of Chicago, Chicago, IL, [2]Brigham and Women's Hospital, Boston, MA, [3]Massachusetts General Hospital, Harvard Medical School, Boston, MA

Disclosures: Aarti Sharma: None; Angelica Moran: None; Sahana Somasegar: None; David Chapel: None; Ricardo Lastra: None; Nita Lee: None; Lauren Ritterhouse: None; Jennifer Bennett: None

Background: Most low-grade, low-stage endometrioid endometrial adenocarcinomas (EEC) have an excellent prognosis; however recurrences occur in a small subset with several studies reporting an increase in *CTNNB1* mutations in this cohort. Herein we evaluated 19 low-grade, low-stage EECs, including 10 that recurred, to further characterize their morphological features and molecular phenotype.

Design: A retrospective cohort of 300 patients with low-grade (FIGO 1-2), low-stage (FIGO IA) EEC were identified. The medical record was reviewed to identify those with biopsy-proven recurrences. Morphologic examination of the primary and recurrent tumors was performed to confirm the diagnosis. This resulted in a total of 10 cases (R-EEC), and all primary tumors underwent next generation sequencing on a 1213 gene panel. Nine non-recurrent low-grade, low-stage EECs (NR-EECs) that had been previously sequenced were included as controls.

Results: Clinicopathological features are summarized in the table. Of all examined features, only depth of invasion was found to be significantly different (p=0.0347) between the 2 groups with deeper invasion occurring in R-EECs. Evaluation of sequencing data revealed 62 pathogenic mutations in R-EECs and 64 in NR-EECs. *ARID1A* (8/10), *PTEN* (8/10), and *FGFR2* (4/10) mutations were most frequent in R-EECs versus *PTEN* (8/9), *ARID1A* (5/9), and *PIK3CA* (5/9) in NR-EECs (Figure 1). *CTNNB1* mutations were detected in 3 R-EECs versus 1 in NR-EECs, but this difference was not significant (p=0.5820). Similarly, no other mutations were significant between the 2 groups.

Clincopathological Feature	R-EEC	NR-EEC	p-value
Age (years)	37-76 (61)	51-71 (63)	0.9822
Size (cm)	2.2-6.5 (4.0)	1.0-4.5 (3.0)	0.2108
Depth of Invasion (mm)	0-45 (15)	0-12 (3.6)	0.0347*
Pattern of Invasion	Conventional - 6	Conventional - 4	0.4965
	MELF - 3	MELF - 0	
Metaplastic Changes	6	6	0.986
Mitoses/10 HPF	0-11 (3)	0-6 (2)	0.4283
PTL	6	3	>0.9999
TILs/HPF	3-22 (13)	4-23 (14)	0.7954
Unstable Microsatellite Loci (%)	0.9-64 (18)	5-56 (26)	0.1564
R-EEC: Recurrent EEC, NR-EEC: Non-Recurrent EEC			
MELF: Microcystic, ELongated, and Fragmented, HPF: high-power fields			
PTLs: PeriTumoral Lymphocytes, TILs: Tumor-Infiltrating Lymphocytes			

Figure 1 - 1187
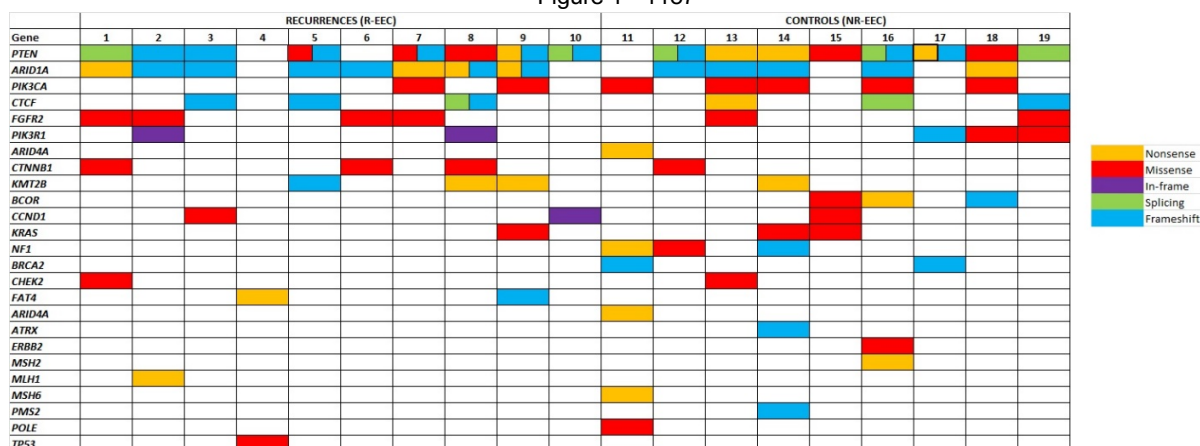
Conclusions: Unlike other studies, we did not identify *CTNNB1* mutations to be significantly associated with recurrent low-grade, low-stage EECs in our cohort. While we identified an association between deeper myometrial invasion and recurrence, our sample size is small, and this feature needs to be corroborated by larger studies. Nonetheless, while *CTNNB1* mutations contribute to recurrence in a subset of EECs, other molecular alterations and epigenetic modifications likely play an important role and remain to be elucidated.

1188 5-hmC Immunohistochemistry is a Reliable Marker for Predicting Leiomyomas with Fumarate Hydratase Mutations

Aarti Sharma[1], Erna Forgo[2], Brooke Howitt[2], Joseph Rabban[3], Karuna Garg[3], Jennifer Bennett[1]
[1]The University of Chicago, Chicago, IL, [2]Stanford University School of Medicine, Stanford, CA, [3]University of California San Francisco, San Francisco, CA

Disclosures: Aarti Sharma: None; Erna Forgo: None; Brooke Howitt: None; Joseph Rabban: *Employee*, Spouse is employee of Merck & Co.; Karuna Garg: None; Jennifer Bennett: None

Background: Fumarate hydratase deficient (FH-d) leiomyomas (LM) have characteristic morphological features, and when present can alert the pathologist to a potential *FH* germline mutation. FH immunohistochemistry (IHC) has low sensitivity/specificity and has not proven complementary to morphologic evaluation. Thus, there is a need for reliable IHC markers to supplement morphology. FH inactivation results in inhibition of demethylases and decreased levels of the epigenetic marker 5-hydroxymethylcytosine (5hmC); thus we interrogated a series of LMs with FH-d morphology for 5hmC expression.

Design: LMs with FH-d morphology (n=17) as well as conventional (n=10) and variant (n=15) LMs were stained with 5hmC. Nuclear 5hmC expression was scored semi-quantitatively (1: <10%, 2: 10-25%, 3: 26-75%, and 4: >75%) as previously published, and univariate analyses were performed.

Results: Patients with FH-d LMs had a mean age of 35 (range 27-52) vs 44 (range 29-76) years in non-FH-d LMs (p=0.0119). Overall, 13 (76%) FH-d LMs had 5hmC scores of 1-2 while all non-FH-d LMs had scores of 3-4 (p<0.0001) (Figure 1). Germline *FH* mutations were

identified in 8 of 9 patients tested (89%), all of whom had 5hmC scores of 1-2. Conversely, the patient without a germline *FH* mutation had a 5hmc score of 3. FH IHC was previously performed in 14 (82%) of FH-d LMs and was lost in 8 (57%), retained in 4 (29%), and heterogeneously expressed in 2 (14%). No correlation was noted between 5hmC and FH IHC (p=0.3044; Figure 2). Morphologic and IHC results of FH-d LMs are summarized in the table.

Case	Age	Extent of FH-d Morphology	Well Developed FH-d Morphology	Staghorn Vessels	Alveolar Edema	Chain-Like Nuclei	Bizarre Nuclei	Eosinophilic Cytoplasmic Inclusions	Nucleoli/ Halos	5hmc Score	FH IHC	Germline FH Status
1	31	Focal	+	+	+	+	+	+	+	1	Het	+
2	28	Diffuse	+	+	+	+	+	+	+	1	Ret	+
3	30	Diffuse	-	+	+	+	-	+	+	1	Ret	+
4	30	Diffuse	+	+	+	+	-	+	+	1	Lost	+
5	43	N/A	N/A	N/A	N/A	N/A	N/A	N/A	N/A	1	Lost	NP
6	31	Diffuse	+	+	+	+	-	+	+	1	Lost	+
7	29	Diffuse	-	+	+	+	-	+	+	1	NP	NP
8	35	Diffuse	+	+	+	+	+	+	+	1	Lost	NP
9	33	Diffuse	+	+	+	-	+	+	+	1	Lost	+
10	27	Diffuse	+	+	-	-	-	-	+	1	Ret	NP
11	44	Diffuse	+	+	+	-	-	+	+	1	Lost	NP
12	34	Diffuse	+	+	+	+	+	+	+	2	Het	+
13	39	Diffuse	+	+	+	+	+	+	+	2	Lost	+
14	44	N/A	N/A	N/A	N/A	N/A	N/A	N/A	N/A	3	Ret	NP
15	52	Focal	+	+	+	-	+	+	+	3	Lost	-
16	47	Focal	-	+	-	-	-	+	+	4	NP	NP
17	37	Focal	-	+	-	-	+	+	+	4	NP	Pending
+ = Present, - = Absent, NP = not performed, N/A = not available, Het: Heterogenous, Ret: Retained												

Figure 1 - 1188

5hmC Expression in Leiomyomas

Figure 2 - 1188

Association Between 5hmC and FH IHC
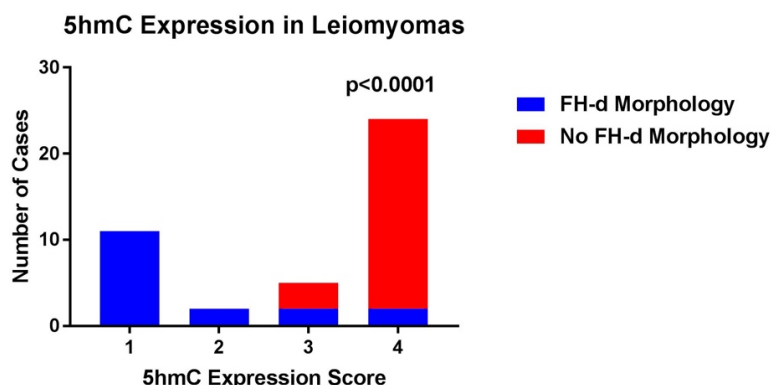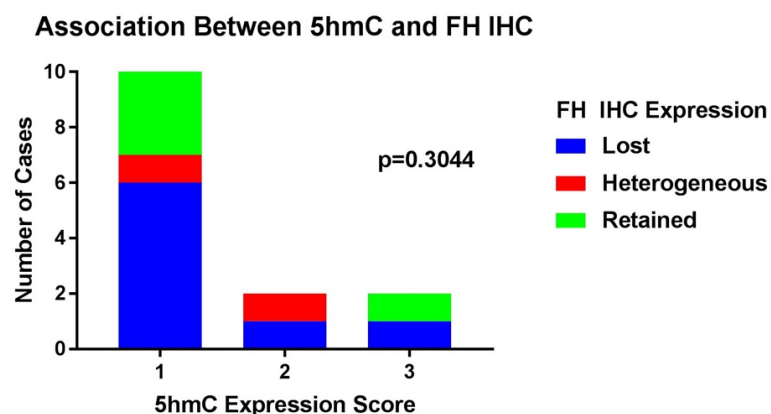
Conclusions: LMs with FH-d morphology are significantly associated with low 5hmC expression ($\leq$ 25% staining) compared to conventional and variant LMs. As FH IHC is unreliable, this study supports a role for 5hmC as an adjunct to morphology in triaging patients for genetic testing. Additional studies evaluating 5hmC in LMs with known somatic *FH* mutations are in process.

1189 Immunohistochemistry for MDM2 is a Useful Tool in the Diagnosis of Malignant Brenner Tumors?

Sindhu Shetty[1], Amy Joehlin-Price[1], Omar Habeeb[1]
[1]Cleveland Clinic, Cleveland, OH

Disclosures: Sindhu Shetty: None; Amy Joehlin-Price: None; Omar Habeeb: None

Background: Malignant Brenner tumors (MBT) are typically diagnosed in the setting of a high grade carcinoma with transitional cell morphology and the presence of a benign Brenner tumor (BBT) in the background. While MBT are rare, there is no marker that permits diagnosis of MBT with certainty outside of this specific histologic scenario. MDM2 amplification was recently reported as part of a massive parallel sequencing study on a small number of MBT. This is significant not only for diagnostic purposes, but also shows potential for targeted therapy, as MDM2 inhibitors are being tested in early clinical trials for multiple tumor types with MDM2 amplification. Immunohistochemistry for MDM2 is widely available and is a candidate immunohistochemical (IHC) stain to aid in the diagnosis of MBT.

Design: We performed MDM2 IHC on whole sections of 4 MBT, 2 borderline Brenner tumors (BLBT), 25 BBT, and 22 epithelial ovarian tumors, most of which exclusively or in part showed transitional cell morphology. Additionally, MDM2 IHC was performed on triplicate core tissue microarrays (TMAs) containing 204 cases of high grade serous carcinomas (HGSC) and 52 high grade urothelial carcinomas (HGUC). MDM2 IHC was considered positive with diffuse (>50%) nuclear reactivity; in cases of patchy staining (20-50% nuclear reactivity) MDM2 was considered equivocal. Less than 20% of cells staining positively was considered negative. In equivocal cases, MDM2 FISH is pending.

Results: Three MBT showed diffuse nuclear reactivity for MDM2. One MBT showed patchy nuclear reactivity, with up to 50% of cells staining in some areas, and is interpreted as equivocal. It is of note, however, that this MBT demonstrates more typical architecture of a BLBT and was diagnosed as a MBT secondary to cytology. One BLBT showed patchy nuclear reactivity and was interpreted as equivocal, and the other BLBT was negative (<5% nuclear reactivity). While rare nuclei showed positivity in 9/25 BBT (<5% of cells), all 25 BBT are negative for MDM2. Whole sections of epithelial ovarian carcinoma with transitional cell morphology, as well as all HGSC and HGUC in TMA sections, are also negative for MDM2.

Conclusions: Diffuse MDM2 expression is 75% sensitive and 100% specific for MBT. MDM2 IHC was not useful in the two cases of BLBT. IHC expression of MDM2 can therefore be a useful diagnostic tool in identifying MBT. Although it requires further study, this finding suggests that MBT may be a candidate for targeted molecular therapy.

1190 Evaluation of Dual MMR IHC and MSI PCR Testing for Gynecologic Cancers

Marie Smithgall[1], Helen Remotti[2], Mahesh Mansukhani[2], Susan Hsiao[3], Helen Fernandes[4], Xiaolin Liu-Jarin[2]
[1]New York-Presbyterian/Columbia University Medical Center, New York, NY, [2]Columbia University Medical Center, New York, NY, [3]New York-Presbyterian/Columbia University Medical Center, Flushing, NY, [4]Columbia University, New York, NY

Disclosures: Marie Smithgall: None; Helen Remotti: None; Mahesh Mansukhani: *Speaker*, Promega; Susan Hsiao: None; Helen Fernandes: None; Xiaolin Liu-Jarin: None

Background: A subset of gynecologic cancers harbor mutations in DNA mismatch repair (MMR) genes, including both germline (Lynch Syndrome) and sporadic cases. Both immunohistochemistry (IHC) of MMR proteins or MSI (microsatellite instability) testing by PCR can be used to detect MMR deficient (dMMR)/MSI-High (MSI-H) tumors which may benefit from treatment with immune checkpoint inhibitors. Recent recommendations from the European Society for Medical Oncology (ESMO), suggest that molecular tests be used for confirmatory analysis of MMR. This study reviewed MMR/MSI test results in gynecologic cancers to evaluate their correlation.

Design: The pathology case database at a large academic medical center was queried to identify gynecological cancer cases between 1/1/2014 and 8/9/2019 with both IHC for MMR proteins and MSI PCR analysis. Cases were reviewed to determine the concordance rate between these methods. Discordant cases were re-reviewed by 2 pathologists, blindly and independently.

Results: 206 gynecologic cancer cases (173, 84% endometrial) with both IHC MMR and MSI results were identified (178 primary and 28 metastatic cases). There were 201 (97.6%) concordant cases. 157 (76.2%) cases were microsatellite stable (MSS) with preserved MMR (pMMR) and 44 (21.4%) cases were MSI-H with dMMR, for three of these cases their MSI status was confirmed with next generation sequencing (NGS). Three endometrial cases (1.4%) showed dMMR but were MSS. For all three, IHC was performed on the initial biopsy and MSI on the resection. IHC re-testing performed on the resection concurred with the original biopsy showing dMMR for MLH1 and PMS2. Two endometrial cases (1.0%) showed pMMR but were MSI-H. For one, IHC was performed on an initial biopsy and MSI on the resection. IHC on the resection showed pMMR. The other case showed clear geographic heterogeneity within the tumor with distinct dMMR and pMMR areas. MSI testing performed on the dMMR area alone, was positive.

Figure 1 - 1190
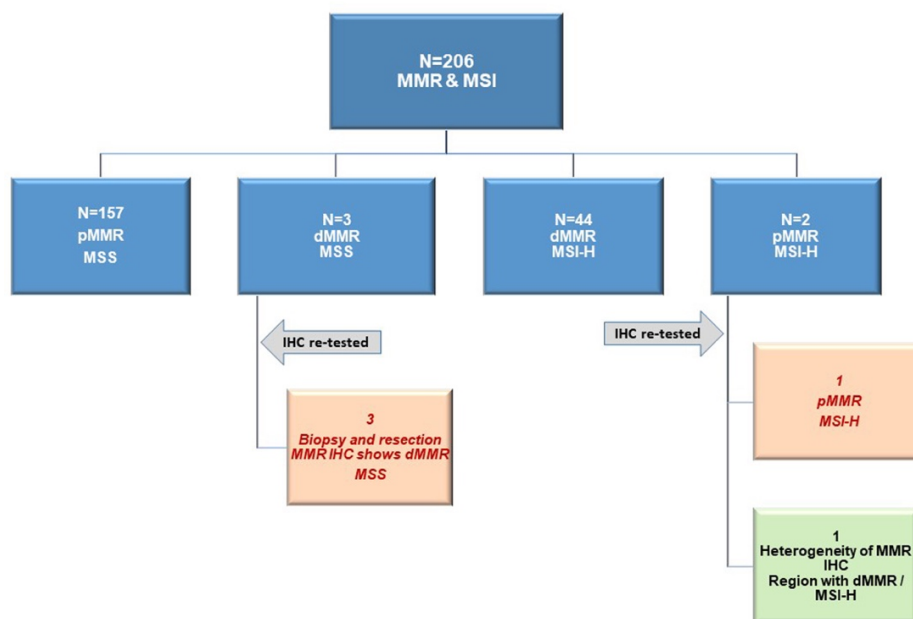
Conclusions: Concordance between MMR IHC and MSI testing among gynecologic cancers was high (98%). Three dMMR cases that were MSS and one case of a MSI-H tumor with pMMR IHC were discordant. Our results highlight the benefit of dual testing with MSI PCR and MMR IHC. Further investigation on the heterogeneity of MMR IHC expression may help understand the importance of appropriate sampling for molecular testing.

1191 Significance of Immunotyping by CD8 and PD-L1 Immune Checkpoint Inhibitor in Epithelial Ovarian Carcinoma

Radhika Srinivasan[1], Akriti Bansal[1], Manish Rohilla[1], Bhavana Rai[1], Arvind Rajwanshi[1], Vanita Suri[1], Subhas Saha[2]
[1]Postgraduate Institute of Medical Education & Research, Chandigarh, India, [2]Department of Obstetrics and Gynecology, Postgraduate Institute of Medical Education and Research, Chandigarh, Chandigarh, India

Disclosures: Radhika Srinivasan: None; Akriti Bansal: None; Manish Rohilla: None; Bhavana Rai: None; Arvind Rajwanshi: None; Vanita Suri: None; Subhas Saha: None

Background: High Grade Serous carcinoma [HGSC] of the ovary is one of the most common and lethal carcinomas among women in spite of multimodality treatment. The aim of this study was to evaluate the interplay of tumor infiltrating lymphocytes [TILs] and PD-L1, an immune check point inhibitor in HGSC and evaluate the clinical significance of 'immunotyping' in HGSC.

Design: A total of 100 cases of HGSC ovary were included in this retrospective analysis. Out of these, 50 underwent upfront surgery (HGSC-upfront) and 50 underwent interval debulking surgery following neoadjuvant chemotherapy (HGSC-post-NACT group). TIL density was scored from 0-3+ on whole tissue sections. Tissue microarrays were constructed from the areas with maximum TILs and evaluated by immunohistochemistry for CD4 and CD8 lymphocytes, CD68 tumour associated macrophages (TAMs), and PD-L1. The cases were then divided into four immunotypes based on PD-L1 (≥10%) and CD8+ T-cell (≥5%) expression (Type I-PDL1+/CD8+; Type II-PDL1-/CD8-; Type III-PD-L1+/CD8-; Type IV-PD-L1-/CD8+) and correlated to disease-free survival (DFS), overall survival and platinum-free interval.

Results: Majority (77%) of HGSC ovary were in FIGO stage 3 with median DFS of 196 days without any difference in survival among the two groups. HGSC-post-NACT had higher TILs and CD8**+**T cells with no difference in TAMs and CD4+ cells. Overall 60% HGSC showed PD-L1 expression of any degree in tumour and TAMs. The HGSC-post-NACT group showed increased PD-L1 levels as compared to the HGSC-upfront group (p=0.01). PD-L1 levels showed a linear association with immune cell infiltration. At 10% cut-off, PD-L1 expression alone did not show any association with DFS. Immunotyping (Fig.1) revealed frequency of Type I, II, III and IV immunotypes in HGSC-upfront group to be 2%, 60%, 16% and 20% whereas in the HGSC-post-NACT group it was 22%, 54%, 2% and 20% respectively. Log-rank test and Kaplan-Meier analysis revealed that immunotype I (PD-L1+/CD8+) showed worst outcome (p=0.04) (Fig.2) with the difference in DFS between type I and type III immunotypes highly significant (p=0.01).

Figure 1 - 1191
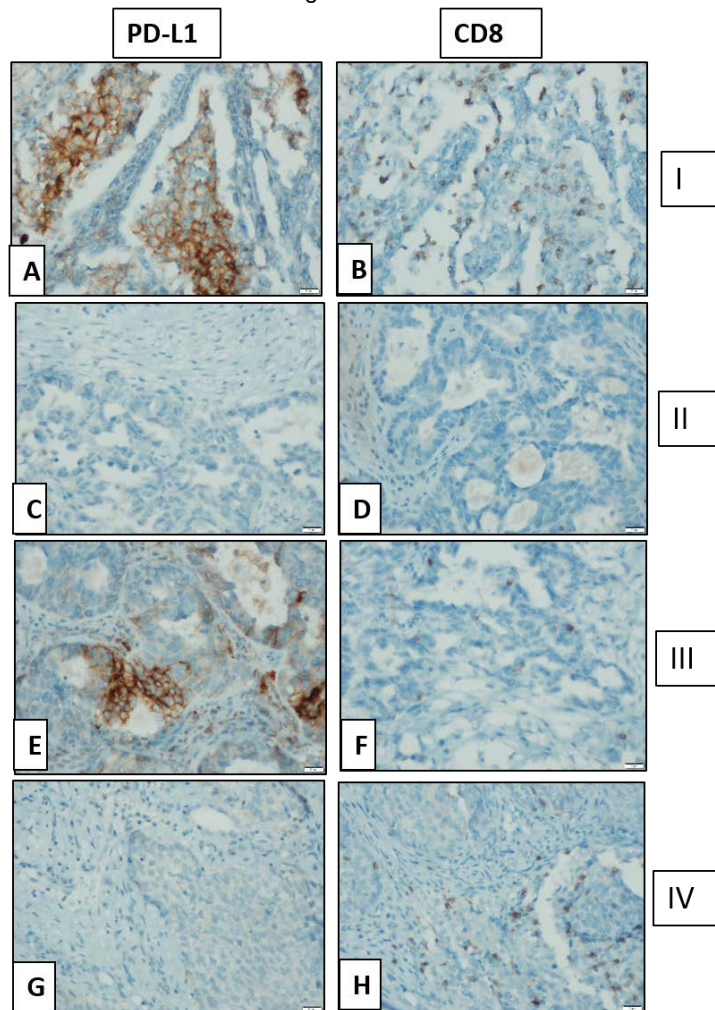
Figure 2 - 1191
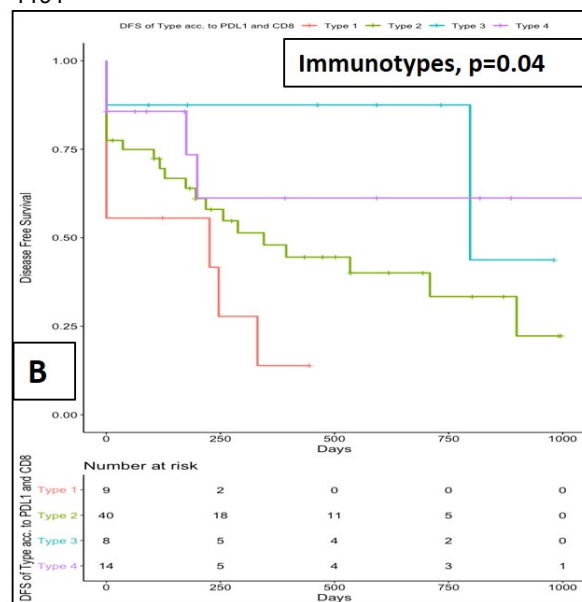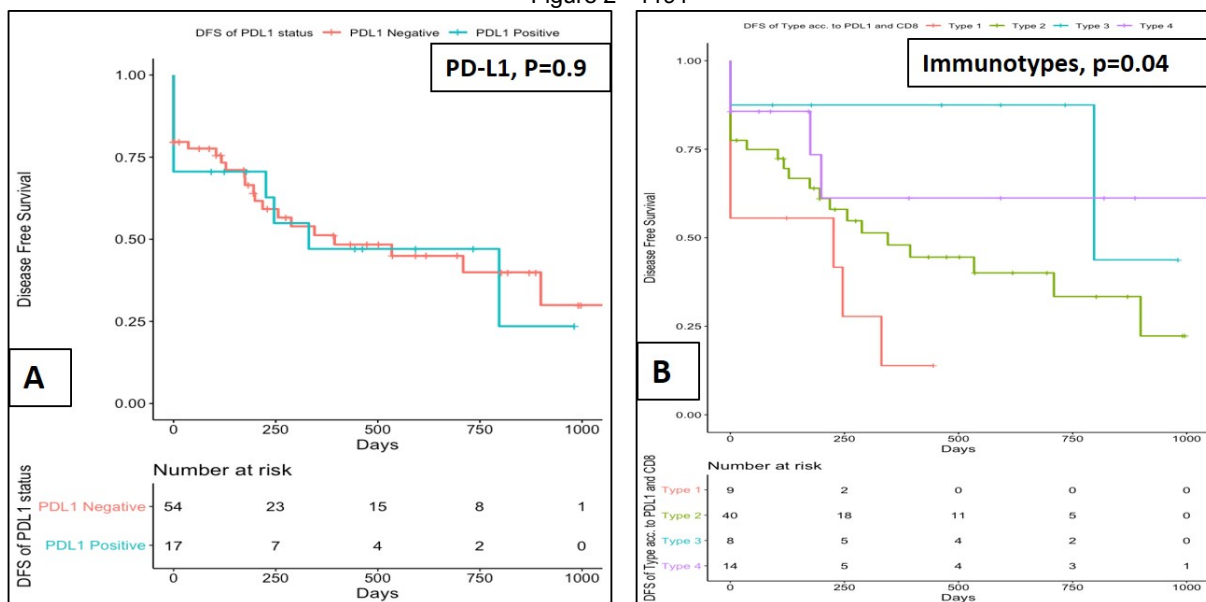
Conclusions: Immunotyping based on PD-L1 and CD8+ T cell levels stratifies patients based on prognosis better than PD-L1 scoring alone. Further, immunotyping helps in selection of patients for treatment and type I (PD-L1+/CD8+) cases may be potential candidates for anti-PD-L1 therapy.

1192   HER2 Expression in Endometrial Cancers Diagnosed as Clear Cell Carcinoma

Bradly Stelter[1], Nhu Vu[2], Alain Cagaanan[3], Ahmed Al-Niaimi[2], Paul Weisman[4], Stephanie McGregor[4]
[1]University of Wisconsin-Madison, Fitchburg, WI, [2]University of Wisconsin-Madison, Madison, WI, [3]Madison, WI, [4]University of Wisconsin, Madison, WI

Disclosures: Bradly Stelter: None; Nhu Vu: None; Alain Cagaanan: None; Paul Weisman: None; Stephanie McGregor: None

Background: There is increasing evidence from immunophenotypic and molecular studies that a large proportion of cases diagnosed as clear cell carcinoma (CC) may be better regarded as either endometrioid (EmC) or serous (SC). A diagnosis of CC in such cases has the potential to exclude patients from targeted regimens or clinical trials that may be of therapeutic benefit, such as HER2-targeted therapy, which has been approved for SC but not for CC. Here we present an assessment of HER2 expression in endometrial cancers in relation to original diagnosis and immunophenotype.

Design: A tissue microarray of archived endometrial cancers was created (1 mm punches in duplicate). Stains for p53, p16, ER, and HER2 were performed in our clinical lab. Representation of all relevant stains was achieved for 26 CC, 78 SC, and 133 EmC (93 FIGO grade 1, 40 FIGO grade 3), according to original diagnosis. Stains were scored as: p53 mutant/null vs. wild type, ER high (>10%) vs. low/negative (10% or less), and p16 strong and diffuse (>90%) vs. patchy/negative. HER2 was scored according to 2007 guidelines for breast carcinoma. Cases were assessed for HER2 expression according to original diagnosis, p53/p16 status, or a dichotomized classification of endometrioid or serous based on immunophenotype according to p53, p16, and ER.

Results: According to original diagnosis, HER2 was 3+ in 7/78 SC (9%) and in 5/26 CC (19%) but in 0/133 EmC (0%). Of the 12 cases that were 3+ for HER2, 11 were p53 mutant/null (92%) and 10 had strong/diffuse expression of p16 (83%). Among p53 mutant/null cases, 11 of 95 (12%) were 3+. When dichotomized as being more similar to serous or endometrioid, all 12 cases were regarded as serous (13%).

Conclusions: Though current recommendations are to test for HER2 in SC, in this series HER2 is more common in cases initially regarded as CC. Irrespective of initial diagnosis, HER2 3+ cases demonstrated serous-like immunophenotype. Though additional study is necessary to determine the utility of HER2-targeted therapy in cases diagnosed as CC, identifying patients with a diagnosis of CC that are HER2+ may open avenues with higher likelihood of therapeutic benefit than those that are otherwise currently available. Such overlap in expression also underscores the biologic similarity between a subset of cases regarded as CC and SC.

1193   Clinical and Pathological Determinants of Outcome in Invasive Stratified Mucinous Carcinoma (iSMILE) of the Cervix: An International Multicentric Study

Simona Stolnicu[1], Monica Boros[2], Carlos Parra-Herran[3], Esther Oliva[4], Nadeem Abu-Rustum[5], Robert Soslow[5], Kay Park[5]
[1]University of Medicine, Pharmacy, Sciences and Technology, Targu Mures, Mures, Romania, [2]Faculty of Medicine and Pharmacy, University of Oradea, Oradea, BH, Romania, [3]Sunnybrook Health Sciences Centre, University of Toronto, Toronto, ON, [4]Massachusetts General Hospital, Harvard Medical School, Boston, MA, [5]Memorial Sloan Kettering Cancer Center, New York, NY

Disclosures: Simona Stolnicu: None; Monica Boros: None; Carlos Parra-Herran: None; Esther Oliva: None; Nadeem Abu-Rustum: *Grant or Research Support*, Stryker, GRAIL; Robert Soslow: *Speaker*, Ebix/Oakstone; Kay Park: None

Background: iSMILE, a tumor characterized by hybrid morphology thought to arise from human papillomavirus (HPV) infected reserve cells of the transformation zone, may represent an aggressive subtype with worse outcomes compared to usual HPV associated (HPVA) cervical adenocarcinoma. We sought to investigate the outcomes in iSMILE and determine which clinical and pathological parameters may influence the prognosis.

Design: Slides from 52 cases of iSMILE were collected and classified as follows: pure iSMILE (>90% of the entire tumor) and iSMILE mixed with other HPVA components (miSMILE) (>10% but <90% of the entire tumor). The following parameters were evaluated: age, FIGO stage, treatment, HPV status, tumor size, lympho-vascular involvement (LVI), Silva pattern of invasion, lymph node metastases (LNM), local/pelvic recurrence, overall survival (OS) and recurrence free survival (RFS).

Results: In most cases (80%) iSMILE occurred in patients <50y and were Silva pattern C. One third of patients with iSMILE presented with LNM and 25% developed local recurrences while 4 developed distant recurrences. 29 cases (55.76%) were pure iSMILE while 23 cases (44.23%) were miSMILE: 13 with usual-type adenocarcinoma, 6 with adenosquamous carcinoma, 3 with mucinous adenocarcinoma NOS and 1 with neuroendocrine carcinoma. Kaplan Meier survival analysis revealed 5-year OS of 78.8% and RFS of 63.6%. OS was 74.7% in pure iSMILE versus 85.2% in miSMILE but not statistically significant (p: 0.267). RFS was 56.5% in pure iSMILE and 72.9% in miSMILE (p: 0.185). OS at 5 years in stage I was 88.9% vs. stage II-IV 30% (p: 0.004). RFS at 5 years in stage I was 73.9%

vs. stage II-IV 38.1% (p: 0.02). Using Log rank Mantel Cox analysis, OS was influenced by FIGO stage (p: 0.013), tumor size (p: 0.02), LNM (p: 0.015) and local recurrence (p:0.022), while RFS was influenced by FIGO stage (p: 0.031), tumor size (p: 0.001), local recurrence (p: 0.009) and LNM (p: 0.008) (Table 1).

	OS			RFS		
	HR	CI 95%	p	HR	CI 95%	p
Tumor type (pure iSMILE vs miSMILE)	2.444	0.471-12.675	0.287	2.158	0.663-7.020	0.201
Age 50<;>50 years	1.834	0.347-9.702	0.476	1.379	0.160-3.273	0.676
FIGO stage (I vs II-IV)	6.765	1.490-30.500	**0.013**	3.469	1.120-10.746	**0.031**
Surgical treatment (without vs with lymph node dissection)	57.526	0.077-42858,438	0.23	4.782	1.041-21.974	**0.044**
Adjuvant treatment (yes vs no)	3.382	0.378-28.493	0.281	3.324	0.700-15.792	0.131
Tumor size (<4cm vs >=4cm)	32.114	3.583-287.821	**0.02**	10.261	2.619-41.794	**0.001**
HPV status (pos vs neg)	3.69	0.055-1.347	0.111	2.197	0.112-1.856	0.273
Tumor grade (1,2 vs 3)	2.032	0.244-16.923	0.512	3.841	0.495-29.831	0.198
Silva pattern (A, B vs C)	22.565	0.000-8545346.7	0.634	1.187	0.109-6.494	0.869
Lympho-vascular invasion (yes vs no)	3.289	0.633-17.093	0.157	2.998	0.893-10.071	0.076
Lymph node metastasis (yes vs no)	14.95	1.694-131.912	**0.015**	5.52	1.569-19.424	**0.008**
Local/pelvic pelvic recurrences (yes vs no)	12.323	1.436-105.770	**0.022**	18.089	2.040-160.361	**0.009**

Conclusions: iSMILE is an aggressive cervical tumor biologically different from other HPVA adenocarcinomas due to propensity for LNM, local/distant recurrence. FIGO stage, tumor size, LNM and presence of local/pelvic recurrences are determinants of outcome in iSMILEs.

1194 FIGO (2018) Stage IB Endocervical Adenocarcinomas: A Detailed Study of Clinical Outcomes Informed by Clinico-Pathological Parameters, including HPV Status

Simona Stolnicu[1], Monica Boros[2], Lynn Hoang[3], Louise De Brot[4], Glauco Baiocchi[4], Graziele Bovolim[4], Carlos Parra-Herran[5], Esther Oliva[6], Kay Park[7], Nadeem Abu-Rustum[7], Robert Soslow[7]
[1]University of Medicine, Pharmacy, Sciences and Technology, Targu Mures, Mures, Romania, [2]Faculty of Medicine and Pharmacy, University of Oradea, Oradea, BH, Romania, [3]Vancouver, BC, [4]A.C.Camargo Cancer Center, São Paulo, SP, Brazil, [5]Sunnybrook Health Sciences Centre, University of Toronto, Toronto, ON, [6]Massachusetts General Hospital, Harvard Medical School, Boston, MA, [7]Memorial Sloan Kettering Cancer Center, New York, NY

Disclosures: Simona Stolnicu: None; Monica Boros: None; Lynn Hoang: None; Louise De Brot: None; Glauco Baiocchi: None; Graziele Bovolim: None; Carlos Parra-Herran: None; Esther Oliva: None; Kay Park: None; Nadeem Abu-Rustum: *Grant or Research Support*, Stryker; *Grant or Research Support*, GRAIL; Robert Soslow: *Speaker*, Ebix/Oakstone

Background: FIGO stage and HPV status pattern are prognostic in endocervical adenocarcinomas (ECAs). 2018 FIGO stage IB is heterogeneous, posing clinical management challenges for gynecologists. We aimed to determine parameters that associate with overall survival (OS) and recurrence free survival (RFS) in stage IB ECAs.

Design: Stage IB ECAs with at least 5-year follow-up were collected from 12 international institutions, all with lymph node evaluation. Preoperative radio- and/or chemotherapy was exclusionary. Full slide sets (n=421) were used to assign microscopic type (IECC classification), HPV status, lympho-vascular invasion (LVI) and lymph node metastases (LNM). Kaplan-Meier survival analysis and Cox regression were used for statistical analysis.

Results: 45.6% were stage IB1, 38.47% IB2 and 14.96% IB3. 7.12% died of disease and 14.25% suffered a recurrence. OS at 5- and 10-years did not differ across substages (p: 0.339), whereas RFS across substages at 5- and 10-years differed (p: 0.012).On univariate analysis, there was a higher risk of recurrence for stage IB3 versus IB2 (p:0.05; HR=1.848). OS was significantly associated with LVI (p:0.021; HR=2.62), LNM (p:0.02, HR=3.825) and local recurrence (p:0.001: HR=32.308), while RFS was associated with HPV status (p=0.017; HR=2.24), LVI (p:0.001; HR=3.614) and LNM (p:0.001; HR=5.696).

Conclusions: Beyond depth of invasion and tumor diameter, HPV-negative Stage IB ECAs with LVI and LNM have the highest recurrence risk, especially in the IB3 subgroup. These parameters are important to be included in any future sub-staging modification of stage IB cervical adenocarcinoma.

1195 Persistent Expression Pattern of Biomarkers in Endometrial Intraepithelial Lesions in Consecutive Biopsies and its Clinical Implications: A Longitudinal Study

Amanda Strickland[1], Hao Chen[2], Elena Lucas[3], Katja Gwin[1], Glorimar Rivera- Colón[1], Shuang Niu[4], Kelley Carrick[3], Diego Castrillon[3], Wenxin Zheng[1]
[1]University of Texas Southwestern Medical Center, Dallas, TX, [2]Coppell, TX, [3]University of Texas Southwestern, Dallas, TX, [4]UTSW Medical Center, Frisco, TX

Disclosures: Amanda Strickland: None; Hao Chen: None; Elena Lucas: None; Katja Gwin: None; Glorimar Rivera- Colón: None; Shuang Niu: None; Kelley Carrick: None; Diego Castrillon: None; Wenxin Zheng: None

Background: Hyperplasia with atypia (HA), or endometrial intraepithelial neoplasia (EIN), is known as the precursor of endometrioid adenocarcinoma. Progestin treatment is common for young patients desiring future fertility. It is thus routine to evaluate progestin-treated endometrial specimens for residual disease, but this may be challenging due to the lack of well-established diagnostic criteria. Biomarkers like PAX2 and PTEN have proved useful in facilitating diagnosis of HA/EIN. Whether the expression pattern of these two biomarkers persists after progestin treatment, and whether biomarker expression can be restored after progestin treatment, are two currently unanswered questions investigated in this study.

Design: 21 patients with initial diagnosis of EIN and n≥2 follow-up (f/u) endometrial biopsies (n=85) were divided into 3 categories based on clinical outcome: A) persistent disease group (8 patients, 26 biopsies); B) recurrent disease group (5 patients, 24 biopsies); C) optimally treated (complete response, CR) group (8 patients, 35 biopsies). PAX2 and PTEN immunohistochemistry (IHC) was performed on all biopsies.

Results: Loss of PAX2 and/or PTEN expression was identified in 19 (90.5%) of 21 available primary biopsies. 19 (90.5%) cases showed lost PAX2 expression, 8 (38.1%) cases exhibited lost PTEN expression, and 2 cases retained both markers (9.5%). All 19 f/u cases (100%) with residual or recurrent EIN had the same expression pattern of PAX2 and PTEN (p<0.00001) in the involved areas as in the initial biopsies. Completely restored PAX2 and PTEN expression was found in all 30 (100%) CR biopsies (p<0.00001) (Figure 1). Five (71.4%) of 7 f/u biopsies not completely meeting EIN diagnostic criteria showed concordant PAX2 and PTEN expression patterns, whereas 2 cases (28.6%) showed normal expression of PAX2 and PTEN. 3 cases (8.8%) initially diagnosed as "no residual hyperplasia identified" were re-classified as "residual hyperplasia identified" based on morphologic features and IHC staining pattern with PAX2 and PTEN. One case with uncertain status regarding residual hyperplasia based on morphologic features was re-classified as "no residual hyperplasia identified".

Figure 1 - 1195
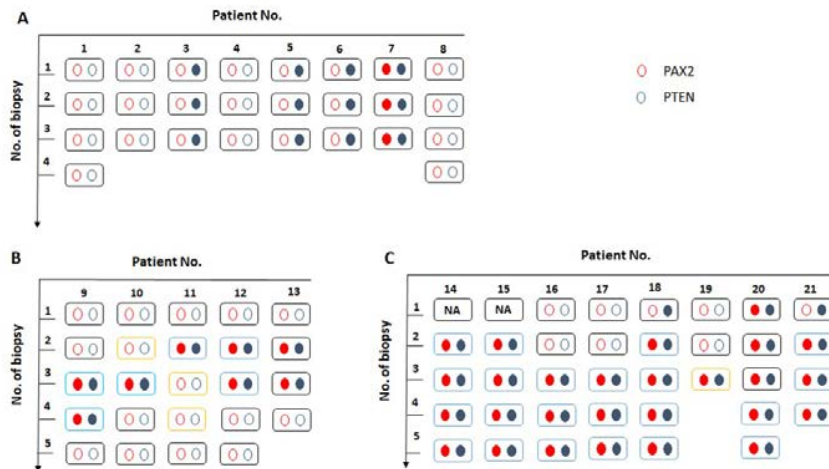
Figure 2 - 1195
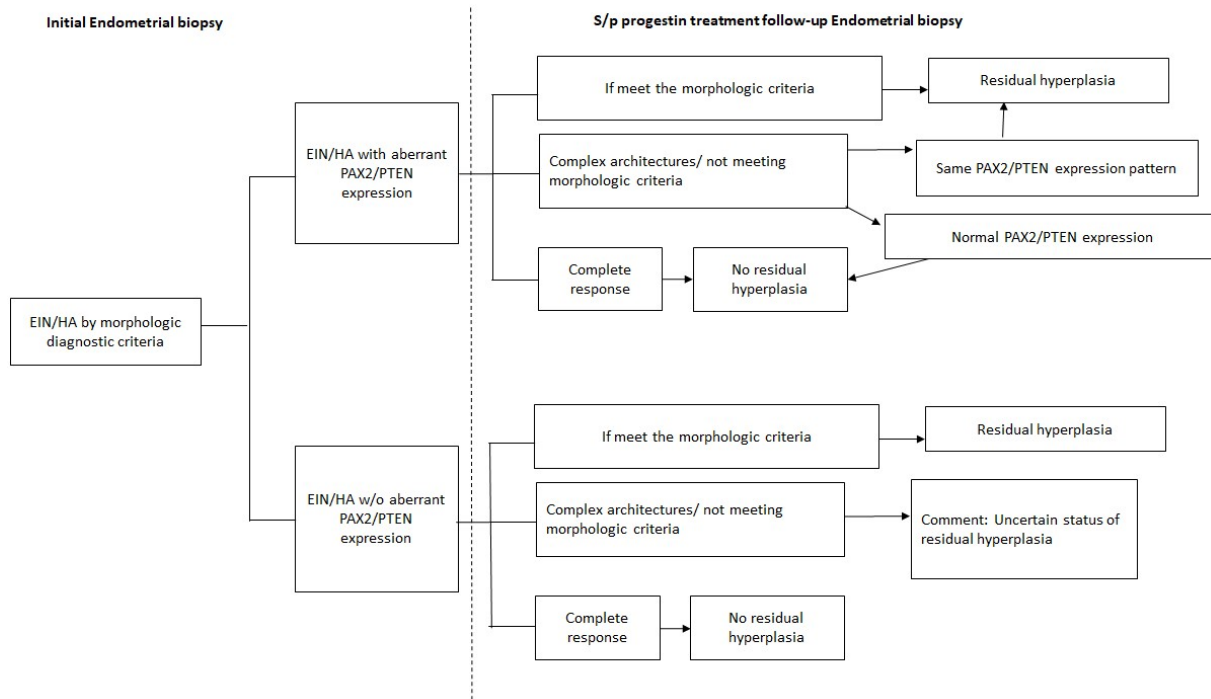
Conclusions: 1) PTEN/PAX2 expression patterns in HA/EIN persist across serial biopsies. 2) Restored PTEN/PAX2 expression is observed in cases with a CR to progestin treatment. 3) PTEN/PAX2 staining in initial and follow-up biopsies is useful in evaluating questionable residual HA/EIN (Figure 2).

1196 FOXO1 Expression and its Potential Role in Endocervical Carcinogenesis

Amanda Strickland[1], Hao Chen[2], Elena Lucas[3], Shuang Niu[4], Diego Castrillon[3], Glorimar Rivera- Colón[1]
[1]University of Texas Southwestern Medical Center, Dallas, TX, [2]Coppell, TX, [3]University of Texas Southwestern, Dallas, TX, [4]UTSW Medical Center, Frisco, TX

Background: FOXO1 is largely considered a tumor suppressor due to its inhibition of cancer cell growth and induction of apoptosis. FOXO1 has been implicated in cervical carcinogenesis. We investigated the presence and quality of FOXO1 expression in endocervical adenocarcinomas.

Design: Thirty-eight (38) cervical adenocarcinoma cases were reviewed by three gynecologic pathologists and classified using the three-tiered Pattern Based Classification System (PBCS). Unstained slides from each case were made, and immunohistochemical (IHC) analysis of FOXO1 antibody (Cell Signaling Technology, catalog # 2880) was performed on a Dako Autostainer Link 48 system at 1:50 antibody dilution. FOXO1 IHC expression was evaluated and results were recorded. Statistical analysis was performed to compare FOXO1 expression in relation to the patterns of invasion.

Results: After the evaluation of 38 cervical adenocarcinoma cases, 6 (16%) were classified as pattern A, 6 (16%) as pattern B and 26 (68%) as pattern C. In all cases, FOXO1 was weak/multifocally positive (n=28; 74%) or lost (n=10; 26%). 22 out of 26 (85%) cases that were classified as pattern C expressed FOXO1 (p=0.024). Importantly, there was also an association between FOXO1 glandular expression and the presence of intraluminal tumor apoptosis (*p=0.0026*). Additionally, only pattern C cases showed intraluminal apoptotic/ghost cells [Figure 1] with expression of FOXO1 [Figure 2] (*p=0.0011*

Conclusions: Our results show a likely correlation of pattern C endocervical adenocarcinoma with positive expression of FOXO1. This finding may have an impact on the evaluation of cervical adenocarcinoma because it could help predict the tumor behavior. In addition, the association between FOXO1 glandular expression and presence of intraluminal tumor apoptosis implies increased apoptotic activity and tumor turnover in FOXO1 expressing tumor cells. This could help explain the more aggressive biologic behavior of this subtype. Our findings suggest that FOXO1 may be a potential prognostic marker of cervical adenocarcinoma.

1197 Endometrial Serous Carcinoma with Shared Features of Ovarian High-Grade Serous Carcinoma: A Distinct Subset of Tumors?

Amanda Strickland[1], Hao Chen[2], Yiying Wang[3], Shuang Niu[4], Elena Lucas[5], Glorimar Rivera- Colón[1], Katja Gwin[1], Kelley Carrick[5], Anais Malpica[6], Wenxin Zheng[1]
[1]University of Texas Southwestern Medical Center, Dallas, TX, [2]Coppell, TX, [3]Henan Provincial People's Hospital, Zhengzhou, China, [4]UTSW Medical Center, Frisco, TX, [5]University of Texas Southwestern, Dallas, TX, [6]The University of Texas MD Anderson Cancer Center, Houston, TX

Disclosures: Amanda Strickland: None; Hao Chen: None; Yiying Wang: None; Shuang Niu: None; Elena Lucas: None; Glorimar Rivera-Colón: None; Katja Gwin: None; Kelley Carrick: None; Anais Malpica: None; Wenxin Zheng: None

Background: Typical endometrial endometrioid (EEC) and serous carcinomas (ESC) have distinct morphologic and immunophenotypic features. WT1 expression in ESC has been reported to range from 0% to 30% while estrogen receptor (ER) expression is variable, up to 80% in a recent study. This causes diagnostic challenges in assigning histologic type (EEC versus ESC) and primary site (endometrium versus ovary) for these cancers. Any implication conferred by ER and WT1 expression in ESC is also unclear. We assessed WT1 expression in whole tumor sections and ascertained whether such expression correlates with ER expression in ESC. We also included a cohort of EEC for comparison.

Design: 84 endometrial cancers were retrieved and re-reviewed. Whole tumor sections were obtained and used for immunohistochemistry (IHC) studies for p53, p16, ER/PR, PTEN, Pax2, mismatch repair proteins (MMR), and WT1. The histotype was confirmed using morphological features and IHC results. Among the 84 cases, 39 were EEC, 43 ESC, 1 true mixed EEC and ESC, and 1 dedifferentiated. To address the above questions, we only present data regarding ER and WT1 in this study. ER high expression and WT1 positivity was each defined as 50% or more tumor cells showing strong positive nuclear staining. Benign fallopian tube sections with positive expression for both ER and WT1 served as positive controls.

Results: 21/43 (48.8%) ESCs were positive for WT1 and the same number of ESCs was positive for ER expression. Among the 21 ESCs with positive ER, 18 (86%) were positive for WT1, while only 3 of 22 (14%) ESCs with negative ER expression were positive for WT1 ($p < 0.00001$). In contrast, 5 of the 39 (13%) EECs were WT1 positive, while the remaining 34 (87%) were WT1 negative ($p < 0.0001$). The mixed EEC-ESC showed WT1 positivity in the serous component only while ER was positive in both components. One dedifferentiated EEC showed WT1 expression in the low-grade cancerous area. The data is summarized in Table 1.

Table 1. WT1 and ER expression in endometrial cancers

	IHC Biomarkers	WT1 positive	WT1 negative
EEC		5	34
ESC	ER positive	18	3
	ER negative	3	19
Mixed EEC-ESC		1 (in serous only)	
Dedifferentiated		1 (in low-grade area)	

Note: EEC: endometrial endometrioid carcinoma; ESC: endometrial serous carcinoma

Conclusions: For the first time, we show that approximately half of ESCs are positive for both WT1 and ER. This finding indicates the need for caution in using these biomarkers to determine the primary site of a serous carcinoma (uterine versus extra-uterine). In addition, WT1 expression in ESCs correlates with a high ER expression, which may suggest the existence of an ovarian high-grade serous carcinoma-like subset within ESCs.

1198 Stratified Mucin-Producing Intraepithelial Lesion (SMILE) of the Uterine Cervix: Squamous Immunohistochemical Phenotype Related to Variable High Risk HPV Genotypes

Margareta Strojan Flezar[1], Neza Nedelko[2], Mario Poljak[2], Anja Oštrbenk Valenčak[2], Helena Gutnik[2]
[1]Institute of Pathology, Faculty of Medicine University, Ljubljana, Slovenia, [2]Faculty of Medicine, University of Ljubljana, Ljubljana, Slovenia

Disclosures: Margareta Strojan Flezar: None; Neza Nedelko: None; Mario Poljak: None; Anja Oštrbenk Valen?ak: *Speaker*, Abbott; *Speaker*, Qiagen; *Speaker*, Seegene; Helena Gutnik: None

Background: Stratified mucin producing intraepithelial lesion (SMILE) is a rare presumably high grade cervical precancerous lesion designated as a variant of AIS in 2014 WHO classification. Histomorphology of SMILE indicates both squamous and glandular differentiation. We analysed immunohistochemical phenotype, mucin presence and HPV genotypes of SMILE.

Design: SMILE was diagnosed in 34 of 6958 (0,5 %) cervical biopsies in 23 patients between 2010 and 2018. Only 26 tissue samples (13 with SMILE alone, 7 with SMILE and SIL (1 LSIL, 6 HSIL), 4 with SMILE and AIS, 1 with SMILE, HSIL and AIS, 1 with SMILE, HSIL, AIS and adenocarcinoma) from 21 patients were available for further studies. Immunohistochemical staining to p16, Ki-67, CK7 and CK19 (both present in endocervical columnar, reserve and basal layer squamous cells), p40 (highly sensitive and specific squamous marker: ΔNp63 - a p63 isoform) and mucin stain (Alcian Blue) were conducted. HPV genotyping was performed using a clinically validated real-time polymerase chain reaction-based Seegene Anyplex II HPV 28 Assay capable of detecting 28 alpha-HPV genotypes.

Results: All SMILEs showed strong positive reaction to p16, CK7, CK19 and high Ki67 proliferation index, also comparable to adjacent HSIL and/or AIS if present. SMILE showed mucin presence that was statistically significantly different from HSIL. Moreover, SMILE showed strong p40 positive staining comparable to HSIL and statistically significantly different from AIS. HPV was detected in 24/26 (92.3 %) cases. In 22 cases, single HPV genotype was identified and in one sample each 2 and 3 HPV genotypes. All HPV genotypes but one were high-risk (23/24, 95.8 %) We have identified 6 different high-risk HPV genotypes (16, 18, 31, 33, 39, 51), the most common being HPV16 (10/23 cases, 43.5 %), HPV18 (8/23 cases, 34.8 %), HPV 31 (5/23 cases, 21.7 %).

Conclusions: Although mucin is an integral glandular marker of SMILE, we found strong expression of p40, confirming squamous differentiation in SMILE and suggesting it is a separate entity from AIS. We confirmed that SMILE is predominantly associated with high-risk HPV infection, but HPV genotypes do not differ from those commonly associated with HSIL and AIS.

1199 Integrative Molecular Profiling of Uterine Smooth Muscle Tumors (USMT) Highlights Potential Utility for Targeted Next-Generation Sequencing (NGS) of Histologically Challenging Cases

Julianne Szczepanski[1], Andrew Sciallis[2], Scott Tomlins[2], Aaron Udager[3]
[1]University of Michigan, Lake Orion, MI, [2]University of Michigan, Ann Arbor, MI, [3]University of Michigan Medical School, Ann Arbor, MI

Disclosures: Julianne Szczepanski: None; Andrew Sciallis: None; Scott Tomlins: *Employee*, Strata Oncology; *Stock Ownership*, Strata Oncology; Aaron Udager: None

Background: Histologic classification of USMTs may be difficult for tumors with unusual combinations of increased mitotic activity, cytologic atypia, and/or geographic tumor necrosis – morphologic features that are subject to inter- and intra-pathologist variability. In addition, intravascular growth and/or distant metastatic dissemination without other overt histologic features of malignancy is present in rare subsets of cases. Despite these clear challenges, few ancillary tools are available to aid pathologists in the evaluation of USMTs with atypical features.

Design: 10 USMTs were retrospectively identified from the surgical pathology records database at a single large academic institution: 3 conventional leiomyomas (LM), 1 intravascular leiomyoma (IVLM), 1 benign metastasizing leiomyoma (BMLM), 2 atypical USMT, and 3 leiomyosarcomas (LMS). Targeted NGS was performed on an Ion Torrent S5 sequencer using custom AmpliSeq panels and FFPE-extracted tumor DNA and RNA. NGS data was processed using in-house bioinformatics pipelines; log2-transformed normalized RNAseq data was visualized using unsupervised hierarchical clustering.

Results: Targeted NGS revealed *MED12* mutations without significant copy number alterations (CNA) in all LM samples; in contrast, all LMS samples harbored frequent high-level CNA and/or deleterious tumor suppressor gene mutations (i.e., *TP53* and/or *RB1*). RNAseq data highlighted clear transcriptomic differences between LM and LMS, including higher expression of cell cycle/proliferation (CCP) genes. The BMLM showed intermediate CCP gene expression without identifiable molecular alterations, while the IVLM demonstrated intermediate CCP gene expression with scattered low-level CNA. One atypical USMT demonstrated focal deep deletion of the *FH* gene and low CCP gene expression, while the other atypical USMT harbored a *MED12* mutation with high CCP gene expression but without significant CNA.

Conclusions: These data highlight distinct molecular features of unequivocally benign and malignant USMT, including *MED12* and tumor suppressor gene mutation status, CNA patterns and genomic complexity, and CCP gene expression levels. In contrast, the molecular spectrum of unusual leiomyoma variants (IVLM and BMLM) and other atypical USMT is heterogeneous and highly idiosyncratic, indicating that integrative targeted NGS may be important to provide a common molecular framework upon which to evaluate USMT in future studies.

1200 Universal Screening for Lynch Syndrome using Mismatch Repair Protein Immunohistochemistry in an Asian Cohort of Endometrial Carcinomas

Nicholas Jin Hong Tan[1], Tuan Zea Tan[2], David Tan[3], Diana Lim[1]
[1]National University Hospital, Singapore, Singapore, [2]Cancer Science Institute of Singapore, National University of Singapore, Singapore, Singapore, [3]National University Cancer Institute of Singapore, Singapore, Singapore

Disclosures: Nicholas Jin Hong Tan: None; Tuan Zea Tan: None; David Tan: *Consultant*, MSD; *Grant or Research Support*, AZD; *Consultant*, ROCHE; *Consultant*, Bayer; Diana Lim: None

Background: Patients with Lynch Syndrome (LS) carry a significantly elevated lifetime risk for several malignancies including endometrial carcinomas (EC). Universal LS screening for patients with EC has been proposed to maximize detection of LS in this population. We examined the clinicopathologic features of EC with mismatch repair protein (MMR) protein deficiency that were identified on universal screening at a single Asian institution.

Design: Slides from all EC screened between January 2016 and December 2018 using MMR immunohistochemistry (IHC) were reviewed and correlated with clinicopathological features including age at diagnosis, tumor type, size, site, grade, stage, tumor-infiltrating lymphocytes (TILs), presence of Crohn's-like lymphoid reaction (CLR) and family/personal history of cancer.

Results: A total of 162 EC were screened with MMR IHC. Deficiency in ≥1 MMR protein was observed in 33 cases (20.3%) and they include cases with: MLH1 and PMS2 loss (16), MSH2 and MSH6 loss (9), PMS2 loss (4) and MSH6 loss (4). These patients ranged in age from 37 to 70 (mean 55.2) years. Thirty-one patients had endometrioid carcinomas (16 G1, 6 G2, 9 G3), 1 had clear cell carcinoma and 1 had MMMT. Twenty-seven patients were stage I, 1 was stage II, 3 were stage III and 2 were stage IV at presentation. One patient had a history of breast and renal cancers and 9 had family histories of LS-related cancers. There were no significant differences in the clinicopathological characteristics of EC with intact and deficient MMR immunoexpression except more TILs (mean 46/10 HPFs versus 19/10 HPFs, p<0.005) and a higher incidence of CLR (p <0.005) were seen in tumors with loss of MMR proteins.

Conclusions: Most patients with loss of MMR immunoexpression do not fulfill the Amsterdam II or Bethesda criteria for LS testing. The presence of increased TILs or CLR can help to identify EC with MMR protein deficiency. Our findings support universal LS screening for Asian patients with EC, as the majority of potential LS patients in this cohort would have been missed by conventional screening algorithms based solely on age at diagnosis and significant personal or family history of cancers.

1201   Size of Lymph Node Metastasis Significantly Affects Overall Survival but not Recurrence-Free Survival in a Cohort of 182 Single-Institution Endometrial Carcinomas

Matthew Thomas[1], Scott Robertson[2], Amy Joehlin-Price[2]
[1]Cleveland, OH, [2]Cleveland Clinic, Cleveland, OH

Disclosures: Matthew Thomas: None; Scott Robertson: None; Amy Joehlin-Price: None

Background: The 8th Edition of the AJCC Cancer Staging Manual adopted size of lymph node (LN) metastasis in the pN staging of endometrial cancer (EC). Little data exist to suggest whether this information has an impact on outcomes of EC.

Design: We reviewed consecutive EC with LN metastases that were diagnosed at our institution between 2002-2015. Sizes of the largest LN metastases were measured histologically and classified as isolated tumor cells (≤0.2 mm), micrometastases (≥0.2 mm to 2 mm) and macrometastases (>2 mm). Clinical outcome data were obtained from the institutional electronic medical records and tumor registry. Logrank tests were performed and Kaplan Meier curves were constructed for both overall survival and recurrence-free survival using Stata version 15.1 (Statacorp, College Station, TX).

Results: 182 EC with LN metastases were identified in patients that ranged from 43 to 84 years (median 63). Cases included 66 (36%) low grade EC, 32 (18%) high grade endometrioid EC, 34 (19%) serous carcinomas, 11 (6%) clear cell carcinomas, 16 (9%) carcinosarcomas, 20 (11%) mixed epithelial carcinomas, and 3 (2%) dedifferentiated or undifferentiated carcinomas. Sixteen (9%) demonstrated ITCs, 27 (15%) demonstrated micrometastases, and 139 (76%) demonstrated macrometastases (ranging from 2.1 mm to 70 mm, median 12 mm). Follow up time ranged from <1 month to 172 months (median 44 months). At the end of the follow up period, 76 (42%) patients remained free of disease, 8 (4%) patients were alive with disease, and 79 (43%) died of disease. The remaining 19 (10%) patients were dead of unrelated or unknown causes. During the follow up period, 71 (39%) patients experienced recurrences; of these, 14 (20%) were local recurrences and 57 (80%) were distant. Overall survival differed significantly between the three groups of EC patients with LN metastases, but recurrence-free survival only trended towards a difference (see Figure 1). Recurrence free survival remained insignificant when considering only distant metastases (as opposed to either local/vaginal or distant metastases) and when the tumor type was restricted to only low grade EC.

Figure 1 - 1201

Overall Survival	Recurrence-Free Survival
p=0.028	p=0.159
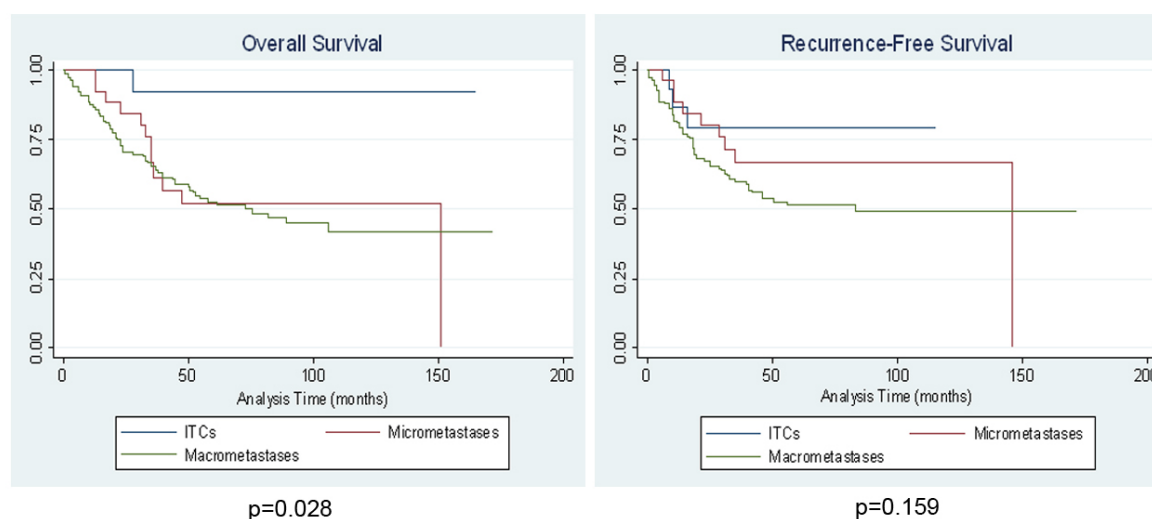
Conclusions: Size of LN metastasis, when classified according to the 8th Edition of the AJCC Cancer Staging Manual, significantly affects overall survival but not recurrence-free survival. Further study is necessary to determine the impact these measurements should have on clinical treatment decisions.

1202 Endometrial Carcinoma Molecular Subtype is Associated with Pathologic and Prognostic Indices: Findings from a National Study

Emily Thompson[1], Samuel Leung[2], Amy Lum[3], Janine Senz[4], Jutta Huvila[5], Marilyn Kinloch[6], Saul Offman[7], Monalisa Sur[8], Alice Lytwyn[9], Katherine Grondin[10], Chantale Morin[11], Carlos Parra-Herran[12], Francois Gougeon[13], Lynn Hoang[14], Jessica McAlpine[5], C. Blake Gilks[15]

[1]Vancouver General Hospital/University of British Columbia, Vancouver, BC, [2]University of British Columbia and British Columbia Cancer Agency, Vancouver, BC, [3]British Columbia Cancer Research Centre, Vancouver, BC, [4]University of British Columbia, Vancouver, BC, [5]University of British Columbia and BC Cancer Agency, Vancouver, BC, [6]Saskatoon, SK, [7]Dalhousie University, Halifax, NS, [8]McMaster University, Burlington, ON, [9]Juravinski Hospital, Hamilton, ON, [10]Quebec, QC, [11]Levis, QC, [12]Sunnybrook Health Sciences Centre, University of Toronto, Toronto, ON, [13]CHUM, Montreal, QC, [14]Vancouver, BC, [15]Vancouver General Hospital, Vancouver, BC

Disclosures: Emily Thompson: None; Samuel Leung: None; Amy Lum: None; Janine Senz: None; Jutta Huvila: None; Marilyn Kinloch: None; Saul Offman: None; Monalisa Sur: None; Alice Lytwyn: *Grant or Research Support*, Astra Zeneca; Chantale Morin: None; Carlos Parra-Herran: None; Francois Gougeon: None; Lynn Hoang: None; Jessica McAlpine: None; C. Blake Gilks: None

Background: Inconsistencies in the management of endometrial carcinoma (EC) persist in part due to inter-observer variability in grading & histotype designation, and thus risk assignment. TCGA-informed molecular classification of EC is reproducible and provides prognostic and predictive information while also identifying women who may have inherited cancer syndromes. Herein we describe the molecular subtype distribution and histo-morphologic correlates in a nation-wide cohort of ECs.

Design: We collected representative tumour samples and clinicopathologic data for all ECs diagnosed in the calendar year 2016 from 24 participating centers. Proactive Molecular risk classifier for Endometrial Cancer (ProMisE) subtype was determined by immunohistochemistry for mismatch repair (MMR) and p53 proteins performed on whole stained sections, and by focused sequencing for mutations in polymerase epsilon (POLE) gene.

Results: 1453 ECs from 24 centers have been identified for entry into this study. Complete molecular and clinical outcome data is available on 278 cases at time of this submission. The distribution of ProMisE subtypes and clinicopathologic features associated with molecular subtype are outlined in Table 1 and depicted in Figure 1.

Highlights

- ProMisE subtype associated with progression-free survival (p=0.047).
- We observed a significant association between MMRd and presence of lymphvascular invasion (LVI) (p=0.002).
- Variation in the routine use of MMR and p53 IHC, and reporting of extent of LVI (i.e. focal versus extensive), was notable across participating sites.

Table 1. Histopathologic characteristics by molecular subtype						
		Total *	**MMRd**	**p53abn**	**p53wt**	**POLE**
Number of Evaluated cases *		278	86 (30.9%)	57 (20.5%)	127 (45.7%)	8 (2.8%)
Histotype	Endometrioid	209 (75.3%)	74 (86.0%)	7 (12.3%)	122 (96.1%)	6(75.0%)
	Serous	33 (11.8%)	3 (3.5%)	29 (50.9%)	1 (0.8%)	0 (0.0%)
	Mixed	15 (5.4%)	2 (2.3%)	9 (15.8%)	2 (1.6%)	2 (25.0%)
	Dediff/undiff	8 (2.9%)	6 (7.0%)	2 (3.5%)	0 (0.0%)	0 (0.0%)
	MMMT	6 (2.2%)	0 (0.0%)	6 (10.5%)	0 (0.0%)	0 (0.0%)
	CCC	4 (1.4%)	0 (0.0%)	3 (5.3%)	1 (0.8%)	0 (0.0%)
	Other**	3 (1.1%)	1 (1.2%)	1 (1.8%)	1 (0.8%)	0 (0.0%)
Tumor grade	Grade 1/2	185 (66.3%)	63 (73.3%)	3 (5.3%)	115 (89.8%)	4 (50.0%)
	Grade 3	94 (33.7%)	23 (26.7%)	56 (98.2%)	12 (9.4%)	4 (50.0%)
FIGO stage	I	211 (75.6%)	66 (76.7%)	33 (57.9%)	106 (83.5%)	7 (87.5%)
	II-IV	55 (19.7%)	17 (19.8%)	23 (40.4%)	15 (11.8%)	1 (12.5%)
LVI	Negative	169 (60.6%)	41 (47.7%)	36 (63.2%)	88 (69.3%)	5 (62.5%)
	Positive	95 (34.1%)	41 (47.7%)	20 (35.1%)	32 (25.2%)	3 (37.5)
	+ focal	7 (2.5%)	4 (4.7%)	1 (1.8%)	1 (0.8%)	1 (12.5%)
	+ extensive	11 (3.9%)	3 (3.5%)	1 (1.8%)	5 (3.9%)	2 (25.0%)
	+ not specified	77 (27.6%)	34 (39.5%)	1 (1.8%)	26 (20.5%)	0 (0.0%)
Local MMR testing performed		45 (16.1%)	17 (19.8%)	5 (8.8%)	22 (17.3%)	1 (12.5%)
Local p53 testing performed		62 (22.2%)	14 (16.3%)	31 (54.4%)	13 (10.2%)	0 (0.0%)
* Indicates columns and rows where percentages have been expressed by total number of evaluated cases. All remaining percentages are expressed by total number of cases per molecular subtype						
** 'Other' histology included intestinal differentiated mucinous adenocarcinoma of the endometrium, a mixed endometrioid and MMMT and dedifferentiated carcinoma and a mixed serous and clear cell carcinoma.						
*** Missing data (FIGO stage, LVI, LND status) for non-surgically managed patients were considered in the calculations for percentage values above.						

Figure 1 - 1202
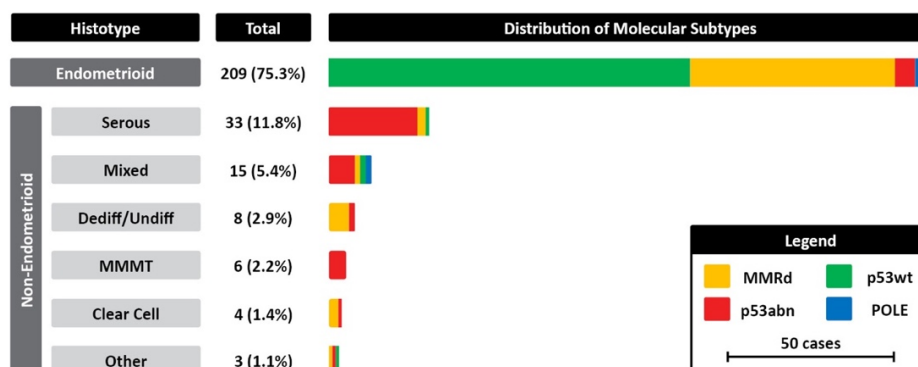
Conclusions: The molecular subtype of EC is of prognostic significance and correlates with histotype, with the most variation in molecular subtype seen in endometrioid carcinomas. We identified considerable variability in the use of immunomarkers that allow for molecular subclassification of EC at the time the cases in this study were reported (2016), and little uptake in the reporting of LVI as focal or extensive.

1203   Subclonal p53 Expression in a National Cohort of Endometrial Carcinomas

Emily Thompson[1], Amy Lum[2], Janine Senz[3], Jamie Vanden Broek[3], Samuel Leung[4], Jutta Huvila[5], Jessica McAlpine[5], C. Blake Gilks[6]
[1]Vancouver General Hospital/University of British Columbia, Vancouver, BC, [2]British Columbia Cancer Research Centre, Vancouver, BC, [3]University of British Columbia, Vancouver, BC, [4]University of British Columbia and British Columbia Cancer Agency, Vancouver, BC, [5]University of British Columbia and BC Cancer Agency, Vancouver, BC, [6]Vancouver General Hospital, Vancouver, BC

Disclosures: Emily Thompson: None; Amy Lum: None; Janine Senz: None; Jamie Vanden Broek: None; Samuel Leung: None; Jutta Huvila: None; Jessica McAlpine: None; C. Blake Gilks: None

Background: Immunohistochemistry (IHC) for p53 is used as a surrogate marker for TP53 mutations, and as part of the TCGA-based molecular sublassification of endometrial carcinoma (EC). p53 staining with abrupt transition between mutational and wild-type patterns, termed 'subclonal' staining, can be observed but the significance of this finding is unclear. Herein we describe a series of cases with subclonal p53 IHC staining encountered as part of a national study assessing the potential clinical impact of molecular subtyping in EC.

Design: We collected representative tumor specimens for all ECs diagnosed in the calendar year 2016 from 24 centers across Canada. IHC was performed at our institution on whole stained sections. The **Pro**active **M**olecular **ris**k classifier for **E**ndometrial Cancer (ProMisE) subtype was determined using p53 IHC in conjunction with MMR IHC and targeted *POLE* mutation testing. Cases showing subclonal p53 expression were interpreted by one resident (ET) and two gynecologic pathologists (CBG, JH). We interpreted any abrupt change in pattern of p53 staining as subclonal.

Results: Complete molecular results from 278 ECs were reportable at the time of this submission. Subclonal p53 IHC staining was observed in 19 (6.8%) of cases. Subclonal p53 staining was observed at levels ranging from 0.5% to 95% (median 11%). 7 of the 19 cases (37%) were classified as MMRd EC, 6 of which showed subclonal p53 expression at rates of <10%. An additional 5 cases (26%) tumors contained pathogenic POLE mutations. The remaining 7 tumors (37%) were MMR intact/POLE wild type, and 6/7 contained a *TP53* mutation, the only exception being a tumor where the subclonal loss was only present in 3% of the tumor cells, and below the limit of detection of the assay used.

Conclusions: Subclonal p53 IHC staining is relatively uncommon, and is most frequently encountered in the context of EC with molecular features known to carry high mutational burden (MMRd, POLE), where TP53 mutation is a secondary event and not associated with an adverse prognosis. There remain, however, cases (7/278, 2.5%) showingwith subclonal mutant expression pattern and an underlying TP53 mutation, a pattern suggestive of tumor progression, and the significance of this finding warrants further study.

1204   Tumor BRCA Testing in High Grade Serous Carcinoma: Somatic BRCA Mutation Rates and Optimal Tissue Requirements

Gulisa Turashvili[1], Shengjie Ying[2], Conxi Lazaro[3], George Charames[1], Aaron Pollett[1], Andrew Wong[1], Jordan Lerner-Ellis[4]
[1]Mount Sinai Hospital, Toronto, ON, [2]Department of Laboratory Medicine and Pathobiology, University of Toronto, North York, ON, [3]Catalan Institute of Oncology, Barcelona, Spain, [4]Sinai Health System, Toronto, ON

Disclosures: Gulisa Turashvili: None; Shengjie Ying: None; Conxi Lazaro: None; George Charames: None; Aaron Pollett: None; Andrew Wong: None; Jordan Lerner-Ellis: None

Background: Mutations in the *BRCA1 and BRCA*2, genes essential in the repair of DNA double-strand breaks by homologous recombination (HR), have been reported in up to 25% of high grade serous carcinomas (HGSC). In *BRCA*-mutation carriers, poly (ADP-ribose) polymerase (PARP) inhibitors selectively target HR-deficient cancer cells, and tumor tissue can also be tested to identify additional patients for drug eligibility. We set out to characterize somatic *BRCA* mutation rates and optimal tissue requirements for tumor *BRCA* testing.

Design: A total of 291 HGSC patients from 15 hospitals underwent somatic *BRCA* testing in October 2018-May 2019. Formalin-fixed paraffin-embedded tissue samples were sequenced using a multiplexed polymerase chain reaction-based approach (Illumina AmpliSeq Library PLUS for BRCA panel kit) on an Illumina MiSeq instrument. All reported variants had a minimum sequencing depth of 500X and an allele frequency of >5%. Variants were assessed based on the American College of Medical Genetics and Genomics guidelines. Pathogenic and likely pathogenic variants were reported as clinically significant.

Results: There were 253 surgical samples (87%), 35 biopsies (12%) and 3 cytology cell blocks (1%). Most patients (207, 71%) were chemotherapy naïve. Nine cases (3%) had insufficient tumor, while 16 (6%) had poor DNA quality. Sequencing was successful in 228 cases (78%), failed in 25 (9%) and deemed incomplete in 38 (13%) due to failed exons or variants below the detection limit. Of 42 retested samples, 23 (55%) were successful. Subsequently, a total of 251 cases were successfully reported (86%). Pathogenic or likely pathogenic variants were found in 48 patients (17%), including 30 in *BRCA1* and 18 in *BRCA2*. Successful sequencing was dependent on sample type (p=0.001), tumor cellularity (p=0.003) and tumor size (p<0.0001) but not on neoadjuvant chemotherapy (p>0.05), with failure

rates at 26%, 33% and 6% in biopsies, cytology and surgical samples, respectively; 29%, 11% and 4% in samples with ≥50%, 20-40% and 10% cellularity, respectively; and 7% and 39% in samples with ≥20% and 10% cellularity, respectively.

Conclusions: Our study shows a 17% somatic *BRCA* mutation rate. Success rates range from 78% on initial testing to 86% following repeat testing. The success rate on repeat testing is 55% suggesting that suboptimal samples should be retested when possible. Biopsy and cytology samples and post-chemotherapy specimens can be used, and optimal tumor should measure >5 mm with >10% cellularity.

1205 Recurrent Chromatin Remodeling Pathway Mutations Identified in Ovarian Juvenile Granulosa Cell Tumors

Theodore Vougiouklakis[1], Varshini Vasudevaraja[2], Guomiao Shen[1], Xiaojun Feng[3], Sarah Chiang[4], Julieta Barroeta[5], Kristen Thomas[6], Lauren Schwartz[7], Rebecca Linn[8], Esther Oliva[9], Pratibha Shukla[10], Anais Malpica[11], Deborah DeLair[12], Matija Snuderl[13], George Jour[6]
[1]New York University Langone Health, New York, NY, [2]New York University Medical Center, New York, NY, [3]NYU Langone, New York, NY, [4]Memorial Sloan Kettering Cancer Center, New York, NY, [5]Cooper University Hospital, Philadelphia, PA, [6]NYU Langone Health, New York, NY, [7]Perelman School of Medicine at the University of Pennsylvania, Bala Cynwyd, PA, [8]Children's Hospital of Philadelphia, Philadelphia, PA, [9]Massachusetts General Hospital, Harvard Medical School, Boston, MA, [10]NYU School of Medicine, New York, NY, [11]The University of Texas MD Anderson Cancer Center, Houston, TX, [12]NYU Langone Medical Center, New York, NY, [13]New York University, New York, NY

Disclosures: Theodore Vougiouklakis: None; Varshini Vasudevaraja: None; Guomiao Shen: None; Xiaojun Feng: None; Sarah Chiang: None; Julieta Barroeta: None; Kristen Thomas: None; Lauren Schwartz: None; Rebecca Linn: None; Esther Oliva: None; Pratibha Shukla: None; Anais Malpica: None; Deborah DeLair: None; Matija Snuderl: None; George Jour: None

Background: The somatic missense mutation *FOXL2* c.C402G (p.C134W) is harbored in 95-97% of adult granulosa cell tumors (AGCTs) and functions as a pathognomonic oncogenic driver. More recently, *KMT2D* and *TERT* promoter mutations have been reported to associate with recurrence in AGCTs. While the molecular pathogenesis of AGCTs has been well investigated, comprehensive genomic analysis of juvenile granulosa cell tumors (JGCTs) is currently lacking.

Design: A total of seventeen (*n*=17) JGCTs were selected for this study. Cases were selected and analyzed based on JGCT histomorphology and lack of *FOXL2* c.C402G (p.C134W) mutational status. Slides were reviewed by two experienced gynecologic pathologists. Formalin-fixed paraffin embedded (FFPE) tissues were subjected to DNA extraction for next generation sequencing (NGS) using our customized NGS580 panel targeting all exonic and select intronic areas in 580 cancer related genes. Matched tumors against normal pools were analyzed and manually curated to filter out single nucleotide polymorphisms (SNPs) and retain pathogenic variants by a molecular pathologist.

Results: Clinical information and follow-up was available for eleven patients. Age at diagnosis ranged from 13 to 65 years of age (median: 28). Fifteen cases (*n*=15) harbored callable mutations while 2 cases only had copy number (CN) losses. Recurrent mutational events were identified in *KMT2C* (73%), *RECQL4* (67%), *FANCD2* (67%), *KMT2D* (53%), and *RAD21* (47%).
Recurrent *FANCD2* c.1278_1278del (p.L426fs) frameshift deletions were identified in ten of fifteen cases (67%), and *RAD21* c.A49T (p.I17F) single nucleotide variants (SNVs) in seven of fifteen cases (47%). Deleterious events included *PALB2* in two cases (13%). Recurrent homozygous CN losses in *ATR (n=3)*, *CDKN2A (n=2)*, *SUFU (n=3)*, *RB1 (n=4)* and *NF1 (n=3)* were present in up to 30% of the cases. *EP400* and *EGFR* CN gains were seen in two cases [Figure 1]. The tumor mutational burden (TMB) ranged from 2.85 to 33.74 mut/mb. Four cases (27%) with a high TMB (>16.0 mut/mb; median cutoff) were associated with mutations in *CD79A* (p.A32G). One case with FIGO stage II and one metastatic to the mesentery were also associated with *KMT2D* mutations.

Figure 1 - 1205
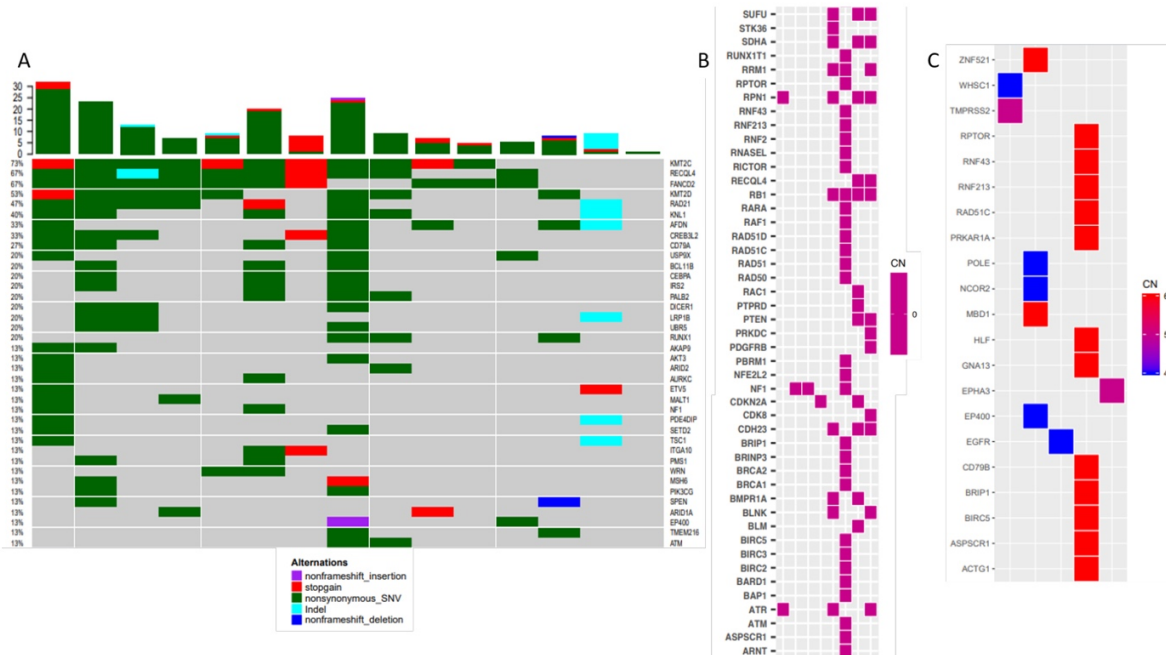
Conclusions: Our findings suggest that JGCTs shows a distinct genomic landscape compared to AGCTs. Alterations affecting chromatin remodeling and hedgehog signaling pathways contribute to the pathogenesis of JGCTs. These findings provide novel insight into the pathogenesis of a rare entity.

1206 Clinicopathologic Analysis and Morphologic Variants of Ovarian Juvenile Granulosa Cell Tumors

Theodore Vougiouklakis[1], Sarah Chiang[2], Pratibha Shukla[3], Kristen Thomas[4], Julieta Barroeta[5], Lauren Schwartz[6], Rebecca Linn[7], Esther Oliva[8], Anais Malpica[9], Matija Snuderl[10], George Jour[4], Deborah DeLair[11]
[1]New York University Langone Health, New York, NY, [2]Memorial Sloan Kettering Cancer Center, New York, NY, [3]NYU School of Medicine, New York, NY, [4]NYU Langone Health, New York, NY, [5]Cooper University Hospital, Philadelphia, PA, [6]Perelman School of Medicine at the University of Pennsylvania, Bala Cynwyd, PA, [7]Children's Hospital of Philadelphia, Philadelphia, PA, [8]Massachusetts General Hospital, Harvard Medical School, Boston, MA, [9]The University of Texas MD Anderson Cancer Center, Houston, TX, [10]New York University, New York, NY, [11]NYU Langone Medical Center, New York, NY

Disclosures: Theodore Vougiouklakis: None; Sarah Chiang: None; Pratibha Shukla: None; Kristen Thomas: None; Julieta Barroeta: None; Lauren Schwartz: None; Rebecca Linn: None; Esther Oliva: None; Anais Malpica: None; Matija Snuderl: None; George Jour: None; Deborah DeLair: None

Background: Juvenile granulosa cell tumors (JGCTs) are rare neoplasms associated with a favorable prognosis, however, a subset of patients develop recurrences. Morphologic overlap frequently renders a diagnostic challenge on account of the rarity of these tumors.

Design: A total of 29 cases from multiple institutions were identified. Select slides were reviewed by two experienced gynecologic pathologists. Paired primary and metastatic tumors were reviewed, except in two cases where only recurrent/metastatic tumors were available. All but one were pure JGCTs. Clinicopathologic features, including morphologic appearance, immunophenotype, and clinical follow-up, when available, were recorded.

Results: Patient age ranged from 2-65 years (mean: 23; median: 16), and tumor size from 4-34 cm (mean: 16; median: 14). Stage at presentation was: I (90%), II (5%), III (5%). Accompanied genetic disorders, Ollier disease and Donahue syndrome, were identified in two patients; the latter associated with bilateral tumors. Morphology showed at least one of these accompanied architectural patterns: follicular (83%), solid (62%), multinodular (31%), cystic (24%) and papillary (10%). Additional recognized features included foamy/bubbly cytoplasm (70%), cells with a rhabdoid appearance (57%) and prominent cell borders (39%). Nuclear atypia was as follows: mild (n=6), moderate (n=17), and moderate with focal severe/severe (n=6). Mitotic index ranged from 1-76/10 HPFs (mean: 12; median: 7). Inhibin (18/18), calretinin (12/12), CD99 (7/7), CD56 (4/4) and WT1 (2/2) were positive when applied. Nuclear grooves were seen in two cases, and no Call-Exner bodies were identified. Clinical follow-up was available for 20 patients (range 1-132 months), and identified four cases with recurrence. Two patients had recurrence in the ovary; one contralaterally at 26 months and one ipsilaterally after cystectomy at 2 months. The remaining two recurred in the colonic serosa. One patient with bilateral tumors died of disease one month after surgery.

Conclusions: JGCTs display a spectrum of morphologic features with variable mitotic activity and nuclear atypia. Recurrent/metastatic disease developed in 20% of patients with available follow-up and 5% died (14% and 3%, respectively, in total series). Recognition of these growth patterns and variable morphology is critical to render the correct diagnosis. Additional outcome data will be forthcoming.

1207   NF1 Mutations Are More Frequent in Metastatic vs. Primary-Site Cervical Squamous Cell Carcinoma Specimens: A Case for NF1 Mutation Testing in Metastatic Squamous Cell Carcinoma of the Cervix

John Wallbillich[1], Radhika Gogoi[1], Joseph Trak[2], Saivaishnavi Kamatham[2], Christopher Walker[1], Rouba Ali-Fehmi[2]
[1]Wayne State University School of Medicine, Detroit, MI, [2]Wayne State University, Detroit, MI

Background: Metastatic squamous cell carcinoma of the cervix (SCC-Cx) is a clinical challenge with poor survival and limited options for effective second- or later-line systemic treatment. We sought to investigate whether there were differences in next generation sequencing (NGS) genomic profiling results between primary squamous cell carcinoma of the cervix (SCC-Cx:primary) and metastatic-site squamous cell carcinoma of the cervix (SCC-Cx:met).

Design: Data for this analysis was obtained from AACR's Project GENIE (Cancer Discov. 2017 Aug;7[8]:818-831), a multi-Institutional dataset of clinical-grade NGS genomic profiling results for many cancer sites and histologic subtypes, through cBioPortal (http://genie.cbioportal.org). Patient/specimen groups used for analysis were SCC-Cx:primary and SCC-Cx:met. The SCC-Cx:met group included lymph node and distant metastases. Mutation frequencies for all available genes were calculated. For each gene, the difference in mutation frequencies between the two groups was evaluated using Fisher's exact test. The threshold for statistical significance was p-value < 0.05.

Results: In the SCC-Cx:primary group, there were 86 samples from 86 patients. In the SCC-Cx:met group, there were 54 samples from 53 patients. 1 patient with SCC-Cx had both primary and met samples in the dataset; that patient was excluded from patient-level analyses. Median age (in years) was 47 and 50 in the SCC-Cx:primary and SCC-Cx:met groups, respectively. 322 genes were available for analysis. PIK3CA was the gene with the highest mutation frequency in both the SCC-Cx:primary (35.2%) and SCC-Cx:met (33.7%) groups. NF1 was the only gene with significantly different mutation frequencies between the SCC-Cx:primary (1.2%) and SCC-Cx:met (11.3%) groups as illustrated in Figure 1 (p-value = 0.013).

Figure 1 - 1207

Figure 1: Genes with highest mutation frequencies in either the SCC-Cx:met or SCC-Cx:primary groups (asterisk denotes p < 0.05).
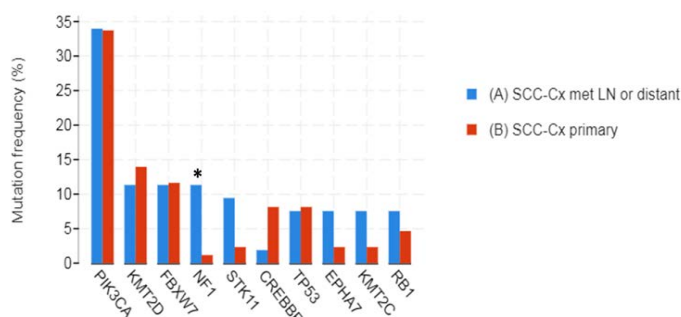
Conclusions: These data suggest NF1 mutations are more frequent in metastatic vs primary SCC-Cx tumors analyzed by NGS genomic profiling. NF1 mutations appear sufficiently prevalent in this setting to merit strong consideration of NF1 testing and targeting in future clinical trial development for metastatic SCC-Cx.

1208   The Combination of p16, IGF2BP3 and p53 Identifies Low Risk Patients with Stage I Ovarian Clear Cell Carcinoma

Linyuan Wang[1], Katharina Wiedemeyer[2], Martin Kobel[3]
[1]University of Calgary, Calgary, AB, [2]Calgary Laboratory Services/University of Calgary, Calgary, AB, [3]University of Calgary/Alberta Public Laboratories, Calgary, AB

Background: Among ovarian carcinomas, together with endometrioid carcinoma, clear cell carcinoma (CCC) is the second most common histotype and it frequently presents at low stage, particular among young women. However, due to its resistance to the standard platinum-based chemotherapy, there is a need to refine the therapeutic threshold and to identify new therapeutic targets. p16, IGF2BP3 and p53 have all been shown to be individual prognostic markers in all comers of CCC. In this study, we sought to evaluate whether a combination of these 3 biomarkers can identify low risk patients within stage I CCC. Additionally, we screened stage II-IV CCC for expression of existing theranostic markers.

Design: Tissue microarrays were constructed using 156 ovarian CCC (53 stage I, 61 stage II, 35 stage III and 8 stage IV). Immunohistochemical (IHC) expression for p53 was categorized as mutant-type versus wild type, while p16 and IGF2BP3 as strong block versus less. IHC status and survival was assessed using Kaplan survival analysis with the endpoint of 5-year ovarian cancer-specific survival (5-Y OCSS). The expression frequency of common theranostic markers including MET, ER, PR, VEGFR2, ALK, ROS1, TRKA-C (NTRK), and BRAF were assessed by IHC. ERBB2 (HER2) was assessed by IHC and SISH.

Results: During univariate analysis of 53 stage I CCC, p16, p53 and IGF2BP3, all identified cases with worse 5-Y OCSS but only p16 reached significance (log rank p = 0.0032). When analyzed in combinations, cases with various combinations of 2 or 3 abnormal markers showed similar survival. Cases with at least 2-marker abnormality showed 5-year OCSS of 33%, while cases with one or no abnormal biomarker expression showed 5-year OCSS of 91% (log rank <0.0001) (Figure 1). Among stage II-IV tumors, the frequency of MET overexpression is 57%, ERBB2 amplification is 6%, expression of ER is 15% and PR is 4%. The remaining theranostic biomarkers were not expressed in CCC.

Figure 1 - 1208

Figure 1: 5-year ovarian specific survival (OCSS) of cases with no abnormal biomarker expression compared to cases with at least two abnormal biomarker expressions in stage I ovarian clear cell carcinomas
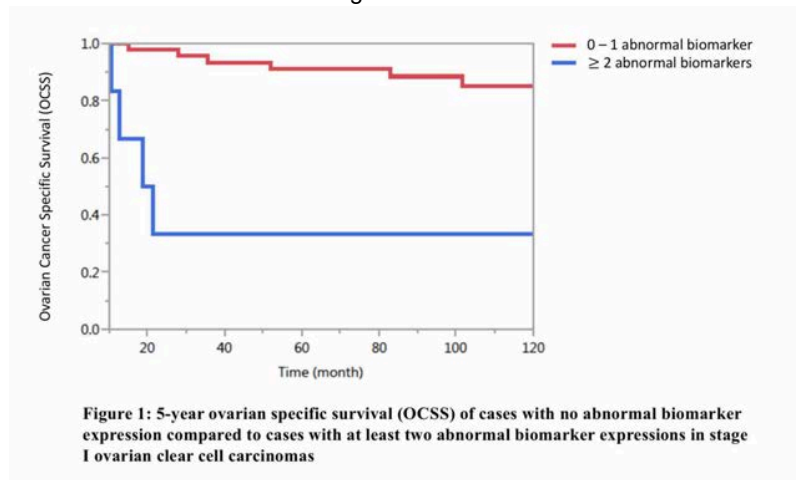
Conclusions: Normal expression in at least 2 of the 3-marker panel (p16, IGF2BP3 and p53) will identify stage I CCC with a survival threshold where clinician may consider withholding adjuvant chemotherapy. We confirm a small proportion of ERBB2 amplification in CCC that might be viable therapeutic option for high stage disease. The expression of hormone receptors is low in CCC and thus does not warrant hormonal therapy. The value of MET overexpression remains elusive. Other theranostic targets are absent and shotgun testing is discouraged.

1209 A Five-Year Retrospective Clinicopathological Analysis of Vulvar Squamous Cell Carcinoma in a Large Tertiary Care Women's Hospital

Tiannan Wang[1], Rohit Bhargava[2], Cheng Zhiqiang[3], Chengquan Zhao[4]
[1]Department of Pathology, Magee-Womens Hospital, University of Pittsburgh Medical Center, Pittsburgh, PA, [2]Magee-Womens Hospital of UPMC, Pittsburgh, PA, [3]Shenzhen People's Hospital, Shenzhen, Guangdong, China, [4]Pittsburgh, PA

Disclosures: Tiannan Wang: None; Rohit Bhargava: None; Cheng Zhiqiang: None; Chengquan Zhao: None

Background: Vulvar squamous cell carcinoma (v-SCCa) is an uncommon malignant neoplasm representing approximately 6% of all female genital cancer in US. HPV associated high grade usual intraepithelial neoplasm (uVIN) and HPV independent differentiated VIN (dVIN) are the two major precursor lesions driven by different pathways and are conclusively linked to v-SCCa carcinogenesis. This study aimed to analyze the clinicopathological features of v-SCCa and its precursor lesions, and to evaluate the clinical significance of two different pathways.

Design: A series of 210 v-SCCa were identified from archived pathology reports during the period July 2014 to June 2019. Clinicopathological features of dVIN associated v-SCCa vs. uVIN associated v-SCCa were analyzed with regard to patient age, tumor size, depth of invasion (DI), lymphovascular invasion (LVI), lymph node status (LN) if sampled, whether associated with adjacent lichen sclerosus, and pathologic stage.

Results: Total 210 v-SCCa cases from 65 (31%) biopsies, 28 (13.3%) excisional biopsies and 117 (55.7%) vulvectomies were retrospectively reviewed. Median age of women with dVIN associated v-SCCa (98 of 210, 46.7%) was 71 years (range: 34-92) vs 60 years (range: 33-98) of women with uVIN associated v-SCCa (p<0.001). 50.26% of v-SCCa women aged >50 years had d-VIN related disease as compared to 14.29% in women aged <50 years. Additionally, tumor size was larger in d-VIN associated v-SCCa cases and dVIN related v-SCCa tends to present at higher FIGO stage. Lastly, 39 of 98 (39.8%) d-VIN cases showed adjacent lichen sclerosus. 1.4% of v-SCCa showed background of low grade VIN (VIN1).

Table1. Summarized Clinicopathological Features of v-SCCa

Invasive v-SCCa No. (%)								
	Total		Negative / VIN-1		uVIN		dVIN	
	210		13 (6.2%)		99 (47.1%)		98 (46.7%)	
Mean±SE /Median age	66.1 ±1.0 / 65		69.7±3.0 / 67		61.9±1.4 / 60		70.1±1.3* / 71	
Tumor size (mm)	16.7±1.6		n/a		16.6±2.9		17.2±1.9	
Depth of Invasion (mm)	5.3±0.7		4.33±1.2		5.23±1.0		5.76±0.6	
Lymphovascular Invasion	26 (12.4%)		1 (6.7%)		12 (12.1%)		13 (13.3%)	
Positive Lymph Node	21 (10%)		1 (6.7%)		9 (9.1%)		11 (11.2%)	
FIGO Stage (AJCC 8th)	Stage IA	48 (22.9%)	2	1 (50%)	81	33 (40.7%)	84	14 (16.7%)
	Stage 1B	88 (41.9%)		1 (50%)		33 (40.7%)		54 (64.3%)
	Stage II	12 (5.7%)		0		7 (8.6%)		5 (6.0%)
	Stage III	19 (9.0%)		0		8 (9.9%)		11 (13.1%)

*p<0.01

Conclusions: Our data elaborate the important clinicopathologic features of v-SCCa and its association with precursor lesions. In summary, dVIN associated v-SCCa occurs in older populations, behaves in a more aggressive manner and presents at higher clinical stage. Moreover, aforementioned age-related disease prevalence is more prominent in our study. P53 and P16 stains can further specify a particular pathway if morphology is ambiguous.

1210 Protein Tyrosine Kinase 2 (PTK2) Overexpression in Ovarian Carcinoma is Associated with Poor Pprognosis and Distant Metastasis

Yaohong Wang[1], Yongchao Li[1], Shuyu E[1], Sonali Lanjewar[1], Jie Zhang[1], Ian Clark[2], Robert Bradley[3], Farhan Khan[3], Joel Gradowski[4], David Robins[5], David McGregor[3], Rodolfo Laucirica[1], Junming Yue[1], Mahul Amin[6]
[1]University of Tennessee Health Science Center, Memphis, TN, [2]University of Tennessee, Memphis, TN, [3]The University of Tennessee Health Science Center, Memphis, TN, [4]University of Tennessee Health Sciences Center, Germantown, TN, [5]West Cancer Clinic, Memphis, TN, [6]Methodist University Hospital, Memphis, TN

Disclosures: Yaohong Wang: None; Yongchao Li: None; Shuyu E: None; Sonali Lanjewar: None; Ian Clark: None; Farhan Khan: None; Joel Gradowski: None; David McGregor: None; Rodolfo Laucirica: None; Junming Yue: None; Mahul Amin: *Consultant*, Urogen; *Consultant*, Advanced Clinical; *Advisory Board Member*, Cell Max; *Advisory Board Member*, Precipio Diagnostics

Background: Ovarian carcinoma is among the leading causes of cancer death in women. The high-grade serous carcinoma is the most common malignant ovarian tumor and initially presents with advanced stage with widespread intrabdominal metastasis. The prognosis is poor with the five-year survival rate of less than 30% because of relapse and aggressive metastasis. There are no specific biomarkers for ovarian carcinoma with prognostic and therapeutic significance. Protein tyrosine kinase 2 (PTK2) is a member of focal adhesion kinase (FAK), which is upregulated or amplified in a variety of cancers including breast, lung, liver and colon cancer and is associated with cancer patient poor survival, tumor recurrence and metastasis. However, role of PTK2 in ovarian cancer is still largely unknown.

Design: TCGA database, SurvExpress database and Kaplan-Meier Survival database were used for gene expression profiling of human PTK2 expression. An orthotopic ovarian cancer mouse model was used for assessment of in-vivo primary tumor growth and metastasis. A complementary part of our study involved tissue selections of patients with ovarian serous carcinoma from Methodist University Hospital and West Cancer Center were stained with PTK2, PCNA, WT-1, P53, P16 and Pax8.

Results: Gene expression profiling from TCGA database shows PTK2 mRNA expression was significantly increased ($p < 0.01$) in ovarian carcinoma (n = 606) compared with control normal ovary surface epithelium (n = 10). High PTK2 mRNA expression is correlated with poor patient progress free survival (PFS) and overall survival (OS) based on Kaplan-Meier Survival database (n = 1435, $p < 0.01$). Knockout of PTK2 resulted in the inhibition of primary tumor growth and metastasis in an orthotopic ovarian cancer mouse model. Immunostaining showed increased PTK2 expression in ovarian cancer patients compared to normal ovarian surface epithelium. Further clinical data analysis showed that high PTK2 expression associates with advanced surgical stage, higher tumor grade, increased lymph node metastases, more disease relapse and poor patient survival.

Conclusions: We report for the first time that PTK2 expression is significantly upregulated in serous ovarian carcinoma promoting ovarian tumor invasion and metastasis and is associated with poor prognosis. PTK2 might be useful for risk stratification and prognostic evaluation of serous ovarian carcinoma and is a potential marker for targeted therapy.

1211 Folate Receptor Alpha Signatures in Mucosal Epithelial Cells of the Fallopian Tube: Further Evidence Supporting Tubal Origin of "Ovarian" Endometriosis

Yiying Wang[1], Yue Wang[2], Yan Wang[3], Wanrun Lin[3], Hao Chen[4], Oluwole Fadare[5], Wenxin Zheng[3]
[1]Henan Provincial People's Hospital, Zhengzhou, China, [2]Henan Provincial People's Hospital, People's Hospital of Zhengzhou University, School of Clinical Medicine, Henan University, Zhengzhou, Henan, China, [3]University of Texas Southwestern Medical Center, Dallas, TX, [4]Coppell, TX, [5]University of California San Diego, La Jolla, CA

Disclosures: Yiying Wang: None; Yue Wang: None; Yan Wang: None; Wanrun Lin: None; Hao Chen: None; Oluwole Fadare: None; Wenxin Zheng: None

Background: Endometriosis is a puzzling and debilitating disease that affects millions of women around the world. Ovary is the most common organ site involved by endometriosis. Despite various hypotheses about its cell of origin, uncertainty remains. Based on our clinicopathologic observations, we hypothesize that fallopian tube contributes the histogenesis of ovarian endometriosis.

Design: To examine if the hypothesis, tubal origin of ovarian endometriosis, has scientific supporting evidence, we identified a set of novel genes which are either highly expressed in the normal fallopian tube or in the endometrium through a gene differential array study. We then detailed examined one of the top differentially expressed gene *FOLR1* (real time qPCR) and its corresponding protein FRA expression (Western blot and immunohistochemistry) in a total of 114 formalin fixed paraffin embedded tissue sections of the fallopian tube, endometrium, and ovarian endometriosis.

Results: The differentially expressed gene *FOLR1* was validated in ovarian sections with foci of endometriosis by comparing their expression levels in the fallopian tube and the endometrium within the same patients with real-time PCR, Western blot and immunohistochemistry analysis. *FOLR1* was highly expressed in the tubal epithelia as well as in the ovarian endometriosis, while low in the paired endometrium. Results of the protein FRA expression were similarly seen by using Western blot and immunohistochemistry. Both the gene *FOLR1* and the protein FRA expression in the tissues (the fallopian tube or the ovarian endometriosis vs the endometrium) were significantly different ($p < 0.001$).

Conclusions: The study provided additional evidence supporting that ovarian endometriosis is likely derived from the fallopian tube instead of the endometrium through a retrograde menstruation. Understanding of tubal contribution to the ovarian endometriosis will certainly illicit ideas of searching for alternative ways of prevention and treatment of endometriosis.

1212 Fumarate Hydratase-Deficiency Should be Considered in the Differential Diagnosis of Uterine and Extra-Uterine Smooth Muscle Tumors of Uncertain Malignant Potential (STUMP)

Julianna J Weiel[1], Kelly Devereaux[2], Ann Folkins[2], Teri Longacre[1]
[1]Stanford University, Stanford, CA, [2]Stanford University School of Medicine, Stanford, CA

Disclosures: Julianna J Weiel: None; Kelly Devereaux: None; Ann Folkins: None; Teri Longacre: None

Background: Fumarate hydratase-deficient (dFH) leiomyomas are recognized as a distinct clinicopathologic entity occurring in the context of Hereditary Leiomyomatosis and Renal Cell Carcinoma (HLRCC) syndrome as well as the sporadic setting. Detection of dFH leiomyomas by pathologic screening can prospectively identify women at increased risk for HLRCC who may benefit from genetic counseling and surveillance for aggressive RCC.

We have recently encountered several smooth muscle tumors with atypical features for which the diagnosis of STUMP was considered; each showed at least focal morphologic features suggestive of dFH. Loss of FH expression by IHC supported classifying these tumors as atypical leiomyomas with dFH rather than STUMP and prompted review of archived STUMP cases to assess the prevalence of dFH tumors in this cohort.

Design: 48 tumors previously diagnosed as a STUMP in 40 cases from 38 patients (2007-2016) with available FFPE material were included in this retrospective study. FH IHC was performed on whole sections, with granular cytoplasmic staining of tumor cells interpreted as intact and absence of cytoplasmic staining interpreted as deficient. Normal myometrium and intratumoral vessels served as positive internal controls.

Results: Three of the 48 tumors (6.3%) were deficient for FH. These occurred in 2 patients (5.3%) including a 40-year-old with multiple abdominopelvic tumors and a 71-year-old with a uterine tumor, both with a history of prior myomectomy. One uterine tumor with dFH features in a 39 year-old showed heterogeneous loss of FH with patchy internal control staining; this was interpreted as an equivocal result (FH eq). None of the tumors with aberrant FH recurred, with a mean follow-up of 81 months.

Table 1: STUMP Cohort Features and Clinicopathologic Characteristics of Cases with Aberrant FH

	Total	dFH	FH eq
STUMP Tumors	48	3	1
NOS	31	3	1
Epithelioid	9	0	0
Myxoid	8	0	0
Site			
Uterus	36	1	1
Pelvis	5	1	0
Abdomen	5	1	0
Retroperitoneum	2	0	0
	Case 1 (dFH)	**Case 2 (dFH)**	**Case 3 (FH eq)**
Age (years)	40	71	39
Site	Pelvis, abdomen	Uterus, LUS	Uterus, Corpus
Size (cm)	9.0, 4.5	-	7.8
Multiple	Yes	No	No
Procedure	Excision	Hysterectomy	Hysterectomy
Prior myomectomy	Yes	Yes	Yes
Follow-up Length (months)	96	51	97
Recurrence	No	No	No
RCC	No	No	No
Features			
HPC-Like vessels	Yes	Yes	Focal
Edema	Yes	Yes	Yes
Atypia	Focal	Diffuse	No
Necrosis	No	Yes (Indeterminate-type)	No
Mitoses (per 10 HPF)	4	1	1
Macronucleoli	Focal	Focal	Rare
Hyaline Globules	No	Focal	No

Conclusions: 6.3% of tumors for which STUMP is a diagnostic consideration show aberrant loss of FH by IHC. Although data are limited, dFH should be considered in the differential diagnosis of STUMP when suggestive features are present, even in the context of extensive extra-uterine disease. Prospective screening for dFH in these cases may identify women at increased risk for HLRCC who may benefit from genetic counseling. Given that loss of FH is reported to occur rarely, if at all, in clinically aggressive smooth muscle tumors, the finding of dFH may support a low biologic potential for a neoplasm otherwise regarded as a STUMP. Indeed, patients with dFH tumors in this study had a benign course after complete resection with no evidence of recurrence on long term follow-up.

1213 PAX7 is a Sensitive Marker of Skeletal Muscle Differentiation in Rhabdomyosarcoma of the Female Gynecologic Tract

Julianna J Weiel[1], Dina Kokh[2], Gregory Charville[3], Teri Longacre[1]
[1]Stanford University, Stanford, CA, [2]Mountain View, CA, [3]Stanford University School of Medicine, Stanford, CA

Disclosures: Julianna J Weiel: None; Gregory Charville: None; Teri Longacre: None

Background: Rhabdomyosarcoma (RMS) is a clinically aggressive and histologically diverse mesenchymal tumor characterized by skeletal muscle differentiation. In the gynecologic tract, RMS may occur rarely in a "pure" form or more commonly as a heterologous constituent of a biphasic neoplasm such as carcinosarcoma or adenosarcoma. Discriminating RMS from its histologic mimics often relies on confirmation of skeletal muscle differentiation by morphology or immunohistochemistry (IHC) for myogenin, which can be challenging to interpret in some cases owing to limited expression. We hypothesized that IHC detection of PAX7, a paired box transcription factor involved in early lineage specification of muscle progenitor cells, may augment current approaches to the identification of RMS in gynecologic malignancies.

Design: A total of 39 cases (2010-2019) previously diagnosed as RMS in a gynecologic site were included. Cases underwent microscopic review to confirm classification. PAX7 and myogenin were assessed by IHC on whole tissue sections. MyoD1 and desmin IHC were also reviewed if available. A positive result was defined as nuclear immunoreactivity for PAX7 or myogenin in at least 5% of tumor cells; less than 5% was regarded as focal. Pattern and percentage of positive staining was recorded.

Results: Positive PAX7 expression was observed in 95% (37/39) of all gynecologic RMS (Table 1) occurring in 36 patients aged 4 to 82 (mean 56.7) years. PAX7 was positive in a greater percentage of tumor cells than myogenin in 19 cases (51%). On average, 52% of tumor cells were positive for PAX7 vs. 47% for myogenin. In most cases, both PAX7 and myogenin were expressed; however, two myogenin-negative tumors expressed PAX7 in 30-50% of cells. No cases exhibited complete absence of both markers. PAX7 expression was localized to primitive-appearing round to spindled cells, whereas myogenin was more commonly detected in maturing rhabdomyoblasts including strap cells. Cytoplasmic immunoreactivity for PAX7 was not observed.

Table 1: Immunohistochemical Expression of Skeletal Muscle Markers in Gynecologic Rhabdomyosarcoma

	Case (n)	PAX7 Positive	Myogenin Positive	MYOD1 Positive	Desmin Positive
Gynecologic Rhabdomyosarcoma (All)	39	37 (95%)	37 (95%)	4/6 (67%)	21/23 (91%)
Pure Rhabdomyosarcoma	15	14 (93%)	14 (93%)	1/3 (33%)	10/11 (91%)
Embryonal	10	10 (100%)	9 (90%)	1/2 (50%)	6/7 (86%)
Pleomorphic	4	4 (100%)	4 (100%)	-	3/3 (100%)
Alveolar (Fusion-Negative)	1	0	1	0	1
Carcinosarcoma	19	18 (95%)	17 (89%)	2/2 (100%)	9/10 (90%)
Adenosarcoma	3	3 (100%)	3 (100%)	-	-
Sertoli-Leydig Cell Tumor	1	1	1	-	-
Indeterminate (Scant Sample)	1	1	1	1/1	1/1
Site of Origin					
Vagina	4	4 (100%)	4 (100%)	-	2/2 (100%)
Cervix	4	4 (100%)	3 (75%)	0/1	3/4 (75%)
Uterus	20	18 (90%)	20 (100%)	1/2 (50%)	13/13 (100%)
Ovary	7	7 (100%)	6 (86%)	1/1	1/2 (50%)
Fallopian Tube	1	1	1	-	-
Pelvic Mass	3	3 (100%)	3 (100%)	2/2 (100%)	2/2 (100%)
Limited Biopsies (i.e. EMB or FNA)	7	6 (86%)	6 (86%)	1/1	6/6 (100%)

Conclusions: Our findings highlight the utility of PAX7 as a diagnostic marker of skeletal muscle differentiation across a broad spectrum of rhabdomyosarcomatous gynecologic tumors. We advise that PAX7 be used in combination with other markers of skeletal muscle differentiation, namely myogenin; it may be particularly helpful in cases where myogenin, MYOD1, and desmin expression is limited. The consistently low background and nuclear localization allow for straightforward interpretation of PAX7 IHC.

1214 Association between Fallopian Tubal Precursors and Adnexal Carcinosarcoma with Serous and Non-Serous Epithelial Components

Arielle Weiss[1], Barbara Norquist[1], Elizabeth Swisher[1], Thing Rinda Soong[1]
[1]University of Washington, Seattle, WA

Disclosures: Arielle Weiss: None; Barbara Norquist: None; Elizabeth Swisher: None; Thing Rinda Soong: None

Background: Pelvic carcinosarcoma (CS) has been suggested to be clonally linked to serous tubal intraepithelial carcinoma (STIC), the latter of which is known to be a precursor to high-grade serous carcinoma. Previous reports of CS with STICs were described in CS with high-grade serous carcinoma being the sole epithelial component. It is unclear whether the association is restricted to STICs or if it is affected by the extent of serous component in the tumor. We aimed to characterize the spectrum of tubal intraepithelial lesions associated with adnexal CSs that exhibit serous, mixed or non-serous epithelial differentiations.

Design: Eleven adnexal CS resection cases with serous, clear cell, and/or endometrioid epithelial components were retrospectively examined. Histologic review and p53 immunohistochemical study of all tubal blocks were performed to assess for the presence of tubal intraepithelial proliferations, including STICs, p53 signatures or serous tubal intraepithelial lesions (STILs) with atypia that did not meet the diagnostic threshold of STIC.

Results: Most (10/11) cases were stage 3 at diagnosis and occurred in post-menopausal *BRCA*-negative women. All presented as expansile masses involving bilateral adnexa. STICs were identified in the fimbriae in 7/11 cases, of which 2 involved the fallopian tubes bilaterally. STICs extended to the proximal fallopian tubes in 2 cases, and were present at multiple tubal sites in 4 patients. P53 signatures and STILs were seen in 4 subjects, with 1 being an isolated lesion in a STIC-negative resection. High-grade serous morphology was identified in 10/11 cases but its extent varied from minimal (<10%) to prominent (>90%) in the tumors. Clear cell and endometrioid morphologies were present as the predominant (>90%) epithelial component in 3 and 2 cases respectively. The majority of tubal intraepithelial lesions shared identical p53 staining profile with the concurrent tumors in the adnexa (Table 1).

Figure 1 - 1214

Table 1. Characteristics of carcinosarcoma and tubal intraepithelial lesions								
	Carcinosarcoma				Tubal intraepithelial lesion			
	Epithelial component		Sarcomatous component		STIC		STIL and/or p53 signature	
Case ID	Morphologic component (% extent in epithelial component)	p53 IHC status	% extent in tumor	p53 IHC status	Present	p53 IHC status	Present	p53 IHC status
1	Endometrioid (95%) Serous (5%)	Variable	50%	Variable	No	N/A	No	N/A
2	Endometrioid (90%) Serous (10%)	Variable	<10%	Variable	Yes	Over-expressed	No	N/A
3	Serous (≥90%) Undifferentiated (<10%)	Over-expressed	30%	Over-expressed	Yes	Over-expressed	No	N/A
4	Serous (≥80%) Undifferentiated (<20%)	Over-expressed	40%	Over-expressed	Yes	Over-expressed	Yes	Over-expressed
5	Serous (≥90%) Undifferentiated (<10%)	Over-expressed	30%	Over-expressed	Yes	Over-expressed	Yes	Over-expressed
6	Serous (≥90%) Undifferentiated (<10%)	Null	10%	Null	Yes	Null	Yes	Null
7	Serous (80%) Endometrioid (20%)	Over-expressed	<10%	Over-expressed	No	N/A	No	N/A
8	Clear cell (>95%)	Null	50%	Null	No	N/A	Yes	Over-expressed
9	Clear cell (≥90%) Serous (<10%)	Null	<10%	Null	No	Null	No	N/A
10	Clear cell (≥95%) Serous (<5%)	Null	10%	Null	Yes	Null	No	N/A
11	Undifferentiated (70%) Serous (30%)	Null	10%	Null	Yes	Null	No	Null

Conclusions: Our series reveals a spectrum of tubal intraepithelial lesions ranging from p53 signatures to STICs in more than 50% of adnexal CS cases with matching p53 profiles. The association is present even in tumors with minor serous component at the time of resection. The observation suggests that a significant portion of CSs might have been derived from serous tubal precursors. The findings have implications for treatment, as well as early detection and prevention of these highly aggressive tumors.

1215 Molecular Triage Strategies for HPV Primary Screening

Christine White[1], Stephen Reynolds[2], Padmaja Naik[3], Roisin O' Brien[3], Trinh Pham[4], Helen Keegan[3], Niamh Kernan[3], Loretto Pilkington[5], Imogen Sharkey Ochoa[1], Fiona Wright[6], Prerna Tewari[1], Sharon O'Toole[7], Charles Normand[1], Linda Sharp[8], Grainne Flannelly[9], Cara Martin[7], John O'Leary[1]
[1]Trinity College Dublin, Dublin, Ireland, [2]CERVIVA, Dublin, Ireland, [3]Coombe Women & Infants University Hospital, Dublin, Ireland, [4]Beacon Hospital, Dublin, Lenster, Ireland, [5]Coombe Women & Infants University Hospital, Dublin, Dublin, Ireland, [6]National Cervical Screening Programme, Limerick, Limerick, Ireland, [7]Trinity St. James's Cancer Institute, Dublin, Ireland, [8]Newcastle University, United Kingdom, [9]National Maternity Hospital, Sandymount, Ireland

Disclosures: Christine White: None; Stephen Reynolds: None; Padmaja Naik: None; Roisin O' Brien: None; Trinh Pham: None; Helen Keegan: None; Niamh Kernan: None; Loretto Pilkington: None; Imogen Sharkey Ochoa: None; Fiona Wright: None; Prerna Tewari: None; Sharon O'Toole: None; Cara Martin: None; John O'Leary: None

Background: Appropriate triage of HPV primary cervical screening is a key challenge. This study investigates a panel of molecular triage options including HPV16/18 genotyping, cytology, p16/Ki-67 and methylation markers [CADM1, MAL, miR1-124] in women who test positive for HPV in primary screening.

Design: In partnership with CervicalCheck, The National Cervical Screening programme, CERVIVA are undertaking a longitudinal observational HPV primary screening study which will evaluate different triage strategies for management of a HPV-positive primary screening test. Cervical cytology samples from approximately 13,000 women undergoing routine cervical screening are tested for HPV DNA (cobas 4800 HPV test) and mRNA (Aptima HPV assay). All HPV-positive women are further assessed with HPV16/18 genotyping, cytology, p16/Ki-67 dual staining and methylation markers [CADM1, MAL, miR1-124]. The performance of different triage strategies will be examined both cross-sectionally and longitudinally over two screening rounds for detection of CIN2+.

Results: From the overall study population 15.7% (1653/10,528) tested positive for HPV DNA and 12.8% (1613/12,601) tested positive for HPV mRNA. Overall, 31.2% (514/1650) of HPV DNA positive women were positive for HPV16/18, 33.2% (548/1650) had an abnormality on cytology, 36.6% (404/1104) tested positive for p16/Ki-67 and 39.9% (393/993) tested positive for methylation markers [CADM1, MAL, miR1-124]. Clinical performance was assessed in a range of combinations for detection of CIN2+, sensitivity ranged from 57-96% and specificity from 46-96%.

Conclusions: Here we present an update on the longitudinal follow up and clinical performance in relation in to each of the putative triage tests.

1216 Combined CCNE1 High-Level Amplification and Overexpression is Associated with Unfavorable Outcome in Tubo-Ovarian High-Grade Serous Carcinoma

Nicholas Wiebe[1], Angela Chan[2], Emeka Enwere[1], John McIntyre[1], Linda Cook[3], Martin Kobel[4]
[1]University of Calgary, Calgary, AB, [2]Alberta Health Services, Caglary, AB, [3]University of New Mexico Health Sciences Center, Albuquerque, NM, [4]University of Calgary/Alberta Public Laboratories, Calgary, AB

Disclosures: Nicholas Wiebe: None; Angela Chan: None; Emeka Enwere: None; John McIntyre: None; Linda Cook: None; Martin Kobel: None

Background: *CCNE1* amplification is one of the few recurrent alterations in chromosomally unstable tubo-ovarian high-grade serous carcinoma (HGSC). High level *CCNE1* amplifications are mutually exclusive to germline BRCA1/2 mutations and associated with unfavorable outcome. We investigated whether immunohistochemistry (IHC) can be used to identify *CCNE1* amplification status and whether *CCNE1* high-level amplification status and overexpression can be prognostic in high-grade serous carcinoma.

Design: A training set of 528 tubo-ovarian high-grade serous carcinoma samples were stained via two optimized IHC assays then subjected to digital image analysis and visual scoring. DNA and RNA CISH for *CCNE1* were performed. Receiver operating characteristic (ROC) curves were used to identify optimal cut-offs. Using the optimal cut offs identified from the training set, survival analyses were performed and validated in an independent testing set of 764 tubo-ovarian high-grade serous carcinomas. Combined amplification/expression status was evaluated in a combined set with complete data (N=1114).

Results: *CCNE1* high-level amplification was present in 10.2% of cases in the training set and 11.2% in the combined cohort. ROC curve analyses identified 60% positive tumor cells by immunohistochemistry as the optimal cut-off to correlate *CCNE1* high-level amplification with 81.6% sensitivity and 77.2% specificity. *CCNE1* high-level amplification and overexpression were associated with survival in both the training and the testing set. The combination *CCNE1* high-level amplification and overexpression was observed in 8.3% of patients and are significantly associated with a higher risk of ovarian cancer caused death in multivariate analysis adjusted for age, stage and cohort (HR=1.78, 95 CI% 1.38-2.26, p<0.0001). There were no significant difference among the other three combinations (high-level amplification/low expression; low-level amplification/high expression; low-level amplification/low expression).

Figure 1 - 1216
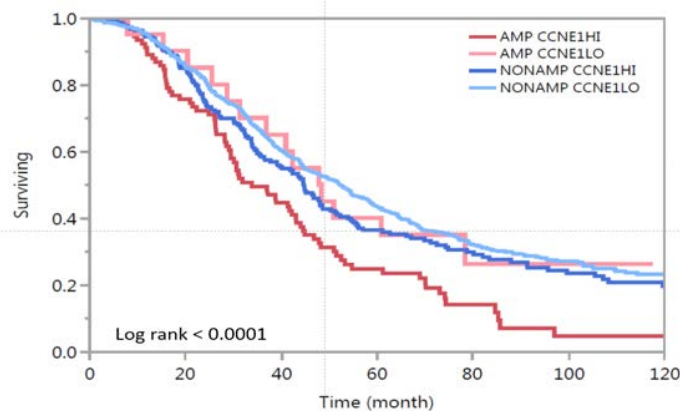
Conclusions: Our results suggest that CCNE1 immunohistochemistry can serve as a prognostic marker because only high-grade serous carcinomas patients whose tumors show the combination of high-level *CCNE1* amplification with overexpression can be expected to have an unfavorable outcome. This may also define a group of patients that require new treatment regimens.

1217 Recurrent Intrachromosomal FOXO1-LINC00598 Rearrangement Characterize a Novel Subtype of Leiomyosarcoma with Variant Cell Morphology

Erik Williams[1], Meagan Montesion[2], Radwa Sharaf[2], Nikunj Shah[2], Julie Tse[1], Vincent Miller[2], Dean Pavlick[2], Natalie Danziger[3], Jo-Anne Vergilio[2], Keith Killian[2], Siraj Ali[4], Julia Elvin[2], Douglas Lin[2]
[1]Boston, MA, [2]Foundation Medicine, Inc., Cambridge, MA, [3]Foundation Medicine, Inc., Somerville, MA, [4]Cambridge, MA

Disclosures: Erik Williams: *Stock Ownership*, F. Hoffman La-Roche, Ltd.; *Employee*, Foundation Medicine, Inc.; Meagan Montesion: *Employee*, Foundation Medicine; *Stock Ownership*, Roche; Radwa Sharaf: *Employee*, Foundation Medicine; Nikunj Shah: None; Julie Tse: *Employee*, Foundation Medicine, Inc.; *Consultant*, Pathology Watch, LLC.; Vincent Miller: *Employee*, Foundation Medicine / Roche; *Stock Ownership*, Foundation Medicine / Roche; *Advisory Board Member*, Revolution Medicines; *Stock Ownership*, Revolution Medicines; Dean Pavlick: *Employee*, Foundation Medicine; *Stock Ownership*, F. Hoffmann-La Roche AG; Natalie Danziger: *Employee*, Foundation Medicine Incorporated; Jo-Anne Vergilio: *Employee*, Foundation Medicine, Inc; *Employee*, Foundation Medicine, Inc; Keith Killian: *Employee*, FMI; Siraj Ali: *Employee*, Foundation Medicine; *Advisory Board Member*, INcysus Therapeutics; *Consultant*, Takeda; Julia Elvin: *Employee*, Foundation Medicine, Inc; *Employee*, Hoffman La Roche; Douglas Lin: *Employee*, Foundation Medicine

Background: Due to their biological significance and tumor-specific expression, gene rearrangements and fusions are often defining molecular events of specific tumor types, particularly in sarcomas. Alveolar rhabdomyosarcoma is characterized by *PAX3-FOXO1* and *PAX7-FOXO1* fusions, where breakpoints occur in *FOXO1* intron 1, and reciprocal transcripts are often expressed. In the current study, we identity a novel recurrent *FOXO1* rearrangement in a subset of leiomyosarcoma (LMS).

Design: Our case archive of >200,000 clinical samples that had undergone comprehensive genomic profiling using a hybrid capture based sequencing platform was searched for leiomyosarcoma with structural variants in *FOXO1.* Pathology reports and histopathology were reviewed. Patient clinical data was collected.

Results: 16 of 2359 (0.7%) soft tissue and visceral LMS had a structural variant in *FOXO1*. All *FOXO1* breakpoints occurred in intron 1. A recurrent intrachromosomal rearrangement involving 5' *FOXO1* and 3' *LINC00598*, a long noncoding RNA gene, was identified in 7 LMS. Additional non-recurrent *FOXO1* partners were identified in remaining 9 LMS, 4 fused with the 5' end of *FOXO1* and 5 with the 3' end. No reciprocal transcript was identified in any LMS. The *FOX01* fusion-positive LMS was observed to occur exclusively in female adults (median age=54, range 45-78 years). 12 of 16 were of known uterine or pelvic origin. The most frequent other genomic alterations (GA) observed in the *FOX01* fusion-positive LMS were in *TP53* (75%), *RB1* (56%), and *ATRX* (50%), and *PTEN* (25%). 11/16 (69%) *FOX01* fusion-positive LMS displayed at least one form of variant-cell morphology: 8 of 16 (50%) with areas of rhabdoid morphology (p<0.05, as compared to 20 *FOX01* fusion-negative LMS; Fig 1) and 7/16 with areas of pleomorphic giant cells (Fig 2). In 10 of the 11 variant-cell cases, we identified 5' *FOXO1* fusion transcripts.

Figure 1 - 1217
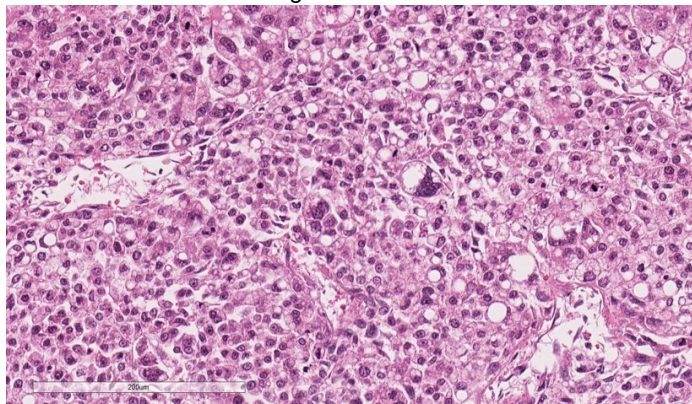
Figure 2 - 1217
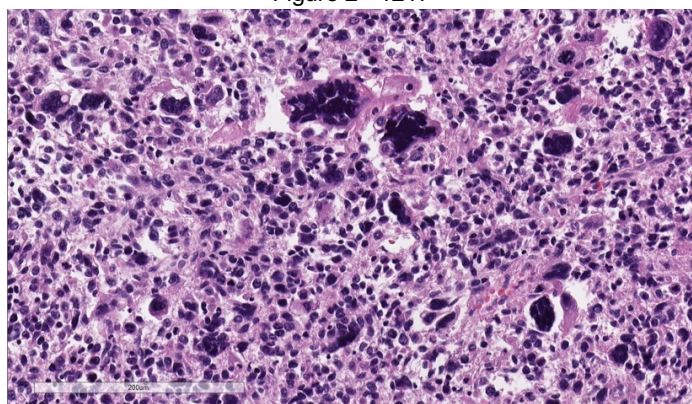
Conclusions: Non-canonical *FOXO1* rearrangements, particularly *FOXO1-LINC00598*, are recurrently identified in female adult LMS, and the majority show variant morphologic features, specifically, focal areas of rhabdoid and/or pleomorphic giant cell morphology. The identification of this fusion may offer insights into the biology of LMS and suggests the need for focused investigation to delineate the pro-oncogenic functions of these novel rearrangements, along with possible sensitivity to targeted therapies.

1218 SATB2 May Be Useful in Distinction of Atypical Polypoid Adenomyoma from Benign Adenomyomatous Polyps and Myoinvasive Carcinoma on Biopsy

Helen Worrell[1], Andrew Sciallis[2], Stephanie Skala[2]
[1]Michigan Medicine, University of Michigan, Novi, MI, [2]University of Michigan, Ann Arbor, MI

Disclosures: Helen Worrell: None; Andrew Sciallis: None; Stephanie Skala: None

Background: Atypical polypoid adenomyoma (APAM) is an uncommon uterine lesion composed of complex endometrioid glands, frequent squamous morular metaplasia, and smooth muscle stroma with short interlacing fascicles. On endometrial curettage, biopsy, or polypectomy specimens, the presence of endometrioid glands and smooth muscle stroma raises the differential diagnosis of myoinvasive endometrioid carcinoma. APAM is thought to behave similar to complex atypical hyperplasia; recurrence is not uncommon and endometrial carcinoma is subsequently diagnosed in approximately 9% of patients. Reproductive age patients with APAM have the option of preservation of fertility, whereas myoinvasive endometrioid carcinoma is treated by hysterectomy. One study has reported an incidental finding that the stroma of APAM is positive for SATB2, whereas the stroma of other polypoid lesions is not. We aim to assess whether SATB2 is useful stain for distinction of APAM from myoinvasive endometrioid carcinoma on endometrial biopsies or curettings.

Design: The surgical pathology and consultative archives of a single large academic institution was searched for cases of "atypical polypoid adenomyoma" (n=27), "adenomyomatous polyp" (n=45), and "myoinvasive endometrioid carcinoma" (n=16) sampled between 1989 and 2019. Study pathologists reviewed all cases to confirm the diagnosis and assess various morphologic features. The intensity and extent of nuclear SATB2 expression in the epithelial and stromal components of each lesion were recorded.

Results: SATB2 expression was seen in the stromal component of 25/27 (93%) APAM, compared to 0/45 (0%) benign adenomyomatous polyps and 4/16 (25%) myoinvasive endometrioid carcinomas. Stromal SATB2 reactivity in myoinvasive carcinomas was limited to rounded stromal cells in the surface component of the tumor; stroma surrounding invasive foci was negative for SATB2. Weak/moderate nuclear SATB2 staining was occasionally seen in vessel walls (focal), lipoleiomyomas, and flat endometrium adjacent to a polyp. All entities showed frequent SATB2 reactivity in squamous morules (when present), as well as scattered positive cells in areas of tubal metaplasia.

Conclusions: Based on our data, SATB2 reactivity in fibromuscular stroma separating atypical endometrioid glands may support a diagnosis of APAM rather than myoinvasive endometrioid carcinoma. SATB2 immunohistochemistry shows potential to be a useful adjunct tool accompanying careful morphologic evaluation of endometrial biopsies or curettings.

1219 Beta-Catenin Expression in Endometrioid Intraepithelial Neoplasia (Atypical Hyperplasia)

Martha Wright[1], Sarah Fitzlaff[2], Autumn Wyeth[3], Matthew Zaragoza-Watkins[4], Mirna Podoll[1], Charles Quick[5], Jaclyn Watkins[1]
[1]Vanderbilt University Medical Center, Nashville, TN, [2]Vanderbilt University School of Medicine, Nashville, TN, [3]University of Arkansas for Medical Science (UAMS), Little Rock, AR, [4]Vanderbilt University, Nashville, TN, [5]University of Arkansas for Medical Sciences, Little Rock, AR

Disclosures: Martha Wright: None; Sarah Fitzlaff: None; Autumn Wyeth: None; Matthew Zaragoza-Watkins: None; Mirna Podoll: None; Charles Quick: None; Jaclyn Watkins: None

Background: Beta-catenin (BC) mutations are associated with a high risk of recurrence in otherwise low-grade, early stage endometrioid adenocarcinomas. Recent literature suggests nuclear BC expression by immunohistochemistry is highly sensitive and specific for BC mutations. The significance of BC expression in endometrioid intraepithelial neoplasia (EIN/atypical hyperplasia) has yet to be explored.

Design: Cases meeting current diagnostic criteria for EIN based on H&E examination were obtained from two institutions (years 1999-2014). Patterns of altered differentiation (e.g., tubal, squamous morular, mucinous, secretory) were noted. Representative blocks were stained for BC and PAX2, and expression patterns recorded. Follow-up and demographic data was obtained from the electronic medical record where available.

Results: 99 cases were included (86 biopsies, 13 hysterectomies). BC nuclear expression outside of squamous morules was identified in 36% of cases. Patients with non-morular nuclear BC staining were significantly younger (mean 44.8 vs 56.7, p<0.005). Non-morular nuclear BC expression in biopsies was not significantly associated with the presence of carcinoma on subsequent hysterectomy (p=0.5). Cases with tubal and mucinous differentiation were significantly less likely to demonstrate non-morular nuclear BC staining than cases with no specific pattern of differentiation (p<0.005, p=0.016, respectively). Results were equally robust when limiting analyses to cases of EIN with PAX2 loss (72% of cases).

Conclusions: EIN, especially in young women and in cases without tubal or mucinous differentiation, commonly demonstrates non-morular nuclear BC positivity. This finding suggests that BC mutation may be an early event in the progression towards endometrioid adenocarcinoma. Further, our data suggests that tubal and mucinous differentiation may be morphologic correlates of non-BC mutated EIN.

1220 Genetic Alterations in Mullerian adenosarcoma with High-Grade Sarcoma Components

Xinyu Wu[1], Amir Momeni Boroujeni[2], Robert Soslow[3], Britta Weigelt[3]
[1]New York, NY, [2]Memorial Sloan Kettering Cancer Center, Brooklyn, NY, [3]Memorial Sloan Kettering Cancer Center, New York, NY

Disclosures: Xinyu Wu: None; Amir Momeni Boroujeni: None; Robert Soslow: *Speaker*, Ebix/Oakstone; Britta Weigelt: None

Background: Mullerian adenosarcoma (AS) is a biphasic tumor composed of benign epithelial and neoplastic mesenchymal elements. These uncommon tumors generally have a low malignant potential. However, patients with high-grade sarcoma component often have poor outcome. We aimed to investigate the clinico-pathologic and molecular characteristics of ASs with high-grade sarcoma components.

Design: A total of 10 ASs with high-grade sarcoma components were included in this study and evaluated using a next-generation-sequencing panel targeting cancer-related genes. Cases were reviewed in detail to evaluate their clinico-pathologic features and outcome.

Results: The patients' age at diagnosis ranged from 23 to 71 years (mean 46 years). Stromal overgrowth was seen in nine cases (90%) and the mitotic index ranged from 6 to 58/10 HPFs. Myometrial invasion was present in 50% (4/8) of tumors with uterine corpus involvement. Three AS showed heterologous elements (chondroid, n=1; rhabdomyosarcoma n=2). Six patients (60%) developed metastatic disease. The ASs harbored few non-synonymous mutations, but were genetically heterogeneous. *DICER1* and *ARID1A* were the most frequently mutated genes (30% each). Two ASs harbored *CDKN2A* deletions (20%), which were mutually exclusive with *TERT* amplification/ promoter mutation in two other Ass (20%). *SMARCB1* loss-of-function mutations were present in one case, and *BAP1* deletions were found in two ASs. *ARID1A, KRAS* and *PIK3CA* mutations were found in 20% of ASs with metastasis. Two ASs with rhabdomyosarcomous differentiation harbored *DICER1* mutations.

Figure 1 - 1220
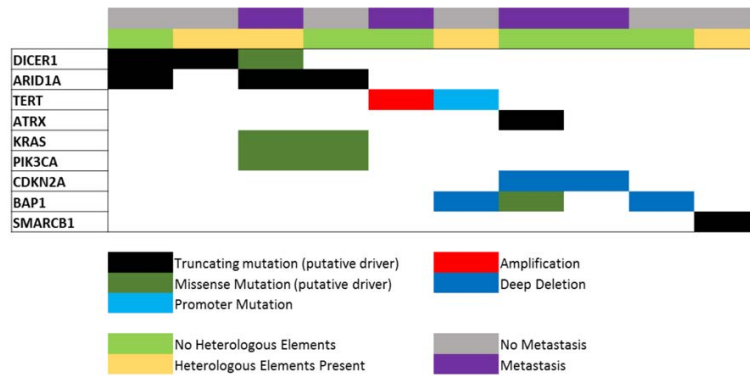
Conclusions: In this series, mullerian AS with high-grade sarcoma components showed high mitotic index and myometrial invasion along with lymphovascular invasion and heterologous elements. ASs were genetically heterogeneous and included *DICER1* mutation, alterations of chromatin remodeling genes (*ARID1A, BAP1, SMARCB1*) as well as *TERT* and *CDKN2A* alterations.

1221 Mutational Analysis of Ovarian Thecomas Suggests Molecular Kinship to Granulosa Cell Tumours

Ellen Yang[1], Anjelica Hodgson[2], Sasha Blay[3], David Swanson[3], George Charames[3], Gulisa Turashvili[3]
[1]Department of Laboratory Medicine and Pathobiology, Faculty of Medicine, University of Toronto, Toronto, ON, [2]University of Toronto, Toronto, ON, [3]Mount Sinai Hospital, Toronto, ON

Disclosures: Ellen Yang: None; Anjelica Hodgson: None; Sasha Blay: None; David Swanson: None; George Charames: None; Gulisa Turashvili: None

Background: Alterations in *FOXL2* are commonly identified in a number of ovarian sex cord-stromal tumours, especially granulosa cell tumours (GCTs). There is considerable debate regarding the genesis of thecomas (TCs) and fibrothecomas (FTCs) and how they relate to pure morphological fibromas and GCTs. With this background information in mind, we aimed to genomically interrogate these tumours, in order to establish any evident mutational relationship.

Design: The study cohort includes 33 tumours originally diagnosed as GCT (n=14), TC (n=8), FTC (n=8) and cellular fibroma (CF; n=3). All cases were reviewed to confirm the original morphological diagnoses and reticulin staining was evaluated in all non-GCTs. TruSight Tumor 15 next generation sequencing assay was used to assess 15 genes commonly mutated in cancers. Detected mutations were confirmed as likely pathogenic or pathogenic based on review of ClinVar and COSMIC databases. P53 immunohistochemistry was performed in all cases with a pathogenic *TP53* mutation and staining was assessed as normal (wild-type) and aberrant (overexpressed or null).

Results: Most (12/19) non-GCTs displayed pericellular reticulin staining pattern around individual cells while focal nested staining pattern was seen in 7 cases including 5/8 TCs and 2/8 FTCs. All 33 tumours were successfully sequenced. CFs did not harbor any mutations in genes surveyed by the TruSight 15 panel. *FOXL2* mutation (all c.402C>G, p.Cys134Trp) was detected in a total of 19 cases including 12 GCTs (86%), 6 TCs (75%), and 1 FTC (13%). Most (6/7) morphological non-GCT tumors with focal nested staining pattern were *FOXL2*-mutated. Only 1 *FOXL2*-mutated TC showed pericellular staining pattern. A variety of *TP53* mutations were identified in 9 cases (8 GCTs, 1 FTC), of which 6 had concurrent *FOXL2* mutations. *EGFR* mutation (c.2369C>T; p.Thr790Met) was detected in 1 GCT which also harbored concurrent *TP53* mutation. P53 protein was expressed in a wild-type pattern in all cases with *TP53* mutation with the exception of 1 GCT which showed a null phenotype.

Conclusions: We confirm that the majority of GCTs harbor mutations in *FOXL2*, in addition to a significant proportion of morphological TCs, most of which show at least focally altered reticulin staining; these tumours may represent GCTs with prominent TC-like foci. In these tumours, *TP53* mutations do not seem to correlate with abnormal p53 protein expression as assessed by immunohistochemistry. CFs and FTCs appear to be mostly unrelated to GCTs and TCs.

1222   Retrospective Review of Products of Conception with Atypical Villous Morphology: Histological, Immunohistochemical and Genetic Features with Clinical Correlation

Ellen Yang[1], William Parks[2], Gulisa Turashvili[3]
[1]Department of Laboratory Medicine and Pathobiology, Faculty of Medicine, University of Toronto, Toronto, ON, [2]University of Toronto, Toronto, ON, [3]Mount Sinai Hospital, Toronto, ON

Disclosures: Ellen Yang: None; William Parks: None; Gulisa Turashvili: None

Background: The finding of chorionic villi with non-specific changes, such as edema, irregular shape, trophoblast pseudoinclusions and focal trophoblast hyperplasia, typically raises a broad differential diagnosis including partial hydatidiform mole (PHM), hydropic abortus (HA), non-molar aneuploidy (NMA), and placental mesenchymal dysplasia (PMD). Distinguishing between PHM and its mimics often requires ancillary studies. We set out to review the clinical, pathologic and genetic features of AVM with the intent of improving diagnostics and use of genotyping in the future.

Design: A retrospective analysis of products of conception (POC) at a large tertiary hospital identified 200 cases of AVM (complete moles excluded) that underwent quantitative fluorescence-polymerase chain reaction analysis (QF-PCR) with molar genotyping. Blinded to the original diagnoses, 180 cases with available slides were reviewed. Clinical findings, p57 immunohistochemistry (IHC) and cytogenetic reports were also assessed.

Results: The cohort includes 93 HAs, 45 PHMs, 34 NMAs, 2 PMDs, and 6 cases with no diagnosis favored. The median maternal age was 33 years (16-49), and the median gestational age was 9 weeks (5-19). Clinical presentations included 57 missed abortions, 6 incomplete abortions, 22 miscarriages (including 7 recurrent miscarriages), 6 pregnancy terminations, and 3 in vitro fertilizations. A total of 36 cases (20%) failed cytogenetic testing, with maternal cell contamination being the culprit in 47%. The presence of diandric triploidy by QF-PCR supported the diagnosis of PHM in 69% of cases, whereas PHM was favored based on the morphology in the remaining 31% with failed QF-PCR. Both PMD cases showed normal genotype with retained p57 in cytotrophoblast and lack of staining in villous stroma. All diagnostic categories showed overlapping morphologic features. The diagnosis of PHM was associated with biphasic morphology (91%), ≥30% villous edema (100%), >50% edematous villi (73%), cistern formation (60%) and trophoblast pseudoinclusions (87%) (p≤0.037).

	Partial Hydatidiform Mole	Hydropic Abortus	Aneuploidy Non-molar	Placental Mesenchymal Dysplasia	Unclassifiable	All
Number of Cases, %	45 (25%)	93 (52%)	34 (19%)	2 (1%)	6 (3%)	180
Maternal Age, median (range); years	31 (20-42)	33.5 (23-49)	37.5 (20-45)	33 (33-33)	27.5 (16-35)	33 (16-49)
Gestational Age, median (range); weeks	11 (6-13)	9 (5-18)	13 (7-19)	7 (5-9)	8 (6-8)	9 (5-19)
Microscopic Description						
Biphasic	41 (91%)	22 (24%)	14 (41%)	2 (100%)	3 (50%)	82
Hydropic (>3 mm/villus)	45 (100%)	83 (89%)	29 (85%)	2 (100%)	4 (67%)	163
Hydropic (% on low power field)						
80-90%	2 (4%)	1 (1%)	0	0	0	3
70-80%	14 (31%)	3 (3%)	0	0	1 (17%)	18
60-70%	7 (16%)	6 (6.5%)	4 (12%)	0	0	17
50-60%	10 (22%)	6 (6.5%)	5 (15%)	1 (50%)	0	22
40-50%	6 (14%)	12 (13%)	5 (15%)	0	0	23
30-40%	2 (4%)	12 (13%)	6 (17%)	0	0	20
20-30%	4 (9%)	22 (24%)	8 (24%)	1 (50%)	2 (33%)	37
10-20%	0	16 (17%)	3 (9%)	0	2 (33%)	21
0-10%	0	15 (16%)	3 (9%)	0	1 (17%)	19
Cistern Formation	27 (60%)	19 (20%)	6 (18%)	1 (50%)	1 (17%)	54
Irregular Shape	45 (100%)	92(99%)	33 (97%)	2 (100%)	6 (100%)	178
Trophoblast Pseudoinclusions	39 (87%)	32 (34%)	17 (50%)	1 (50%)	3 (50%)	92
Trophoblast Hyperplasia (focal)	10 (22%)	25 (27%)	6 (18%)	0	1 (17%)	42
Stromal Karyorrhexis	4 (9%)	7 (7.5%)	6 (17%)	0	0	17
Nucleated Red Blood Cells	9 (20%)	12 (13%)	2 (6%)	0	1 (17%)	24
P57 Immunohistochemistry						
Retained in Both Cytotrophoblast and Villous Stroma	39 (87%)	74 (80%)	15 (44%)	0	5 (83%)	133
Retained in Cytotrophoblast, Lost in Villous Stroma	1 (2%)	0	0	2 (100%)	0	3
Retained in Cytotrophoblast, reduced in Villous Stroma	2 (4%)	2 (2%)	1 (3%)	0	0	5
Not performed	3 (7%)	17 (18%)	18 (53%)	0	1 (17%)	39
Quantitative Fluorescence-Polymerase Chain Reaction						
Trisomy 4	0	0	1 (3%)	0	0	1
Trisomy 13	0	0	5 (15%)	0	0	5
Trisomy 18	0	0	10 (24%)	0	0	10
Trisomy 21	0	0	7 (21%)	0	0	7
Trisomy 22	0	0	2 (6%)	0	0	2
Monosomy X	0	0	5 (15%)	0	0	5
Monosomy 16 and trisomy 21	0	0	1 (3%)	0	0	1
Diandric Triploidy	31 (69%)	0	0	0	0	31
13q14 Deletion	0	0	1 (3%)	0	0	1
Xp22.31 Deletion	0	0	2 (6%)	0	0	2
Normal	0	77 (83%)	0	2 (100%)	0	79
Failed	14 (31%)	16 (17%)	0	0	6 (100%)	36

Conclusions: Most POCs with AVM represent non-molar HAs. Both HA and NMA exhibit morphologic features closely mimicking PHM. Although the presence of some features may indicate a higher likelihood of PHM, p57 IHC in conjunction with QF-PCR is crucial for accurate diagnosis of PHM and recognition of its mimics. A low threshold should be maintained for these ancillary studies and/or subspecialty consultation when the diagnosis of PHM is in question.

1223 Distinct Clinicopathological Features of Endometrial Mesonephric-like Adenocarcinoma

Mitsutake Yano[1], Tomomi Katoh[1], Akira Yabuno[1], Naoki Ogane[2], Kozue Ito[1], Mariko Miyazawa[3], Masaki Miyazawa[3], Kosei Hasegawa[1], Hisashi Narahara[4], Masanori Yasuda[1]
[1]Saitama Medical University International Medical Center, Hidaka, Japan, [2]Kanagawa Prefectural Ashigarakami Hospital, Ashigarakami, Japan, [3]Tokai University School of Medicine, Isehara, Japan, [4]Oita University Faculty of Medicine, Yufu, Japan

Disclosures: Mitsutake Yano: None; Tomomi Katoh: None; Akira Yabuno: None; Naoki Ogane: None; Kozue Ito: None; Mariko Miyazawa: None; Masaki Miyazawa: None; Kosei Hasegawa: None; Hisashi Narahara: None; Masanori Yasuda: None

Background: Endometrial mesonephric-like adenocarcinoma is morphologically and immunophenotypically similar to mesonephric carcinoma. Diffuse positive reaction of GATA binding protein 3 (GATA3) or transcription termination factor 1 (TTF-1) is of diagnostic significance for mesonephric-like adenocarcinoma. However, its clinicopathological features have not yet been clarified.

Design: 533 cases of endometrial carcinoma were recruited to analyze their clinical, morphological, and immunohistochemical features. Immunohistochemical analysis was performed to evaluate GATA3, TTF-1, estrogen receptor, and TP53 expression using tissue microarray sections.

Results: Mesonephric-like adenocarcinoma, low-grade endometrial carcinomas (endometrioid carcinoma G1/2), and high-grade endometrial carcinomas (endometrioid carcinoma G3, serous carcinoma, clear cell carcinoma, and others) accounted for 3.2% (17 cases), 75% (401 cases), and 22% (115 cases), respectively. Mesonephric-like adenocarcinoma was closely associated with advanced age ($p = 0.012$), high lymphovascular invasion ($p = 0.048$), deep myometrial invasion ($p = 0.038$), and mortality ($p = 0.032$) compared with low-grade endometrial carcinoma. Patients with mesonephric-like adenocarcinoma showed unfavorable progression-free survival and overall survival compared with patients with low-grade endometrioid carcinoma ($p = 0.048$ and $p = 0.032$, respectively). However, there were no significant associations between mesonephric-like adenocarcinoma and high-grade endometrial carcinomas with regard to clinicopathological characteristics, and no significant differences in progression-free or overall survival were observed. In multivariate survival analyses, independent prognostic factors included histology of mesonephric-like adenocarcinoma in comparison with low-grade endometrial carcinoma (progression-free survival, hazard ratio: 2.73, $p = 0.037$; overall survival, hazard ratio: 3.06, $p = 0.028$), high-grade endometrial carcinoma compared with low-grade endometrial carcinoma (progression-free survival, hazard ratio: 2.52, $p < 0.001$; overall survival, hazard ratio: 3.62, $p < 0.001$), myometrial invasion, and FIGO stage.

Conclusions: We would like to emphasize that endometrial mesonephric-like adenocarcinoma may be not infrequent (approximately 3%) among variable endometrial carcinomas and that it is potentially identical to high-grade endometrial carcinoma. Therefore, it should be distinguished from low-grade endometrial carcinoma in order to select an appropriate therapy.

1224 Mutational Spectrum in Clinically Aggressive Low-Grade Serous Carcinoma/Serous Borderline Tumors of the Ovary

Ju-Yoon Yoon[1], Kyle Devins[2], Emily Ko[3], Robert Burger[2], Carolina Reyes[4], Ronny Drapkin[1], Lauren Schwartz[5]
[1]Perelman School of Medicine at the University of Pennsylvania, Philadelphia, PA, [2]Hospital of the University of Pennsylvania, Philadelphia, PA, [3]University of Pennsylvania Health System, Philadelphia, PA, [4]University of Pennsylvania, Philadelphia, PA, [5]Perelman School of Medicine at the University of Pennsylvania, Bala Cynwyd, PA

Disclosures: Ju-Yoon Yoon: None; Kyle Devins: None; Robert Burger: *Consultant*, Tesaro; *Consultant*, Merck; *Consultant*, Morphotek; *Consultant*, Roche; Carolina Reyes: None; Ronny Drapkin: *Advisory Board Member*, Repare Therapeutics; *Advisory Board Member*, Siamab Therapeutics; *Consultant*, Mersana Therapeutics; Lauren Schwartz: None

Background: While reported to be generally driven by mutations in the Ras/MAPK signaling pathway genes, the mutational spectra of low-grade serous carcinoma (LGSC) and serous borderline tumors (SBTs) of the ovary remain poorly characterized. We present a case series of clinically aggressive LGSC/SBT with comprehensive molecular profiling.

Design: Molecular profiling of 17 LGSCs/SBTs (13 LGSC, 4 SBTs) was performed, all with FIGO stage III disease. 15/17 cases were profiled using a 592 gene panel (Caris Molecular Intelligence), and 2 cases by a 46-gene panel (Caris, including *BRCA1/2*). Retrospective chart review was performed for clinico-patho-molecular correlations.

Results: Tumor mutational burdens (TMB) were generally low, with mean TMB of 5.2 mutation/Mb (range 3-10, based on 14 cases). Microsatellites were stable in 12/12 cases examined. Driver mutations were identified in 11/17 cases, namely in KRAS (5 cases), BRAF (2), NRAS (2), and ERBB2 (2). Among the cases without a clear driver mutation, one case harbored a pathogenic NF2 mutation (p.Y192X) with an FGFR4 kinase domain alteration. Surprisingly, 5/17 cases harbored BRCA2 alterations, all

variants of unknown significance (VUSs), with allele frequencies ranging 11-51%. 2/3 of those patients tested were found to harbor germline BRCA2 alterations. In other cases, VUSs in additional genes in the homologous recombination DNA repair pathway were found, including BARD1, BRIP1, and CHEK2. During the median follow-up period of 3.6 years, two patients had succumbed to their disease, both of whom had received a PARP inhibitor during the terminal disease course.

Conclusions: In our series, besides the previously reported driver mutations, we identified NF2 and FGFR4 alterations. Unexpectedly, BRCA2 was the second most commonly altered gene, some being confirmed be germline. The benefit of targeting VUSs in the homologous recombination DNA repair pathway genes by PARP inhibition appears unclear.

1225 Histopathological Scoring of Activated Stromal Reaction and its Associations with Tumor Molecular Subtypes and Prognosis in High-Grade Serous Ovarian Carcinoma

Lin Yuan[1], Ruifeng Guo[2], Chen Wang[3], Yajue Huang[2]
[1]Shanghai General Hospital, Shanghai Jiaotong University School of Medicine, Hongkou District, Shanghai, China, [2]Mayo Clinic, Rochester, MN, [3]Mayo Clinic College of Medicine, Rochester, MN

Disclosures: Lin Yuan: None; Ruifeng Guo: None; Chen Wang: None; Yajue Huang: None

Background: As a leading lethal women malignancy, high grade serous ovarian carcinoma (HGSOC) has been previously characterized as four tumor transcriptome subtypes: proliferation (PRO), differentiated (DIF), immunoreactive (IMM) and mesenchymal (MES) subtypes. Among which, MES subtype has been associated with the worst survival outcome and extensive desmoplasia. The purpose of this study is to establish a systematic histopathological criterion for scoring of activated stroma in tumor areas and to investigate associations of stromal reactions with HGSOC molecular subtypes and clinical outcomes.

Design: Totally 298 advanced-stage (FIGO stage III/IV) treatment-naïve HGSOC cases underwent surgery between 1990 and 2009 were recruited from the institutional surgical pathology archives. Tumor molecular subtypes were previously characterized according to transcriptome profiling of primary tumors. H&E slides of primary tumor were reviewed by at least two pathologists independently. Activated stroma was defined as reactive desmoplastic stroma of HGSOC with fibroblasts and/or myofibroblasts proliferation. According to proportion of activated stroma component in examined slides, the stroma reaction of tumors were scored as 1 (<5%), 2 (5-10%), 3 (10-30%) and 4 (>30%). Score =3 or 4 were categorized as strong stroma reaction (SSR) and rest as weak stroma reactions (WSR) groups.

Results: Statically significant association (p=1.6e-5) was found between molecular subtypes and scored stromal reactions (SSR or WSR). As shown in table 1, PRO subtype was over-represented in WSR group (44.1%) comparing to other three subtypes; MES subtype had the highest percentage in SSR group (35.7%). When evaluating prognosis associations using 242 cases with available follow-up, median survivals of SSR group was 11 months shorter than WSR group (median survival =36.7 and 47.8 months, respectively; Hazard-ratio = 1.37, p-value = 9.7e-3).

Table 1: Scored Stromal Reactions in Different Molecular Subtypes of High Grade Serous Ovarian Carcinoma

Molecular Subtypes/Score	1	2	WSR（%）	3	4	SSR（%）
PRO	24	21	45（44.1）	22	17	39（19.9）
DIF	8	15	23（22.5）	33	11	44（22.4）
IMM	9	10	19（18.6）	28	15	43（21.9）
MES	6	9	15（14.7）	37	33	70（35.7）

Conclusions: We defined scoring system to characterize activated stromal reactions and found statistically significant associations between stromal reactions and tumor molecular subtypes. In addition, we showed that stromal reaction had significant associations with patient prognosis in HGSOCs. This pilot study suggests that activated stroma scoring can serve as prognostic factor for HGSOC; upon further validations, it can be reported as a routine assessment in pathological diagnosis for advanced stage HGSOC.

1226 Gastric Type Cervical Adenocarcinoma: The Spectrum of Molecular Alterations and Strong Association with Family History of Cancer

Michael Zaleski[1], Anais Malpica[1], DongHyang Kwon[1], Elizabeth Euscher[1], Preetha Ramalingam[1]
[1]The University of Texas MD Anderson Cancer Center, Houston, TX

Disclosures: Michael Zaleski: None; Anais Malpica: None; DongHyang Kwon: None; Elizabeth Euscher: None; Preetha Ramalingam: None

Background: Gastric type endocervical adenocarcinoma (GECA) is an aggressive subtype of non-HPV associated CxCa, which has a worse outcome and increased recurrence rate compared to usual type CxCa. Up to 10% of GECAs are associated with Peutz-Jeghers syndrome (PJS) while rare case are seen in the context of Lynch syndrome. However, no study has reported the incidence of familial

history (FH) of Ca in patients (pts) with GECA. In addition, limited information is available on the molecular landscape of this tumor. The aims of this study are to present a clinicopathology study on a cohort of GECAs with emphasis on the incidence of FH of Ca and to describe the molecular findings obtained by next generation sequencing (NGS).

Design: 39 cases of GECAs were identified from our database (2012-2019). The following information was collected: age, FH, stage, molecular testing (MT), and overall survival. MT was performed using NGS platform for detection of somatic mutations (mut) in the coding sequence of 50 genes.

Results: Mean age at diagnosis was 52 yrs (range 27-88). FH was available in 36 cases; 29 (81%) had a family member with cancer. Total number of family members with Ca was 63; ranged from 1-6 (mean 2.3) per pt. The most common Cas were breast (13/63; 21%), prostate (8/63; 13%), colon (7/63; 11%), melanoma (7/63; 11%), uterine 4/63; 6%), miscellaneous (16/63; 25%) and unknown (8/63; 13%). 5/39 (12%) pts. had a personal history (PH) of Ca (1, pulmonary large cell neuroendocrine Ca, 1 vulvar squamous cell Ca, 2 reported ovarian Ca (5 and 13 yrs. prior to GECA). One pt. had PJS (molecular testing not performed).13/39 (33%) pts. presented with FIGO stage III or IV. 11/39 (28%) had biopsy proven metastatic Ca (5 to ovary/adnexa, 4 omentum, 2 liver). Molecular studies were available for 11/39 (28%) cases. 81% (9/11) of cases had mut. [*TP53* (78%), *KRAS* (44%), STK11 (18%), *SMAD4* (18%) *CDKN2A* (18%), *PTEN* (9%), *MSH6* (9%)]. 5/9 (55%) pts.with muts. had FH of breast Ca.

Conclusions: GECA of the cervix is an uncommon aggressive tumor with advanced stage at presentation and frequent ovarian metastases. A novel finding is that the majority of our pts. have FH and or PH of Ca, most commonly breast, especially in those with molecular alterations. As reported there is genetic heterogeneity in GECA with *TP53* being the most frequent mutation followed by *KRAS* and *CDKN2A*. *SMAD4* mutation in 2 of our cases is also a novel finding. The 2 pts. with STK11 somatic mut. were postmenopausal and did not have clinically known PJS.

1227 Tumor Budding Activity and Cell Nest Size are Strong Determinants of Patient Outcome in Squamous Cell Carcinoma of the Uterine Cervix: Independent Validation of a Novel Grading System

Somaye Zare[1], Omonigho Aisagbonhi[2], Farnaz Hasteh[1], Oluwole Fadare[1]
[1]University of California San Diego, La Jolla, CA, [2]University of California San Diego, Inglewood, CA

Disclosures: Somaye Zare: None; Omonigho Aisagbonhi: None; Farnaz Hasteh: None; Oluwole Fadare: None

Background: Novel grading systems that are based on tumor budding and cell nest size have been proposed for squamous cell carcinomas (SCC) of various sites, including lung, oral cavity, and esophagus. A similar grading scheme has recently been proposed for SCC of the uterine cervix (PMID: 29665323). In this study, we appraise this grading system in an institutional cohort of cervical SCC to assess its prognostic value in an independent dataset.

Design: Our study cohort included 94 cases of cervical SCC with clinical follow-up whose slides were available for review. Tumor budding activity and cell nest size were scored and cases were stratified using a 3-tiered grading system that includes level of budding per 10 HPF and nest size (see PMID: 29665323). In addition, a variety of other tumoral histomorphologic parameters, including keratinization, differentiation by WHO criteria, nuclear size, mitotic activity, and stroma content, were evaluated and correlated with clinicopathologic factors and outcome.

Results: High tumor budding and small cell nest size were strongly associated with poor prognosis, including reduced overall survival (OS), disease-specific survival (DSS), and disease-free survival (DFS) (p<0.001). The novel grading scheme showed excellent prognostic separation of Grade 1, 2, and 3 cases (p<0.001). The strong prognostic impact of the grading scheme was independent of age, pathologic stage, and lymph node status for OS, DSS, and DFS (OS: p <0.0001). Multivariate statistical analysis showed a hazard ratio (HR) for OS of 2.2 for Grade 2 and 4.3 for Grade 3, in comparison to Grade 1 tumors (p=.02). Among the other potentially prognostic factors, higher pathological stage and nodal metastasis correlated with decreased survival (p<.001 and =.004). However, histomorphologic factors, including keratinization, nuclear size, mitotic count and WHO-based 3-tiered grading system were not significantly associated with survival. Higher grade tumors in the novel system were significantly associated with higher stage and lymph node metastasis (p=.03 and p=.01 respectively).

Figure 1 - 1227
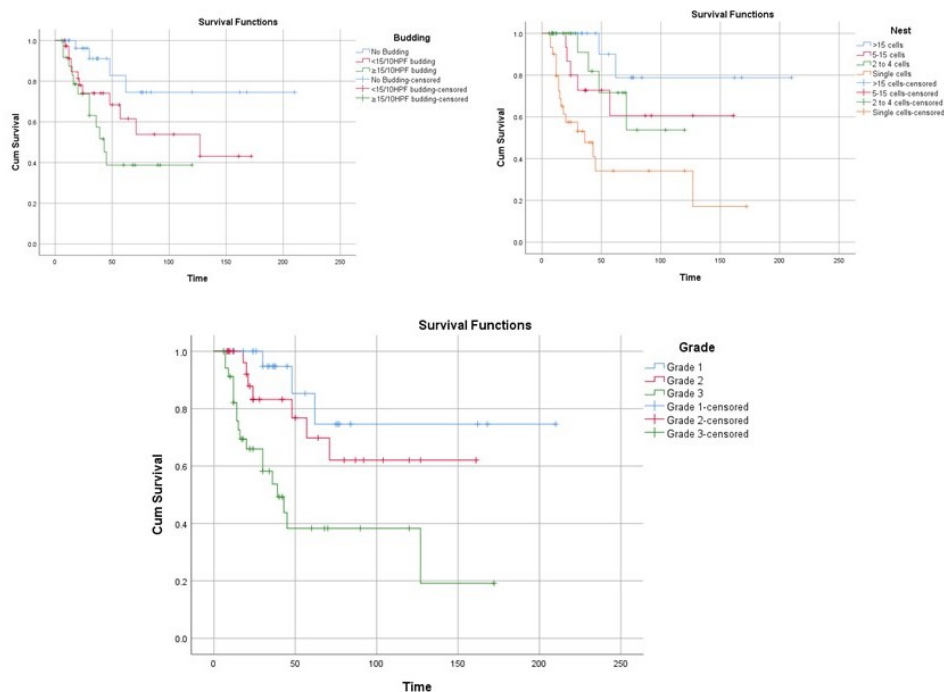
Conclusions: The proposed 3-tiered grading system, which is based on tumor budding activity and cell nest size, is an excellent prognostic indicator and outperforms the widely used, WHO grading systems. Our findings validate the previous study that proposed this system for prognostically stratifying cervical SCC.

1228 Application of a Novel Histological Grading System in Squamous Cell Carcinoma of the Uterine Cervix: Interobserver Reproducibility

Somaye Zare[1], Omonigho Aisagbonhi[2], Farnaz Hasteh[1], Oluwole Fadare[1]
[1]University of California San Diego, La Jolla, CA, [2]University of California San Diego, Inglewood, CA

Disclosures: Somaye Zare: None; Omonigho Aisagbonhi: None; Farnaz Hasteh: None; Oluwole Fadare: None

Background: Histopathological grading of cervical squamous cell carcinomas (SCC) is currently performed using WHO guidelines, which imprecisely combine the extent of squamous differentiation, nuclear pleomorphism, nucleoli size, necrosis, and mitotic activity. However, this system has been found to suboptimally stratify patients regarding prognosis and outcome. A novel histopathological 3-tiered grading system based on tumor budding and cell nest size has recently been proposed for grading SCC of various sites, including the uterine cervix, and has been proffered to be superior to the WHO system. We assess herein the diagnostic reproducibility of this system

Design: 22 cases of cervical SCC with clinical follow-up were selected from a cohort of 94 resected cervical SCCs. The 4 observers were gynecologic pathologists at various levels of experience that practice in an academic medical center. Blinded to FIGO stage and clinical outcomes, the 4 pathologists were asked to independently review one representative slide on each case, score tumor budding and cell nest size and assign the grade of tumor using the 3-tiered budding/nest system (see PMID: 29665323). Briefly, in the budding/nest system, a score is assigned (1 to 3) based on the degree of budding in 10 HPF, with a bud being defined as <5 cells. Another score is assigned based on the smallest nest size (1 to 4). The budding and nesting scores are then added to generate a final score (grade I: 2 and 3; grade 2: 4 and 5; grade 3: 6 and 7). Additionally, observers assigned a separate grade on each case based on the WHO system as they apply it in their routine practice. Interobserver agreement was assessed with the κ statistic (Fleiss' kappa).

Results: The overall agreement in assigning the tumors to grade 1, 2, and 3 based on the budding/nest system was 74.24%. The overall chance-adjusted agreement was substantial (κ = 0.61), with a Cronbach's alpha of 0.83. Observers showed better agreement in evaluation of budding activity (overall agreement: 59.85%, κ = 0.40) than in scoring cell nest size (overall agreement: 48.48%, κ = 0.31). Participants had a moderate agreement in stratifying the tumors by WHO-based grading system (overall agreement= 77.27%, κ = 0.55).

Conclusions: There is substantial reproducibility between gynecologic pathologists in assigning grade for cervical SCC using a 3-tiered grading system that is based on tumor budding activity and nest size, which enhances its potential applicability in routine practice.

1229 Morphological and Immunohistochemical Screening of FH-deficiency in Atypical Leiomyomas

Gloria Zhang[1], Bin Yang[1]
[1]*Cleveland Clinic, Cleveland, OH*

Disclosures: Gloria Zhang: None; Bin Yang: None

Background: The hereditary leiomyomatosis and renal cell carcinoma syndrome (HLRCC) is an autosomal dominant syndrome that results from germline mutations in the fumarate hydratase (FH) gene. FH-deficient (FH-d) uterine leiomyomas display characteristic morphologic features. However the interobserver reproducibility based on morphology alone varies and therefore hinders its effectiveness as a universal tool for screening. Immunohistochemistry for FH can help detect loss of FH protein in leiomyomas. But immunochemical staining for FH may be retained in the presence of an FH gene mutation. Combining immunohistochemistry for FH with morphological screening may help enhance the sensitivity and specificity of identification of FH-d leiomyomas and trigger the genetic consultation.

Design: We studied the FH-d morphologic features and immunohistochemical patterns on 50 cases of atypical leiomyoma, leiomyoma with bizarre nuclei and smooth muscle tumors of uncertain malignant potential (STUMP). Fifty cases consist of 28 atypical leiomyoma, 15 bizarre leiomyomas, and 7 STUMPs. Patient's age arranges from 25 to 72 years with a median of 44.

Results: Histopathologically we assessed five key FH-d features, including staghorn vessels, patchy alveolar edema, nuclei arranged in chains or palisading, macronucleoli with peri-nucleolar halos, and eosinophilic cytoplasmic inclusions. We identified 15 (30%) cases with at least three FH-d features. Among FH-d features, macronucleoli with halos, eosinophilic cytoplasmic inclusions, and staghorn vessels were consistently present in all 15 cases. Three cases did not show patchy alveolar edema, and four cases did not show nuclei arranged in chains or palisading. Immunohistochemical staining showed that 13 out of 15 cases with FH-d morphology had complete loss of FH staining in neoplastic smooth muscle cells while FH staining in intratumor vessels retained. None of the atypical leiomyomas lack of FH-d morphology showed loss of FH protein immunohistochemically.

Conclusions: Our study showed that FH-d morphology can be seen in as high as 30% of atypical leiomyomas. Careful evaluation of key FH-d features is important in identifying suspicious cases. Our study found that FH immunohistochemistry had approximately 87% concordance with FH-d morphology. Since immunohistochemistry has a relatively high specificity and positive predictive value, it could be an excellent tool to confirm the morphological impression especially when FH-d features are less fulfilled.

1230 Podoplanin and Collagen IV are Potential Diagnostic Markers for Early Invasion of Squamous Cell Carcinoma in Uterine Cervix

Wanyu Zhang[1], Sufang Tian[2]
[1]*Wuhan, Hubei, China,* [2]*Wuhan University Zhongnan Hospital, Los Angeles, CA*

Disclosures: Wanyu Zhang: None; Sufang Tian: None

Background: Cervical squamous cell carcinoma (CSCC) is usually developed from high grade squamous intraepithelial lesion (HSIL). Diagnosis of early invasion is difficult but vital for patients' treatment and survival. Podoplanin (PDPN, D2-40 clone) is a specific marker for lymphatic endothelium; collagen IV is an important component of basal membrane network structure. Both may be essential to restrict tumor progression and metastasis.

Design: 34 cases diagnosed of HSIL with suspicious for early invasion were collected. The H&E slides were reviewed by 2 pathologists independently, one with more than 10-year experience and the other 5 years, and classified into negative (no early invasion), positive (early invasion) and uncertain (hard to judge). All the cases were subjected to immunohistochemistry staining (IHC) for D2-40 and collagen IV. Comprehensive interpretation (combining H&E and IHC) was analyzed by two additional pathologists with more than 10-year experience. The results were divided into positive (basement membranes/ basolateral staining completely or intermittently, no invasion) and negative (no staining, invasion) expression.

Results: For H&E review, concordance of 34 cases between the two pathologists was 85.3% (29/34, 20 positive, 8 negative and 1 uncertain). For comprehensive interpretation, concordance between the two pathologists was 100%. Concordance between comprehensive interpretation and at least one pathologist who reviewed H&E sections only was 94.1% (32/34). Statistically, the sensitivity and specificity of D2-40 were 75.9% and 75%, respectively; those of collagen IV were 91.3% and 90.9%, respectively; those of combined use of D2-40 and collagen IV were both 100% (24 cases expressed in consistent pattern and 10 cases in complementary pattern).

Figure 1 - 1230
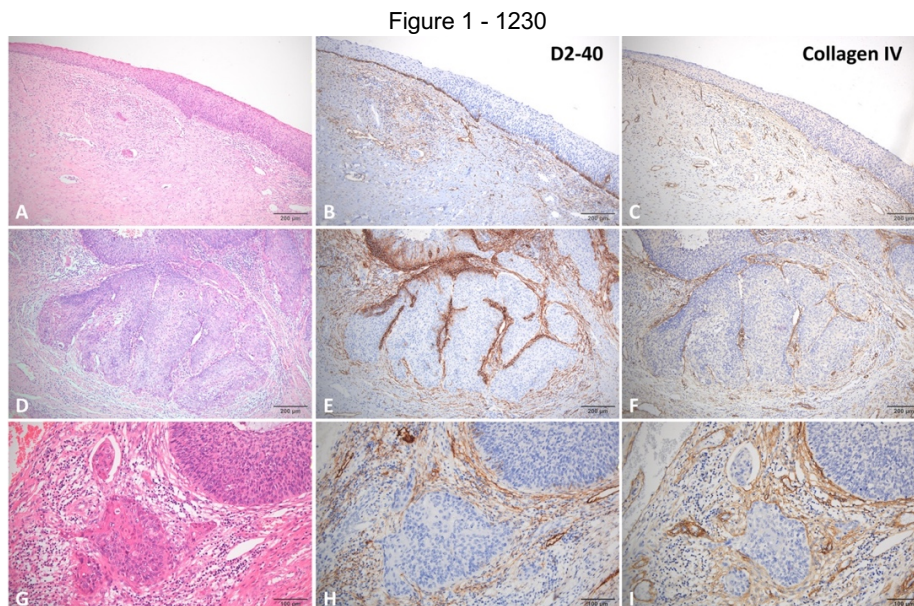
Conclusions: Diagnosis of CSCC with early invasion based on H&E alone lacks objective features. We propose that the combination of morphology and IHC of D2-40 and collagen IV can provide a strong and objective reference for accurate diagnosis of CSCC with early invasion.

1231   p53, but not BRCA Mutational Status, Affects the p16 Immunostaining Patterns in High-Grade Serous Carcinoma of the Ovary

Longmei Zhao[1], Gloria Zhang[2], Bin Yang[2]
[1]Cleveland Clinic Foundation, Cleveland, OH, [2]Cleveland Clinic, Cleveland, OH

Disclosures: Longmei Zhao: None; Gloria Zhang: None; Bin Yang: None

Background: Immunohistochemical staining for p53 is used as a surrogate for mutational analysis in the diagnostic workup of high-grade serous carcinomas (HGSC) of the ovary. Overexpression of p16 is also seen in HGSC and is useful in differential diagnosis from endometrioid carcinoma. However, p16 staining is not always diffuse and strong in ovarian HGSC in our practice. This study is aimed at assessing whether the mutational status of p53 and BRCA genes has an impact on the p16 staining patterns in ovarian HGSC.

Design: A total of 78 cases of ovarian high-grade serous carcinoma was selected for the study. Germline mutations of BRCA1 and BRCA2 have been characterized in 44 cases. Immunohistochemical study for p53 and p16 were performed on selected tissue blocks. For p53, diffuse strong nuclear positivity involving >85% of the tumor cells was considered as positive representing missense mutations and lack of p53 staining was considered as negative representing nonsense mutations. For p16, strong nuclear and cytoplasmic staining involving >85% of tumor cells was considered as diffuse positivity and otherwise was considered as patchy positivity.

Results: Immunohistochemical abnormality of p53 protein was seen in all cases of ovarian HGSC, including 74.4% cases with diffuse staining pattern and 25.6% cases with negative staining. Immunostaining for p16 showed 70.5% cases with diffuse staining pattern and 29.5% cases with patchy staining pattern. When correlates with p53 status, p16 patchy staining pattern is seen in 90% of cases with p53 nonsense mutations, compared to only 10% in those cases with p53 missense mutations (p<0.001, Table 1). We further correlated p53 and p16 staining patterns with BRCA1/2 germline mutations. Although HGSC harboring BRCA1/2 germline mutations had a higher frequency of p53 negativity compared to those with wild type BRCA1/2 (35.7% vs 16.7%), there is no significant statistical difference in each p53/p16 staining patterns between groups of HGSC with wild type and germline BRCA1/2 mutations (p>0.05, Table 2).

Table 1. p53 and p16 Immunostaining Patterns in Ovarian High-Grade Serous Carcinoma

Immunostaining Patterns	p16 Diffuse	p16 Patchy	Total Cases
p53 Diffuse (Missense)	53 (91.4%)	5 (9.6%)	58 (74.4%)
p53 Negative (Nonsense)	2 (10%)	18 (90%)	20 (25.6%)
Total Cases	55 (70.5%)	23 (29.5%)	78

Table 2. Impact of BRCA1/2 Germline Mutational Status on P53 and P16 Immunostaining Patterns

	BRCA1/2 Mutations	BRCA1/2 Wild type	Total cases
Diffuse p53 / Diffuse p16	8 (57.2%)	22(73.3%)	30
Diffuse p53 / Patchy p16	1 (7.1%)	3 (10%)	4
Negative p53/ Diffuse p16	0 (0%)	1 (3.4%)	1
Negative p53/ Patchy p16	5(35.7%)	4 (13.3%)	9
Total cases	14	30	44

Conclusions: Our study shows that diffuse p53 and diffuse p16 immunostaining patterns are seen in the vast majority of ovarian high-grade serous carcinoma. However patchy p16 staining pattern can be seen in up to 30% of cases. We found that patchy p16 staining pattern correlates significantly with null p53 status. Ovarian HGSC harboring germline mutations of BRCA1/2 have a higher frequency of p53 null status but have no impact on p16 staining pattern.

1232 Association of Obesity and Diabetes Mellitus with High-Grade Serous Carcinoma: Does the Risk Vary with Population? A Study in a Safety-Net Hospital

Xiaofeng Zhao[1], Congli Wang[1], Suad Taraif[2]
[1]Temple University Hospital, Philadelphia, PA, [2]Temple University Hospital, Conshohocken, PA

Disclosures: Xiaofeng Zhao: None; Congli Wang: None; Suad Taraif: None

Background: Obesity and Diabetes Mellitus are epidemic public health problems in the United States and worldwide. In contrast to their established role as risk factors in endometrioid carcinoma, the role of obesity and Diabetes Mellitus in high-grade serous carcinoma is debated. The purpose of our study was to examine the association between obesity and/or Diabetes and high-grade serous carcinoma of various sites in our high-risk patient population.

Design: We retrospectively retrieved from the departmental pathology archives all cases diagnosed as high-grade serous carcinoma over a ten-year period including concurrent/subsequent cytopathology samples. Patient demographics, including age, BMI, and diabetic status were obtained from electronic medical records.

Results: Between June 2008 and June 2018, a total of 84 patients were diagnosed with high-grade serous carcinoma (median age 61-year old, range 34-89 years). 38% of our patients were Caucasians, 32.14% were African Americans, 8.33% were Hispanics, and the rest were among other ethnic minorities or of unknown ethnicity. The majority of serous carcinomas originated from the ovary, followed by the endometrium. 25 of our patients were diabetics (29.76%) and 25 were obese defines as BMI>30 (29.76%). The prevalence of diabetes in our study population is 60% and 26.5% among patients with endometrial and ovarian serous carcinomas, respectively. Peritoneal fluid cytology was available for 44 cases (Table 1). Out of 6 diabetic patients with ovarian serous carcinoma, 5 had positive peritoneal fluid cytology (83.3%). 8 patients with ovarian serous carcinoma were deceased, 4 of which had diabetes and one was obese.

High-grade serous carcinoma							
	Ovary	Endometrium	Fallopian tube	Ovary and tube	Peritoneum	Unknown	Total
	34 (40.47%)	20 (23.81%)	8 (9.52%)	10 (11.90%)	3 (3.51%)	9 (10.71%)	84
diabetes	9	12	1	1	0	2	25
obesity	7	13	1	3	0	1	25
overweight	14	5	3	5	1	3	31
Normal BMI	8	2	3	0	1	3	17
Peritoneal fluid	20	14	3	4	0	3	44
Positive cytology	13	4	2	4	0	3	26
Rate of positivity	65%	28.6%	66.7%	100%	N/A	100%	59.1%

Race	Overall	Diabetic	BMI			
			Obese (BMI ≥30)	Overweight (BMI 25-29.9)	Normal (BMI <25)	Unknown
African American	27	12	12	9	3	3
Caucasian	32	6	3	16	12	1
Hispanic	7	4	3	3	0	1
Other	8	2	5	1	1	1
Unknown	10	1	2	2	1	5
Total	84	25	25	31	17	11

Conclusions: Patients with ovarian and endometrial serous carcinomas were more likely to be diabetics compared to serous carcinomas of other sites. Patients with diabetes were more likely to present with advanced stage disease. For ovarian and endometrial serous carcinoma, diabetes seems to be an independent risk factor from obesity. Although rates of diabetes and obesity are higher among African American patients, our study population seems to have a higher number of Caucasian patients which makes the likelihood of race as a confounding factor less likely. Obesity and diabetes may be associated with serous carcinoma of the ovary and endometrium in high-risk populations. Additional studies are needed to further explore this association.

1233 CTNNB1 Mutations and Aberrant β-Catenin Expression in Ovarian Endometrioid Carcinoma: Correlation with Patient Outcome

Roman Zyla[1], Yutaka Amemiya[2], Ekaterina Olkhov-Mitsel[3], Dina Bassiouny[4], Arun Seth[4], Bojana Djordjevic[5], Sharon Nofech-Mozes[4], Carlos Parra-Herran[4]
[1]Toronto, ON, [2]Sunnybrook Research Institute, Toronto, ON, [3]Sunnybrook Health Sciences Centre, Toronto, ON, [4]Sunnybrook Health Sciences Centre, University of Toronto, Toronto, ON, [5]University of Toronto, Toronto, ON

Disclosures: Roman Zyla: None; Yutaka Amemiya: None; Ekaterina Olkhov-Mitsel: None; Dina Bassiouny: None; Arun Seth: None; Bojana Djordjevic: None; Sharon Nofech-Mozes: None; Carlos Parra-Herran: None

Background: *CTNNB1* mutations are associated with worse survival in patients with early-stage, low-grade endometrial carcinoma. Interestingly, it has been recently shown that nuclear β-catenin (βCAT) expression is a good prognostic factor in ovarian endometrioid carcinoma (OEC). The prognostic value of the *CTNNB1* mutational status and its relationship with other clinical and pathologic variables in OEC has not been documented.

Design: We performed immunohistochemistry for βCAT (M3539, Dako) and a 9-gene next-generation sequencing panel in 51 OECs, previously classified as per the PROMISE classifier as: p53 wild-type (wt, n=31), p53 abnormal (abn, n=10), POLE-abn (n=6) and MMR-abn (n=4). The panel included whole-exome sequencing of *CTNNB1, PTEN* and *TP53*, and hotspot coverage of *PIK3CA, KRAS, HRAS, BRAF* and *CDKN2A*. Results were correlated with clinic-pathologic variables including disease-free survival (DFS) and disease-specific survival (DSS).

Results: Median patient age was 55 years (range 36-89). Median follow-up period was 61 months (range 3-176). Tumor recurrence was documented in 14 patients (27%), and OEC-related death in 8 (16%). *CTNNB1* mutations were found in 22 cases (43%), and nuclear βCAT in 12 (24%). Mutated *CTNNB1* status was statistically associated with better DFS (p=0.04, log rank test) and approached significance for better DSS (p=0.07, Figure 1). It also correlated with nuclear βCAT expression, no surface involvement and early FIGO stage (p<0.05, Chi-square test). There was no association between *CTNNB1* status and PROMISE group. On univariate Cox regression analysis, *CTNNB1* mutations, *TP53* mutations, age, PROMISE group, surface involvement, tumor grade and stage correlated with DFS. There was no correlation between nuclear βCAT expression and DFS (p=0.1) or DSS (p=0.4). There was no statistical association between *CTNNB1* mutations and survival when analysis was restricted to patients in p53-wt, low grade and FIGO stage I groups.

Figure 1 - 1233
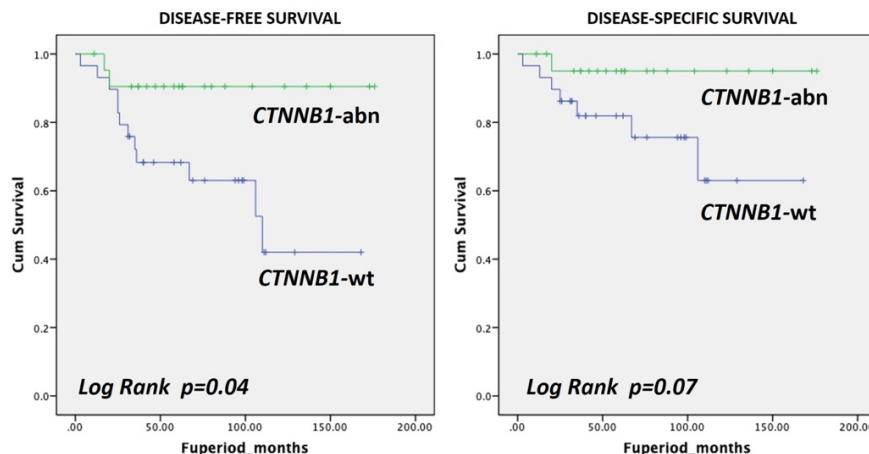
Conclusions: *CTNNB1* mutations are associated with better progression-free survival in patients with OEC, unlike those with endometrial carcinoma. This relationship may be in part due to a trend of *CTNNB1*-mutated tumors to present at early stage. This is in keeping with previous observations of better survival in OECs with nuclear βCAT (although we did not observe such association in our study). Further investigation in larger samples is required to establish whether this relationship is independent from other variables.

1234 Horizontal Tumor Extent is an Independent Prognostic Variable in Cervical Cancer: Implications for the 2018 FIGO Staging Update

Roman Zyla[1], Ekaterina Olkhov-Mitsel[2], Lilian Gien[3], Jelena Mirkovic[4], Sharon Nofech-Mozes[4], Bojana Djordjevic[5], Carlos Parra-Herran[4]

[1]Toronto, ON, [2]Sunnybrook Health Sciences Centre, Toronto, ON, [3]Sunnybrook Odette Cancer Center, Toronto, ON, [4]Sunnybrook Health Sciences Centre, University of Toronto, Toronto, ON, [5]University of Toronto, Toronto, ON

Disclosures: Roman Zyla: None; Ekaterina Olkhov-Mitsel: None; Lilian Gien: None; Jelena Mirkovic: None; Sharon Nofech-Mozes: None; Bojana Djordjevic: None; Carlos Parra-Herran: None

Background: The FIGO 2018 update on staging of cervical cancer (CxCA) removes horizontal tumor extent (HZTE) as a staging variable, arguing that it is a poorly reproducible metric without providing data against its prognostic significance. As evidence to support this shift is needed, we aimed to determine the association of HZTE with patient outcome.

Design: We identified patients with CxCA from 01/2009 to 12/2017 in our institution, where HZTE is routinely reported. When documented, the % of cervix circumference involved by tumor (%CIR) was also recorded. Pathologic variables were extracted from synoptic reports including lymphovascular invasion (LVI) and grade (G1-G3). Only squamous cell, adenocarcinoma, adenosquamous and glassy cell carcinomas were included. HZTS and %CIR were correlated with other clinical and pathologic variables including recurrence-free (RFS), overall (OS) and disease-specific survival (DSS). Stage as per 2018 FIGO recommendations was determined for each case (thus not using the horizontal extent metric).

Results: After exclusion of lesions with no HZTE recorded and/or no follow-up, a total of 400 patients were included. Median follow-up was 40 months (mean 41, range 1-123). Both HZTE (in mm) and %CIR correlated with FIGO 2018 tumor stage (p<0.001, log rank test). HZTE also correlated with lymph node metastases (p<0.001). On KM curve analysis (Figure 1) and univariate Cox regression, HZTE correlated with worse RFS, OS and DSS (p≤0.001). Indeed, none of the women with HZTE <7 mm had recurrence or cancer-related death. Other variables correlating with DFS, OS and DSS included invasive depth, grade, LVI and 2018 FIGO stage (IA1-IB2 vs IB3-IV). %CIR and histotype correlated with RFS. On multivariate analysis of variables significant on univariate regression (Table 1), HZTE was associated with worse OS [hazard ratio (HR) 1.05, 95% confidence interval (CI) 1-1.1, p=0.02] and approached significance for RFS (p=0.07); RFS also correlated with grade (G2 vs G1 p=0.03; G3 vs G1 p=0.02) and histotype (p=0.04).

	RFS				OS				DSS			
Univariate Cox Regression Analysis	HR	95% CI		P-value	HR	95% CI		P-value	HR	95% CI		P-value
Horizontal extent	1.08	1.06	1.10	*<0.001*	1.06	1.04	1.08	*<0.001*	1.06	1.04	1.08	*<0.001*
% circumference	1.02	1.01	1.04	*0.008*	1.02	0.99	1.04	0.15	1.02	0.99	1.04	0.15
Age	1.00	0.98	1.03	0.73	1.01	0.98	1.04	0.55	1.01	0.97	1.04	0.77
Histotype				*0.001*				0.06				0.08
SCC vs HPV adenoCA	0.81	0.33	2.01	0.65	0.27	0.06	1.22	0.09	0.29	0.06	1.34	0.11
SCC vs adenosquamous CA	4.27	1.72	10.59	*0.002*	2.06	0.65	6.50	0.22	1.77	0.49	6.46	0.39
SCC vs glassy CC	5.21	0.68	39.94	0.11	6.22	0.80	48.48	0.08	6.56	0.84	51.43	0.07
SCC vs non-HPV adenoCA	6.32	1.43	27.85	*0.015*	2.46	0.32	19.14	0.39	2.78	0.35	21.82	0.33
Grade				*0.001*				*0.03*				*0.05*
G2 vs G1	9.34	2.14	40.87	*0.003*	5.93	1.28	27.46	*0.02*	5.24	1.11	24.69	*0.04*
G3 vs G1	16.17	3.65	71.69	*0.0002*	7.91	1.68	37.29	*0.01*	7.06	1.47	34.01	*0.02*
Depth	1.11	1.08	1.15	*<0.001*	1.07	1.04	1.10	*<0.001*	1.07	1.04	1.10	*<0.001*
LVI	3.79	1.82	7.91	*<0.001*	7.31	2.42	22.06	*<0.001*	6.44	2.10	19.79	*0.001*
FIGO 2018 (IA1-IB2 vs IB3-IV)	5.49	2.71	11.14	*<0.001*	8.88	3.37	23.38	*<0.001*	9.89	3.48	28.09	*<0.001*

	RFS				OS				DSS			
Multivariate Cox Regression Analysis	HR	95% CI		P-value	HR	95% CI		P-value	HR	95% CI		P-value
Horizontal extent	1.07	0.99	1.14	0.07	1.06	1.01	1.10	*0.02*	1.04	0.99	1.09	0.12
% circumference	1.00	0.98	1.02	0.87								
Histotype				*0.05*								
SCC vs HPV adenoCA	2.81	0.84	9.42	0.10								
SCC vs adenosquamous CA	2.72	0.56	13.20	0.22								
SCC vs glassy CC	0.00	0.00	.	0.99								
SCC vs non-HPV adenoCA	126.6	5.08	3155	*0.003*								
Grade				0.07				0.66				0.73
G2 vs G1	23.86	1.20	472.92	*0.04*	1.87	0.36	9.78	0.46	1.84	0.35	9.81	0.48
G3 vs G1	31.28	1.69	578.25	*0.02*	2.17	0.42	11.35	0.36	1.94	0.36	10.54	0.44
Depth	1.02	0.93	1.12	0.71	0.96	0.90	1.03	0.25	0.98	0.91	1.05	0.56
LVI	0.87	0.25	3.01	0.83	2.73	0.79	9.46	0.11	2.30	0.65	8.22	0.20
FIGO 2018 (IA1-IB2 vs IB3-IV)	1.08	0.33	3.51	0.90	2.42	0.71	8.21	0.16	3.45	0.94	12.71	0.06

Figure 1 - 1234
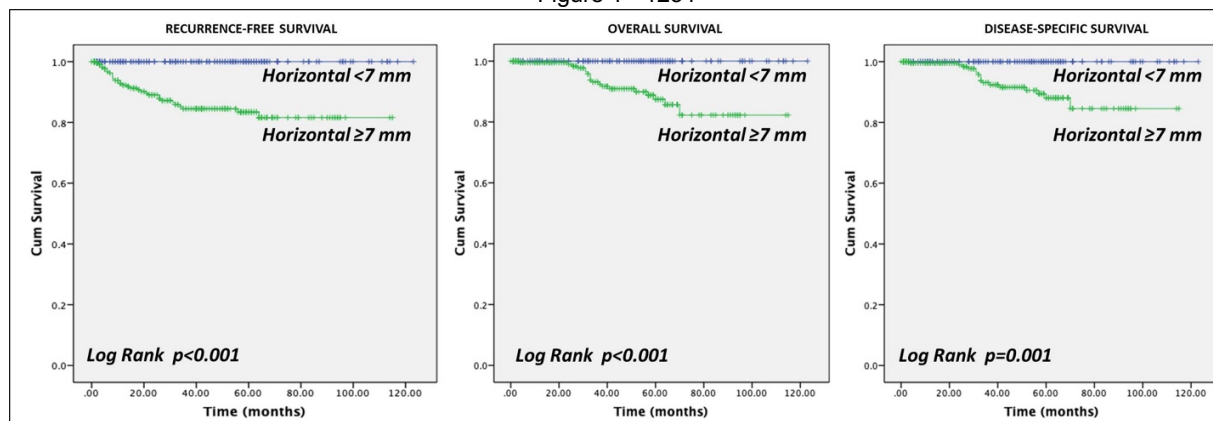
Conclusions: Based on this large retrospective series, horizontal tumor size is an important prognostic variable in cervical cancer, predictive of overall survival independent from other factors including the 2018 FIGO stage. The % of circumferential tumor involvement may also have a prognostic role. Despite recent recommendations by FIGO, our findings support continuing to include these variables in the pathologic assessment and management of patients with cervical cancer.